With all the scientific and technological advances in all disciplines in every single corner of the globe, our understandings of the systems in the Universe and even within the planet Earth is limited and without internationally hand-in-hand interdisciplinary collaborations, it is hard to believe we can proceed toward the right pathway of expanding our knowledge. Acting on all the experiences in the last thirsty-two years, the author of this book has found that the strength is in unity from small scales up to larger ones which enables us to search for the philosophy behind a phenomenon, like how fractals are mesmerizing.

Detection, attribution and quantification of methane emissions...

Hossein Maazallahi

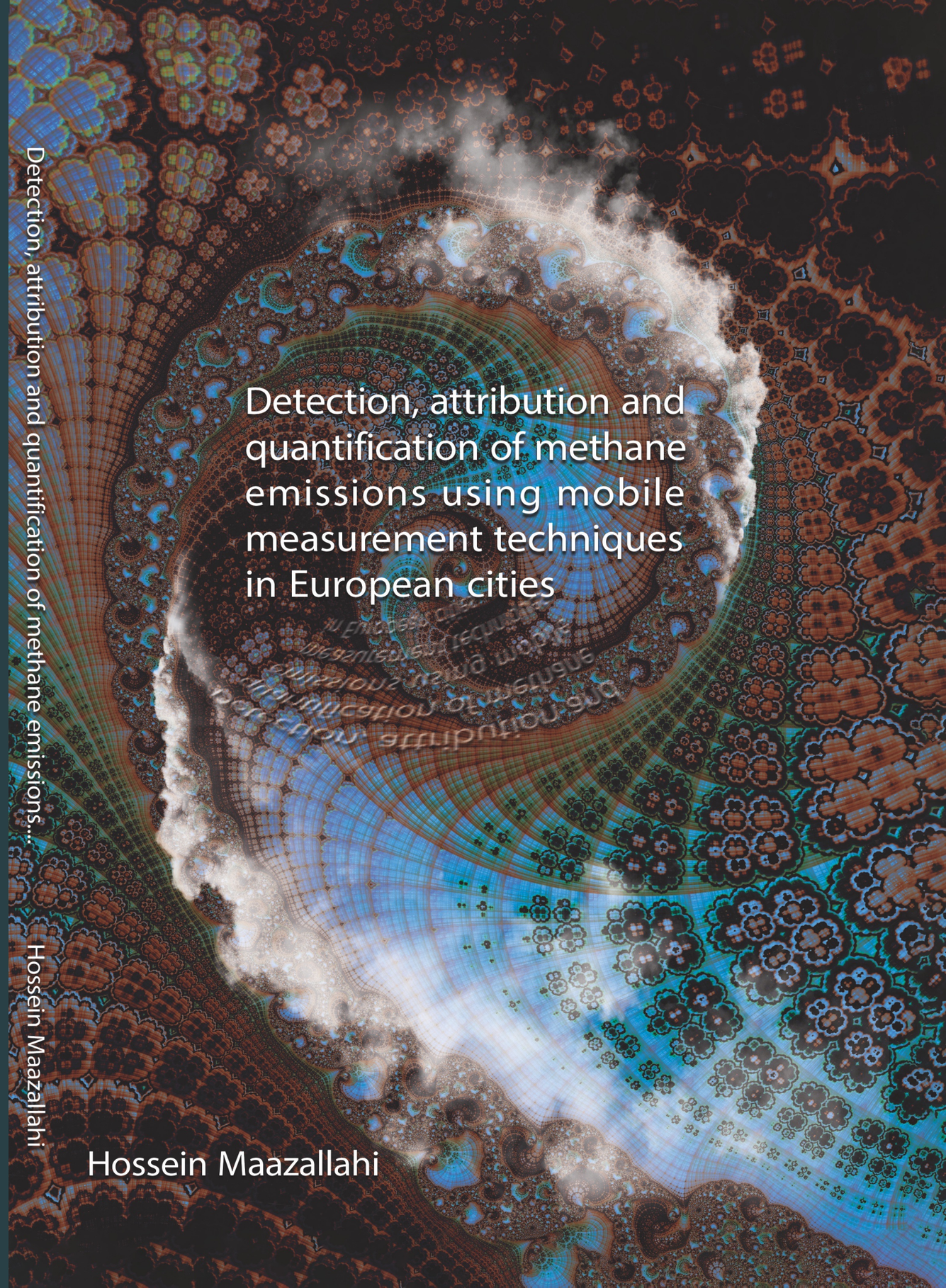

Detection, attribution and quantification of methane emissions using mobile measurement techniques in European cities

Hossein Maazallahi
September 2022

Institute for Marine and Atmospheric research Utrecht (IMAU)
Faculty of Science, Department of Physics, Utrecht University
Princetonplein 5, 3584 CC Utrecht, The Netherlands

Cover designed by Hamid Shams
The design is inspired by a combination of infrared vision of methane plumes, ancient Persian architecture and fractal structures.
Pattern Studio
112-2799 Gilmore Ave., BC V5C 6S5, Burnaby, Vancouver, Canada
Website: www.patternstudio.ca
Instagram: @patternstudio.ca

ISBN: 978-94-6419-577-4
Printed by Gilderprint
Auke Vleerstraat 145, 7547PH, Enschede, the Netherlands

Detection, attribution and quantification of methane emissions using mobile measurement techniques in European cities

Detectie, attributie en kwantificatie van methaan emissies in Europese steden met behulp van mobiele meettechnieken

(met een samenvatting in het Nederlands)

Detektierung, Zuordnung und Quantifizierung von Methanemissionen in europäischen Städten unter Verwendung mobiler Messtechniken

(mit einer Zusammenfassung auf deutsch)

Detección, atribución y cuantificación de emisiones de metano usando técnicas de medición móvil en ciudades Europeas

(con resumen en Espanol)

Détection, attribution et qualification des émissions de méthane en utilisant des mesures mobiles et techniques dans des villes européennes

(avec un résumé en français)

Deteksjon, attribusjon og kvantifisering av metanutslipp ved bruk av mobile måleteknikker i europeiske byer

(med oppsummering på norsk)

شناسایی، نسبت‌دهی و کمی‌سازی انتشارات متان برپایه اندازه‌گیری‌های سیار در شهرهای اروپا

(به همراه خلاصه فارسی)

Proefschrift

ter verkrijging van de graad van doctor aan de Universiteit Utrecht op gezag van de rector magnificus, prof.dr. H. R. B. M. Kummeling, ingevolge het besluit van het college voor promoties in het openbaar te verdedigen op
dinsdag 27 september 2022 des ochtends te 10.15 uur

door
Hossein Maazallahi
22 September 1990, Rayn, Iran

Promoter
Prof. dr. Thomas Röckmann

Co-promoter
Dr. Hugo Denier van der Gon

Beoordelingscommissie
Prof. dr. Euan Nisbet
Dr. Martina Schmidt
Prof. dr. Jia Chen
Prof. dr. Guus Velders
Prof. dr. Huib E. de Swart
Prof. dr. Maarten Krol
Dr. Daniel Zavala-Araiza

This thesis was accomplished within the MEMO^2 (Methane goes Mobile, Measurements and Modelling) project, one of the European Union's Horizon 2020 research and innovation programmes under the Marie Skłodowska–Curie grant No. 722479.

Table of Contents

International summaries

The mixing ratio increase of atmospheric greenhouse gases, hence global warming and climate changes are not bounded to the borders. This is a global issue and should be addressed internationally with robust, transparent and continuous efforts.

Summary

Global actions are required to reduce Greenhouse Gas (GHG) emissions, and thus mitigate global warming. On the 4th of November 2016 the Paris agreement (UNFCCC, 2015) between 196 countries entered into force which aims to limit global warming to less than 2 °C. Methane (CH_4) has a relatively short atmospheric lifetime (≈10 years) which makes it an effective mitigation target to slow down global warming on the short to medium term (Rogelj et al., 2019). The CH_4 mitigations can be implemented faster and have less severe economic effects than reduction of carbon dioxide (CO_2) emissions because CO_2 emission is directly proportional to energy consumption. Despite the attractiveness of CH_4 reduction, on the longer term also CO_2 emission will need to be reduced to zero around the middle of this century to reach the goals of the Paris agreement. Among all the CH_4 sources, emission mitigation in the energy sectors seems to be the most time efficient and cost effective compared to emission reduction from other sectors (UNEP and CCAC, 2021; Dlugokencky et al., 2011).

CH_4 emissions from the energy sector, particularly from production, storage, transportation, distribution and end-use of fossil fuels (oil, gas and coal) contribute 19% to total anthropogenic CH_4 emissions in Europe. This contribution can increase to more than 60% in fossil fuel producing countries (UNFCCC, 2017). Fossil fuel related emission have been identified as an interesting target within the CH_4 reduction strategy of the EU (EC, 2020).

The emissions from these activities are mainly estimated using Emission Factors (EFs) and Activity Data (AD) in inventories. The EFs are the ratio of emission rate per activity unit, e.g. kg of CH_4 emitted per amount of gas produced. The EFs are tabulated in reports from national or international agencies, and standard EFs for emission reporting have been tabulated by the Intergovernmental Panel on Climate Change (IPCC). However, the EFs can vary temporally and spatially which increases the uncertainty in the estimated emissions. To reduce the uncertainty, independent measurement campaigns are required to update or verify these EFs, some of which are outdated or are possibly affected by sampling and / or emission rate biases.

Detailed information is required on where and how large the emissions are, for effective mitigation policies. This thesis was carried out within the MEMO^2 (MEthane goes MObile, MEasurements and MOdelling) project, with the objective to use mobile measurement techniques to improve our understanding of CH_4 emissions. The main focus was on emissions in the energy sector. In this thesis, we provide detailed results from detection, quantification and attribution of CH_4 emissions from extensive measurement campaigns focusing on emissions from the gas distribution networks in cities. These measurements showed that the contribution of CH_4 emissions from natural gas leaks, microbial or combustion sources are different from one city to another, thus dedicated emission mitigation policies are required for different cities.

In chapter 2 we provide results of street-level mobile measurements in two different European cities; Hamburg (DE), Utrecht (NL). We demonstrate the benefit of detecting and attributing natural gas leaks with mobile measurements. A key aspect is that the use of vehicle platforms can considerably speed up the gas leak detection process, allowing in principle more frequent maintenance, which will help reduce emissions. The method can also be used to quantify emission rates, but we show that estimates from individual transects have a large uncertainty. On the other hand, a snapshot of emissions in an entire city can be derived in days to weeks. The aggregated city-scale emission rates will be more reliable than estimates at individual locations. In addition, very large emitters can be easily detected, and thus also reported and subsequently mitigated. We quantified total CH_4 emission of 440±70 t yr^{-1} and 150±50 t yr^{-1} to Hamburg and Utrecht, out of which 50%–80% and 70%–90%, respectively were attributed to CH_4 emissions from urban natural gas distribution network in these two cities. Our measurement show that the emission rate distribution is a skewed distribution where only a few leak locations can account for half of the city scale emissions. This opens attractive mitigation options for CH_4 emissions from gas distribution networks.

CH_4 signals from mobile measurements in urban areas are prone to be reported as a false alarm for a natural gas leak if the CH_4 signals are not properly attributed with robust constraints. The use of co-emitted species with CH_4, e.g. ethane (C_2H_6), CO_2 and/or the stable isotope signatures of carbon and hydrogen in CH_4 ($\delta^{13}C$-CH_4 and δD-CH_4 respectively) can be used individually or together in CH_4 emission attribution. In chapter 2, we introduced new constraints and showed the value of simultaneous use of C_2H_6 and CO_2 signals to attribute CH_4 signals from mobile measurements. These constraints do not only improve our understanding about the contribution of different sources to total CH_4 emissions in an urban area but can indirectly also contribute to maintaining the safety of the gas distribution system. We used the C_2H_6:CH_4 (C_2:C_1) ratio from the measurements and correlations of CO_2 with observed CH_4 signals, together with prior knowledge on the C_2:C_1 ratio in natural gas pipelines, and introduced a systematic approach to attribute CH_4 emissions to fossil, microbial and combustion sources. In cities, fossil emissions are generally due to CH_4 emissions from leaks in the natural gas distribution system. Microbial emissions mostly point to the biogenic, non-fossil CH_4 being released from open street-level outlets connected to rain or wastewater systems, e.g. manholes from the sewer system. The combustion category refers to unburned CH_4 from incomplete combustion which can happen in cars, house heating and cooking systems. By applying this attribution approach to the CH_4 signals, we reported the potential natural gas leak locations (with high confidence) to the local gas utilities which resulted in the repair of a large number of gas leaks in Utrecht and Hamburg.

In chapter 3 we report and discuss our results from mobile surveys in Bucharest where we used measurements of $\delta^{13}C$-CH_4 and δD-CH_4 collected in air sample bags, and online C_2H_6 measurements to attribute CH_4 signals. While in Utrecht or Hamburg more than 50% and up to 90% of emissions can be attributed to the CH_4 emissions from leaks from natural gas pipelines (chapter 2), the situation in Bucharest is different and about 60% of total emissions could be attributed to microbial sources, likely from the sewer system. We show that δD-CH_4 is a better attributor than $\delta^{13}C$-CH_4 in separating natural gas leaks from signals of other sources. This was also observed in a smaller isotopic sample size in Hamburg (chapter 2).

In chapter 4 we report results from an intercomparison of three different gas leak quantification methods in Hamburg, Germany. Our reports of CH_4 emissions from natural gas distribution networks in chapter 2 sometimes showed very high emission rates. These are larger than what is normally found with the suction method, which is used to provide information for the official German national emission inventory. Hence, we designed an intercomparison campaign to understand the discrepancy. In addition to the mobile and suction methods we deployed the tracer method which is more labor intensive but has a low quantification uncertainty for emission estimates using atmospheric measurements. The direct comparison between methods is difficult because of limitations of the different methods for different types of locations, and we discuss in detail the strengths and limitations of each method. A key result is that all three methods showed that emissions from leaks in the high safety risk categories of A1&A2 have higher emission rates than leaks in the lower risk B&C categories. We also generally encountered large subsurface CH_4 emissions around the A1&A2 gas leak locations. The suction method could in several cases not be applied at these locations because official regulations required immediate repair, or the team could not complete the measurement within the allotted time. Due to such time constraints and safety issues, it is likely that the suction method is usually not deployed at the A1&A2 locations, where CH_4 emissions are generally higher than at the B&C locations. This could induce a low bias to the German CH_4 emission inventory for gas leaks from urban natural gas distribution networks.

In chapter 5 we provide general conclusions of our research results from the urban measurement campaigns. We discuss the importance of attribution techniques to distinguish the contributions of different CH_4 sources to total emission in the urban area. We present the strengths and limitations of mobile detection and quantification methods and provide outlook on how to improve these methods. We also show an outlook of the application of the mobile method in the commercial market, with the goal to reduce CH_4 emissions in cities and to speed up our understanding of the state of CH_4 emissions in urban areas in the framework of CH_4 mitigation policies.

Samenvatting

Wereldwijde acties zijn nodig om de uitstoot van broeikasgassen te verminderen en zo de opwarming van de aarde te beperken. Op 4 november 2016 is het akkoord van Parijs (UNFCCC, 2015) tussen 196 landen in werking getreden met als doel de opwarming van de aarde te beperken tot minder dan 2 °C. Methaan (CH_4) heeft een relatief korte atmosferische levensduur (≈10 jaar), waardoor het een effectief mitigatiedoel is om de opwarming van de aarde op korte tot middellange termijn te vertragen (Rogelj et al., 2019). De CH_4-beperkingen kunnen sneller worden geïmplementeerd en hebben minder ernstige economische effecten dan vermindering van de uitstoot van kooldioxide (CO_2), omdat de CO_2-uitstoot recht evenredig is met het energieverbruik. Ondanks de aantrekkelijkheid van CH_4-reductie zal op langere termijn ook de CO_2-uitstoot rond het midden van deze eeuw naar nul moeten worden teruggebracht om de doelen van het Parijs-akkoord te halen. Van alle CH_4-bronnen lijkt emissiebeperking in de energiesectoren het meest efficiënt en kosteneffectief in vergelijking met emissiereductie van andere sectoren (UNEP and CCAC, 2021; Dlugokencky et al., 2011).

CH_4-emissies van de energiesector, met name van productie, opslag, transport, distributie en eindgebruik van fossiele brandstoffen (olie, gas en steenkool) dragen 19% bij aan de totale antropogene CH_4-emissies in Europa. Deze bijdrage kan oplopen tot meer dan 60% in landen die fossiele brandstoffen produceren (UNFCCC, 2017). Emissies gerelateerd aan fossiele brandstoffen zijn geïdentificeerd als een interessant doel binnen de CH_4-reductiestrategie van de EU (EC, 2020).

De emissies van deze activiteiten worden voornamelijk geschat met behulp van emissiefactoren (EF's) en activiteitsgegevens (AD) in inventarissen. De EF's zijn de verhoudingen van de emissiesnelheid per activiteitseenheid, b.v. kg CH_4 uitgestoten per geproduceerde hoeveelheid gas. De EF's zijn genoteerd in rapporten van nationale of internationale instanties, en standaard EF's voor emissierapportage zijn genoteerd door het Intergouvernementeel Panel voor klimaatverandering (IPCC). De EF's kunnen echter in tijd en ruimte variëren, wat de onzekerheid in de geschatte emissies vergroot. Om deze onzekerheid te verminderen en de EF's bij te werken of te verifiëren zijn onafhankelijke meetcampagnes vereist. Dit is ook nodig omdat sommige van de EF's verouderd zijn of mogelijk worden beïnvloed door bemonstering en/of vertekening in de emissiesnelheid.

Om een effectief mitigatiebeleid te vormen is gedetailleerde informatie nodig over waar en hoe groot de emissies zijn. Dit proefschrift werd uitgevoerd binnen het MEMO^2 (MEthane goes MObile, MEasurements and MOdelling) project, met als doel om mobiele meettechnieken te gebruiken om ons begrip van CH_4-emissies te verbeteren. De focus lag op de emissies in de energiesector. In dit proefschrift leveren we gedetailleerde resultaten van detectie, kwantificering en attributie van CH_4-emissies van uitgebreide meetcampagnes gericht op emissies van de gasdistributienetwerken in steden. Deze metingen toonden aan dat de bijdrage van CH_4-emissies van aardgaslekken, microbiële of verbrandingsbronnen van stad tot stad verschilt, dus een specifiek emissiebeperkingsbeleid is vereist voor verschillende steden.

In hoofdstuk 2 geven we resultaten van mobiele metingen op straatniveau in twee verschillende Europese steden; Hamburg (DE) en Utrecht (NL). Met mobiele metingen demonstreren we het voordeel van het opsporen en toekennen van aardgaslekken. Een belangrijk aspect is dat het gebruik van voertuigplatforms het gaslekdetectieproces aanzienlijk kan versnellen, waardoor in principe frequenter onderhoud mogelijk is, wat de emissies zal helpen verminderen. De methode kan ook worden gebruikt om emissiesnelheden te kwantificeren, maar we laten zien dat schattingen van individuele transecten een grote onzekerheid hebben. Aan de andere kant kan een momentopname van de uitstoot in een hele stad worden afgeleid in dagen tot weken. De geaggregeerde emissiecijfers op stadsschaal zullen betrouwbaarder zijn dan schattingen op individuele locaties. Bovendien kunnen zeer grote uitstoters eenvoudig worden gedetecteerd, en dus ook worden gerapporteerd en vervolgens worden gemitigeerd. We kwantificeerden de totale CH_4-emissie van 440±70 t yr^{-1} voor Hamburg en 150±50 t yr^{-1} voor Utrecht, waarvan respectievelijk 50%–80% en 70%–90% werd toegeschreven aan CH_4-emissies van het stedelijk aardgasdistributienetwerk in deze twee steden. Onze metingen laten zien dat de emissiesnelheidsverdeling een scheve verdeling is waarbij slechts een paar leklocaties verantwoordelijk

kunnen zijn voor de helft van de emissies op stadsschaal. Dit opent aantrekkelijke mitigatiemogelijkheden voor CH_4-emissies uit gasdistributienetwerken.

Als de CH_4-signalen niet correct worden toegeschreven met robuuste beperkingen worden CH_4-signalen van mobiele metingen in stedelijke gebieden vaak als vals alarm van een aardgaslek gerapporteerd. Het gebruik van gelijktijdig uitgestoten soorten met CH_4, b.v. ethaan (C_2H_6), CO_2 en/of de stabiele isotoopsignaturen van koolstof en waterstof in CH_4 (respectievelijk $\delta^{13}C$-CH_4 en δD-CH_4) kunnen afzonderlijk of samen worden gebruikt bij de toekenning van CH_4-emissie. In hoofdstuk 2 hebben we nieuwe manieren geïntroduceerd om CH_4-emissies te karakteriseren en we hebben de waarde aangetoond van gelijktijdig gebruik van C_2H_6- en CO_2-signalen om CH_4-signalen van mobiele metingen aan bronnen toe te kennen. Deze nieuwe methoden verbeteren niet alleen ons begrip van de bijdrage van verschillende bronnen aan de totale CH_4-emissies in een stedelijk gebied, maar kunnen ook indirect bijdragen aan het handhaven van de veiligheid van het gasdistributiesysteem. Om CH_4-emissies toe te schrijven aan fossiele, microbiële en verbrandingsbronnen gebruikten we de C_2H_6:CH_4 (C_2:C_1)-verhouding van de metingen en correlaties van CO_2 met waargenomen CH_4-signalen, samen met voorkennis over de C_2:C_1-verhouding in aardgaspijpleidingen, en we introduceerden hiervoor een systematische benadering. In steden zijn fossiele emissies over het algemeen te wijten aan CH_4-emissies door lekken in het aardgasdistributiesysteem. Microbiële emissies wijzen er meestal op dat biogene, niet-fossiele CH_4 vrijkomt uit open stopcontacten op straatniveau die zijn aangesloten op regen- of afvalwatersystemen, b.v. mangaten uit het riool. De verbrandingscategorie verwijst naar onverbrande CH4 van onvolledige verbranding die kan voorkomen in auto's, huisverwarming en kooksystemen. Door deze attributiebenadering toe te passen op de CH_4-signalen, rapporteerden we de potentiële aardgasleklocaties (met veel vertrouwen) aan de lokale gasbedrijven, wat resulteerde in de reparatie van een groot aantal gaslekken in Utrecht en Hamburg.

In hoofdstuk 3 rapporteren en bespreken we onze resultaten van mobiele onderzoeken in Boekarest, waar we metingen gebruikten van $\delta^{13}C$-CH_4 en δD-CH_4 verzameld in luchtmonsterzakken en online C_2H_6-metingen om CH_4-signalen toe te kennen. Terwijl in Utrecht of Hamburg meer dan 50% tot 90% van de emissies kan worden toegeschreven aan de CH_4-emissies door lekkage van aardgaspijpleidingen (hoofdstuk 2), is de situatie in Boekarest anders en kan ongeveer 60% van de totale emissies worden toegeschreven naar microbiële bronnen, waarschijnlijk uit het riool. We laten zien dat δD-CH_4 een betere onderscheider is dan $\delta^{13}C$-CH_4 bij het scheiden van aardgaslekken van signalen van andere bronnen. Dit werd ook waargenomen in een kleinere isotopische steekproefomvang in Hamburg (hoofdstuk 2).

In hoofdstuk 4 rapporteren we resultaten van een onderlinge vergelijking van drie verschillende gaslekkwantificeringsmethoden in Hamburg, Duitsland. Onze rapporten over CH_4-emissies van aardgasdistributienetwerken in hoofdstuk 2 lieten soms zeer hoge emissiewaarden zien. Deze zijn groter dan wat normaal wordt gevonden bij de zuigmethode, die wordt gebruikt om informatie te verstrekken voor de officiële Duitse nationale emissie-inventaris. Daarom hebben we een onderlinge vergelijkingscampagne ontworpen om de discrepantie te begrijpen. Naast de mobiele en afzuigmethoden hebben we de traceermethode toegepast die arbeidsintensiever is maar een lage kwantificeringsonzekerheid heeft voor emissieschattingen met atmosferische metingen. De directe vergelijking tussen methoden is moeilijk vanwege de beperkingen van de verschillende methoden voor verschillende soorten locaties. In dit hoofdstuk bespreken we in detail de sterke punten en beperkingen van elke methode. Een belangrijk resultaat is dat alle drie de methoden hebben aangetoond dat emissies van lekken in de categorieën met een hoog veiligheidsrisico van A1&A2 hogere emissiewaarden hebben dan lekken in de B&C-categorieën met een lager risico. Ook rond de gasleklocaties A1&A2 kwamen we doorgaans grote ondergrondse CH_4-emissies tegen. De afzuigmethode kon op deze locaties in een aantal gevallen niet worden toegepast omdat officiële voorschriften onmiddellijke reparatie vereisten, of omdat het team de meting niet binnen de gestelde tijd kon voltooien. Vanwege dergelijke tijdsdruk en veiligheidsproblemen is het waarschijnlijk dat de afzuigmethode meestal niet wordt toegepast op de A1&A2-locaties, waar de CH_4-emissies over het algemeen hoger zijn dan op de B&C-

locaties. Dit zou kunnen leiden tot een lage bias in de Duitse CH_4-emissie-inventaris voor gaslekken uit stedelijke aardgasdistributienetwerken.

In hoofdstuk 5 geven we algemene conclusies van onze onderzoeksresultaten van de stedelijke meetcampagnes. We bespreken het belang van attributietechnieken om de bijdragen van verschillende CH_4-bronnen aan de totale emissie in stedelijke gebieden te onderscheiden. We presenteren de sterke punten en beperkingen van mobiele detectie- en kwantificeringsmethoden en geven inzicht in hoe deze methoden kunnen worden verbeterd. We tonen ook een vooruitblik op de toepassing van de mobiele methode op de commerciële markt, met als doel de CH_4-emissies in steden te verminderen en ons inzicht in de toestand van de CH_4-emissies in stedelijke gebieden in het kader van CH_4-mitigatiebeleid te versnellen.

Zusammenfassung

Globale Maßnahmen sind erforderlich, um die Treibhausgasemissionen (THG) zu reduzieren und damit die globale Erwärmung abzuschwächen. Am 4. November 2016 trat das Pariser Abkommen (UNFCCC, 2015) zwischen 196 Staaten in Kraft, das zum Ziel hat, die globale Erwärmung auf weniger als 2 °C zu begrenzen. Methan (CH_4) hat eine relativ kurze atmosphärische Lebensdauer (ca. 10 Jahre), was es zu einem wirksamen Reduzierungsmittel macht, um die globale Erwärmung kurz- bis mittelfristig zu verlangsamen (Rogelj et al., 2019). Die CH_4-Reduzierung kann schneller umgesetzt werden und hat weniger schwerwiegende wirtschaftliche Auswirkungen als die Reduzierung von Kohlendioxid (CO_2)-Emissionen, da die CO_2-Emission direkt proportional zum Energieverbrauch ist. Trotz der Attraktivität der CH_4-Reduktion müssen längerfristig auch die CO_2-Emissionen um die Mitte dieses Jahrhunderts auf Null reduziert werden, um die Ziele des Pariser Abkommens zu erreichen. Unter allen CH_4-Quellen scheint die Emissionsminderung im Energiesektor im Vergleich zur Emissionsminderung aus anderen Sektoren am zeiteffizientesten und kostengünstigsten zu sein (UNEP und CCAC, 2021; Dlugokencky et al., 2011).

CH_4-Emissionen aus dem Energiesektor, insbesondere aus Produktion, Lagerung, Transport, Verteilung und Endverbrauch von fossilen Brennstoffen (Öl, Gas und Kohle), tragen mit 19% zu den gesamten anthropogenen CH_4-Emissionen in Europa bei. Dieser Beitrag kann in Ländern, die fossile Brennstoffe produzieren, auf über 60 % steigen (UNFCCC, 2017). Emissionen aus fossilen Brennstoffen wurden als interessante Möglichkeit innerhalb der CH_4-Reduktionsstrategie der EU identifiziert (EC, 2020).

Die Emissionen aus diesen Aktivitäten werden hauptsächlich anhand von Emissionsfaktoren (EFs) und Aktivitätsdaten (AD) in Inventaren geschätzt. Die EFs sind das Verhältnis der Emissionsrate pro Aktivitätseinheit, z.B. kg emittiertes CH_4 pro erzeugter Gasmenge. Die EFs sind in Berichten nationaler oder internationaler Behörden tabelliert, und Standard-EFs für die Emissionsberichterstattung wurden vom Zwischenstaatlichen Ausschuss für Klimaänderungen (IPCC) tabelliert. Die EFs können jedoch zeitlich und räumlich variieren, was die Unsicherheit bei den geschätzten Emissionen erhöht. Um die Unsicherheit zu verringern, sind unabhängige Messkampagnen erforderlich, um diese EFs zu aktualisieren oder zu verifizieren, von welchen einige veraltet sind oder möglicherweise durch Stichproben- und / oder Emissionsratenverzerrungen beeinflusst werden.

Detaillierte Informationen darüber, wo und wie hoch die Emissionen sind, sind für wirksame Klimaschutzmaßnahmen erforderlich. Diese Doktorarbeit wurde im Rahmen des MEMO^2-Projekts (MEthane goes MObile, MEasurements and MOdelling) mit dem Ziel durchgeführt, mobile Messtechniken einzusetzen, um unser Verständnis von CH_4-Emissionen zu verbessern. Das Hauptaugenmerk lag dabei auf den Emissionen im Energiesektor. Diese Arbeit liefert detaillierte Ergebnisse aus der Erfassung, Quantifizierung und Zuordnung von CH_4-Emissionen aus umfangreichen Messkampagnen, die sich auf Emissionen aus den Gasverteilungsnetzen in Städten konzentrieren. Diese Messungen zeigten, dass der Beitrag von CH_4-Emissionen aus Erdgaslecks, mikrobiellen oder Verbrennungsquellen von Stadt zu Stadt unterschiedlich ist, weshalb für verschiedene Städte spezielle Emissionsminderungsstrategien erforderlich sind.

In Kapitel 2 liefern wir Ergebnisse von mobilen Messungen auf Straßenebene in zwei verschiedenen europäischen Städten; Hamburg (DE) und Utrecht (NL). Wir demonstrieren den Nutzen der Erkennung und Zuordnung von Erdgaslecks mit mobilen Messungen. Ein wichtiger Aspekt dabei ist, dass der Einsatz von Fahrzeugplattformen den Prozess der Gaslecksuche erheblich beschleunigen kann, was im Prinzip häufigere Wartungen ermöglicht, was zur Reduzierung von Emissionen beitragen wird. Die Methode kann auch zur Quantifizierung von Emissionsraten verwendet werden, allerdings zeigen wir auch, dass Schätzungen aus einzelnen Transekten eine große Unsicherheit aufweisen. Andererseits kann eine Momentaufnahme der Emissionen in einer ganzen Stadt in Tagen bis Wochen abgeleitet werden. Die aggregierten Emissionsraten auf Stadtebene sind zuverlässiger als Schätzungen an einzelnen Standorten. Darüber hinaus können sehr große Emittenten leicht erkannt und somit auch gemeldet und anschließend beseitigt werden. Wir quantifizierten die CH_4-Gesamtemissionen von

Hamburg und Utrecht mit jeweils 440±70 t yr^{-1} und 150±50 t yr^{-1}, wovon 50–80% bzw. 70–90% den CH_4-Emissionen aus den städtischen Gasverteilungsnetzen in diesen beiden Städten zugeschrieben werden kann. Unsere Messung zeigt, dass die Emissionsratenverteilung eine schiefe Verteilung ist, bei der nur wenige Leckstellen für die Hälfte der Emissionen im städtischen Maßstab verantwortlich sein können. Dies eröffnet attraktive Reduzierungsmöglichkeiten für CH_4-Emissionen aus Gasverteilungsnetzen.

CH_4-Signale von mobilen Messungen in städtischen Gebieten neigen dazu, als Fehlalarm für ein Erdgasleck gemeldet zu werden, wenn den CH_4-Signalen keine robusten Einschränkungen zugeordnet werden. Die Verwendung von co-emittierten Spezies von CH_4, z.B. Ethan (C_2H_6), CO_2 und/oder die stabilen Isotopensignaturen von Kohlenstoff und Wasserstoff von CH_4 ($\delta^{13}C$-CH_4 bzw. δD-CH_4) können einzeln oder zusammen in der CH_4-Emissionszuordnung verwendet werden. In Kapitel 2 haben wir neue Randbedingungen eingeführt die zeigen, welchen Wert die gleichzeitige Verwendung von C_2H_6- und CO_2-Signalen hat, um CH_4-Signale aus mobilen Messungen zuzuordnen. Diese Randbedingungen verbessern nicht nur unser Verständnis über den Beitrag verschiedener Quellen zu den gesamten CH_4-Emissionen in einem städtischen Gebiet, sondern können indirekt auch zur Aufrechterhaltung der Sicherheit des Gasverteilungssystems beitragen. Wir haben das C_2H_6:CH_4 (C_2:C_1)-Verhältnis aus den Messungen und Korrelationen von CO_2 mit beobachteten CH_4-Signalen zusammen mit Vorkenntnissen über das C_2:C_1-Verhältnis in Erdgaspipelines verwendet und einen systematischen Ansatz eingeführt, um CH_4-Emissionen fossilen Brennstoffen zuzuordnen, sowohl für mikrobielle als auch für Verbrennungsquellen. In Städten sind fossile Emissionen im Allgemeinen auf CH_4-Emissionen aus Lecks im Erdgasverteilungssystem zurückzuführen. Mikrobielle Emissionen weisen meist darauf hin, dass das biogene, nicht fossile CH_4 aus offenen Straßenabflüssen freigesetzt wird, die an Regen- oder Abwassersysteme angeschlossen sind, z.B. Schächte aus der Kanalisation. Die Verbrennungskategorie bezieht sich auf unverbranntes CH_4 aus unvollständiger Verbrennung, die in Autos, Hausheizungen und Kochsystemen auftreten kann. Durch die Anwendung dieses Zuordnungsansatzes auf die CH_4-Signale haben wir die potenziellen Standorte von Erdgaslecks (mit hoher Zuverlässigkeit) an die örtlichen Gasversorgungsunternehmen gemeldet, was zur Beseitigung einer großen Anzahl von Gaslecks in Utrecht und Hamburg führte.

In Kapitel 3 berichten und diskutieren wir unsere Ergebnisse aus mobilen Messungen in Bukarest, bei denen wir Messungen von $\delta^{13}C$-CH_4 und δD-CH_4, die in Luftprobenbeuteln gesammelt wurden, und Online-C_2H_6-Messungen verwendet haben, um CH_4-Signale zuzuordnen. Während in Utrecht oder Hamburg mehr als 50% und bis zu 90% der Emissionen auf die CH_4-Emissionen aus Lecks von Erdgasleitungen zurückzuführen sind (Kapitel 2), ist die Situation in Bukarest anders; dort können etwa 60% der Gesamtemissionen auf mikrobielle Quellen zurückgeführt werden, wahrscheinlich aus dem Abwassersystem. Wir zeigen, dass δD-CH_4 ein besserer Proxy als $\delta^{13}C$-CH_4 ist, um Erdgaslecks von Signalen anderer Quellen zu trennen. Dies wurde auch bei einer kleineren Isotopenprobe in Hamburg beobachtet (Kapitel 2).

In Kapitel 4 berichten wir über Ergebnisse eines Vergleichs von drei verschiedenen Gasleck-Quantifizierungsmethoden in Hamburg, Deutschland. Unsere Berichte über CH_4-Emissionen aus Erdgasverteilungsnetzen in Kapitel 2 zeigten teilweise sehr hohe Emissionsraten. Diese sind größer als bei der Ansaugmethode, die als Informationsquelle für das amtliche, deutsche, nationale Emissionsinventar verwendet wird. Daher haben wir eine Vergleichskampagne entwickelt, um die Diskrepanz zu verstehen. Zusätzlich zu den mobilen und Ansaugmethoden haben wir die Tracer-Methode eingesetzt, die arbeitsintensiver ist, aber eine geringe Quantifizierungsunsicherheit für Emissionsschätzungen mit atmosphärischen Messungen aufweist. Der direkte Vergleich zwischen den Methoden ist aufgrund der Einschränkungen der verschiedenen Methoden für verschiedene Arten von Standorten schwierig, und wir diskutieren ausführlich die Stärken und Schwächen jeder Methode. Ein wichtiges Ergebnis ist, dass alle drei Methoden zeigten, dass Emissionen aus Lecks in den hohen Sicherheitsrisikokategorien A1 & A2 höhere Emissionsraten aufweisen als Lecks in den niedrigeren Risikokategorien B & C. Wir stießen im Allgemeinen auch auf große unterirdische CH_4-Emissionen

rund um A1 und A2 Gasleckagen. Das Absaugverfahren konnte an solchen Standorten in mehreren Fällen nicht angewendet werden, weil behördliche Vorschriften eine sofortige Reparatur erforderten oder das Team die Messung nicht innerhalb der vorgegebenen Zeit abschließen konnte. Aufgrund dieser zeitlichen Einschränkungen und Sicherheitsbedenken wird das Absaugverfahren in der Regel nicht an A1 und A2 Standorten eingesetzt, wo die CH_4-Emissionen im Allgemeinen höher sind als an B&C Standorten. Dies könnte zu einer geringen Verzerrung des deutschen CH_4-Emissionsinventars für Gasleckagen aus städtischen Erdgasverteilungsnetzen führen.

In Kapitel 5 stellen wir allgemeine Schlussfolgerungen unserer Forschungsergebnisse aus den städtischen Messkampagnen vor. Wir diskutieren die Bedeutung von Zuordnungstechniken, um die Beiträge verschiedener CH_4-Quellen zur Gesamtemission im Stadtgebiet zu unterscheiden. Wir stellen die Stärken und Grenzen mobiler Detektions- und Quantifizierungsmethoden vor und geben einen Ausblick, wie diese Methoden verbessert werden können. Wir zeigen auch einen Ausblick auf die Anwendung der mobilen Methode auf dem kommerziellen Markt mit dem Ziel, die CH_4-Emissionen in Städten zu reduzieren und unser Verständnis des Zustands der CH_4-Emissionen in städtischen Gebieten im Rahmen der CH_4-Reduzierungspolitik zu beschleunigen.

Resumen

Se requieren acciones globales para reducir las emisiones de Gases de Efecto Invernadero (GEI) y, por tanto, mitigar el calentamiento global. El 4 de noviembre de 2016 entró en vigor el Acuerdo de París (UNFCCC, 2015) para 196 países, que tiene como objetivo limitar el aumento del calentamiento global a menos de 2 °C. El metano (CH_4) tiene una vida atmosférica relativamente corta (≈10 años), lo cual lo convierte en un objetivo de reducción efectivo para frenar el calentamiento global a corto y medio plazo (Rogelj et al., 2019). Las reducciones de CH_4 se pueden implementar más rápido y tienen efectos económicos menos severos que la reducción de emisiones de dióxido de carbono (CO_2), ya que la emisión de CO_2 es directamente proporcional al consumo de energía. A pesar de la posible reducción del CH_4, a mediados de este siglo también será necesario reducir a cero las emisiones de CO_2 para alcanzar los objetivos del Acuerdo de París. De todas las fuentes de CH_4, la reducción de emisiones en sectores energéticos parece ser la más eficiente en comparación con otros sectores, tanto económicamente como en cuanto al tiempo necesario (PNUMA y CCAC, 2021; Dlugokencky et al., 2011).

Las emisiones de CH_4 del sector energético, en particular proveniente de los procesos de producción, almacenamiento, transporte, distribución y el uso final de combustibles fósiles (petróleo, gas y carbón), contribuyen en un 19% a las emisiones totales de CH_4 provenientes de actividades humanas en Europa. Esta contribución puede llegar a aumentar a más del 60% en países productores de combustibles fósiles (UNFCCC, 2017). Las emisiones relacionadas con los combustibles fósiles se han identificado como un objetivo de interés en la estrategia para la reducción del CH_4 de la UE (CE, 2020).

Las emisiones de estas actividades se estiman principalmente utilizando Factores de Emisión (FE) y Datos de Actividad (DA) para la creación de inventarios. Los FE son la tasa de emisión por unidad de actividad, p. ej. los kg de CH_4 emitidos por cantidad de gas producido. Los FE están tabulados en informes de agencias nacionales o internacionales, y el Grupo Intergubernamental de Expertos sobre el Cambio Climático (IPCC) ha tabulado los FE estándar en el informe de emisiones. Sin embargo, los FE pueden variar temporal y espacialmente, lo cual aumenta la incertidumbre en las emisiones estimadas. Para reducir esta incertidumbre y actualizar o verificar los FE, se requieren campañas de medición independientes, ya que algunos FE están desactualizados o posiblemente afectados por sesgos de muestreo o de tasa de emisión.

Para obtener políticas de reducción efectivas es necesaria información detallada sobre dónde y cuan grandes son las emisiones de CH_4. Esta tesis se llevó a cabo dentro del proyecto MEMO^2 (MEthane goes MObile, MEasurements and MOdelling), con el objetivo de utilizar técnicas de medición móvil para mejorar nuestra comprensión de las emisiones de CH_4. Las emisiones en el sector energético fueron el objetivo principal. En esta tesis proporcionamos resultados detallados de la detección, cuantificación y atribución de las emisiones de CH4 en extensas campañas de medición, centradas en las emisiones de redes de distribución de gas en diferentes ciudades. Estas mediciones mostraron que la contribución de las emisiones de CH_4 provenientes de fugas de gas natural y fuentes microbianas o de combustión es diferente en cada ciudad. Por tanto, para diferentes ciudades se requieren regulaciones específicas para la reducción de emisiones.

En el capítulo 2 proporcionamos resultados de mediciones móviles a nivel de superficie en dos ciudades europeas: Hamburgo (DE) y Utrecht (NL). Demostramos el beneficio de detectar y atribuir fugas de gas natural a través de mediciones móviles. Un aspecto clave es que el uso de instrumentos en el coche de medición puede acelerar considerablemente el proceso de detección de fugas de gas, permitiendo, en principio, un mantenimiento más frecuente, lo cual ayudará a reducir emisiones. El método también se puede utilizar para cuantificar tasas de emisión, aunque las estimaciones de tramos individuales son menos fiables. Sin embargo, es posible obtener mediciones de las emisiones de toda una ciudad en días o semanas. Las tasas de emisiones totales a escala de ciudad serán más fidedignas que las estimaciones por ubicación individual. Además, de esta manera los grandes emisores se pueden detectar fácilmente y, por lo tanto, también pueden ser denunciados y posteriormente mitigados.

Cuantificamos la emisión total de CH_4 de 440±70 t yr^{-1} y 150±50 t yr^{-1} en Hamburgo y Utrecht, de los cuales 50%–80% y 70%–90% respectivamente se atribuyeron a emisiones de CH4 de redes de distribución de gas natural urbanas en estas dos ciudades. Nuestras mediciones muestran que la distribución de la tasa de emisión es sesgada: algunas ubicaciones de fugas pueden llegar a representar la mitad de las emisiones a escala de ciudad. Esto crea oportunidades interesantes para la reducción de emisiones de CH_4 en las redes de distribución de gas.

Las señales de CH_4 de mediciones móviles en áreas urbanas son propensas a ser reportadas como falsas alarmas de fugas de gas natural si estas no se atribuyen correctamente en un rango con restricciones sólidas. Las especies emitidas simultáneamente con CH_4, p. ej. etano (C_2H_6), CO_2 y/o las firmas de isótopos estables de carbono e hidrógeno en CH_4 ($\delta^{13}C$-CH_4 y δD-CH_4 respectivamente), se pueden usar individualmente o conjuntamente en la atribución de emisiones de CH_4. En el capítulo 2 presentamos nuevas restricciones y mostramos el valor del uso simultáneo de señales de C_2H_6 y CO_2 para atribuir señales de CH_4 en mediciones móviles. Estas restricciones no solo mejoran nuestra comprensión de la contribución de diferentes fuentes a las emisiones totales de CH_4 en un área urbana, sino que también pueden contribuir indirectamente a mantener la seguridad del sistema de distribución de gas. Usamos la relación cuantitativa del C_2H_6:CH_4 (C_2:C_1) de las mediciones y correlaciones con CO_2 con las señales de CH_4 observadas, junto con el conocimiento previo sobre la relación C_2:C_1 en tuberías de gas natural, e introdujimos un enfoque sistemático para atribuir las emisiones de CH_4 a fuentes microbianas, de combustión y de combustibles fósiles. En ciudades, las emisiones de combustibles fósiles generalmente se deben a emisiones de CH_4 por fugas en el sistema de distribución de gas natural. Las emisiones microbianas apuntan principalmente a que el CH_4 biogénico no fósil se libera de salidas abiertas a nivel de calle conectadas a sistemas de recolección de lluvias o aguas residuales, p. ej. bocas de acceso al sistema de alcantarillado. Las emisiones de combustión son el CH_4 que no ha sido quemado en combustiones incompletas. Esto puede ocurrir en automóviles y sistemas de calefacción y de cocina. Al aplicar este enfoque de atribución a las señales de CH_4, informamos a servicios de gas locales sobre posibles ubicaciones de fugas de gas natural (con un alto nivel de certeza), lo cual resultó en la reparación de una gran cantidad de fugas de gas en Utrecht y Hamburgo.

En el capítulo 3 informamos y discutimos nuestros resultados de mediciones móviles en Bucarest, donde usamos mediciones de $\delta^{13}C$-CH_4 y δD-CH_4 recolectadas en bolsas de muestreo de aire y mediciones online de C_2H_6 para atribuir señales de CH_4. Si bien en Utrecht o Hamburgo más del 50% y hasta el 90% de las emisiones pueden atribuirse a fugas de tuberías de gas natural (capítulo 2), la situación en Bucarest es diferente: alrededor del 60% de las emisiones totales pudieron atribuirse a fuentes microbianas, probablemente provenientes del sistema de alcantarillado. Mostramos que para separar fugas de gas natural de señales de otras fuentes, δD-CH_4 es más útil para la atribución de las señales de CH_4 que $\delta^{13}C$-CH_4. Esto también se observó en una muestra isotópica más pequeña en Hamburgo (capítulo 2).

En el capítulo 4 presentamos los resultados de la comparación de tres métodos diferentes de cuantificación de fugas de gas en Hamburgo, Alemania. Nuestros informes de emisiones de CH_4 de las redes de distribución de gas natural (tratados en el capítulo 2) a veces mostraban tasas de emisión muy altas. Estas eran más altas que las que resultan normalmente con el método de succión, que se utiliza para proporcionar información al inventario nacional de emisiones de Alemania. Para entender esta discrepancia, diseñamos una campaña de comparación. Además del método móvil y de succión, implementamos también el método del gas trazador. Este método requiere más trabajo, pero, utilizando mediciones atmosféricas, tiene un grado de incertidumbre de cuantificación bajo para la estimación de emisiones. La comparación directa entre métodos es difícil debido a las limitaciones de los diferentes métodos en distintos tipos de ubicaciones, pero discutimos en detalle las fortalezas y limitaciones de cada método. Un resultado clave es que los tres métodos mostraron que las emisiones de fugas en categorías de alto riesgo de seguridad de A1 y A2 tienen tasas de emisión más altas que las fugas en las categorías B y C, de menor riesgo. En general, también encontramos grandes emisiones de CH_4 en el subsuelo alrededor de las ubicaciones de fugas de gas A1 y A2. En varios casos, el método de succión

no se pudo aplicar en estos lugares porque las normas oficiales requerían una reparación inmediata o porque el equipo no pudo completar la medición dentro del tiempo asignado. Debido a tales limitaciones de tiempo y problemas de seguridad, es probable que el método de succión generalmente no se implemente en las ubicaciones A1 y A2, donde las emisiones de CH_4 son generalmente más altas que en las ubicaciones B y C. Esto podría llevar a un reporte de emisiones más bajas de lo real en el inventario alemán de emisiones de CH_4 proveniente de fugas de gas en redes de distribución de gas natural urbanas.

En el capítulo 5 proporcionamos conclusiones generales de los resultados de nuestra investigación en campañas de medición urbana. También discutimos la importancia de las técnicas de atribución para distinguir las contribuciones de diferentes fuentes de CH_4 a la emisión total en el área urbana. Presentamos las fortalezas y limitaciones de los métodos de cuantificación y detección móvil y proporcionamos pronósticos sobre cómo mejorar estos métodos. También mostramos un pronóstico sobre la aplicación del método móvil en el mercado comercial, con los objetivos de reducir emisiones de CH_4 en ciudades y acelerar nuestra comprensión del estado de emisiones de CH_4 en áreas urbanas para contribuir a políticas de reducción de CH_4.

Résumé

Des mesures à échelle mondiale sont nécessaires pour réduire les émissions de gaz à effet de serre (GES) et ainsi atténuer le réchauffement climatique. Le 4 novembre 2016 est entré en vigueur l'Accord de Paris (UNFCCC, 2015) entre 196 pays qui vise à limiter le réchauffement climatique à moins de 2°C. Le méthane (CH_4) a une durée de vie atmosphérique relativement courte (≈10 ans), ce qui en fait une cible d'atténuation efficace pour ralentir le réchauffement climatique à court et moyen terme (Rogelj et al., 2019). Les mesures d'atténuation du CH_4 peuvent être mises en œuvre plus rapidement et avoir des effets économiques moins graves que la réduction des émissions de dioxyde de carbone (CO_2) car les émissions de CO_2 sont directement proportionnelles à la consommation d'énergie. Malgré l'attrait de la réduction du CH_4, à plus long terme, les émissions de CO_2 devront également être réduites à zéro vers le milieu de ce siècle pour atteindre les objectifs de l'Accord de Paris. Parmi toutes les sources de CH_4, l'atténuation des émissions dans les secteurs de l'énergie semble être la plus efficace en termes de temps et de coût par rapport à la réduction des émissions des autres secteurs (UNEP and CCAC, 2021; Dlugokencky et al., 2011).

Les émissions de CH_4 du secteur de l'énergie, en particulier de la production, du stockage, du transport, de la distribution et de l'utilisation finale des combustibles fossiles (pétrole, gaz et charbon), contribuent à hauteur de 19 % aux émissions anthropiques totales de CH_4 en Europe. Cette contribution peut monter à plus de 60 % dans les pays producteurs d'énergies fossiles (UNFCCC, 2017). Les émissions liées aux combustibles fossiles ont été identifiées comme une cible intéressante dans le cadre de la stratégie de réduction du CH_4 de l'UE (EC, 2020).

Les émissions de ces activités sont principalement estimées à l'aide des facteurs d'émission (FE) et des données d'activité (DA) dans les inventaires. Les FE sont le rapport du taux d'émission par unité d'activité, par ex. kg de CH_4 émis par quantité de gaz produite. Les FE sont tabulés dans des rapports d'organismes nationaux ou internationaux, et les FE standard pour les rapports sur les émissions ont été tabulés par le Groupe d'experts intergouvernemental sur l'évolution du climat (GIEC). Cependant, les FE peuvent varier dans le temps et dans l'espace, ce qui augmente l'incertitude des émissions estimées. Pour réduire l'incertitude, des campagnes de mesures indépendantes sont nécessaires pour mettre à jour ou vérifier ces FE, dont certains sont obsolètes ou sont éventuellement affectés par des biais d'échantillonnage et/ou de taux d'émission.

Des informations détaillées sur le lieu et l'ampleur des émissions sont nécessaires pour des politiques d'atténuation efficaces. Cette thèse a été réalisée dans le cadre du projet MEMO^2 (MEthane goes MObile, MEsuresements and MOdelling), avec l'objectif d'utiliser des techniques de mesures mobiles pour améliorer notre compréhension des émissions de CH_4. L'accent a été mis sur les émissions dans le secteur de l'énergie. Dans cette thèse, des résultats détaillés de la détection, de la quantification et de l'attribution des émissions de CH_4 sont fournis à partir de vastes campagnes de mesure portant sur les émissions des réseaux de distribution de gaz dans les villes.

Dans le chapitre 2, les résultats de mesures mobiles au niveau de la rue dans deux villes européennes différentes ; Hambourg (DE), Utrecht (NL) sont indiqués. L'avantage de détecter et d'attribuer les fuites de gaz naturel avec des mesures mobiles est démontré. Un aspect clé est que l'utilisation de plates-formes de véhicules peut considérablement accélérer le processus de détection des fuites de gaz, permettant en principe un entretien plus fréquent, ce qui contribuera à réduire les émissions. La méthode peut également être utilisée pour quantifier les taux d'émission, mais il est montré que les estimations des transects individuels sont d'une grande incertitude. D'autre part, un instantané des émissions dans une ville entière peut être obtenu en quelques jours ou semaines. Les taux d'émission agrégés à l'échelle de la ville seront plus fiables que les estimations à des emplacements individuels. De plus, les grands émetteurs peuvent être facilement détectés, et donc également signalés et ensuite atténués. Nous avons quantifié les émissions totales de CH_4 de 440±70 t an^{-1} et 150±50 t an^{-1} à Hambourg et Utrecht, dont 50 % à 80 % et 70 % à 90 %, respectivement, ont été attribués aux émissions de CH_4 provenant du réseau urbain naturel de distribution de gaz dans ces deux villes.

Les signaux CH_4 provenant de mesures mobiles dans les zones urbaines sont susceptibles d'être indiqués comme une fausse alarme pour une fuite de gaz naturel si les signaux CH_4 ne sont pas correctement attribués avec des contraintes robustes. L'utilisation d'espèces co-émises avec le CH_4, par ex. l'éthane (C_2H_6), le CO_2 et/ou les signatures isotopiques stables du carbone et de l'hydrogène dans le CH_4 ($\delta^{13}C$-CH_4 and δD-CH_4 respectivement) peuvent être utilisés individuellement ou ensemble dans l'attribution des émissions de CH_4. Dans le chapitre 2, des nouvelles contraintes sont introduites et l'intérêt de l'utilisation simultanée des signaux C_2H_6 et CO_2 pour attribuer les signaux CH_4 issus des mesures mobiles est démontré. Ces contraintes améliorent non seulement notre compréhension de la contribution des différentes sources aux émissions totales de CH_4 dans une zone urbaine, mais peuvent également contribuer indirectement au maintien de la sécurité du système de distribution de gaz. Le rapport C_2H_6:CH_4 (C_2:C_1) a été utilisé à partir des mesures et des corrélations du CO_2 avec les signaux de CH_4 observés, ainsi que des connaissances antérieures sur le rapport C_2:C_1 dans les gazoducs, et nous avons introduit une approche systématique pour attribuer les émissions de CH_4 aux sources fossiles, microbiennes et de combustion. Dans les villes, les émissions fossiles sont généralement dues aux émissions de CH_4 provenant de fuites dans le système de distribution de gaz naturel. Les émissions microbiennes indiquent principalement que le CH_4 biogénique non-fossile est rejeté par des points de vente ouverts au niveau de la rue connectés aux systèmes de pluie ou d'eaux usées, par ex. les couvercles de regard du système d'égouts. La catégorie de combustion fait référence au CH_4 non brûlé provenant d'une combustion incomplète qui peut se produire dans les voitures, le chauffage domestique et les systèmes de cuisson. En appliquant cette approche d'attribution aux signaux CH_4, les emplacements potentiels des fuites de gaz naturel sont signalés (avec une grande conviction) aux services publics de gaz locaux, ce qui a entraîné la réparation d'un grand nombre de fuites de gaz à Utrecht et Hambourg.

Dans le chapitre 3, les résultats d'enquêtes mobiles à Bucarest sont examinés. Dans cette ville nous avons utilisé des mesures de $\delta^{13}C$-CH_4 et δD-CH_4 collectées dans des sacs d'échantillons d'air, et des mesures de C_2H_6 en ligne pour attribuer des signaux CH_4. Alors qu'à Utrecht ou à Hambourg plus de 50 % et jusqu'à 90 % des émissions peuvent être attribuées aux émissions de CH_4 provenant des fuites des gazoducs (chapitre 2), la situation à Bucarest est différente et environ 60 % des émissions totales pourraient être attribuées à des sources microbiennes, probablement du réseau d'égouts. Il est montré que δD-CH_4 est un meilleur attribut que $\delta^{13}C$-CH4 pour séparer les fuites de gaz naturel des signaux d'autres sources. Cela a également été observé dans un échantillon isotopique plus petit à Hambourg (chapitre 2).

Dans le chapitre 4, les résultats d'une comparaison de trois méthodes différentes de quantification des fuites de gaz à Hambourg, en Allemagne sont présentés. Nos rapports sur les émissions de CH_4 des réseaux de distribution de gaz naturel au chapitre 2 ont parfois montré des taux d'émission très élevés. Celles-ci sont plus grandes que ce que l'on trouve normalement avec la méthode d'aspiration, qui est utilisée pour fournir des informations pour l'inventaire national des émissions officiel allemand. Par conséquent, nous avons conçu une campagne d'intercomparaison pour comprendre la disparité. En plus des méthodes mobiles et d'aspiration, il a été déployé la méthode du traceur qui demande plus de main-d'œuvre mais présente une faible incertitude de quantification pour les estimations d'émissions à l'aide de mesures atmosphériques. La comparaison directe entre les méthodes est difficile en raison des limites des différentes méthodes pour différents types d'emplacements, et nous étudions en détail des forces et des limites de chaque méthode. Un résultat décisif est que les trois méthodes ont montré que les émissions provenant de fuites dans les catégories à haut risque pour la sécurité A1 et A2 ont des taux d'émission plus élevés que les fuites dans les catégories à faible risque B et C. De même, nous avons généralement rencontré d'importantes émissions souterraines de CH_4 autour des emplacements des fuites de gaz A1 et A2. Dans plusieurs cas la méthode d'aspiration ne pouvait pas être appliquée à ces endroits car les réglementations officielles exigeaient une réparation immédiate ou l'équipe n'a pas pu terminer la mesure dans le délai imparti. En raison de ces contraintes de temps et de problèmes de sécurité, il est probable que la méthode d'aspiration ne soit généralement pas déployée sur les sites A1 et A2, où les émissions de CH_4 sont généralement plus

élevées que sur les sites B et C. Cela pourrait induire un faible biais des émissions de CH_4 dans l'inventaire allemand des fuites de gaz des réseaux urbains de distribution de gaz naturel.

Dans le chapitre 5, les conclusions générales de nos résultats de recherche issus des campagnes de mesures urbaines sont présentées. Nous examinons l'importance des techniques d'attribution pour distinguer les contributions des différentes sources de CH_4 aux émissions totales dans la zone urbaine. Les forces et les limites des méthodes de détection et de quantification mobiles sont présentés et nous exposons des perspectives sur la façon d'améliorer ces méthodes. De même, un aperçu de l'application de la méthode mobile sur le marché commercial est montré, dans le but de réduire les émissions de CH_4 dans les villes et d'accélérer notre compréhension de l'état des émissions de CH_4 dans les zones urbaines dans le cadre des politiques d'atténuation du CH_4.

Sammendrag

Det kreves globale handlinger for å redusere utslippene av drivhusgasser (GHG), og dermed begrense global oppvarming. Den 4. november 2016 trådte Paris-avtalen (UNFCCC, 2015) mellom 196 land i kraft som tar sikte på å begrense global oppvarming til under 2 °C. Metangass (CH_4) har en relativt kort atmosfærisk levetid (≈10 år) som gjør det til et effektivt avbøtende mål for å bremse global oppvarming på kort til mellomlang sikt (Rogelj et al., 2019). CH_4-reduksjonene kan implementeres raskere og ha færre negative økonomiske konsekvenser enn reduksjon av karbondioksid (CO_2)-utslipp fordi CO_2-utslipp er direkte proporsjonalt med energiforbruk. I tillegg til en reduksjon av metanutslipp vil også CO_2-utslipp på lengre sikt måtte reduseres til null rundt midten av dette århundret for å nå målene i Paris-avtalen. En reduksjon i metanutslipp fra energisektorene er det mest tids- og kostnadseffektive sammenlignet med utslippsreduksjoner fra andre sektorer (UNEP og CCAC, 2021; Dlugokencky et al., 2011).

CH_4-utslipp fra energisektoren, spesielt fra produksjon, lagring, transport, distribusjon og forbruk av fossilt brensel (olje, gass og kull) bidrar med 19 % av de totale menneskeskapte CH_4-utslippene i Europa. Dette bidraget kan øke til mer enn 60% i land som produserer fossilt brensel (UNFCCC, 2017). Fossilt brenselrelatert utslipp har blitt identifisert som et mål innenfor metanreduksjonsstrategien til EU (EC, 2020).

Utslippene fra disse aktivitetene er i hovedsak estimert ved bruk av utslippsfaktorer (UF) og aktivitetsdata (AD) i inventar. EF er forholdet mellom utslippsraten per aktivitetsenhet, f.eks. kg CH_4 utslipp per mengde produsert gass. EF er tabellert i rapporter fra nasjonale eller internasjonale institutter, og standard EF for utslippsrapportering er tabellert av Intergovernmental Panel on Climate Change (IPCC). Imidlertid kan EF variere over tid og areal, noe som øker usikkerheten i de estimerte utslippene. For å redusere usikkerheten kreves det uavhengige måleinger for å oppdatere eller verifisere EF, hvorav noen er utdaterte eller muligens påvirket av prøvetakings- og/eller utslippshastigheter.

Detaljert informasjon om plassering og størrelse på utslippene er nødvendig for effektive avbøtningspolitikker. Denne avhandlingen tilhørte MEMO^2-prosjektet (MEthane goes MObile, MEasurements and MOdelling), med mål om å bruke mobil måleteknikker for å forbedre vår forståelse av CH_4-utslipp. Hovedfokuset var på utslipp i energisektoren. I denne avhandlingen gir vi detaljerte resultater fra deteksjonen, kvantifiseringen og attribueringen av CH_4-utslipp i omfattende målekampanjer med fokus på utslipp fra gassdistribusjonsnettverk i byer. Disse målingene viste at bidraget fra CH_4-utslipp fra naturgasslekkasjer, mikrobiologi og forbrenning er forskjellig fra by til by, og derfor kreves det forskjellig utslippsreduksjonspolitikk for forskjellige byer.

I kapittel 2 presenteres resultater fra mobil målinger på gatenivå i to europeiske byer; Hamburg (DE) og Utrecht (NL). Vi demonstrerer fordelene ved å oppdage naturgasslekkasjer med mobil målinger. Et sentralt tema er at bruk av bil kan øke gasslekkasjedeteksjonen betraktelig, noe som øker vedlikeholdet av gassledninger og derfor vil bidra til å redusere utslippene. Metoden kan også brukes til å kvantifisere utslippshastighetet, men vi viser at estimater fra enkeltmålinger har stor usikkerhet. På en annen side kan et estimat av utslipp i en hel by utledes på dager til uker. De samlede utslippene i byskala vil være mer pålitelige enn estimater på enkeltsteder. I tillegg kan svært store utslipsskilder lett oppdages, og dermed også rapporteres og deretter reduseres. Vi målte totale metanutslipp på 440 ±70 tonn år^{-1} i Hamburg og 150±50 tonn år^{-1} i Utrecht, hvorav henholdsvis 50%–80% og 70%–90% var metanutslipp fra urbane distribusjonsnettverk av naturgass. Våre målinger viser at utslippsfordelingen er en skjev fordi bare noen få lekkasjesteder kan står for halvparten av utslippene i byskala. Dette åpner for gode reduksjonsmuligheter for metanutslipp fra gassdistribusjonsnettverk.

Mobil metanmålinger i urbane områder har en tendens til å bli rapportert som falsk alarm for naturgasslekkasjer hvis metanmålingene ikke er riktig attribuert med robuste begrensninger. Gasser som slippes ut samtidig som metan, slik som etan (C_2H_6), CO_2 og/eller de stabile isotopene til karbon og hydrogen i CH_4 (henholdsvis $\delta^{13}C$-CH_4 og δD-CH_4) kan brukes individuelt eller sammen for å bestemme kilden til metanutslippet. I kapittel 2 introduserte vi nye begrensende faktorer og demonstrerte viktigheten ved bruk av både C_2H_6- og CO_2-målinger for å bestemme kilden til

metanutslippet i utførelsen av mobilmålinger. Disse grenseverdiene øker ikke bare vår forståelse av ulike kilders bidrag til det samlede metanutslippet i et byområde, men kan også indirekte bidra til å opprettholde sikkerheten til gassdistribusjonssystemet. Vi brukte forholdet mellom C_2H_6:CH_4 (C_2:C_1) fra målinger, og korrelasjoner mellom CO_2 og observerte CH_4-målinger, sammen med kjennskap om C_2:C_1-ratioen i naturgassrørledninger, og introduserte en systematisk tilnærming for å attribuere CH_4-utslipp til fossile, mikrobielle og forbrennings-kilder. I byer skyldes utslipp av fossilt metan generelt CH_4-utslipp fra lekkasjer i naturgassdistribusjonssystemet. Mikrobielt produsert metan blir stort sett sluppet ut fra åpne avløpssystemer, som f.eks. kummer fra kloakksystemet.
Forbrenningskategorien refererer til uforbrent CH_4 fra ufullstendig forbrenning som kan skje i biler, under oppvarming av hus og matlaging med gass. Ved å bruke denne attribusjonstilnærmingen på CH_4-målingene rapporterte vi de potensielle naturgasslekkasjestedene (med høy sikkerhet) til de lokale gassselskapene, noe som resulterte i reparasjon av et stort antall gasslekkasjer i Utrecht og Hamburg.

I kapittel 3 rapporterer og diskuterer vi resultatene våre fra mobil undersøkelser i Bucuresti hvor vi brukte målinger av δ^{13}C-CH_4 og δD-CH_4 samlet inn i luftprøveposer, og online C_2H_6-målinger for å tilskrive CH_4-signaler. I Utrecht eller Hamburg kan mer enn 50%, og opptil 90% av metanutslippene attribueres til lekkasjer fra naturgassrørledninger (kapittel 2), men situasjonen i Bucharest er annerledes, og rundt 60 % av de totale utslippene kan komme fra mikrobielle kilder, sannsynligvis fra kloakksystemet. Vi viser at δD-CH_4 er mer kildespesifik enn δ^{13}C-CH_4 når det gjelder å skille naturgasslekkasjer fra andre kilder til metan. Dette ble også observert i en mindre studie om metanisotoper i Hamburg (kapittel 2).

I kapittel 4 rapporterer vi resultater fra en sammenlikning av tre forskjellige gasslekkasjekvantifiseringsmetoder i Hamburg i Tyskland. Våre rapporter om metanutslipp fra distribusjonsnettverk for naturgass i kapittel 2 viste noen ganger svært høye utslippsrater. Utslippene var større enn det man vanligvis finner med pumpemetoden som brukes for å gi informasjon til den tyske nasjonale utslippsdatabasen. Derfor utviklet vi en sammenlikningskampanje for å forstå avviket. I tillegg til mobil- og pumpemetoden har vi implementert sporingsmetoden som er mer arbeidskrevende, men har lav usikkerhet knyttet til utslippsestimater ved bruk av atmosfæriske målinger. Den direkte sammenligningen mellom metoder er vanskelig på grunn av ulempene ved de ulike metodene for ulike typer lokasjoner, og vi diskuterer i detalj fordeler og ulemper ved hver metode. Et sentralt resultat er at alle tre metodene viste at utslipp fra lekkasjer med høy risikokategori A1&A2 har høyere utslippsrater enn lekkasjer i B&C-kategoriene med lavere risiko. Vi har også generelt sett store metanutslipp under overflaten rundt A1&A2-gasslekkasjestedene. Pumpemetoden kunne i flere tilfeller ikke brukes på disse stedene fordi offisielle forskrifter krevde umiddelbar reparasjon, eller fordi teamet ikke kunne fullføre målingen innen den tildelte tiden. På grunn av slike tidsbegrensninger og sikkerhetsproblemer, er det sannsynlig at pumpemetoden vanligvis ikke brukes på A1&A2-lokasjonene, der CH_4-utslippene generelt er høyere enn på B&C-lokasjonene. Dette kan indusere en skjevhet mot lavere måleverdier til den tyske CH_4-utslippsdatabasen for gasslekkasjer fra urbane naturgassrørledninger.

I kapittel 5 gir vi generelle konklusjoner av resultatene fra de urbane målingskampanjene. Vi diskuterer viktigheten av attribueringsteknikker for å skille mellom ulike CH_4-utslippskilders bidrag til det totale utslippet i byområdet. Vi presenterer fordelene og ulempene til mobil deteksjons- og kvantifiseringsmetoder og gir forslag til hvordan disse metodene kan forbedres. Vi diskuterer også bruken av den mobil metoden i det kommersielle markedet, med mål om å redusere CH_4-utslipp i byer og å bedre forstå tilstanden til CH_4-utslipp i urbane områder. Dette blir også sett på i kontekst av CH_4-reduksjonspolitikk.

آب باران و یا فاضلاب شهری مربوط هستند. انتشارات احتراقی به گاز متان سوخته نشده گفته می‌شود که برای مثال حاصل سوخت ناقص در ماشین، سیستم گرمایش و پخت و پز منازل است. با استفاده از این روش نسبت‌دهی گاز متان به منبع انتشار، با استفاده ازاین روش نسبت‌دهی گاز متان به منبع انتشار، ما نقاط احتمالی نشت گاز متان از خطوط لوله را به شرکت‌های توزیع گزارش دادیم که موجب برطرف سازی بسیاری از نشتی ها در اوترخت و هامبورگ گردید.

در فصل سوم، ما نتایج و مباحث پیرامون اندازه‌گیری‌های صورت گرفته در بخارست جایی که ما با استفاده از اندازه‌گیری‌های $\delta^{13}C\text{-}CH_4$ و $\delta D\text{-}CH_4$ جمع‌آوری شده در نمونه‌های کیسه‌ای، و اندازه‌گیری همزمان C_2H_6 سیگنال‌های CH_4 را به منابع انتشار نسبت‌دهی کردیم. در حالی که در اوترخت و هامبورگ بیش از ۵۰٪ و تا حدود ۹۰٪ کل انتشار می‌تواند به انتشار از خطوط لوله گاز شهری نسبت داده شود، شرایط در بخارست متفاوت و حدود ۶۰٪ انتشار کل متان را می‌توان به منابع میکروبی، احتمالا سیستم فاضلاب شهری، نسبت داد. ما نشان می‌دهیم که برای نسبت‌دهی و جداسازی نقاط انتشار از دیگر منابع انتشار اندازه‌گیری $\delta D\text{-}CH_4$ نتایج بهتری نسبت به $\delta^{13}C\text{-}CH_4$ را حاصل می‌آورد. ما با استفاده از نمونه‌های کمتر نتایج مشابهی را در هامبورگ نیز مشاهده کردیم.

در فصل چهارم ما نتایج مربوط به مقایسه سه روش اندازه‌گیری میزان انتشار از نشتی‌های خطوط لوله را در هامبورگ ارائه می‌نماییم. گزارش‌های ما نشان می‌دهد که انتشار متان از خطوط لوله توزیع گاز شهری که در فصل دوم ارایه گردید، در بعضی نقاط بسیار بالا بوده است. این نتایج با اندازه‌گیری‌های روش ساکشن (suction) که برای گزارش‌دهی میزان انتشار از نقاط نشتی در فهرست انتشارهای رسمی آلمان استفاده می‌شود، بالاتر بوده است. بنابراین، ما یک پروژه اندازه‌گیری برای مطالعه این تفاوت طراحی کردیم. علاوه بر روش سیار و ساکشن، ما از روش نشر گاز ردیاب نیز استفاده کردیم که نیازمند کار بیشتر برای اندازه‌گیری می‌باشد، اما دارای قطعیت بالاتری می‌باشد.مقایسه مستقیم روش‌ها به دلیل محدودیت مربوط به هر روش دشوار می‌باشد، و ما نقاط ضعف و قوت هر کدام از این روش‌ها را بررسی می‌کنیم. یک نتیجه کلیدی از تمامی این روش‌ها نشان‌دهنده این است که میزان انتشار در دسته‌بندی‌های براساس ایمنی در طبقه‌بندی A1 وA2 بیشتر از طبقه‌بندی B و C است. به صورت کلی ما همچنین میزان تجمع بیشتر گاز زیرسطحی ناشی از نشتی خطوط لوله را در طبقه‌بندی A1 وA2 مشاهده نمودیم. امکان گزارش‌دهی از روش ساکشن در نقاط متعددی به دلیل محدودیت‌های ایمنی و یا عدم تکمیل اندازه‌گیری میسر نبود. به دلیل محدودیت‌های ایمنی و زمانی، احتمالا این روش در نقاط A1&A2، جایی که میزان انتشار بیشتر از B&C است، انجام نگردیده است. این می‌تواند سوگیری پایین در گزارش‌دهی میزان انتشار از خطوط لوله در فهرست انتشارات آلمان را موجب شود.

در فصل پنجم ما نتیجه‌گیری های کلی از تحقیقات خود را از اندازه‌گیری‌های شهری ارائه می‌نماییم. ما پیرامون روش‌های نسبت‌دهی و درک میزان سهم هر منبع در انتشارات کلی مناطق شهری بحث میکنیم. ما نقاط قوت و ضعف روش‌های شناسایی و کمی سازی سیار و چشم‌انداز مرتبط برای بهبود این روش را ارائه می‌نماییم. ما همچنین چشم‌انداز مربوط به تجاری‌سازی این روش با هدف کاهش میزان انتشارات در شهرها و سرعت‌بخشیدن به درک ما از انتشارات گاز متان در مناطق شهری در چهارچوب سیاست‌گزاری کاهش انتشار را نشان می‌دهیم.

خلاصه

انتشار گاز های گلخانه‌ای یکی از عوامل گرمایش زمین می‌باشد، به همین علت نیاز به اقدامات بین المللی در راستای کاهش انتشار گاز های گلخانه‌ای وجود دارد. به همین منظور قرارداد پاریس (UNFCCC, 2015) با هدف محدود کردن گرمایش زمین به دو درجه منعقد گردیده و روز چهارم نوامبر سال ۲۰۱۶، به اجرا گذاشته شد. به طور نسبی گاز متان دارای طول عمر کوتاه (≈۱۰ سال) است که این ویژگی باعث میگردد که کاهش انتشار این گاز یک هدف مناسب برای کاهش روند صعودی گرمایش زمین شود (Rogelj et al., 2019). کاهش میزان انتشار گاز متان میتواند به نسبت گاز دی اکسید کربن سریعتر و از لحاظ اقتصادی بهینه تر باشد، زیرا انتشار گاز دی اکسید کربن به صورت مستقیم به میزان مصرف انرژی مربوط می‌باشد. با وجود جذابیت‌های مربوط به کاهش گاز متان، انتشار گاز دی اکسید کربن نیز باید تا نیمه قرن به میزان صفر نزول پیدا کند تا به اهداف قرارداد پاریس نیل پیدا کنیم. به نظر میرسد، در میان تمامی منابع انتشار گاز متان، کاهش انتشار این گاز در بخش انرژی علاوه بر پربازده بودن از لحاظ زمانی، مقرون به صرفه تر می‌باشد.

انتشار گاز متان از بخش انرژی، به ویژه در مراحل تولید، ذخیره سازی، انتقال، توزیع و مصرف نهایی سوخت های فسیلی (نفت، گاز و ذغال سنگ) حدود ۱۹٪ از کل انتشار گاز های گلخانه‌ای حاصل از فعالیت‌های انسانی در اروپا را شامل می‌شود. این سهم در کشورهای تولید کننده سوخت های فسیلی می تواند تا ۶۰٪ افزایش یابد (UNFCCC, 2017). انتشار مربوط به فعالیت‌های مرتبط با سوخت های فسیلی به عنوان یک برنامه جالب در برنامه کاهش میزان انتشار گاز متان در اتحادیه اروپا مشخص گردیده است (EC, 2020).

فاکتورهای انتشار (EFs) و میزان فعالیت (AD) به عنوان شاخص انتشار از منابع مختلف معرفی میگردند. فاکتورهای انتشار به صورت میزان انتشار در واحد یک فعالیت خاص تعریف می‌شود. فاکتورهای انتشار برای گزارش دهی میزان انتشار توسط هیئت بین‌دولتی تغییر اقلیم (IPCC) تعریف و دسته بندی گردیده است. با این وجود، این فاکتورها می‌توانند در زمان و مکان تغییر کنند که باعث افزایش در عدم قطعیت مرتبط با گزارش‌های انتشار می‌گردد. برای کاهش این عدم قطعیت‌ها، کمپین‌های اندازه‌گیری مستقل برای به‌روز رسانی و یا تایید این فاکتورها نیاز می‌باشد، که بعضی از این فاکتورها منسوخ شده‌اند و یا دارای سوگیری در نقاط و یا میزان انتشار می‌باشند.

برای دستیابی به یک برنامه تاثیر گذار در کاهش میزان انتشار نیاز به دریافت جزئیات مربوط به مکان و میزان انتشار از منابع مختلف می‌باشد. این پایان‌نامه در پروژه $MEMO^2$ (Methane goes Mobile, Measurements and MOdelling) با هدف افزایش دانش ما در رابطه با انتشار متان با تمرکز بر انتشار از بخش انرژی با استفاده از روش اندازه‌گیری سیار انجام گردید. در این پایان نامه، ما نتایج دقیقی از شناسایی، اندازه‌گیری و نسبت دهی انتشار متان از پروژه‌های اندازه‌گیری گسترده با تمرکز بر انتشار این گاز از شبکه توزیع گاز شهری بررسی کرده ایم.این اندازه‌گیری ها نشان داده‌اند که سهم انتشار گاز متان از نشتی‌های خطوط لوله، انتشارات میکروبی و یا موتورهای احتراقی در شهرهای مختلف، متفاوت می‌باشد.

در فصل دوم، ما نتایج اندازه‌گیری سیار در دوشهر اروپایی هامبورگ (آلمان) و اوترخت (هلند) را ارائه مینماییم. ما منفعت‌های استفاده از سیستم اندازه‌گیری سیار برای شناسایی نقاط نشتی گاز متان از خطوط توزیع گاز شهری را نشان می‌دهیم. نقطه قوت کلیدی استفاده از این روش، بالارفتن سرعت روند شناسایی نقاط نشت می‌باشد، که باعث بالارفتن تعدد بازرسی خطوط می‌گردد، این موضوع باعث کاهش انتشار می‌گردد. از این روش می‌توان برای کمی سازی میزان انتشار نیز استفاده نمود، اما ما نشان می‌دهیم که تخمین‌های این روش حول میزان انتشار با استفاده از پیمایش سیار دارای خطای بالا می‌باشد. در عوض، این اندازه‌گیری‌ها یک دید مقطعی در واحد زمان از کل شهر در اختیار قرار می‌دهند. در این روش، میزان انتشار کلی در سطح شهر دقیق‌تر از میزان انتشار نسبت داده شده به هر نشتی می باشد. علاوه بر این، در این روش نشتی‌های بزرگ به راحتی قابل شناسایی و گزارش دهی و در نهایت باعث کاهش انتشار می‌شوند. ما برای شهر هامبورگ میزان کلی انتشارمتان را در حدود ۷۰ ±۴۴۰ تن در سال و برای شهر اوترخت میزان ۵۰ ±۱۵۰ تن در سال تخمین زده‌ایم، که از میزان ۵۰-۸۰ درصد و ۷۰-۹۰ درصد انتشار به ترتیب در هامبورگ و اوترخت به نشتی‌های خطوط لوله نسبت داده می‌شود. اندازه‌گیری های ما نشان می‌دهد که توزیع آماری انتشار یک توزیع ناهنجار است و تنها تعداد کمی از نشتی‌ها حدود ۵۰ درصد انتشار کلی شهر را شامل می‌شوند. این باعث به وجود آمدن یک موقعیت جذاب برای کاهش میزان انتشار از خطوط لوله می‌گردد.

در صورتی که سیگنال‌های اندازه گیری سیار در سطح شهر به درستی به نشتی‌های خطوط لوله نسبت داده نشوند، این سیگنال‌ها مستعد گزارش نادرست در مورد موقعیت نشت از خطوط هستند. آنالیز گازهای همراه متان، برای نمونه گاز اتان (C_2H_6) و یا ایزوتوپ‌های پایدار کربن و هیدروژن در اتم متان (به ترتیب $\delta^{13}C\text{-}CH_4$ و $\delta D\text{-}CH_4$) می‌توانند به صورت انفرادی و یا باهم در نسبت‌دهی انتشار به منبع مرتبط مورد استفاده قرار بگیرند. در فصل دوم، ما محدودیت‌های جدیدی را ارائه میکنیم اهمیت بررسی سیگنال‌های CO_2 و C_2H_6 را نشان می‌دهیم. این محدودیت‌ها نه تنها باعث بهبود آگاهی ما نسبت به میزان مشارکت منابع مختلف در میزان انتشار کلی می‌شوند، بلکه به صورت غیرمستقیم باعث بالارفتن ایمنی خطوط لوله می‌شوند. با استفاده از نسبت $C_2H_6{:}CH_4$ ($C_2{:}C_1$) از اندازه‌گیری‌ها و نسبت میزان اضافی گاز CO_2 به سیگنال‌های CH_4، به همراه اطلاعات مربوط به میزان نسبت اتان به متان در خطوط لوله یک روش سیستماتیک برای نسبت‌دهی میزان انتشار گاز متان به انتشار از نشتی‌های خطوط لوله، میکروبی و یا احتراق نسبت داده شود. در شهرها، انتشارهای مربوط به سوخت‌های فسیلی عموما مربوط به انتشار از خطوط لوله گاز شهری هستند. انتشارهای میکروبی عموما به انتشارهای غیرفسیلی مربوط به دریچه‌های باز متصل به سیستم جمع آوری

1 Introduction

1.1 Importance of methane mitigation

Anthropogenic Greenhouse Gas (GHG) emissions have resulted in altering global climate patterns. This is primarily driven by the increase of atmospheric GHGs concentrations which have increased global mean temperature. To limit future global warming and climate change, effective mitigation policies will need to be implemented. Although carbon dioxide (CO_2) is the main GHG contributing to global warming, methane (CH_4) is an interesting target to reduce global warming on the short term. However, there are significant uncertainties involved in our current understanding about the strengths of the various CH_4 emission sources and sinks, which hamper the implementation of mitigation policies.

CH_4 is a short-lived GHG with a global warming potential of 84 over a time frame of 20 years, and its atmospheric abundance increased by a factor 2.5 since pre-industrial times, which makes it the second most important anthropogenic GHG after CO_2 (Myhre et al., 2013). The short tropospheric CH_4 lifetime of less than 10 years (Shindell et al., 2012), makes it an interesting emission mitigation target (UNEP, 2021), because mitigation effects will be effective already after few years. This is in contrast to CO_2 with an atmospheric residence time of more than 100 years. Therefore, emission reduction of this gas will not have an immediate impact on climate change unless extraordinary large scale atmospheric CO_2 removal actions are initiated. On the other hand, CO_2 emission mitigation is definitely required to reach the goals of the Paris agreement (UNFCCC, 2015) since it is the dominant GHG.

CH_4 has a positive climate forcing (Naik et al., 2022) with direct and indirect contributions to global warming. The direct impact happens by atmospheric heat-trapping of CH_4 itself and the indirect effects originate from its precursor role in the production of e.g. ozone (O_3), water vapor (H_2O) and CO_2. For example, anthropogenic CH_4 emissions lead to tropospheric O_3 formation and thus part of the radiative forcing from O_3 is due to CH_4 emissions (Myhre et al., 2013). The total radiative forcing of CH_4 by emissions is ≈1 W m^{-2}, about double the radiative forcing due to the increase in CH_4 mixing ratio alone (≈0.5 W m^{-2}) (Myhre et al., 2013). This shows that the indirect effects of anthropogenic CH_4 emissions have about the same contribution to global warming as the direct effects from CH_4 mixing ratio increase.

1.2 Global CH_4 atmospheric mixing ratio trend

Systematic measurements of the abundance of atmospheric CH_4 started in 1978 (Rasmussen and Khalil, 1981) and these measurements show that the global mean mixing ratio of CH_4 is increasing. Before this period, measurements of air trapped in polar ice cores from firn has provided a detailed picture about the evolution of CH_4. On geological timescales CH_4 has varied due to natural processes, but ice core reconstructions dating back from the pre-industrial era all the way to 650 kyr ago show that CH_4 mixing ratios did not exceed 773 ± 15 ppb (Spahni et al., 2005) before the industrial period. In 1972 the atmospheric CH_4 mixing ratio was recorded in the Northern and Southern Hemisphere at about 1410 ppb and 1300 ppb respectively (Ehhalt and Schmidt, 1978). In October 2021, the globally averaged CH_4 mixing ratio was reported at 1907.2 ppb (NOAA, 2022).

Fig. 1.1 shows the temporal evolution of the globally averaged mixing ratio of atmospheric CH_4 as derived from the program for systematically monitoring CH_4 abundance (NOAA, 2022). Although the general trend is positive, clear variations of the increase rate have been observed over the past decades. While the average global CH_4 mixing ratio trend in 1984 was ≈14 ppb yr^{-1}, this growth dropped to ≈3 ppb yr^{-1} in 1996 (Dlugokencky et al., 1998). Between 2000 to 2006 the atmospheric CH_4 mixing ratio was stabilized at 1773 ± 3 ppb (Kirschke et al., 2013). The atmospheric CH_4 mixing ratio again increased in 2007 with a further accelerated growth rate in the later years, e.g. 12.7 ± 0.5 ppb yr^{-1} in 2014 (Nisbet et. al., 2019). The renewed increase in CH_4 emissions can put the Paris climate agreement at risk because such an increase in CH_4 mixing ratio was not foreseen (Nisbet et al., 2019). The post 2006 increase is reported to be equivalent to ≈25 Tg CH_4 yr^{-1} extra (Worden et al. 2017).

The variability of atmospheric CH_4 mixing ratio can be studied at different scales, for example seasonal, annual and / or spatial scales. As an example related to spatial scales, the atmospheric CH_4

abundance in the Northern Hemisphere is about 5% higher than in the Southern Hemisphere (Ehhalt et al., 2018).

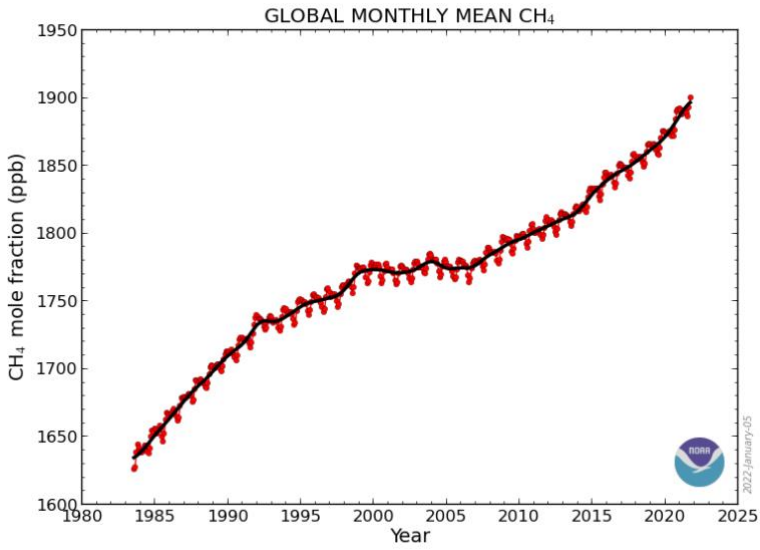

Figure 1.1. Variability of CH_4 mixing ratio observed global in-situ measurements network retrieved from NOAA (2022)

There have been tremendous efforts in understanding the underlying reasons of the variations in the CH_4 growth rate over the past decades, but CH_4 has a complex mix of sources and sinks (see following section) and a definitive answer is not yet available (Canadell et al., 2021, Ehhalt et al., 2018).

1.3 Methane sources and sinks

The growth rate of the atmospheric CH_4 mixing ratio is dependent on the strengths of different sources and sinks. CH_4 sources can be broadly categorized into natural and anthropogenic sources, or alternatively into CH_4 molecules that are formed by biogenic, thermogenic or pyrogenic processes. Generally, the breakdown of organic matter under anoxic conditions leads to the formation of CH_4. This process occurs naturally in wetlands, permafrost and lakes but also in anthropogenic sources such as landfills, wetlands, rice fields or ruminants (livestock) and these processes together constitute the largest anthropogenic source category (Fig. 1.2). CH_4 emissions related to the exploitation, transport and use of fossil fuels (coal, oil and gas) are another important anthropogenic source category (Fig. 1.2). They can have thermogenic or biogenic origin, and the same is true for natural gas seeps. Biomass or biofuel burning are two human-related activities which cause formation of pyrogenic CH_4, but have a relatively small contribution to the global source strength (Fig. 1.2).

According to the review of the global CH_4 budget (Saunois et al., 2020), 60% of total global CH_4 emissions are from anthropogenic sources and 40% are from natural sources. As a feedback to global warming, natural emissions may increase in the future (Christensen et al., 2019; Dean et al., 2018). Saunois et al. (2020) also showed that ≈64% of global emissions are from the tropics, ≈32% from the middle latitudes and ≈4% from higher (> 60° N) latitudes. Although global CH_4 sources and sinks are qualitatively known, their contributions to the total global CH_4 budget include uncertainties (Kirschke et al., 2013; Forster et al., 2007, see also Fig. 1.2).

1.3.1 Recent methane sources

The main three sectors contributing to the current global anthropogenic CH_4 emissions are energy, agriculture and waste and the contribution rankings are dependent on the spatial scale of the target area, e.g. countries or regions. The imbalance between CH_4 sources and sinks has resulted an instability of the CH_4 atmospheric abundance, with an overall positive trend in the global background

mixing ratio of CH_4 with annual variabilities (NOAA, 2022) in the last 4 decades (Fig. 1.1). However, the causes of this increase have not been answered consistently from different scientific articles.

Figure 1.2 shows the state of the art of the understanding of the CH_4 sources and sinks on the global scale, as evaluated by (Saunois et al., 2020). They used Bottom-Up (BU) and Top-Down (TP) approaches and on average they reported 128 Tg CH_4 yr^{-1} (range 113 – 154) and 111 Tg CH_4 yr^{-1} (range 81 - 131) Tg CH_4 yr^{-1} for the fossil fuel related activities from the BU and TD approaches respectively. For the agriculture and waste sectors together the best estimates of emission rates are 206 Tg CH_4 yr^{-1} and 217 Tg CH_4 yr^{-1}, using BU and TP approaches respectively. The contribution of biomass and biofuel burning to total global CH_4 emissions was reported from anthropogenic and natural sources combined, yielding 30 Tg CH_4 yr^{-1} from both BU and TD approaches. Wetlands are the main natural CH_4 emission source with best estimate contributions of 149 Tg CH_4 yr^{-1} and 181 Tg CH_4 yr^{-1} from BU and TD analyses, with overlap in the uncertainty ranges. The largest difference between the BU and TP estimates is for other natural sources, where the BU estimate of 222 Tg CH_4 yr^{-1} is significantly larger than the TD estimate of 37 Tg CH_4 yr^{-1}, which cannot be reconciled within the combined errors.

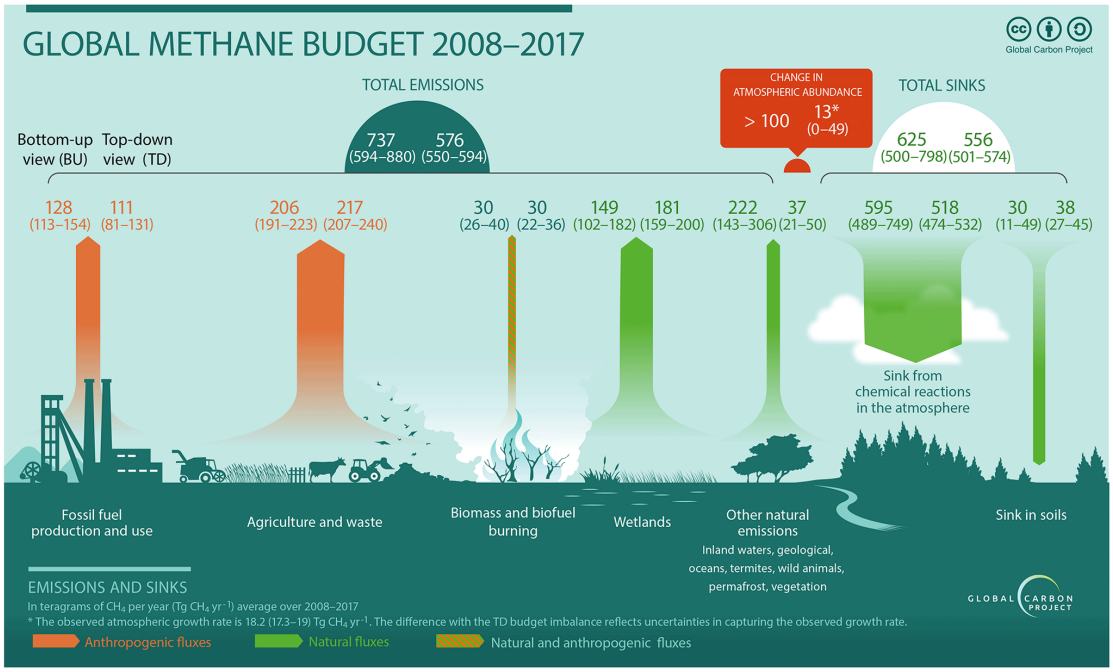

Figure 1.2. Global CH_4 budget for the period from 2008 to 2017, (Figure from Saunois et al. (2020))

1.3.2 Historical methane emissions

Isotope measurements of air trapped in ice cores and historical data related to human activities can help to understand variations in the sources of CH_4 emissions at times where no direct atmospheric measurements were available. Several studies investigated an influence of anthropogenic activities on the atmospheric CH_4 burden before the start of the industrialization.

Sapart et al. (2012) studied $\delta^{13}C$-CH_4 from ice cores from Greenland and found out that the variabilities in isotopic composition between 100 BC and ad 1600 AD can be attributed in changes of pyrogenic and biogenic sources which can be explained partly by climate variability and partly by early anthropogenic pyrogenic emissions.

Subak (1994) estimated anthropogenic CH_4 emissions in the 16th century, the last century before the pre-industrial era. They used historical data over the e.g. lifestyle of people and environmental conditions and concluded that in 15th century anthropogenic emissions contributed at least 55 Tg CH_4 yr^{-1} to total CH_4 emission of 210 Tg CH_4 yr^{-1}.

Stern and Kaufmann (1996) used historical data and reports of CH_4 emissions for different decades and estimated anthropogenic CH_4 emissions between 1860 and 1990. They concluded that

anthropogenic CH_4 emissions rose from 80 Tg CH_4 yr^{-1} in the 1860s to 360 Tg CH_4 yr^{-1} in 1990. This shows that within 130 years, anthropogenic CH_4 emissions increased by more than a factor 4.

1.3.3 Methane sinks

CH_4 can be removed from the atmosphere through several atmospheric odixation reactions and also via soil uptake (Fig. 1.2). Reaction with the hydroxyl radical (OH) is the main sink for the CH_4 molecules (Prather et al., 2001). The lifetime of CH_4 is the ratio of its global burden to its global loss rate (Prather, 2007). The CH_4 atmospheric lifetime is thus dependent on the sinks. Naik et al., (2013) suggested that the CH_4 lifetime decreased by 4.3 ± 1.9% from 1980 to 2000 due to a 3.5 ± 2.2% increase in the mixing ratio of OH. Dalsøren et al. (2016) reported that atmospheric CH_4 lifetime decreased by 8% from 1970 to 2012. However, trends in OH and thus the CH_4 lifetime are discussed controversially.

1.4 Attribution of CH_4 mixing ratio increase at the global scale

As mentioned above, CH_4 can be produced via different pathways and measurements of the relative abundances of the stable carbon or hydrogen isotopes of CH_4 provide information about the formation processes. The analysis of isotope datasets (and other approaches) can help to understand the reason behind the variations in the global atmospheric mixing ratio.

Also, ethane (C_2H_6) is a component which is emitted concurrently with CH_4 from fossil fuel activities, thus investigations on its variation can help in understanding the contributions from fossil fuel related activities. Oil and gas activities and biomass burning are the two major sources of global C_2H_6 emissions (Ehhalt and Prather, 2001).

1.4.1 Global methane attributions using C_2H_6

Simpson et al. (2006) used CH_4 and C_2H_6 measurements from remote locations since 1978 in the Pacific Basin (Simpson et al. 2002) to explain the variations in the atmospheric CH_4 mixing ratio. They attributed synchronous peaks of CH_4 and C_2H_6 to the events of biomass burning episodes in 1998 and 2000-2003 in Indonesia and Russia.

Aydin et al. (2011) measured the C_2H_6 content of air samples collected from firn air in Greenland and Antarctica. They observed a positive growth trend for C_2H_6 from the beginning of the 20th century until the 1980s, but a decline afterwards. They suggested that reduced emissions from fossil fuel sources were the primary reason for the decline in C_2H_6. They also showed that the global C_2H_6 emissions peaked (14-16 Tg C_2H_6 yr^{-1}) in the 1960s and 1970s and declined to 8-10 Tg C_2H_6 yr^{-1} at the end of the 20th century.

1.4.2 Global methane attributions using δ^{13}C-CH_4

Quay et al. (1999) were the first to use global scale isotope measurements to constrain the contribution from different sources. Using δ^{13}C-CH_4 measurements from 6 stations globally, and additional latitudinal gradient samples collected during ship cruises between 1988 and 1995. They attributed 18 ± 9% of the atmospheric CH_4 to fossil fuel emissions.

Numerous studies have attempted to explain the growth rate variations in the past decades using isotope analysis. Bousquet et al. (2006) used isotope data in inversion models and speculated that if wetlands emission returned to their level before 2000, atmospheric CH_4 rise would be observed.

Schaefer et al. (2016) used measurements of CH_4 mixing ratio and δ^{13}C-CH_4 from the NOAA-GMD network at global scale to investigate the cause of the post-2007 rise. They concluded that the cause for the renewed increase after 2007 was from biogenic sources, and more from agriculture rather than wetlands, although inventories show an increase in anthropogenic fossil fuel CH_4 emissions.

Nisbet et al. (2019) offered three hypotheses to explain the CH_4 increase after 2006 (i) increase in natural CH_4 emission with low δ^{13}C-CH_4 values (ii) increase in fossil fuel emissions combined with a decrease in natural emissions and (iii) a decrease in the removal rate of CH_4 through OH. They investigated in detail how these hypotheses individually or together could explain the observations.

Saunois et al. (2020) from a TD and BU budgeting using the Global Carbon Project (GCP) dataset concluded that the CH_4 increase was primarily due to anthropogenic sources and Jackson et al. (2020) with the same methods and datasets attributed the anthropogenic emissions equally to fossil fuel emissions and agriculture.

Schwietzke et al. (2016) reanalyzed the global $\delta^{13}C\text{-}CH_4$ database and updated the isotopic source signatures for biogenic, thermogenic and pyrogenic sources. They reported a decrease from 8% to 2% of gas production in the last three decades prior to their publication. In particular the revision of the global average $\delta^{13}C\text{-}CH_4$ signature towards lighter values requires an upward revision by 20 to 60% of emissions from fossil fuel sources compared to the reports in inventories.

Recent shale gas exploitation has increased exponentially since 2008. Milkov et al. (2020) studied $\delta^{13}C\text{-}CH_4$ signatures of >1600 samples from shale gas exploration which covers >97% of global shale gas productions. They concluded that increased emissions from shale gas and oil exploitations could not explain the global decrease of $\delta^{13}C\text{-}CH_4$. However, Howarth (2019) concluded that emissions from shale gas activities have contributed to about half of increased CH_4 emissions from global fossil fuel activities, which is equivalent to one-third of total additional CH_4 emissions.

1.4.3 Global methane attributions using C_2H_6 and $\delta^{13}C\text{-}CH_4$

Worden et al. (2017) evaluated the increase in atmospheric C_2H_6 mixing ratio and $\delta^{13}C\text{-}CH_4$ and used satellite imageries to derive the variabilities of carbon monoxide (CO) and CH_4. They reported an increase in C_2H_6 mixing ratio, a depletion in $\delta^{13}C\text{-}CH_4$ and a decrease in biomass burning emissions in 2008-2017 compared to the 2001-2007. Their results attribute the post-2006 increase to both biogenic and fossil emissions. The contribution of fossil emissions is estimated within range of 12–19 Tg CH_4 yr^{-1} (out of ≈25 Tg CH_4 yr^{-1}). This suggests that at least half of the emission increase after 2006 can be attributed to fossil emissions.

1.5 Emission inventories

1.5.1 Design of an emission inventory

A GHG emission inventory lists emission rates of sources contributing to the total emissions in a specific domain within a definite period. In the context of contribution to different sources, the domain is normally at the scale of a country but can be bigger or smaller depending on the purpose. The emission inventories (mainly related to the countries' inventories) normally cover emissions related to a certain source over the period of a year.

There are different purposes to use or design an emission inventory. The inventories are the foundations for the discussions around prioritization of emission mitigation policies. However, if spatial and/or temporal resolutions and/or information about strength of emissions of sources within an inventory are incorrect, this can negatively affect the emission mitigation policies. Inventories are also used in atmospheric models because they contain a priori information on the contribution of different sources.

Emission inventories report CH_4 emissions from different sectors using EFs and AD. EFs are the CH_4 emissions per unit of associated activity. For example, in the contexts of fossil fuel production, CH_4 emissions per mass unit of oil produced, or CH_4 emissions per km transportation pipelines of oil or gas. The CH_4 emission rate are the product of Activity Data (AD) and Emission Factor (EFs) (Emission = Activity data * Emission Factor).

Differences or similarities in methods (tiers) or datasets used to design different inventories can lead to either similarities or discrepancies between inventories. If inventories agree on the emission rate from a specific source / sector, this does not necessarily mean that the emission estimate is close to the real emission rate, as the inventories may have been built upon the same foundations, i.e. tiers and datasets (Petrescu et al., 2020).

Uncertainties in an inventory can arise, for example, from using outdated tiers or numbers that are not representative of current emission status. In addition, emission rates from sources can vary over

time, so using simple constant values that were derived for a specific condition (e.g. summer or winter) may not be adequate to derive annual average emission rates. The AD used in emission inventories can also be missing or are uncertain and may not always reflect real activities. These uncertainties are high for CH_4 inventories especially in the energy sector, which implies a need for independent verifications.

There are several CH_4 emission inventories at regional, national and global scales, and they are described below. Continuous efforts have been made over the years to improve temporal and spatial resolutions of inventories, which also include cross-checking the inventory reports with independent measurement campaigns

One example is the recent work to improve the CH_4 emission inventory in the energy sector in US. The Environmental Protection Agency (EPA) is responsible for preparing the US National Inventory Report (NIR) and reporting it to the United Nations Framework Convention on Climate Change (UNFCCC). The emissions and sinks of CH_4 and other GHGs have been provided since 1990. In the latest report of the EPA (EPA, 2022), they recalculated CH_4 emission estimates for the previous years together with a team from Harvard University and found out that the previous reports underestimated the emissions on average by 4% with the highest underestimation in 2012 by 8%. The increase reported in the recalculations is mainly due to adjusted emissions from the hydraulic fracturing of oil basins. For example, in the report of 2021, total CH_4 emissions of the US natural gas system were estimated at 157.6 MMT CO_2-eq while this number was recalculated to 171.5 (MMT CO_2-eq) (EPA, 2022), i.e. an 8.9% increase.

This illustrates the need for continuous efforts to improve emission inventories by carrying out extensive quantification and attribution campaigns, long-term measurements of atmospheric mixing ratio and isotopic compositions, running atmospheric transport models, updating quantification methods, using newly developed instruments and finding unreported emission sources in inventories. The improved understanding of emissions then results in designing well-suited mitigation policies. The comparison between measurements and model outputs is extremely beneficial in understanding locations, strength and variabilities of target sources.

1.5.2 Main global emission inventories

Table 1.1 shows a comparison of CH_4 emission rates from 5 different emission inventories with different spatial and temporal resolutions.

The Emissions Database for Global Atmospheric Research (EDGAR) inventory provides emission rate estimates for anthropogenic CH_4 emissions based on publicly available data and international reports. EDGAR is a high-resolution gridded inventory, 0.1° ×0.1°, and it is a commonly used inventory for the inverse modelling analysis of global CH_4 budget (Janssens-Maenhout et al., 2019). Janssens-Maenhout et al. (2019) listed (i) agriculture (154 ± 92 Tg yr^{-1}) (ii) energy (121 ± 91 Tg yr^{-1}) and (iii) waste (67 ± 61 Tg yr^{-1}) as the three largest anthropogenic contributors to the global anthropogenic emissions. The majority of CH_4 emissions from the energy sector originates from oil, gas and coal exploitations, and partially from biofuel. However, the CH_4 emissions from oil and gas activities are highly uncertain due to e.g. missing or unrepresentative Activity Data (AD) and sources, sampling biases.

The Monitoring Atmospheric Composition and Climate (MACC) is another inventory with the primary goal of supporting modelling efforts in air quality studies (Kuenen et al., 2014). The emissions from each sector were distributed over the same time frame but with different hourly weights, e.g. for the combustion-related emissions, rush hours are weighted higher. The MACC datasets are hosted by TNO and the inventories are known as TNO_MACC. The most recent (fourth) version of this inventory has a spatial resolution of 0.05° × 0.1° and includes emissions from 2000 to 2017 in Europe (Kuenen et al., 2022). The data comes from the NIR that are provided by the countries to UNFCCC. If the quality of the data from NIR does not pass the quality check, MACC uses data from the Greenhouse gas Air pollution Interaction and Synergies (GAINS, https://gains.iiasa.ac.at/models/, last access: 08 April 2022) model instead.

The Community Emissions Data System (CEDS) inventory collected the data and reports from already existing inventories and articles to provide data on anthropogenic emissions of reactive gases and aerosols. The 2014 version of CEDS includes historical anthropogenic emission for CH_4 (Hoesly et al., 2018). For example, they reported that in 1850, the only source of combustion was from coal and biomass burning, related to residential and industrial activities. The most recent version (McDuffie et al., 2020) does not include CH_4 as the historical emissions were released in the earlier version.

Table 1.1 shows the large uncertainties of the emission estimates in each inventory, but also the differences between inventories. While in the EDGAR v4.3.2 and EPA inventories emissions from agriculture are highest, followed by the energy sector, in GAINS the energy sector is the main contributor. Nevertheless, uncertainties are large and these bottom-up estimates agree within the reported uncertainties.

Table 1.1. Intercomparison of 5 different emission inventories, retrieved from Table 4 in Janssens-Maenhout et al. (2019), the values in bold are for 2010 and in italic for 2000

CH_4 totals in Tg yr^{-1} for 2010 (2000)	EDGAR v4.3.2	EPA (2012)	GAINS ECLIPSEv5 (2015)	Kirschke et al. (2013) BU & TD	Saunois et al. (2016) BU & TD
Time series	1970–2012	1990–2005 (projected to 2030)	1990–2010	1980–2009	2000–2012
spatial resolution	0.1°×0.1°	None	1°×1°		
temporal resolution	Monthly	Annual	Annual	Annual	Annual
Geo-coverage	227 countries	224 countries	77 countries and 5 regions	Global	Global
Agricultural	**154** (± **92**) (*137*)	**147** (*136*)	**129** (*123*)	BU: **263** (*219*)	BU: **197** (*190*)
				TD: **286** (*204*)	TD: **200** (*183*)
Waste and wastewater	**67** (± **61**) (*59*)	**65** (*58*)	**51** (*46*)	–	–
energy and fossil fuel production	**121** (± **91**) (*96*)	**129** (*107*)	**144** (*116*)	BU: **105** (*85*)	BU: **164** (*142*)
				TD: **123** (*77*)	TD: **147** (*136*)
Other	**21** (± **20**) (*18*)	–	**19** (*17*)	–	–
Total	**342** (± **160**) (*293*)	–	**343** (*302*)	BU: **368** (*304*)	BU: **370** (*338*)
				TD: **409** (*273*)	TD: **347** (*319*)

1.5.3 National emission inventories in support of UNFCCC

The parties (mostly in this context, this term is equivalent to countries) need to submit their annual total CH_4 emissions as NIR to the UNFCCC. The reported CH_4 emissions reflect emissions from different sectors within a country but the spatial distribution and temporal breakdown of the total annual emissions are not included. This limits their use for the implementation of the most suitable mitigation policies at the right place and time.

The IPCC provided guidelines to the national authorities responsible for reporting anthropogenic GHG emissions of their parties as NIR to UNFCCC. These guidelines are from 2006 with refinements that were proposed in 2016 and accepted in May 2019 (IPCC, 2019). The refinements in the energy sector are only related to the fugitive emissions and methodologies for the other categories

are unchanged. The changes are related to reporting in the coal, oil and gas and fuel transformation categories in the energy sector. In the 2019 refinements, EFs were updated including the EFs for the unconventional oil and gas activities, e.g. shale gas exploration. These updates also contain EFs to estimate CH_4 emissions from abandoned oil and gas wells. The new guideline from 2019 also contains a section on the methodologies for estimating fugitive emission during the practices of transforming fuels, e.g. biomass to liquid fuels or gas). The guidelines and EFs from the IPCC are widely used in reporting the CH_4 emissions of parties, however, it is known that the EFs can differ in different countries, related to management and maintenance practices of the underlying activities. Therefore, country specific emission factors are also used.

1.5.4 Discrepancies between research-based and current inventories

The inventories can be evaluated by independent measurements. The comparisons often point to the sources of discrepancies which can subsequently be improved in the inventories, leading to a better understanding of CH_4 emissions sources. Better and more accurate representation of CH_4 emissions in the inventories can helps with the implementation of emission mitigation policies.

Massakkers et al. (2016) introduced a high resolution gridded inventory for the anthropogenic sources of the US and to be consistent with the existing inventory, they followed the categories introduced in the inventory of EPA in 2016. They also reported that there is a large difference between their analysis and the reports in EDGAR v4.2 for the US CH_4 emissions.

In other cases, the estimate from a measurement study can be of the same order as the reports from inventories but wrongly distributed in a country or region. Hristov (2017) estimated CH_4 emissions from livestock in the US. They found out that their estimate of 8.916 Tg CH_4 yr^{-1} is in the same order of magnitude as the estimate from EPA but the distribution of CH_4 emissions was significantly different. This wrong distribution of CH_4 emission strength will then most likely have an impact on the TD modeling and source attributions.

Alvarez et al. (2018) used information from a large set of measurement campaigns carried out in the previous years to reassess CH_4 emissions from the oil and gas supply chain in the US and compared the results with the EPA inventory. They reported emissions of 13 Tg yr^{-1} (min: 11.3 max: 15.1) from atmospheric measurements, which is about 60% higher than the inventory, 8.1 Tg yr^{-1} (min: 6.7 max: 10.2). The biggest difference is related to the emissions at the production sites, where Alvarez et al. (2018) reported 7.6 Tg yr^{-1} (min: 6.0 max: 9.5) while it is 3.5 Tg yr^{-1} from the EPA report.

Scarpelli et al. (2020) designed a 0.1° ×0.1° gridded inventory for the global fossil fuel emissions. In this study, they reported emissions of 41.5 Tg-CH_4 yr^{-1}, 24.4 Tg-CH_4 yr^{-1} and 31.3 Tg-CH_4 yr^{-1} in 2016 for oil, natural gas and coal respectively at global scale. Their analysis and comparison with current inventories suggest that the location of emissions can be significantly different from other inventories at large scales. They suggested that this updated high resolution inventory can be beneficial to be used in inverse modeling studies of the global CH_4 budget. In another study by Sheng et al. (2017) related to anthropogenic CH_4 emissions from oil and gas activities in Mexico and Canada, they found out that although the EDGAR v4.2 inventory has small errors for the livestocks and waste categories, large errors were observed for anthropogenic oil and gas emission over North America.

Maasakkers et al. (2021) analyzed anthropogenic US CH_4 emissions and concluded that although their total anthropogenic CH_4 emission for the US is close to the reports from the EPA (EPA, 2020) for the years between 2010 and 2015, 30.6 Tg yr^{-1} (min 29.4, max: 31.3) vs 28.7 Tg yr^{-1} (min: 26.4 and max: 36.2) respectively, there is a large discrepancy between their estimates for the US oil and gas activities and the EPA inventory. They showed that their estimates for CH_4 emissions from oil and gas activities is 35% and 22% higher than EPA reports. And the latest report of EPA (after publication of Maasakkers et al. (2021)) reports 2 times lower emissions from oil and gas than the estimates from Maasakkers et al. (2021).

Petrescu et al. (2021) reviewed the data sources, and outputs from process-based models for ecosystems and applied inverse modelling to compare their BU and TD estimates with inventories of

anthropogenic CH_4 emissions for the EU27 + UK for the period of 1990 - 2017. For the years between 2011 and 2015, the anthropogenic BU CH_4 estimates from National Greenhouse Gas Inventories (NGHGIs), EDGAR v5.0 and GAINS are in the same order, 18.9 ± 1.7 Tg-CH_4 yr^{-1}, 20.8 Tg-CH_4 yr^{-1} and 19.0 Tg-CH_4 yr^{-1} respectively. The datasets and approaches of these inventories are not fully independent from each other (see Fig. 4 in Petrescu et al., 2020). The TD estimate derived from atmospheric observations and high-resolution inverse models yields 28.8 Tg CH_4 yr^{-1}. A TD estimate including satellite data from the GOSAT instrument yields 23.3 Tg CH_4 yr^{-1} and the TD estimate using observations from the surface network is 24.4 Tg CH_4 yr^{-1}. This shows that TD estimates are higher than NGHGIs estimate for the EU27 + UK. Petrescu et al. (2021) suggested that this gap can be explained by 5.2 Tg-CH_4 yr^{-1} of emissions estimated for the rivers, lakes and geological sources.

1.6 CH_4 emissions from the energy sector

It is expected that fossil fuels (coal, natural gas and oil) will remain an important energy source in the next decades (IEA, 2020). The transition to renewable energy will likely proceed via an increase in natural gas consumption, successively replacing coal and oil (Alvarez et al., 2012). Among the fossil fuel sources, coal has the highest negative climate impact while use of natural gas has the lowest impact when only the energy content of the fuel is taken into account. However, CH_4 emissions during production, transportation and distribution of natural gas can offset the climate benefit of this natural resource. It has been shown that if CH_4 emissions from natural gas activities exceed 3.2% (Alvarez et al., 2012) or even 2.4–3.2% (Howarth, 2014), or 1 to 5% (Allen, 2014) of the production, then the climate benefits of natural gas is fully counteracted by the additional radiative forcing due to CH_4 emissions.

The CH_4 emissions from oil and gas facilities are uncertain and extensive measurement campaigns with different instruments (in-situ, optical, etc) on different platforms (car, drones, satellites, etc.) have been carried out in the past decade to provide more reliable information. For example, Zavala-Araiza et al. (2015) reported 1.5% CH_4 loss in the Barnett shale basin, and this loss from the upstream activities only increases the climate impact of consumption of natural gas by 50% over a 20 year time horizon.

The Airborne visible/infrared imaging spectrometer (AVIRIS) instrument offers high resolution imagery to better detect and quantify CH_4 emissions from local or regional sources (Thorpe et al., 2014). Cusworth et al. (2021) studied CH_4 emissions from the Permian Basin which accounts for the rapid growth of oil and gas activities in the US. They sampled 1100 unique locations and included samples which were observed at least 3 times. They reported that 50% of emissions were originated from production, 38% from collection facilities and 12% in the processing phase. Maazallahi (2015) used AVIRIS data to detect fugitive CH_4 emissions from the shale gas production wellheads in the Marcellus shale basin, PA, USA (limited number of locations). The derived CH_4 emissions were then compared to the production rate of the wells and the loss to production ratio was retrieved, 0.7 to 3.0%. Haworth et al. (2011) estimated CH_4 escape of 3.6 to 7.9% for the shale gas activities, while this ratio is 1.7 to 6.0% for the conventional gas production.

1.6.1 CH_4 emissions in EU27+UK

According to the national emission reports, the three sectors contributing most to total anthropogenic CH_4 emissions in Europe are agriculture (53%), waste (25%) and the energy sector (19%) (EC, 2020). Major CH_4 emissions in the energy sector in the EU originate from activities related to oil, gas and coal.

The majority of CH_4 emissions related to the fossil fuel use in Europe may happen in other regions of the world, as the union imports 70%, 97% and 90% of their demand for hard coal, oil and gas from outside the EU, and the emissions related to these imports are not clear (EC, 2020).

Table 1.2 summarizes the CH_4 emissions from category 1B2, fugitive CH_4 emissions from oil and gas activities in EU27+UK. The total reported emissions in 1990 were 65182 kt CO_2-eq and the

top five contributing countries were Romania, UK, Italy, Germany and the Netherlands. The largest reduction of emissions from the oil and gas activities was reported for Romania and the UK, increased emissions were reported in Poland for these activities. The emission reduction of fugitive emissions in Romania in 2015 compared to 1989 was 76.8% (Table 1.2). In 2015, total EU27+UK emissions in the 1B2 category were 33930 kt CO_2-eq and the first five contributors were Romania, Germany and the UK, Italy and Poland (Table 1.2). In 2016, total EU27+UK CH_4 emissions dropped further to 33107 ktCO_2-eq and in 2017 reported CH_4 emissions dropped by 14% to 28343 kt CO_2-eq, with another huge reduction in Romania, who was then no longer the largest producer. In 2018, total reported CH_4 emissions in the 1B2 category reported for the EU27+UK were 26899 kt CO_2-eq, only 41% of the emissions in 1990.

This illustrates progress in climate change mitigation, but the sometimes very large changes in the reported emissions (e.g. more than 50% reduction in Romania from 2016 to 2017) call for independent verification. The ROmanian Methane Emissions from Oil and gas (ROMEO) project aimed at independent quantification of the CH_4 emissions from the Romanian energy sector (Röckmann et al., 2020).

Table 1.2. Contributions of CH_4 emissions in 1B2 category (fugitive emissions from oil and gas activities) in EU27+UK

Highest contributor	1990 (kt CO_2-eq)	2015 (kt CO_2-eq)	2016 (kt CO_2-eq)	2017 (kt CO_2-eq)	2018 (kt CO_2-eq)
1	Romania 24186 kt	Romania 9408	Romania 8812	Germany 5011	Germany 4900
2	UK 12379	Germany 5057	Germany 5066	UK 4935	UK 4920
3	Italy 8735	UK 5057	UK 4863	Italy 4696	Italy 4460
4	Germany 8300	Italy 4915	Italy 4686	Romania 3618	Romania 3618
5	Netherlands 1932	Poland 2423	Poland 2530	Poland 2648	Poland 2687
Total EU	65182	33930	33107	28343	26899

Coal mining is another major anthropogenic CH_4 emission source in the EU. In 1990, 95180 kt CO_2-eq were emitted from coal mining activities (category of 1.B.1.a) of EU27+UK with the top highest contributions from Germany, UK, Poland, Czech Republic and France. In 2015 reported emissions were reduced more than three-fold to 28638 kt CO_2-eq and to 26327 kt CO_2-eq in 2016 (Table 1.3).

Table 1.3. Contributions of CH_4 emissions in category 1B1a (CH_4 emissions for the coal activities) in EU27+UK (UNFCCC, 2018)

Highest contributor	1990 (kt CO_2-eq)	2015 (kt CO_2-eq)	2016 (kt CO_2-eq)
1	Germany 25494	Poland 16856	Poland 16930
2	UK 21809	Czech Republic 3581	Czech Republic 3260
3	Poland 21217	Germany 3037	Germany 2426
4	Czech Republic 10322	UK 1375	Romania 907
5	France	Greece	Bulgaria

	4780	1007	821
Total EU	95180	28638	26327

1.7 CH_4 emissions in urban areas

1.7.1 Underestimation of urban CH_4 emission in inventories

Compared to emissions from the production regions, relatively little effort has been invested to estimate CH_4 emissions from and implemention of CH_4 mitigations in cities (Hopkins et al., 2016a). Recent studies related to CH_4 emissions from urban areas have shown mostly underestimations in the reports from the inventories (O'Shea et al., 2014; McKain et al., 2015; Helfter et al.; 2016; Sargent et al., 2021). Thus, studies in various cities are required to gain a better understanding of the situation in different cities as each city may require unique emission mitigation pathways.

O'Shea et al. (2014) used in-situ measurements of CH_4, CO_2 and CO onboard an aircraft and estimated total emissions from the greater London area. Using a mass balance method, they reported net emission rates of 0.13 ± 0.02 μmol-CH_4 m^{-2} s^{-1}, 21 ± 3 μmol-CO_2 m^{-2} s^{-1} and 0.12 ± 0.02 μmol-CO m^{-2} s^{-1}. Their comparison with the NAEI shows that their results are 3.4, 2.3 and 2.2 times higher than reports from the inventory for CH_4, CO_2 and CO respectively.

McKain et al. (2015) studied total CH_4 emissions in the Boston area using measurements from four stationary analyzers and modelling. They reported total emissions of 18.5 ± 3.7 g CH_4 m^{-2} yr^{-1} and attributed most of the emissions to leaks from gas pipelines (60 to 100 %). They also noticed that the CH_4 emission loss compared to the amount of gas distributed was 2.7 ± 0.6% which is significantly higher than the 1.1% reported in the inventories. Phillips et al. (2013) also showed (using δ^{13}C-CH_4 measurements), that the majority of emissions in Boston can be attributed to leaks from gas pipelines.

Helfter et al. (2016) carried out eddy covariance measurements from 2012 to 2014 of CH_4, CO_2 and CO in central London and compared their estimates with the reports from the London Atmospheric Emissions Inventory. They estimated 72 ± 3 t-CH_4 km^{-2} yr^{-1}, 39.1 ± 2.4 kt-CO_2 km^{-2} yr^{-1} and 89 ± 16 t-CO km^{-2} yr^{-1}. Their CH_4 emission estimates are twice larger than the reports from the inventory. They found 33% seasonal variability for CO_2 and 21% for CH_4, higher in the winter than summer which shows anticorrelation between mean seasonal mean temperature and GHG emissions. They correlated 90% and 99% of the spatial variability of CO_2 and CH_4 respectively to the residential population distributions. They suggested revision on the CH_4 emission reports of the inventories which consists of updating reporting methodology and also including missing sources.

Sargent et al. (2021) investigated about 8 years of CH_4 and C_2H_6 measurements from 2012 to 2020 using a transport model (McKain et al., 2015), and they reported total emissions of 198 ± 47 Gg-CH_4 yr^{-1}, with 127 ± 24 Gg-CH_4 yr^{-1} emissions originating from the natural gas system in Boston. They also indicated that over a course of 8 years, emissions had not been reduced significantly despite an increase in gas pipeline repairing practice in Boston in the last years. They provided an estimate of 2.5 ± 0.5% natural gas loss in the distribution network of Boston which is about threefold higher than estimates from the BU approach. They also reported that their estimate for the emissions from the leaky pipeline system in Boston is six times greater than the inventory reports from the EPA. Sargent et al. (2021) concluded that 3.3 to 4.7% of natural gas is lost in the total supply chain of urban areas in the US, totally eliminating the climate benefit of gas compared to coal.

1.7.2 Mobile urban CH_4 emission quantification

1.7.2 Mobile urban CH_4 emission quantification

Von Fischer et al. (2017) carried out mobile street-level surveys with fast response laser instruments on vehicles to study urban CH_4 emissions. They published an empirical equation based on release tests at ground level, aiming to quantify street-level CH_4 sources with the focus on the quantification of emissions from gas leaks. In their release experiment, emission rates from 2 to 40 L min^{-1} were used and the plumes were measured 5 to 40 m downwind from the release point. Their empirical equation was designed to quantify gas leaks without prior information about the main

emission outlet of gas leaks, aiming to quantify total CH_4 emissions from gas leaks in urban area by relatively quick vehicle surveys. The emission rate was then derived from a logarithmic correlation with maximum CH_4 mixing ratio, plume area (integration of CH_4 mixing ratio along the driving track within a plume) and the ratio of these two. They stated that the best derived emission rate occured when the mobile measurement car was about 10 m downwind the release point. To attribute CH_4 signals to gas leaks, they used the persistency of CH_4 signals at a location and the plume stretch along the driving track. The CH_4 signals should be observed at least twice to be persistent, and they did not include CH_4 plumes greater than 160 m, because the plumes with extents of more than 160 m could not be attributed to gas leaks from natural gas pipelines.

Weller et al. (2018) reevaluated the data from the von Fischer et al. (2017) release experiment and provided a revised version of the equation to convert the mobile measurement data to emission rates. The quantification equation of Weller et al. (2018), which is also used in the work presented in this thesis, only considers the maximum CH_4 enhancement from each pass next to a gas leak. They used the same attribution criteria from the first algorithm. Fig. 1.3 shows the correlation they found between the known emission rate and the maximum CH_4 enhancement from each transect downwind the release location using the release experiments first presented in Fischer et al. (2017). Similar to the first equation, distance is not included in the equation and the emission rate is derived when performing several transects next to an emission outlet location. The maximum CH_4 signals from different transects along the same leak (not necessarily on the same street) are clustered and averaged together within 30 m distance. In this equation, CH_4 enhancements are only considered for the quantification if those are greater than 10% above the threshold which gives the minimum CH_4 emission rate of 0.5 L min^{-1}.

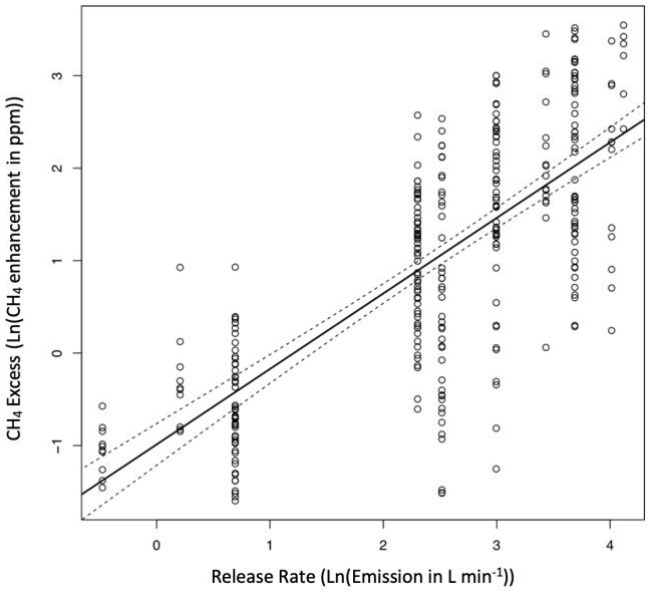

Figure 1.3. Correlation of CH_4 enhancement in ppm and the known release rates, basis for the empirical mobile quantification method, both axes are on natural logarithmic scale (Figure from Weller et al., 2018).

In the first algorithm, they defined CH_4 background in a moving average time window to 2 minutes to be large enough to cover the CH_4 variation in time and small enough to not be affected by large plumes. However, in the second algorithm they redefined the background extraction method to a median of all CH_4 values 2.5 minutes before and after each point. After applying the second method they reported that this method results higher number of CH_4 signals on the same datasets because background is less affected by large plumes in the second version. For example, in Dallas (Texas, USA) they reported 390 CH_4 signals based on the second algorithm, while it was 353 signals from the first version. In the second version, they used larger buffer (30 m) which resulted in lowering emission points. In the case of Dallas,

they reported 23 emission points compared to the 57 emission points from the first algorithm. The total emission report for this city were 1226 L min^{-1} and 1913 L min^{-1} from the first and second equations respectively.

1.7.3 Urban CH_4 emission attribution

In urban areas, natural gas leaks, emissions from the sewage system, and combustion-related emissions are the most prominent sources. Concurrent emissions of C_2H_6, CO_2, and the isotopic signatures of CH_4 can help to attribute the observed emissions. All these datasets individually or together can give a better understanding of spatially distributed CH_4 plumes.

Townsend-Small et al. (2012) used stationary measurements of $\delta^{13}C\text{-}CH_4$, $\delta D\text{-}CH_4$ and radiocarbon ($\Delta^{14}C\text{-}CH_4$) in Los Angeles, USA. Their results show that the main source of CH_4 emission in Los Angeles has $\delta^{13}C\text{-}CH_4$ of −41.5‰, $\delta D\text{-}CH_4$ between −229 and −208‰ and $\Delta^{14}C\text{-}CH_4$ in the range of +262 to +344‰. They conclude that the major source of emission in Los Angles can be attributed to emissions from fossil fuel activities.

Gioli et al. (2012) evaluated long-term CH_4 and CO_2 measurements from a 3-m high eddy-covariance tower in the city center of Florence, Italy and reported contributions of CH_4 emissions from road traffic, heating systems and gas leaks from the distribution network using multi-regression modelling with the use of traffic and natural gas consumption data from inventory. They concluded that about 15% of the CH_4 emissions can be attributed to the road traffic and heating system emissions while 85% of the CH_4 can be attributed to the leaks from the natural gas distribution network.

Zazzeri et al. (2017) evaluated continuous measurements of CH_4, CO_2, and $\delta^{13}C\text{-}CH_4$ from a stationery measurement location in central London and compared their finding with the reports from the National Atmospheric Emissions Inventory (NAEI) which has spatial resolution of 1*1 km to report emissions on yearly basis for the UK. They also carried out mobile measurements for source mapping around the stationary location. They found out that $\delta^{13}C\text{-}CH_4$ from the inventory was 2‰ more depleted than what they found in their measurements, −45.7 ±0.5‰. From the inventory the emission contribution is mostly from the waste sector which accounts for 53% of emissions in the study area while the contribution of fossil emissions was 29%. This is not in line with the measurements of this study which suggest a higher contribution of fossil emissions in this study area in London.

Zimnoch et al. (2019) measured atmospheric mixing ratio of CH_4 along with its isotopic signatures to quantify and attribute emissions in the urban area of Krakow, Poland, which is the second most populated city in this country. They reported emission fluxes of 140 μmol-CH_4 m^{-2} h^{-1} for the period of 1996 to 1997 for this city and by evaluating $\delta^{13}C\text{-}CH_4$, they found very close atmospheric isotopic signatures of CH_4 ($\delta^{13}C\text{-}CH_4 = 54.2$‰) to the $\delta^{13}C\text{-}CH_4$ signature of natural gas in the network ($\delta^{13}C\text{-}CH_4 = -54.4 \pm 0.6$‰), and concluded that the majority of anthropogenic emissions in Krakow could be attributed to the leaky pipelines.

1.8 Scope of the present thesis

Although urban areas significantly contribute to the total anthropogenic GHGs emissions, there have been few studies prior to this thesis about mobile CH_4 emissions in Europe. Thus, we designed four campaigns in three European cities and provide the results in this thesis.

In chapter 2 and 3, we present results and analyses of street-level CH_4 measurements in three European cities. We use these datasets to investigate how the CH_4 emissions are distributed across the urban areas and how the emissions are distributed in terms of emission rate (large and small emission points). We focus on using co-emitted tracers and isotopic composition for source attribution and estimate the contributions of the different source categories in the different cities to the total emissions that we derive from the street-level measurements.

In chapter 4 we report results form an intercomparison campaign of three different methods to quantify CH_4 emissions from urban gas pipeline leaks and discuss the strengths and limitations of methods, and the relevance for national emission inventories.

In chapter 5 we provide the conclusions from the measurement campaigns we had in urban areas with details about strengths and limitations of the mobile detection and quantification method. We describe the importance of source attribution for data interpretation and its benefit for network maintenance. At the end, we provide an outlook on how these studies could be extended or adapted in other countries and how they can be brought out of the academic world to the commercial market for speeding up CH_4 emission mitigation policies.

2 Methane mapping, emission quantification, and attribution in two European cities; Utrecht, NL and Hamburg, DE

Hossein Maazallahi[1,2], Julianne M. Fernandez[3], Malika Menoud[1], Daniel Zavala-Araiza[1,4], Zachary D. Weller[5], Stefan Schwietzke[6], Joseph C. von Fischer[7], Hugo Denier van der Gon[2], and Thomas Röckmann[1]

[1]Institute for Marine and Atmospheric research Utrecht (IMAU), Utrecht University (UU), Utrecht, The Netherlands
[2]Netherlands Organisation for Applied Scientific Research (TNO), Utrecht, The Netherlands
[3]Department of Earth Sciences, Royal Holloway University of London (RHUL), Egham, United Kingdom
[4]Environmental Defense Fund (EDF), Utrecht, The Netherlands
[5]Department of Statistics, Colorado State University (CSU), United States of America
[6]Environmental Defense Fund (EDF), Berlin, Germany
[7]Department of Biology, Colorado State University (CSU), United States of America

Abstract. Characterizing and attributing CH_4 emissions across varying scales is important from environmental, safety, and economic perspectives, and is essential for designing and evaluating effective mitigation strategies. Mobile real-time measurements of CH_4 in ambient air offer a fast and effective method to identify and quantify local CH_4 emissions in urban areas. We carried out extensive campaigns to measure CH_4 mole fractions at the street level in Utrecht, The Netherlands (2018 and 2019) and Hamburg, Germany (2018). We detected 145 leak indications (LIs, i.e., CH_4 enhancements of more than 10% above background levels) in Hamburg and 81 LIs in Utrecht. Measurements of the ethane-to-methane ratio (C_2:C_1), methane-to-carbon dioxide ratio (CH_4:CO_2), and CH_4 isotope composition (δ^{13}C-CH_4 and δD-CH_4) show that in Hamburg about 1/3 of the LIs, and in Utrecht 2/3 of the LIs (based on a limited set of C_2:C_1 measurements), were of fossil fuel origin. We find that in both cities the largest emission rates in the identified LI distribution are from fossil fuel sources. In Hamburg, the lower emission rates in the identified LI distribution are often associated with biogenic characteristics, or partly combustion. Extrapolation of detected LI rates along the roads driven to the gas distribution pipes in the entire road network yields total emissions from sources that can be quantified in the street-level surveys of 440 ± 70 t yr^{-1} from all sources in Hamburg, and 150 ± 50 t yr^{-1} for Utrecht. In Hamburg, C_2:C_1, CH_4:CO_2, and isotope-based source attributions shows that 50 - 80 % of all emissions originate from the natural gas distribution network, in Utrecht more limited attribution indicates that 70 - 90 % of the emissions are of fossil origin. Our results confirm previous observations that a few large LIs, creating a heavy tail, are responsible for a significant proportion of fossil CH_4 emissions. In Utrecht, 1/3 of total emissions originated from one LI and in Hamburg >1/4 from 2 LIs. The largest leaks were located and fixed quickly by GasNetz Hamburg once the LIs were shared, but 80 % of the (smaller) LIs attributed to the fossil category could not be detected/confirmed as pipeline leaks. This issue requires further investigation.

2.1 Introduction

CH_4 is the second most important anthropogenic greenhouse gas (GHG) after CO_2 with a global warming potential of 84 compared to CO_2 over a 20-year time horizon (Myhre et al., 2013). The increase of CH_4 mole fraction from about 0.7 parts per million (ppm) or 700 parts per billion (ppb) in pre-industrial times (Etheridge et al., 1998; MacFarling Meure et al., 2006) to almost 1.8 ppm at present (Turner et al., 2019) is responsible for about 0.5 W m^{-2} of the total 2.4 W m^{-2} radiative forcing since 1750 (Etminan et al., 2016; Myhre et al., 2013). In addition to its direct radiative effect, CH_4 plays an important role in tropospheric chemistry and affects the mixing ratio of other atmospheric compounds, including direct and indirect greenhouse gases, via reaction with the hydroxyl radical (OH), the main loss process of CH_4 (Schmidt and Shindell, 2003). In the stratosphere CH_4 is the main source of water vapor (H_2O) (Noël et al., 2018), which adds another aspect to its radiative forcing. Via these interactions the radiative impact of CH_4 is actually higher than what can be ascribed to its mixing ratio increase alone, and the total radiative forcing ascribed to emissions of CH_4 is estimated to be almost 1 W m^{-2}, ≈ 60 % of that of CO_2 (Fig 8.17 in Myhre et al., 2013). Given this strong radiative effect, and its relatively short atmospheric lifetime of about 9.1 ± 0.9 yr (Prather et al., 2012), CH_4 is an attractive target for short- and medium-term mitigation of global climate change as mitigation will yield rapid reduction in warming rates.

CH_4 emissions originate from a wide variety of natural and anthropogenic sources, for example emissions from natural wetlands, agriculture (e.g. ruminants or rice agriculture), waste decomposition, or emissions (intended and non-intended) from oil and gas activities that are associated with production, transport, processing, distribution, and end-use of fossil fuel sector (Heilig, 1994). Fugitive unintended and operation-related emissions occur across the entire oil and natural gas supply chain. In the past decade, numerous large studies have provided better estimates of the emissions from extended oil and gas production basins (Allen et al., 2013; Karion et al., 2013; Omara et al., 2016; Zavala-Araiza et al., 2015; Lyon et al., 2015), the gathering and processing phase (Mitchell et al., 2015), and transmission and storage (Zimmerle et al., 2015; Lyon et al., 2016) in the United States (US). A recent synthesis

concludes that the national emission inventory of the US Environmental Protection Agency (EPA) underestimated supply chain emissions by as much as 60 % (Alvarez et al., 2018). McKain et al. (2015) discussed how inventories may underestimate the total CH_4 emission for cities. Also, an analysis of global isotopic composition data suggests that fossil related emissions may be 60 % higher than what has been previously estimated (Schwietzke et al., 2016). A strong underestimate of fossil fuel related emissions of CH_4 was also implied by analysis of $\delta^{14}C$-CH_4 in pre-industrial air (Hmiel et al., 2020). These emissions do not only have adverse effects on climate, but also represent an economic loss (Xu and Jiang, 2017) and a potential safety hazard (West et al., 2006). While CH_4 is the main component in natural gas distribution networks (NGDNs), composition of natural gas varies from one country or region to another. In Europe the national authorities provide specifications on components of natural gas in the distribution network (Table 8 in UNI MISKOLC and ETE, 2008).

Regarding CH_4 emissions from NGDNs, a number of intensive CH_4 surveys with novel mobile high precision laser-based gas analyzers in US cities have recently revealed the widespread presence of leak indications (LIs: CH_4 enhancements of more than 10 % above background level) with a wide range of magnitudes (Weller et al., 2020; Weller et al., 2018; von Fischer et al., 2017; Chamberlain et al., 2016; Hopkins et al., 2016b; Jackson et al., 2014; Phillips et al., 2013). The number and severity of natural gas leaks appears to depend on pipeline material and age, local environmental conditions, pipeline maintenance and replacement programs (von Fischer et al., 2017; Gallagher et al., 2015; Hendrick et al., 2016). For example, NGDNs in older cities with a larger fraction of cast iron or bare steel pipes showed more frequent leaks than NGDNs that use the newer plastic pipes. The data on CH_4 leak indications from distribution systems in cities have provided valuable data for emission reduction in the US cities which allows local distribution companies (LDCs) who are in charge of NGDN to quickly fix leaks and allocate resources efficiently (Weller et al., 2018, von Fischer et al., 2017, Lamb et al., 2016; McKain et al., 2015).

Urban European cities CH_4 emissions are not well known, which requires carrying out extensive campaigns to collect required observation data. Few studies have estimated urban CH_4 fluxes using eddy covariance measurements (Gioli et al., 2012; Helfter et al., 2016), airborne mass balance approaches (O'Shea et al., 2014) and the Radon-222 flux and mixing layer height techniques (Zimnoch et al., 2019). Gioli et al. (2012) showed that about 85 % of CH_4 emissions in Florence, Italy originated from natural gas leaks. Helfter et al. (2016) estimated CH_4 emissions of 72 ± 3 t km^{-2} yr^{-1} in London, UK mainly from sewer sesytem and NGDNs leaks, which is twice as much as reported in the London Atmospheric Emissions Inventory. O'Shea et al. (2014) also showed that CH_4 emissions in greater London is about 3.4 times larger than the report from UK National Atmospheric Emission Inventory. Zimnoch et al. (2019) estimated CH_4 emissions of $(6.2 \pm 0.4) \times 10^6$ m^3 $year^{-1}$ for Kraków, Poland, based on data for the period of 2005 to 2008 and concluded that leaks from NGDNs are the main emission source in Kraków, based on carbon isotopic signature of CH_4. Chen et al. (2020) also showed that incomplete combustion or loss from temporarily installed natural gas appliances during big festivals can be the major source of CH_4 emissions from such events, while these emissions have not been included in inventory reports for urban emissions.

Here we present the result of mobile in-situ measurements at street level for whole-city surveys in two European cities, Utrecht in the Netherlands (NL) and Hamburg in Germany (DE). In this study, we quantified LIs emissions using an empirical equation from Weller et al. (2019), which was designed based on controlled release experiments from von Fischer et al. (2017), to quantify ground-level emissions locations in urban area such as leaks from NGDN. In addition to finding and categorizing the CH_4 enhancements (in a similar manner as done for the US cities in order to facilitate comparability), we made three additional measurements to better facilitate source attribution: the concomitant emission of C_2H_6 and CO_2, and the carbon and hydrogen isotopic composition of the CH_4. These tracers allow an empirically based source attribution for LIs. In addition to emission quantifications of LIs across the urban areas in these two cities, we also quantified CH_4 emissions from some of facilities within the municipal boundary of Utrecht and Hamburg using Gaussian plume dispersion model (GPDM).

2.2 Materials and methods

2.2.1 Data collection and instrumentation

2.2.1.1 Mobile measurements for attribution and quantification

Mobile atmospheric measurements at street level were conducted using two Cavity Ring-Down Spectroscopy (CRDS) analyzers (Picarro Inc. model G2301 and G4302) which were installed on the back seat of a 2012 Volkswagen Transporter, (see supplementary information (SI), Sect. 2.S.1.1, Figure 2.S1). The model G2301 instrument provides atmospheric mole fraction measurements of CO_2, CH_4 and H_2O, each of them with an integration time of about 1 s., which results in a data frequency of ≈ 0.3 Hz for each species. The reproducibility for CH_4 measurements was ≈ 1 ppb for 1 s integration time. The G2301 instrument was powered by a 12 V car battery via a DC-to-AC converter. The flow rate was ≈ 187 ml min^{-1}. Given the volume and pressure of the measurement cell (volume = 50 ml and pressure ≈ 190 mbar) the cell is flushed approximately every 3 s, so observed enhancements are considerably smoothed out. The factory settings for CH_4 and CO_2 were used for the water correction.

The G4302 instrument is a mobile analyzer that provides atmospheric mole fraction measurements of C_2H_6, CH_4, and H_2O. The flow rate is 2.2 L min^{-1} and the volume of the cell is 35 ml (operated at 600 mb, thus 21 ml STP) so the cell is flushed in 0.01 s, which means that mixing is insignificant given the 1 s measurement frequency of the G4302. The additional measurement of C_2H_6 is useful for source attribution since natural gas almost always contains a significant fraction of C_2H_6, whereas microbial sources generally do not emit C_2H_6 (Yacovitch et al., 2014). The G4302 runs on a built-in battery which lasts for ≈ 6 h. The instrument can be operated in two modes at ≈ 1 Hz frequency for each species: the CH_4-only mode and the CH_4 - C_2H_6 mode. In the CH_4-only mode the instrument has a reproducibility of ≈10 ppb for CH_4. The factory settings for CH_4 and C_2H_6 were used for the water correction. In the CH_4 - C_2H_6 mode the reproducibility is about 100 ppb for CH_4 and 15 ppb for C_2H_6. For Utrecht surveys (see SI, Sect. 2.S.1.2, Figure 2.S2a), the G4302 was not yet available for the initial surveys in 2018, but it was added for the later re-visits (see SI, Sect. 2.S.1.2, Table 2.S1). For Hamburg (see SI, Sect. 2.S.1.2, Figure 2.S2b), both instruments operated during the entire intensive 3-week measurement campaign in Oct/Nov 2018 (see SI, Sect. 2.S.1.2, Table 2.S2). The time delay from the inlet to the instruments was measured and accounted for in the data processing procedure. The Coordinated Universal Time (UTC) time shifts between the Global Positioning System (GPS) and the two Picarro instruments were corrected for each instrument in addition to the inlet delay (see SI, Sect. 2.S.1.2, Table 2.S1 and Table 2.S2). The clocks on the Picarro instruments were set to UTC but showed drift over the period of the campaigns. We recorded the drifts for each day's survey and corrected to UTC time. The data were also corrected for the delay between air at the inlet and the signal in the CH_4 analyzers. This delay was determined by exposing the inlet to three small CH_4 pulses from exhaled breath, ranging from 5-30 seconds, depending on the instrument and tubing length. We averaged the three attempts to determine the delay for each instrument and used the delays for each instrument. Individual attempts were 1 to 2 s different from each other. For the G4302 the delay was generally about 5 s and for the G2301 it was about 30 s; the difference is mainly due to the different flow rates. The recorded CH_4 mole fractions were projected back along the driving track according to this delay.

One-quarter inch Teflon tubing was used to pull in air either from the front bumper (0.5 m above ground level) to the G2301 or from the rooftop (2 m above ground level) to the G4302. To avoid dust into the inlets for both instruments, Acrodisc® syringe filter, 0.2 μm was used for G2301 and Parker Balston 9933-05-DQ was used for G4302. The G2301 was used for quantification and attribution purposes and the G4302 mainly for attribution. After data quality check, a comparison between the two instruments during simultaneous measurements showed that all LIs were detectable by both instruments despite difference in inlet height (see SI, Sect. 2.S.1.3, Figure 2.S3). A comparison between the two instruments during simultaneous measurements showed that all LIs were detected by both instruments despite difference in instrument characteristics and inlet height. In the majority of cases CH_4 enhancements for each LI from both instruments were similar to each other. We note that there is likely a compensation of differences from two opposing effects between the two measurement systems. The

inlet of the G2301 was at the bumper, thus closer to the surface sources, but the rather low flow rate and measurement rate of the instrument lead to some smoothing of the signal in the cavity. Because of the high gas flow rate, signal smoothing is much reduced for the G4302, but the inlet was on top of the car, thus further away from the surface sources (see Table 2.S3 in SI, Sect. 2.S.1.3). The vehicle locations were registered using a GPS system that recorded the precise driving track during each survey.

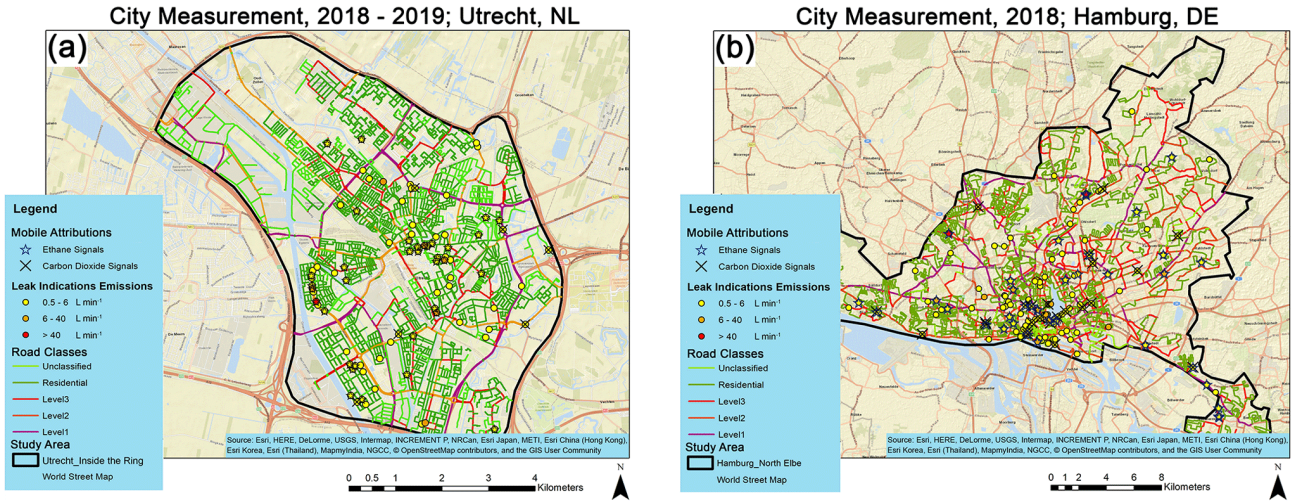

Figure 2.1. Locations of significant LIs for the categories on different street classes in (a) Utrecht and (b) Hamburg. Road colors indicate the street classes according to the OSM. Black polygons show urban study areas.

2.2.1.2 Target cities: Utrecht and Hamburg

Utrecht is the 4th largest city in the Netherlands with population of approximately 0.35 million inhabitants within an area of roughly 100 km^2. It is located close to the center of the Netherlands and is an important infrastructural hub in the country. The Utrecht city area that we target in this study is well constrained by a ring of highways around the city (A27, A12, A2, and N230) with inhabitants of approximately 0.28 million living within this ring on roughly 45 km^2 of land. Figure 2.S2a (see SI, Sect. 2.S.1.2) shows the streets that were driven in Utrecht and Figure 2.1a shows the street coverage over four street categories (level 1, 2, 3, residential, and unclassified) obtained from the Open Street Map (OSM; www.openstreetmap.org). Table 2.S4 (see SI, Sect. 2.S.1.5) provides information on road coverage based on different street categories. The hierarchy of OSM road classes is based on the importance of roads in connecting parts of the national infrastructure. Level 1 roads are primarily larger roads connecting cities, level 2 roads are the second most important roads and part of a greater network to connect smaller towns, level 3 roads have tertiary importance level and connect smaller settlements and districts. Residential roads are roads which connect houses and unclassified roads have the lowest importance of interconnecting infrastructure. Moreover, several transects were also made to measure the atmospheric mole fraction of CH_4 from the road next to the waste water treatment plant (WWTP) in Utrecht – a potentially larger single source of CH_4 emissions in the city (see SI, Sect. 2.S.1.6, Table 2.S5).

Hamburg is the 2nd largest city in Germany (about 1.9 million inhabitants, 760 km^2 area) and hosts one of the largest harbors in Europe. The study area in Hamburg is North of the Elbe river (Figure 2.1b) with ≈1.4 million inhabitants on about 400 km^2 land. Figure 2.S2b (see SI, Sect. 2.S.1.2) shows the streets that were covered in Hamburg and Figure 2.1b shows the street coverage categorized in the four categories of OSM. More information on road coverage based on OSM street categories are provided in Table 2.S4 (see SI, Sect. 2.S.1.5). The Local Distribution Companies (LDCs) in Utrecht (STEDIN; https://www.stedin.net/, last access: 30 September 2020) and Hamburg (GasNetz Hamburg;

https://www.gasnetz-hamburg.de, last access: 20 October 2020) confirmed that full pipeline coverages are available beneath all streets. Therefore, the length of roads in the study area of Utrecht and Hamburg are representatives of NGDNs length. The Hamburg harbor area hosts several large industrial facilities that are related to the midstream / downstream oil and gas sector including refineries and storage tanks. An oil production site (oil well, separator and storage tanks) at Allermöhe (in Hamburg-Bergedorf) was also visited. Information from the State Authority for Mining, Energy and Geology (LBEG, 2018) was used to locate facilities. Precise locations of the facilities surveyed are given in the Table 2.S6 (see SI, Sect. 2.S.1.6). In order to separate these industrial activities from the NGDNs emissions in this study, CH_4 emissions from these locations were estimated, but evaluated apart from the emissions found in each city. The reported in-situ measurement, GPS data, and boundary of study areas reported here are available on the Integrated Carbon Observation System (ICOS) portal (Maazallahi et al., 2020b).

2.2.1.3 Driving strategy

The start/end point for each day's measurement surveys across Utrecht and Hamburg were the Institute for Marine and Atmospheric research Utrecht (IMAU; Utrecht University) and the Meteorological Institute (MI; Hamburg University), respectively. From these starting locations, each day's surveys targeted the different districts and neighborhoods of the cities (see SI, Sect. 2.S.1.2, Table S1 and Table 2.S2). Measurement time periods and survey areas were chosen to select favorable traffic and weather conditions and to avoid large events (e.g., construction; see SI, Sect. 2.S.1.5, Figure 2.S4), which normally took place between 10 - 18 LT. Average driving speeds on city streets were in the range of 17 ± 7 km h^{-1} in Utrecht and 20 ± 6 km h^{-1} in Hamburg.

As part of our driving strategy, we revisited locations where we had observed enhanced CH_4 readings (see SI, Sect. 2.S.1.7, Figure 2.S5). Not all recorded CH_4 mole fraction enhancements are necessarily the result of a stationary CH_4 source. For example, they could be related to emissions from vehicles which run on compressed natural gas, or vehicles operated with traditional fuels but with faulty catalytic converter systems. Later we will discuss how to exclude or categorize these unintended signals (see Sect. 2.2.2 and Sect. 2.3.1). Therefore, we revisited a large number of locations (65 in Utrecht (≈80 %) and 100 in Hamburg (≈70 %)) where enhanced CH_4 had been observed in during the first survey in order to confirm the LIs. In contrast to the measurements carried out in many cities in the United States (US) (von Fischer et al., 2017), our measurements were not carried out using Google Street View cars, but with a vehicle from the Institute for Marine and Atmospheric research Utrecht (IMAU), Utrecht University (see SI, Sect. 2.S.1.1, Figure 2.S1). Due to time and budget restrictions, it was not possible to cover each street at least twice, as done for the US cities. After evaluation of the untargeted first surveys that covered each street at least once, targeted surveys were carried out for verification of observed LIs and for collection of air samples at locations with high CH_4 enhancements. The rationale behind this measurement strategy is that if an enhancement was not recorded during the first survey, it obviously cannot be verified in the second survey. The implications of the difference in the measurement strategy will be discussed in the Results and Discussion sections below.

In total, approximately 1,300 km of roads were driven during Utrecht surveys and about 2,500 km during the Hamburg campaign. In Utrecht, some re-visits were carried out several months to a year after the initial surveys in order to check on the persistence of the LIs. In Hamburg, revisits were also performed within the 4-week intensive measurement period. Further details about the driving logistics are provided in the SI (Sect. 2.S.1.6, Table 2.S1 and Table 2.S2). It is possible that pipeline leaks that were detected during the initial survey were repaired before the revisit, and the chance of this occurring increases as the time interval between visits gets longer.

2.2.1.4 Air sample collection for attribution

In addition to the mobile measurement of C_2H_6 and CO_2 for LIs attributions purposes, samples for lab isotope analysis of $\delta^{13}C$-CH_4 and δD-CH_4 were collected during the revisits at locations that had displayed high CH_4 enhancements during the first surveys. Depending on the accessibility and traffic,

samples were either taken inside the car (see SI, Sect. 2.S.1.8, Figure 2.S6a) using a tubing from the bumper inlet, or outside the car on foot using the readings from the G4302 to find the best location within the plume (see SI, Sect. 2.S.1.8, Figure 2.S6b). All the samples taken in the North Elbe study area and from most of the facilities were collected when the car was parked, but the samples inside the New Elbe tunnel and close to some facilities where there was no possibility to park were taken in motion while we were within the plume. The sampling locations across the North Elbe study area of Hamburg were determined based the untargeted surveys, and the confirmation during revisits. The C_2H_6 information was not used in the selection of sampling locations in order to avoid biased sampling. Sampling locations from the facilities were determined based on wind direction, traffic, and types of different activities. Samples for isotope analysis were collected in non-transparent aluminum-coated Tedlar Supelco, Seupel^{TM} Inert SCV Gas Sampling Bag (2 L) and SKC, Standard FlexFoil® Air Sample Bags (3 L) using a 12 V pump and 1/4-inch Teflon tubing which pumps air with flow rate of ≈0.25 L min^{-1}. In total, 103 bag samples were collected at 24 locations in Hamburg, 14 of them in the city area North of the Elbe river and 10 at larger facilities. Usually, three individual samples were collected at each source location, plus several background air samples on each sampling day. This sampling scheme generally results in a range of mole fractions that allow source identification using a Keeling plot analysis (Keeling, 1958, 1961). Fossil CH_4 sources in the study areas of this paper (inside the ring for Utrecht and north Elbe in Hamburg) refers to emissions originating from natural gas leaks.

2.2.1.5 Meteorological Data

Meteorological information reflecting the large scale wind conditions during the campaigns were obtained from measurements at the Cabauw tower (51.970263° N, 4.926267° E) operated by Koninklijk Nederlands Meteorologisch Instituut (KNMI) (Van Ulden and Wieringa, 1996) for Utrecht and Billwerder tower (53.5192° N, 10.1029° E) operated by the MI at Hamburg University (Brümmer et al., 2012) for Hamburg. The wind direction and wind speed data from the masts were used for planning the surveys. Pressure and temperature measurements were used to convert volume to mass fluxes for CH_4. We also used information from the towers for the GPDM calculations of the emission rates from larger facilities, because the local wind measurements from the 2-D anemometer were not logged continuously due to failure in logging setup of the measurements. In Utrecht, the Cabauw tower is located about 20 km from the WWTP. In Hamburg Billwerder tower is about 18 km from the Soil and Compost company and about 8 km from oil production facilities. Uncertainties over the wind data will be described later.

2.2.2 Emission quantification

2.2.2.1 Data preparation and background extraction of mobile measurements

The first step of the evaluation procedure is quality control of the data from both CH_4 analyzers and the GPS records. Periods of instrument malfunction and unintended signals based on notes written during each day's measurements were removed from the raw data. Extraction of the LIs from in-situ measurements requires estimation of the background levels (see SI, Sect. 2.S.2.1, Figure 2.S7). We estimated CH_4 background as the median value of ± 2.5 min of measurements around each individual point as suggested in Weller et al. (2019). For estimating the CO_2 background level we used the 5th percentile of ± 2.5 min of measurements around each individual point (Brantley et al., 2014; Bukowiecki et al., 2002). The background determination method for CH_4 was selected from Weller et al. (2019) to follow the emission quantification algorithm for the urban studies, and while this algorithm doesn't include background extraction for CO_2, we chose commonly adopted method of background determination for this component. These background signals were subtracted from the measurement time series to calculate the CH_4 and CO_2 enhancements. For C_2H_6, the background was considered zero as it is normally present at a very low mole fraction; between ~0.4-2.5 ppb (Helmig et al., 2016), and is lower than the G4302 detection limit.

2.2.2.2 Quantification of methane emissions from leak indications

We wrote an automated MATLAB® script (available on GitHub from Maazallahi et al. (2020a)) based on the approach initially introduced in von Fischer et al. (2017), and improved in Weller et al. (2019). This algorithm was designed to quantify CH_4 emissions from ground-level emission release locations within 5-40 m from the measurement (von Fischer et al., 2017), such as pipeline leaks and has been demonstrated that the algorithm adequately estimates the majority of those emissions from a city (Weller et al., 2018). Using the same algorithm also ensures that results are comparable between European and US cities. The individual steps will be described below. Mapping and spatial analysis were conducted using Google Earth and ESRI ArcMap software. A flow diagram of the evaluation procedure is provided in the SI (Sect. 2.S.2.2, Figure 2.S8).

Following the algorithm from von Fischer et al. (2017), measurements at speeds above 70 km h^{-1} were excluded, as the data from the controlled release experiments (von Fischer et al., 2017) were not reliable at high speed (Weller et al., 2019). We also excluded measurements during periods of zero speed (stationary vehicle) to avoid unintended signals coming from other cars running on compressed natural gas when the measurement car was stopped in traffic. In order to merge the sharp 1 Hz-frequency records of the GPS with the ≈ 0.3 Hz data from the G2301 analyzer, the CH_4 mole fractions were linearly interpolated to the GPS times.

Weller et al., (2019) established an empirical equation to convert LIs observed with a Picarro G2301 in a moving vehicle in urban environments into emission rates based on a large number of controlled release experiments in various environments (Eq. (2.1)).

$$\mathrm{Ln}(C) = -0.988 + 0.817 * \mathrm{Ln}(Q) \quad (2.1)$$

In this equation, C represents CH_4 enhancements above the background in ppm and Q is the emission rate in L min^{-1}. Weller et al., (2019) used controlled releases to demonstrate that the magnitude of the observed CH_4 enhancement is related to the emission rate and carefully characterized the limitations and associated errors of this equation. We used Eq. (1) to convert CH_4 enhancements encountered during our measurements in Utrecht and Hamburg to emission rates, and we use these estimates to categorize LIs into three classes: high (emission rate > 40 L min^{-1}), medium (emission rate 6− 40 L min^{-1}) and low (emission rate 0.5 - 6 L min^{-1}), following the categories from von Fischer et al. (2017) (Table 2.1).

Table 2.1. Natural gas distribution network CH_4 emission categories.

Class	CH_4 Enhancement (ppm)	Equivalent Emission Rate (L min^{-1})	Equivalent Emission Rate (≈ kg hr^{-1})	LI Location Colour (Figure 2.1, Figure 2.2, and Figure 2.S14)
High	>7.6	>40	>1.7	Red
Medium	1.6-7.59	6 - 40	0.3 – 1.7	Orange
Low	0.2-1.59	0.5 - 6	0.0 – 0.3	Yellow

The spatial extent of individual LIs was estimated as the distance between the location where the CH_4 mole fraction exceeded the background by more than 10 % (≈ 0.200 ppm; as used in von Fischer et al. (2017) and Weller et al. (2019)) to the location where it fell below this threshold level again. LIs which stay above the threshold for more than 160 m were excluded in the automated evaluation because we suspect that such extended enhancements are most likely not related to leaks from the NGDN (von Fischer et al., 2017).

In a continuous measurement survey on a single day, consecutive CH_4 enhancements above background observed within 5 seconds were aggregated and the location of the emission source was

estimated based on the weighted averaging of coordinates (Eq. (2.2)). Decimal degree coordinates were converted to Cartesian coordinates (see SI, Sect. 2.S.2.3, Figure 2.S9) relative to local references (see SI, Sect. 2.S.2.3, Table 2.S7). In Utrecht, the Cathedral tower (Domtoren) and in Hamburg the St. Nicholas' Church were selected as local geographic datums. LIs observed on different days at similar locations were clustered and interpreted as one point source when circles of 30 m radius around the centre locations overlapped, similar to Weller et al., (2019). The enhancement of the cluster was assigned the maximum observed mole fraction and located as the weighted average of the geographical coordinates of the LIs within that cluster (Eq. (2.2) from Weller et al. (2019)), where w_i is CH_4 enhancement of each LI.

$$(\text{lon, lat}) = \frac{\sum_{i=1}^{n} w_i * (lon_i, lat_i)}{\sum_{i=1}^{n} w_i} \quad (2.2)$$

We compared the outputs of our software to the one developed by Colorado State University (CSU) for the surveys in US cities (von Fischer et al., 2017; Weller et al., 2019). 30 LIs were detected and no significant differences were observed (linear fit equation y = 1.00 * x - 0.00, $R^2 = 0.99$) (see SI, Sect. 2.S.2.4, Figure 2.S10). As mentioned above, in our campaign-type studies not all streets were visited twice, so this criterion was dropped from the CSU algorithm. Instead, we used explicit source attribution by co-emitted tracers.

The emission rate per km of road covered during our measurements was then scaled up to the city scale using the ratio of total road length within the study area boundaries derived from OSM to the length of streets covered, and converted to a per-capita emission using the population in the study areas based on LandScan data (Bright et al., 2000). Note that in this up-scaling practice, emission quantified from facilities were excluded.

To account for the emission uncertainty, similar to Weller et al. (2018) for the US city studies, we used a bootstrap technique which was initially introduced in Efron (1979, 1982), as this technique is adequate in resampling of both parametric and non-parametric problems with even non-normal distribution of observed data. Tong et al. (2012) indicated that bootstrap resampling technique is sufficiently capable in estimating uncertainty of emissions with sample size of equal or larger than 9. Efron and Tibshirani (1993) suggested that minimum of 1,000 iterations are adequate in bootstrap technique. In this study, we used non-parametric bootstrap technique to account for the uncertainty of total CH_4 emissions from all LIs in each city with 30,000 replications. As mentioned above the algorithm is based on CH_4 enhancements of measurement with 5-40 m distance from controlled release location, and can produce large uncertainty for emission quantification of individual LI (Figure 4 in Weller et al. (2019)), but with sufficient number of sample size, the uncertainty associated with total emission quantified in an urban area is more precise.

2.2.2.3 Quantification of methane emissions from larger facilities

Apart from the natural gas distribution network, there are larger facilities in both cities that are potential CH_4 sources within the study area. Several facilities in or around the cities were visited during the mobile surveys to provide emission estimates. We applied a standard point source GPDM (Turner, 1969) to quantify CH_4 emissions from these larger facilities. A flowchart describing the steps taken during quantification from facilities in given in SI (Sect. 2.S.2.5., Figure 2.S11). We note that emission quantification using GPDM with data from mobile measurements is prone to large errors (factor of 3 or more) (Yacovitch et al., 2018) especially when the measurements are carried out close to the source. In this study, we also report the data obtained from larger facilities, since rough emission estimates from facilities can be obtained in the city surveys. Caulton et al. (2018) discuss uncertainties of emission quantification with GPDM. Individual facilities were visited during the routine screening measurements and during revisits for LI confirmation and air sampling.

In Utrecht, the WWTP is located in the study area and streets around this facility were passed several times during surveys. In Hamburg, we initially performed screening measurements in the harbor area (extensive industrial activities) and near an oil production site and then revisited these sites for further quantification and isotopic characterization. The data from the oil production site can be fit reasonably well with a GPDM and were therefore selected for quantification, similar to studies in a shale gas production basin in the USA (Yacovitch et al., 2015) and in the Netherlands (Yacovitch et al., 2018).

$$C(x,y,z) = \frac{Q}{2*\pi*u*\sigma_y*\sigma_z} * \{ \exp\left(\frac{-(z-z_{source})^2}{2*\sigma_z^2}\right) + \exp\left(\frac{-(z+z_{source})^2}{2*\sigma_z^2}\right)\} * \exp\left(\frac{-y^2}{2*\sigma_y^2}\right)\} \quad (2.3)$$

In Eq. (2.3), C is the CH_4 enhancement converted to the unit of g/m^3 at cartesian coordinates x, y, and z relative to the source ($[x\ y\ z]_{source} = 0$), x is the distance of the plume from the source aligned with the wind direction, y is the horizontal axis perpendicular to the wind direction, z is the vertical axis. Q is emission rate in $g\ s^{-1}$, u ($m\ s^{-1}$) is the wind speed along the x-axis, and σ_y and σ_z are the horizontal and vertical plume dispersion parameters (described below), respectively.

Determination of an effective release location is a challenge for the larger facilities. Effective emission locations for each facility were estimated based on wind direction measurements and the locations of maximum CH_4 enhancements. The facilities were generally visited multiple times under different wind conditions. The locations of the maximum CH_4 enhancements were then projected against the ambient wind, and the intersection point of these projections during different wind conditions was defined as effective emission location of the facility. At least two measurement transects with different wind direction were used to estimate the effective location of the source. If wind directions, road accessibility or the shape of plumes were not sufficient to indicate the effective source location, the geographical coordinates of centroids of the possible sources using Google Earth imageries and field observations were used to determine the effective emission location. For the WWTP in Utrecht we also contacted the operator and asked for the location of sludge treatment as it is the major source of CH_4 emissions (Paredes et al., 2019; Schaum et al., 2015).

Neumann and Halbritter (1980) showed that the main parameters in sensitivity analysis of GPDM are the wind speed and source emission height in close distance and the influence of emission height become less further downwind compared to the mixing layer height. In this study, the heights of emission sources were low (<10m) and estimated during surveys and/or using Google Earth imageries, and considering that such a larger measurement distance from the facilities, the main sources of uncertainty of the emission estimates for the WWTP and Compost and Soil company are most likely the mean wind speed and for the upstream facilities in Hamburg the major sources of uncertainties can be the mean wind speed and emission height. We considered 0-4 m source height for the WWTP in Utrecht, and for the upstream facilities in Hamburg we considered 0-5 m emission height for the Compost and Soil site, 0-2 m for the separator, 0-10 m for the storage tank, and 0-1 m for the oil extraction well-head. We used 1 m interval for each of these height ranges to quantify emissions in GPDM.

Cross wind horizontal dispersions σ_y were estimated from the measured plumes by fitting a Gaussian curve to the individual plumes from each set during each day's survey. A set of plumes is defined as a back to back transects during a period of time downwind each facility on different days. Later average emissions from all sets of plumes were used to report CH_4 emission for each of the facilities. A suitable Pasquill–Gifford stability class was then determined by selecting a pair of parameters (Table 1-1 in EPA, 1995) that matches best and give the closest number to the with the fitted value of σ_y. Vertical dispersions σ_z were then estimated using the identified Pasquill–Gifford stability class in the first step, using the distances to the source locations (Table 1-2 in EPA, 1995). Uncertainties due to these estimates will be discussed below. Mass emission rates were calculated using the metric

volume of CH_4 at 1 bar of atmospheric pressure (0.715 kg m^{-3} at 0 °C and 0.666 kg m^{-3} at 20 °C, P. 1.124 in IPCC, 1996), and linear interpolation was used for temperatures in between.

Due to technical issues, local wind data were not logged continuously and thus we used wind data from two towers which are 8 to 20 km away from the facilities we focused for emission quantifications. These distances introduce extra uncertainties in analyzing the emissions using GPDM mainly on the wind speed. By comparing some of the local high-quality wind data to data from the towers, we estimated that the local wind speed is within the range of ± 30 % of the collected tower data. This range was adopted to estimate the wind speed for emission quantifications for the set of plumes measured downwind of the facilities. The wind directions were aligned at local scale of each facility based on the locations of sources and locations of maxima of average CH_4 enhancements from a set of transects in each day's survey and we considered ± 5° uncertainty in wind direction for the GPDM quantification.

2.2.3 Emission attribution

2.2.3.1 Mobile C_2H_6 and CO_2 measurements

During the Utrecht campaign, the overall mole fraction of CH_4 and C_2H_6 in the NGDN was ≈ 80 % and ≈ 3.9 % (STEDIN, personal communication, 2020) and in Hamburg the mole fraction of CH_4 and C_2H_6 in the NGDN was about ≈ 95% and ≈ 3.4% (GasNetz Hamburg, personal communication, 2020) respectively. This ratio can vary depending on the mixture of gas compositions from different suppliers, but should meet the standards on the gas compositions in the Netherlands (65 – 96 mol-% for CH_4 and 0.2 – 11 mol-% for C_2H_6 (ACM, 2018)) and in Germany (83.64 – 96.96 mol-% for CH_4 and 1.06 – 6.93 mol-% for C_2H_6 (DVGW, 2013)). Compressed natural gas vehicles can be mobile CH_4 emission sources (E. K. Nam et al., 2004; Curran et al., 2014; Naus et al., 2018; Popa et al., 2014) and in this study we also observed CH_4 signals from vehicles. For example, the point to point C_2H_6:CH_4 ratio (C_2:C_1) calculated from road measurements of a car exhaust shown in Figure 2.S12 (see SI, Sect. 2.S.2.6) is 14.2 ± 7.1%. During the campaigns in Utrecht and Hamburg the C_2:C_1 of NGDNs was less than 10 % and in our study, we removed all the locations where the C_2:C_1 ratio was greater than 10%. CH_4 emissions from combustion processes are always accompanied by large emissions of CO_2 and can therefore be identified based on the low CH_4:CO_2 emission ratio. In this study, LIs with CH_4:CO_2 ratio between 0.02 and 20 with R^2 greater than 0.8 were attributed to combustion.

2.2.3.2 Lab isotopic analysis of δ^{13}C-CH_4 and δD-CH_4

After sample collections, the bag samples were returned to the IMAU for analysis of both δ^{13}C-CH_4 and δD-CH_4 (Brass and Röckmann, 2010) and some samples were analyzed at the Greenhouse Gas Laboratory (GGL) in the department of Earth Sciences, Royal Holloway University of London (RHUL) for δ^{13}C-CH_4 (Fisher et al., 2006) (see SI, Sect. 2.S.2.7, Figure 2.S13).

At the IMAU, we used isotope ratio mass spectrometry (IRMS) instrument of ThermoFinnigan MAT DeltaPlus XL (Thermo Fisher Scientific Inc., Germany). We used a reference cylinder calibrated against Vienna Pee Dee Belmnite (V-PDB) for δ^{13}C-CH_4 and Vienna Standard Mean Ocean Water (V-SMOW) for δD-CH_4 at the at the Max Planck Institute for Biogeochemistry (MPI-BGC), Jena, Germany (Sperlich et al., 2016). The cylinder contained CH_4 mole fraction of 1975.5 ± 6.3 ppb, δ^{13}C-CH_4 = -48.14 ± 0.07 ‰ vs V-PDB and δD-CH_4 = -90.81 ± 2.7 ‰ vs V-SMOW. The samples were pumped through a magnesium perchlorate ($Mg(ClO_4)_2$) dryer before the CH_4 extraction steps. Each sample was measured at least 2 times (up to four times) for each isotope. Every other sample, the reference gas was also measured 3 times for δ^{13}C-CH_4 and δD-CH_4. Each measurement, from the CH_4 extraction to the mass spectrometer, took ≈ 30 minutes.

At the GGL, Flex foil SKC bag samples were each analyzed for CH_4 mole fractions and δ^{13}C-CH_4. CH_4 mole fractions were determined using a Picarro G1301 CRDS, which measured every 5 seconds for 2 minutes resulting in a precision ± 0.3 ppb (Lowry et al., 2020; France et al., 2016; Zazzeri et al., 2015). Each sample was then measured for stable isotopes (δ^{13}C-CH_4) using an Elementar Trace

gas and continuous-flow gas chromatography isotope ratio mass spectrometry (CF-GC-IRMS) system (Fisher et al., 2006), which has an average repeatability of ± 0.05 ‰. CH_4 extraction was preceded by drying process using $Mg(ClO_4)_2$. Each sample was measured 3 times for $\delta^{13}C\text{-}CH_4$, where the duration of each analysis was ≈ 20 minutes. Both instruments are calibrated weekly to the WMO X2004A CH_4 scale using air filled cylinders that were measured by the National Oceanic and Atmospheric Administration (NOAA), and cylinders that were calibrated against the NOAA scale by the MPI-BGC (France et al., 2016; Lowry et al., 2020).

The analytical systems for isotope analysis have been described, used and/or compared in several previous publications (Fisher et al., 2011; Röckmann et al., 2016; Umezawa et al., 2018; Zazzeri et al., 2015). Measurement uncertainties in $\delta^{13}C\text{-}CH_4$ and $\delta D\text{-}CH_4$ are 0.05-0.1 ‰ and 2-5 ‰ respectively.

After the LIs were analyzed and quantified, the measurements of C_2H_6, CO_2, and isotopic composition from the air samples were used for source attribution. We characterize the observed LIs as of fossil origin when they had a concomitant C_2H_6 signal between 1 % and 10 % of the CH_4 enhancements and when the isotopic composition was in the range -50 to -40 ‰ for $\delta^{13}C\text{-}CH_4$ and -150 to -200 ‰ for $\delta D\text{-}CH_4$. A LI was characterized as microbial when there was no C_2H_6 signal (<1 % of the CH_4 enhancements larger than 500 ppb), $\delta^{13}C\text{-}CH_4$ was between -55 ‰ and -70 ‰ and $\delta D\text{-}CH_4$ was between -260 and -360 ‰ (Figure 7 in Röckmann et al., 2016). LIs with enhancements of CH_4 lower than 500 ppb and no C_2H_6 signals were categorized as unclassified. LIs with no C_2H_6 signals, no significant CH_4:CO_2 ratio, and no information on $\delta^{13}C\text{-}CH_4$ and $\delta D\text{-}CH_4$ were also categorized as unclassified. The source signatures for each sampling location were determined by a Keeling plot analysis of the three samples collected in the plumes and a background sample taken on the same day.

2.3 Results

2.3.1 Quantification of CH_4 emissions across Utrecht and Hamburg

Table 2.2 summarizes the main results from the surveys in Hamburg and Utrecht. The amount of km of roads covered in Hamburg is roughly a factor of 2 larger than in Utrecht, and also the number of detected LIs is roughly a factor of 2 larger, for all three categories. This shows that the overall density of LIs (km covered per LI) in both cities is not very different. Specifically, a LI is observed every 5.6 km in Utrecht and every 8.4 km in Hamburg. While not all streets were visited twice in both cities (see SI, Sect. 2.S.1.5, Table 2.S4) 80% of LIs in Utrecht and 69% of LIs in Hamburg were revisited which account for 91 % and 86% of emissions respectively in the study areas. During revisits, 60% of CH_4 emissions in Utrecht and 46% of emissions in Hamburg were confirmed. In both cities, all LIs in the high emission category were re-observed. In some cases, re-visits were carried out several months after first detection, and the LIs were still confirmed (e.g. see SI, Sect. 2.S.1.7, Figure 2.S5).

Table 2.2. Measurements and result summaries across the study area inside the ring in Utrecht and north Elbe in Hamburg.

Study Area			Utrecht (inside the Ring)	Hamburg (North Elbe)
≈ km street driven		Total km driven	1,000 km	1,800 km
		Driven once	220 km	900 km
		Driven more than once	780 km	900 km
≈ km street covered		Total km covered	450 km	1,200 km
		covered once	230 km	900 km
		covered more than once	220 km	300 km
LIs and emissions		Total number	81 LIs	145 LIs
		LI density	5.6 km covered LI^{-1}	8.4 km covered LI^{-1}
		Total emission rate	290 L min^{-1}	490 L min^{-1}
		Average emission rate per LI	3.6 L min^{-1} LI^{-1}	3.4 L min^{-1} LI^{-1}
		Total emission rate per year	107 t yr^{-1}	180 t yr^{-1}
LIs visited	Once	Number	16 LIs	45 LIs
		Emissions	26 L min^{-1}	68 L min^{-1}

		Average emission rate per LI		1.6 L min^{-1} LI^{-1}	1.5 L min^{-1} LI^{-1}
	More than once	Number		65 LIs	100 LIs
		Emissions		264 L min^{-1}	423 L min^{-1}
		Average emission rate per LI		4.1 L min^{-1} LI^{-1}	4.2 L min^{-1} LI^{-1}
Total LIs categorized based on von Fischer et al. (2017) categories	High (>40 L min^{-1})	Number		1 LI	2 LIs
		Emissions		102 L min^{-1}	145 L min^{-1}
		Average emission rate per LI		101.5 (L min^{-1} LI^{-1})	72.4 L min^{-1} LI^{-1}
		% of emissions		35 % of total emissions	30 % of total emissions
	Medium (6-40 L min^{-1})	Number		6 LIs	16 LIs
		Emissions		84 L min^{-1}	176 L min^{-1}
		Average emission rate per LI		14.0 L min^{-1} LI^{-1}	11 L min^{-1} LI^{-1}
		% of emissions		30 % of total emissions	36 % of total emissions
	Low (0.5-6 L min^{-1})	Number		74 LIs	127 LIs
		Emissions		105 L min^{-1}	169 L min^{-1}
		Average emission rate per LI		1.4 L min^{-1} LI^{-1}	1.3 L min^{-1} LI^{-1}
		% of emissions		36 % of total emissions	35 % of total emissions
Total LIs categorized based on OSM road classes	Level 1	Number		6 LIs	29 LIs
		Emissions		5 L min^{-1}	68 L min^{-1}
		Average emission rate per LI		0.76 L min^{-1} LI^{-1}	2.3 L min^{-1} LI^{-1}
	Level 2	Number		16 LIs	34 LIs
		Emissions		145 L min^{-1}	99 L min^{-1}
		Average emission rate per LI		9.0 L min^{-1} LI^{-1}	2.9 L min^{-1} LI^{-1}
	Level 3	Number		3 LIs	23 LIs
		Emissions		10 L min^{-1}	43 L min^{-1}
		Average emission rate per LI		3.4 L min^{-1} LI^{-1}	1.9 L min^{-1} LI^{-1}
	Residential	Number		45 LIs	52 LIs
		Emissions		93 L min^{-1}	274 L min^{-1}
		Average emission rate per LI		2.1 L min^{-1} LI^{-1}	5.3 L min^{-1} LI^{-1}
	Unclassified	Number		11 LIs	7 LIs
		Emissions		38 L min^{-1}	6 L min^{-1}
		Average emission rate per LI		3.4 L min^{-1} LI^{-1}	0.8 L min^{-1} LI^{-1}
Attribution	C_2:C_1 ratio analysis	Fossil (Inc. combustion)	% of emissions	93% of total emissions	64% of total emissions
			% of LIs	69% of LIs	33% of LIs
		Microbial	% of emissions	6% of total emissions	25% of total emissions
			% of LIs	10% of LIs	20% of LIs
		Unclassified	% of emissions	1% of total emissions	11% of total emissions
			% of LIs	21% of LIs	47% of LIs
	$\delta^{13}C$-CH_4 and δD-CH_4 analysis	Fossil	% of emissions	----------	79% of total emissions
			% of LIs	----------	38% of LIs
		Microbial	% of emissions	----------	20% of total emissions
			% of LIs	----------	54% of LIs
		Other	% of emissions	----------	1% of total emissions
			% of LIs	----------	8% of LIs (Pyrogenic)
	CH_4:CO_2 ratio analysis	Combustion	% of emissions	2%	10%
			% of LIs	7%	17%
		Other	% of emissions	98%	90%
			% of LIs	93%	83%
	C_2:C_1 ratio, CH_4:CO_2 ratio, and $\delta^{13}C$-CH_4 - δD-CH_4 analyses	Fossil	% of emissions	73%	48%
			% of LIs	43%	31%
		Combustion	% of emissions	2%	10%
			% of LIs	7%	17%
		Microbial	% of emissions	8%	35%
			% of LIs	4%	33%
		Unclassified	% of emissions	16%	7%

			% of LIs	46%	19%
Average emission rate per km driven				0.29 L min^{-1} km^{-1}	0.27 L min^{-1} km^{-1}
km driven / total LIs				12.5 km LI^{-1}	12.36 km LI^{-1}
Emission factors to scale-up emissions per km covered				0.64 L min^{-1} km^{-1}	0.40 L min^{-1} km^{-1}
km covered per LIs		km covered / total LIs		5.6 km LI^{-1}	8.4 km LI^{-1}
		km covered / red LIs		454.8 km LI^{-1}	611.4 km LI^{-1}
		km covered / orange LIs		75.8 km LI^{-1}	76.4 km LI^{-1}
		km covered / yellow LIs		6.1 km LI^{-1}	9.6 km LI^{-1}
km road from OSM (≈ km pipeline)				≈ 650 km	≈ 3000 km
Up-scaled methane emissions to total roads				420 L min^{-1} (≈150 t yr^{-1})	1,200 L min^{-1} (≈440 t yr^{-1})
Bootstrap emission rate estimate and error				420 ± 120 L min^{-1}	1,200 ± 170 L min^{-1}
Population in study area				≈ 0.28 million	≈ 1.45 million
Average LIs emissions per capita (kg yr^{-1} $capita^{-1}$)				0.54 ± 0.15	0.31 ± 0.04
Yearly natural gas consumption				≈ 0.16 bcm yr^{-1}	≈ 0.75 bcm yr^{-1}
Fossil emission factors	C_2:C_1 ratio attribution analysis		Average emission rate per km gas pipeline	0.60 ± 0.2 L min^{-1} km^{-1}	0.26 ± 0.04 L min^{-1} km^{-1}
			Average emission rates per capita	0.50 ± 0.14 kg yr^{-1} $capita^{-1}$	0.20 ± 0.03 kg yr^{-1} $capita^{-1}$
	$\delta^{13}C$-CH_4 and δD-CH_4 attribution analysis		Average emission rates per km gas pipeline	----------	0.32 ± 0.05 L min^{-1} km^{-1}
			Average emission rates per capita	----------	0.25 ± 0.04 kg yr^{-1} $capita^{-1}$
	C_2:C_1 ratio, CH_4:CO_2 ratio, and $\delta^{13}C$-CH_4 - δD-CH_4 analyses		Average emission rates per km gas pipeline	0.47 ± 0.14 L min^{-1} km^{-1}	0.19 ± 0.03 L min^{-1} km^{-1}
			Average emission rates per capita	0.39 ± 0.11 kg yr^{-1} $capita^{-1}$	0.15 ± 0.02 kg yr^{-1} $capita^{-1}$
			Average emission rates / yearly consumption	0.10 – 0.12%	0.04 – 0.07%

The distribution of CH_4 LIs across the cities of Utrecht and Hamburg is shown in Figure 2.2. As shown in Table 2.2, a total of 145 significant LIs were detected in Hamburg and 81 in Utrecht; these LIs cover all three LI categories. Two LIs in Hamburg and one LI in Utrecht fall in the high (red) emission category; the highest LI detected in Utrecht and Hamburg corresponded to emission rates of ≈ 100 L min^{-1} and ≈ 70 L min^{-1}, respectively. Noted that estimates for individual leaks with the Weller et al. (2019) algorithm can have large error, thus these results are indicative of large leaks, but the precise emission strength is very uncertain. Six LIs in Utrecht and 16 LIs in Hamburg fall in the middle (orange) emission category, and 127 LIs in Hamburg and 74 LIs in Utrecht fall in the low (yellow) emission category. The distribution of emissions over the three categories is also similar between the two cities, with roughly one third of the emissions originating from each category (Figure 2.2), but the number of LIs in each category is different. The contribution of LIs in the high emission category is about a third of the total observed emissions (35 % in Utrecht is (one LI) and in 30 % in Hamburg (two LIs)).

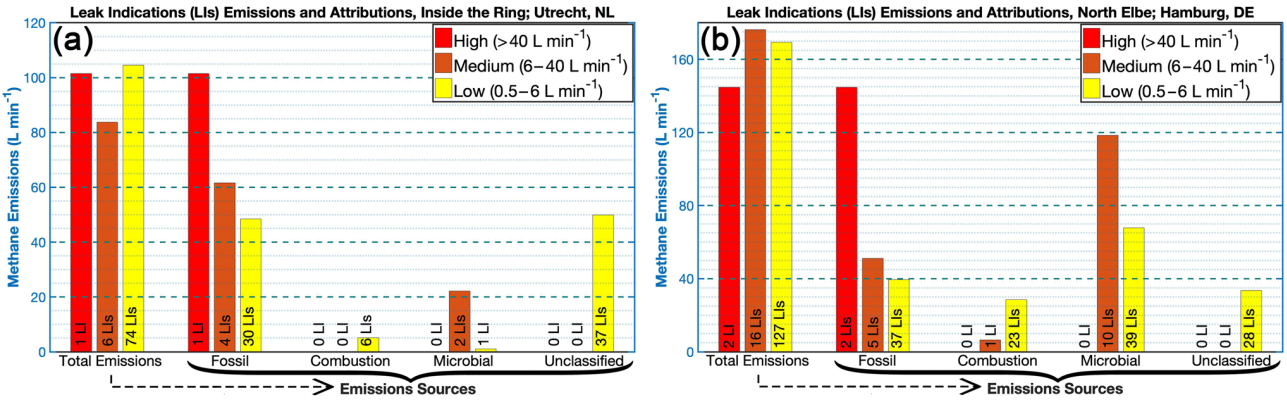

Figure 2.2. Total CH_4 emission rates from different sources in (a) Utrecht and (b) Hamburg; the arrow shows how the emissions are attributed to different sources.

CH_4 emitting locations were categorized based on the roads where the LIs were observed (Figure 2.1, Figure 2.2, Figure 2.3, and Table 2.S8 in SI, Sect. 2.S.3.1). Average emission rates per LI as derived from equation (1) are similar for the two cities with 3.6 L min^{-1} LI^{-1} in Utrecht and 3.4 L min^{-1} LI^{-1} in Hamburg, but they are distributed differently across the road (Figure 2.1). In Utrecht, emitting locations on level 2 roads contributed the most (50 % of emissions) to the total emissions while in Hamburg the majority of the emissions occurred on residential roads (56 % of total emissions). This shows that the major leak indications may happen on different road classes in different cities and there is no general relation to the size of streets between these two cities.

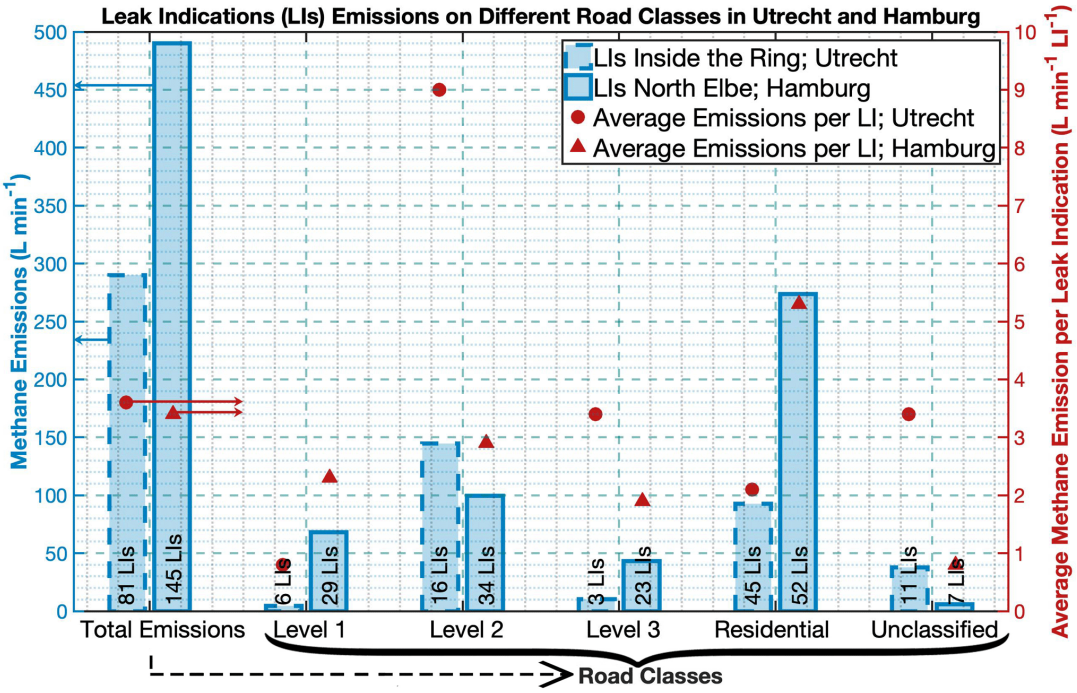

Figure 2.3. Total CH4 emissions in Utrecht and Hamburg; the arrow shows how the total emissions are distributed on different road classes.

In Figure 2.4, we compare cumulative CH_4 emissions for Utrecht and Hamburg to numerous US cities (Weller et al., 2019). After ranking the LIs from largest to smallest, it becomes evident that the largest 5 % of the LIs account for about 60 % of emissions in Utrecht, and 50 % of the emissions in Hamburg.

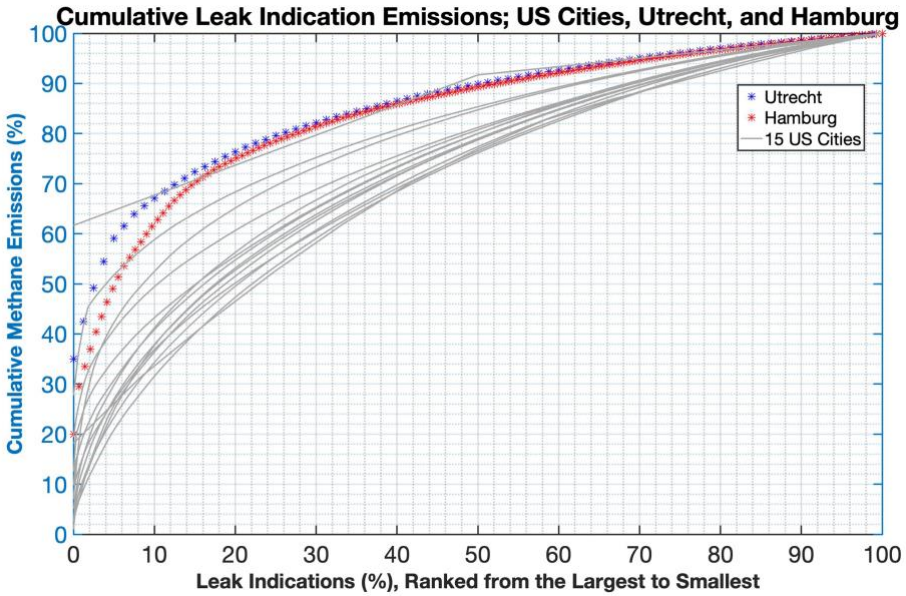

Figure 2.4. Cumulative plot of CH_4 emissions across US cities, Utrecht, and Hamburg; datasets for the US cities are from Weller et al. (2019).

As mentioned above, the observed total emission rates observed on roads in urban environment in the two cities are relatively similar when normalized by the total amount of km covered, 0.64 L min^{-1} km^{-1} for Utrecht and 0.4 L min^{-1} km^{-1} for Hamburg (Table 2.2). Using these two emission factors, the observed emission rates (≈110 t yr^{-1} in Utrecht and ≈180 t yr^{-1} in Hamburg) were up-scaled to the entire road network in the two cities, ≈ 650 km in Utrecht and ≈ 3,000 km in Hamburg. This includes the implicit assumption that the pipeline network is similar to the street network. Total up-scaled emission rates based on mobile measurements on roads in urban environment before considering attribution analysis over LI locations are 150 t yr^{-1} and 440 t yr^{-1} across the study areas of Utrecht and Hamburg respectively. Distributing the calculated emission rates over the population in the city areas yields emission rates of 0.54 ± 0.15 kg yr^{-1} $capita^{-1}$ for Utrecht and 0.31 ± 0.04 kg yr^{-1} $capita^{-1}$ for Hamburg (see SI, Sect. 2.S.3.2, Figure 2.S14).

2.3.2 Attribution of CH_4 emissions across Utrecht and Hamburg

Figure 2.5 shows the results of the isotope analysis for the 21 locations in Hamburg where acceptable Keeling plots were obtained (see SI, Sect. 2.S.3.3, Table 2.S9 and Table 2.S10). The results cluster mostly in three groups, which are characterized by the expected isotope signatures for fossil, microbial, and pyrogenic samples as described in Röckmann et al., (2016).

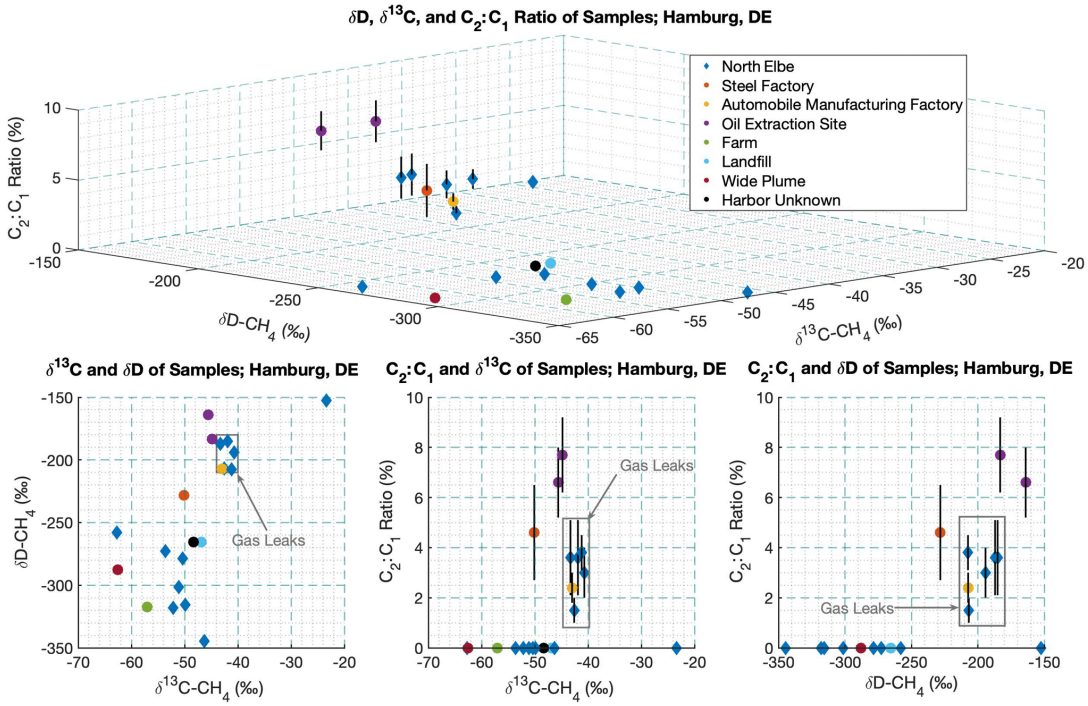

Figure 2.5. Results from the attribution measurements in Hamburg: C_2:C_1 ratios and isotopic signatures (δ^{13}C-CH_4 and δD-CH_4) of collected air samples; measurement uncertainty in δ^{13}C-CH_4 is 0.05 ‰–0.1 ‰ and in δD-CH_4 2 ‰ – 5 ‰.

Average isotope signatures for the LIs in the city of Hamburg were δ^{13}C-CH_4 = -52.3 ± 5.1 ‰ and δD-CH_4 = -298.4 ± 30.3 ‰ for the samples characterized as microbial and δ^{13}C-CH_4 = -41.9 ± 1.0 ‰ and δD-CH_4 = -196.1 ± 10.6 ‰ for the samples characterized as fossil (Figure 2.5). One sample from the Hamburg city area displays a very high source signature of δ^{13}C-CH_4 = -23 ‰ and δD-CH_4 = -153 ‰. The origin of CH_4 with such an unusual isotopic signature could not be identified and it is considered an outlier. In Hamburg, 10% of the LI locations (38% of emissions) on the north side of Elbe were sampled for isotope analysis. The lab isotopic attributions show that the LIs with the higher emission rates are mostly caused by emission of fossil CH_4. 79% of the inferred emissions at 38 % of the LIs were identified as of fossil origin, 20% of emissions at 54% of the LIs as of microbial origin (for an identified source see SI, Sect. 2.S.3.3, Figure 2.S15), 1% of emissions at 8% of LIs as of pyrogenic origin.

In Hamburg, during three passes through the new Elbe tunnel (see SI, Sect. 2.S.3.4, Figure 2.S16) a CH_4:CO_2 of 0.2 ± 0.1 ppb:ppm was derived for combustion-related emission. During the surveys of open roads, clear CH_4:CO_2 correlations were observed for several LIs and an example of a measurement of car exhaust is shown in Figure 2.S12a (see SI, Sect. 2.S.2.6) with CH_4:CO_2 = 1.6 ppb:ppm. Previous studies have shown relatively low CH_4:CO_2 ratios of $4.6*10^{-2}$ ppb:ppm (Popa et al., 2014), 0.41 ppb ppm^{-1} (E. K. Nam et al., 2004), and 0.3 ppb:ppm (Naus et al., 2018) when cars work under normal conditions. During cold engine (Naus et al., 2018) or incomplete combustion conditions, the fuel to air ratio is too high, which results in enhanced emission of black carbon particles and reduced carbon compounds, so higher CH_4:CO_2 ratios. Hu et al. (2018) reported 2 ± 2.1 ppb:ppm in a tunnel, but 12 ± 5.3 $ppb:ppm^{-1}$ on roads. In addition to car exhaust, there are other combustion sources which can affect CH_4 and CO_2 mole fractions at the street level including natural gas water heater (CH_4:CO_2 ratio of ≈ 2 ppb:ppm; Lebel et al., 2020), restaurant kitchens, etc. Based on the CH_4:CO_2 ratio (ppb:ppm) criterion defined above (see Sect. 2.3.1), 17 % of LIs (10 % of emissions) can be attributed to combustion (see SI, Sect. 2.S.3.4, Figure 2.S17) with a mean CH_4:CO_2 ratio of 3.2 ± 3.9 ppb:ppm (max = 18.7 and min = 0.8 ppb:ppm). The C_2:C_1 ratio for these LIs attributed to combustion in Hamburg was

7.8 ± 3.5%. In Utrecht 7% of LIs (2% of emissions) are attributed to combustion with a mean CH_4:CO_2 ratio of 9.8 ± 5.8 ppb:ppm (max = 16.7 and min = 3.0 ppb:ppm).

Based on the C_2H_6 signals, 64% of the emissions (33% of LIs) were characterized as fossil, while 25% of emissions (20% of LIs) were identified as microbial. Due to low CH_4 and C_2H_6 enhancements, 47% of the locations (11% of emission) were considered unclassified. The C_2:C_1 ratio for the LIs attributed to emissions from NGDNs in Hamburg study area (North Elbe) is 4.1 ± 2.0%. The oil production site in south-east Hamburg had a higher C_2:C_1 ratio of 7.1 ± 1.5%.

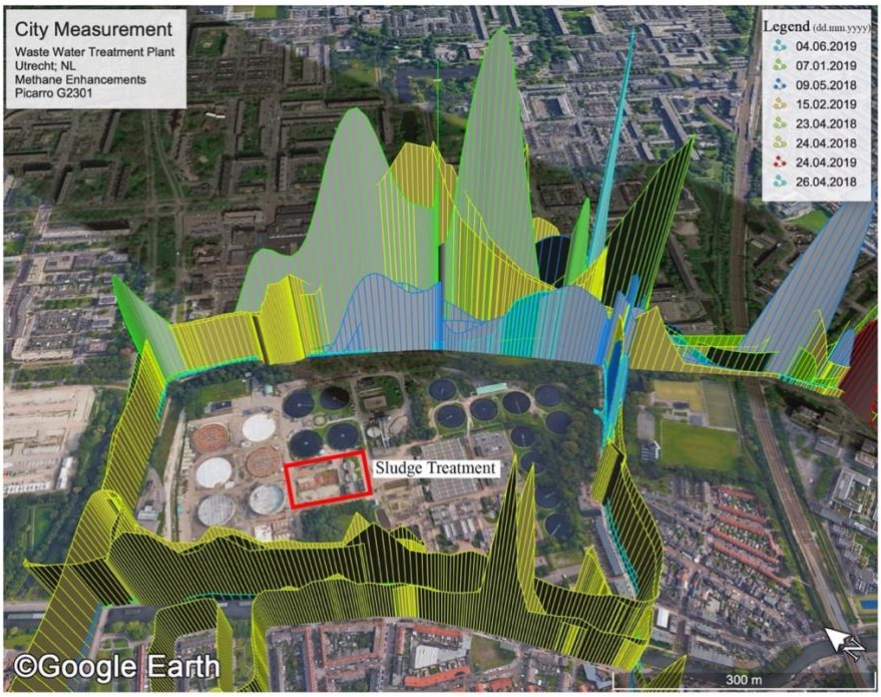

Figure 2.6. CH_4 enhancements measured downwind of the waste water treatment plant on Brailledreef Street and later used for quantifications from this facility in Utrecht; the center of the area where the sludge treatment is located was considered the effective CH_4 emission source. The plumes are plotted on the same scale, and maximum CH_4 enhancement is ≈ 0.3 ppm.

In Utrecht, C_2H_6 was measured only during four surveys in February, April, and June 2019 (revisits of 2-day surveys across the city center and 2 days to LIs with high emission rates) as the CH_4 - C_2H_6 analyzer was not available during the first campaign. The C_2:C_1 ratios from this limited survey indicates that 93% of emissions (69% of the LIs across the city centre, including combustions) are likely from fossil sources (Table 2.2) and 73% of emissions (43% of the LIs, including combustion) out of all LIs. In Utrecht, the C_2:C_1 ratio for the LIs attributed to NGDNs is 3.9 ± 0.8%.

2.3.3 Quantification of CH_4 plume from larger facilities

Table 2.3 shows the emission rate estimates from the larger facilities in Utrecht and Hamburg. CH_4 plumes from the WWTP (Figure 2.6 and in SI, Sect. 2.S.1.6., Table 2.S5) were intercepted numerous times during the city transects, and the error estimate in Table 2.3 represents one standard deviation of 5 sets of measurements where each measurement comprises 2-4 transects during three measurement days (12-Feb.-2018, 24-Apr.2018, and 07-Jan.-2019). Figure 2.7 shows an example of a fit of a Gaussian plume to the measurements from the Utrecht WWTP. The derived distance to the source was 215 ± 90 m, the hourly average wind speed was 3.5 ± 1.1 m s^{-1} and the wind direction was 178 ± 5 degrees (see SI, Sect. 2.S.1.6, Table 2.S5).

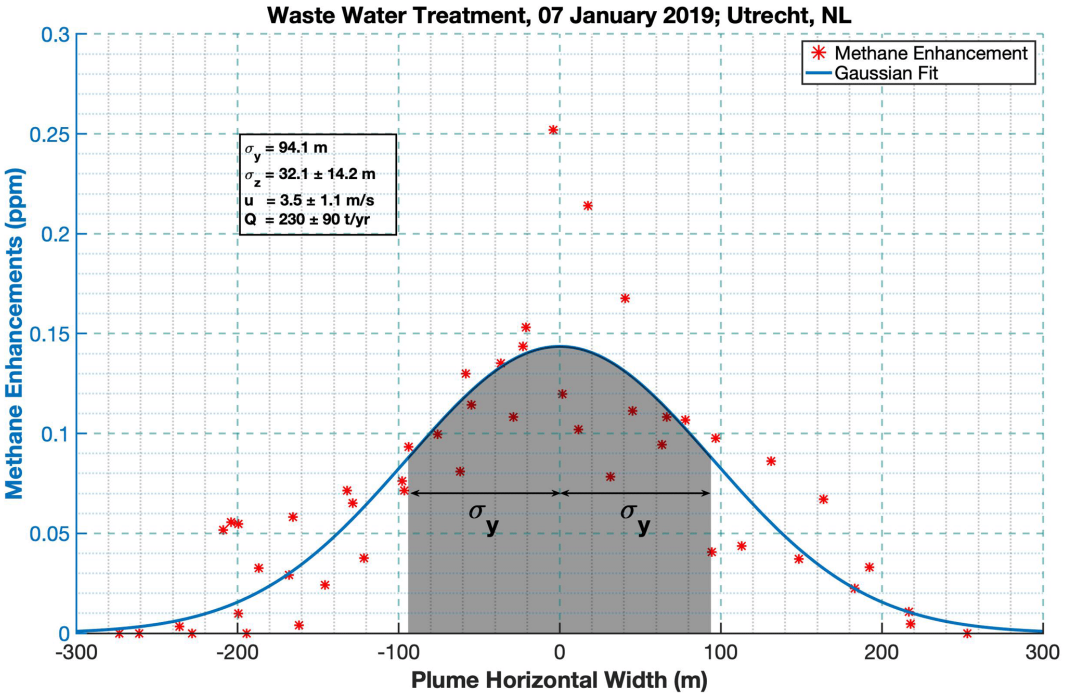

Figure 2.7. Gaussian curve fitted to some transects downwind of the waste water treatment plant in Utrecht.

Table 2.3. CH_4 emissions from larger facilities in Utrecht and Hamburg estimated with the Gaussian plume model.

Facility	Emission rate (t yr^{-1})
Utrecht	
Waste Water Treatment Plant (52.109791° N, 5.107605° E)	160 ± 90
Hamburg	
F: Compost and Soil Company (53.680233° N, 10.053751° E)	70 ± 50
Upstream D1: 53.468774° N,10.184481° E (separator) D2: 53.468443° N,10.187408° E (storage tanks) D3: 53.466694° N,10.180647° E (oil well)	 D1: 4.5 ± 3.7 D2: 5.2 ± 3.0 D3: 4.8 ± 4.0

The total emission rate of the WWTP in Utrecht was estimated at 160 ± 90 t yr^{-1}. The reported errors include stability classes, wind speed and directions, and effective point source coordinates. Not all transects provided datasets that allowed an adequate Gaussian fit, these were not included in total estimates from the facilities, e.g. measurements during the visits of the harbor area in Hamburg were excluded. In Hamburg, plumes from several facilities were also intercepted several times (see SI, Sect. 2.S.1.6, Table 2.S6). For a Compost and Soil Company in Hamburg we estimate an emission rate of 70 ± 50 t yr^{-1}. The mobile quantifications at the upstream sites in Hamburg from a separator, a tank, and an oil well yield annual CH_4 emission of 4.5 ± 3.7 t yr^{-1}, 5.2 ± 3.0 t yr^{-1}, and 4.8 ± 4.0 t yr^{-1} respectively.

2.4 Discussion

2.4.1 Detection and quantification

As mentioned above (see Sect. 2.2.2.2), we used methods similar to the ones introduced by von Fischer et al. (2017) and updated in Weller et al. (2019) that were used to characterize CH_4 emission from local gas distribution systems in the US. An important difference is that we did not visit each street twice in the untargeted survey, and the revisits were specifically targeted at locations where we had found a LI during the first visit. A consequence of the different sampling strategy is that we do not base our city-level extrapolated emissions estimates on “confirmed” LIs, as done in Weller et al. (2019) but

on all the LIs observed. In our study, 60% of CH_4 LIs in Utrecht and 46% of LIs in Hamburg were confirmed. This number may be biased high, since we preferentially revisited locations that had shown higher LIs, and the percentage of confirmed LIs may have been lower if we had visited locations with smaller LIs. Von Fischer et al. (2017) reported that LIs in the high emission rate category have a 74% chance of detection, which decreased to 63% for the middle category and 35% frequency for the small category. In our study, all LIs within the high emission rate category (n = 1 and n = 2 LIs in Utrecht and Hamburg respectively) were confirmed in both cities. Overall, the confirmation rates found in Hamburg and Utrecht were similar to the ones reported in the US cities by von Fischer et al. (2017), suggesting that the results from both driving strategies can be compared when we take into account an overall confirmation percentage of roughly 50%.

In 13 US cities the "LI density" ranged from 1 LI per 1.6 km driven to 1 LI per ≈ 320 km driven (EDF, 2019). This illustrates that cities within one country can be very different in their NGDN infrastructure. In Utrecht, one LI was observed every 5.6 km of street covered and in Hamburg every 8.4 km covered. Note that we normalize the number of LIs per km of road covered, not km of road driven, since the revisits were targeted to confirm LIs, which would bias the statistics if we normalize by km of road driven. After accounting for the confirmation percentage of 50%, the LI densities in Utrecht and Hamburg become 1 LI per 11.2 km covered in Utrecht, and 1 LI per 16.8 km covered in Hamburg. When we take into account the attributions (fraction fossil/total LIs is 43% in Utrecht and 31% in Hamburg), confirmed LIs from the NGDN are found every 26 km in Utrecht and every 54 km in Hamburg. The highest 1% of the LIs in Utrecht and Hamburg account for approximately 30% of emissions, emphasizing the presence of a skewed distribution of emissions. The emissions distribution is even more skewed for these two European cities than for countrywide US cities, where approximately 25% of emissions comes from the highest 5% of the LIs. Skewed emission distributions appear to be typical for emissions from the oil and gas supply chain across different scales. For example, a synthesis study reviewing the distribution of upstream emissions from the US natural gas system shows that in the US 5% of the leaks are responsible for 50% of the emissions (Brandt et al., 2016).

2.4.2 Attribution

Four different approaches were combined in Hamburg for emission source attribution, which allows an evaluation of their molecular consistency. Figure 2.5 shows that measurements of the C_2:C_1, δD-CH_4, and δ^{13}C-CH_4 provide a very consistent distinction between fossil and microbial sources of CH_4. Except for one outlier with a very enriched δ^{13}C-CH_4 and δD-CH_4 contents and no C_2H_6 signal, all samples that are classified as "microbial" and depleted in δ^{13}C-CH_4 and δD-CH_4 signatures contain no measurable C_2H_6. Samples that are characterized as "fossil", based on δ^{13}C-CH_4 and δD-CH_4 signatures, bear a C_2H_6 concomitant signal. This strengthens the confidence in source attribution using these tracers. The fossil δ^{13}C-CH_4 signature of bag samples from natural gas leaks in Hamburg (δ^{13}C-CH_4 = -41.9 ± 1.0 ‰) is higher than recent reports from the city of Heidelberg, Germany (δ^{13}C-CH_4 = −43.3 ± 0.8 ‰ (Hoheisel et al., 2019)). This shows that within one country, δ^{13}C-CH_4 from NGDNs can vary from one region to another. These numbers do not agree within combined errors, but are also not very different. δ^{13}C-CH_4 values of CH_4 from the NGDN can vary regionally and temporally, e.g. due to differences in the mixture of natural gas from various suppliers for different regions in Germany (DVGW, 2013). In a comprehensive study at global scale, it is also shown that how δ^{13}C-CH_4 values of fossil fuel CH_4 have significant variabilities in different regions within an individual basin (Figure 4 in Sherwood et al. (2017)).

In Hamburg both C_2:C_1 and CH_4:CO_2 analysis along with δ^{13}C-CH_4 and δD-CH_4 signatures suggest that ≈ 50% to ≈ 80% of estimated emissions (≈ 30% and ≈ 40% of LIs respectively) originate from NGDNs, whereas CH_4:CO_2 analysis and the smaller sample of C_2:C_1 measurements in Utrecht suggests that the overwhelming fraction (70 - 90% of emissions; 40 – 70% of LIs) originated from NGDNs. We note that although it is widely assumed that microbial CH_4 is not associated with C_2H_6, some studies have reported microbial production of C_2H_6, so it may not be a unique identifier (Davis

and Squires, 1954; Fukuda et al., 1984; Gollakota and Jayalakshmi, 1983; Formolo, 2010). The online C_2:C_1 analysis to attribute LIs is fast and can be used at larger scale, but with the instrument we used we were not able to clearly attribute sources with CH_4 enhancements of less than 500 ppb. Isotopic analysis by IRMS can attribute sources for smaller LIs (down to 100-200 ppb) but is clearly more labor intensive, and it would be a considerable effort to take samples from all LIs observed across an urban area. Overall, C_2H_6 and CO_2 signals are very useful in eliminating non-fossil LIs in mobile urban measurements and with improvements in instrumentations, analyzing signals of these two species along with evaluation of CH_4 signals can make process of detecting pipeline leaks from NGDN more efficient.

In Hamburg, most of the LIs were detected in the city center (Figure 2.1). This means that the LI density is higher than the average value in the center, but much lower than the average value in the surrounding districts and residential areas. Many of the LIs in the city center were attributed to combustion and microbial sources, thus they do not originate from leaks in the NGDN. Many of the microbial LIs encountered in Hamburg are around the Binnenalster lake (see SI, Sect. 2.S.3.3, Figure 2.S15), which suggests that anaerobic methanogenesis (Stephenson and Stickland, 1933; Thauer, 1998) can cause these microbial emissions in this lake, as seen in other studies focused on emissions from other lakes (e.g., DelSontro et al., 2018; Townsend-Small et al., 2016a). Microbial CH_4 emissions from sewage system (Guisasola et al., 2008) can also be an important source of in this area, as seen in US urban cities (Fries et al., 2018). Fries et al. (2018) performed direct measurement of CH_4 and nitrous oxide (N_2O) from a total of 104 sites, and analyzed $\delta^{13}C$-CH_4 and δD-CH_4 signatures of samples from 27 of these locations, and attributed 47% of these locations to microbial emissions in Cincinnati, Ohio, USA.

2.4.3 Comparison to national inventory reports

In the national inventory reports, total upscaled emissions from NGDNs are based on sets of emission factors for different pipeline materials (e.g., grey cast iron, steel, or plastic) at different pressures (e.g., <= 200 mbar or >200 mbar). The reported emission factors are based on IPCC tier 3 approach (Buendia et al., 2019). However, emission estimates do not exist for individual cities including Utrecht and Hamburg. Also, it is not possible to calculate a robust city-level estimate using the nationally reported emission factors because there is no publicly available associated activity data, i.e., pipeline materials and lengths for each material, at the level of individual cities. As a result, a robust direct comparison between nationally reported emissions and our measurements, akin to a recent study in the United States (Weller et al., 2020), is currently not possible. The following juxtaposition of our estimates and national inventory downscaling to city-level is therefore provided primarily as illustration of the data gaps rather than a scientific comparison. In Utrecht, we attributed 70 – 90% of the mobile measurement inferred emissions of ≈ 150 t yr^{-1} to the NGDN, thus 105 – 135 t yr^{-1}.

The Netherlands National Institute for Public Health and the Environment (RIVM) inventory report derived an average NGDN emission factor of ≈ 110 kg km^{-1} yr^{-1} using 65 leak measurements from different pipeline materials and pressures in 2013. This weighted average ranged from a maximum of 230 kg km^{-1} yr^{-1} for grey cast iron pipelines to a minimum of 40 kg km^{-1} yr^{-1} for pipelines of other materials with overpressures <= 200 mbar (for details, see P. 130 in Peek et al. (2019)). This results in an average CH_4 emissions of ≈ 70 t yr^{-1} (min = 30 t yr^{-1} and max = 150 t yr^{-1}) for the study area of Utrecht, assuming ≈ 650 km of pipelines inside the ring, and further assuming that Utrecht's NGDN is representative of the national reported average (see qualifiers above). The average emissions for the Utrecht study, based on emissions factors reported for the Netherlands, is smaller by a factor of 1.5 - 2 compared to the emissions derived here. The variability factor of 5, from the reported emission (resulting from the variability in pipeline materials) highlights the need for city-level specific activity data for a robust comparison. In Hamburg, 50 – 80% of the upscaled emissions of 440 t yr^{-1} (220 – 350 t yr^{-1}), can be attributed to the emission from NGDN. The national inventory from the Federal Environment Agency (UBA) in Germany, reports an average CH_4 emission factor for NGDN from low pressure pipelines as ≈ 290 kg km^{-1} yr^{-1} (max = 445 kg km^{-1} yr^{-1} (grey cast iron) and min = 51 kg km^{-1}

yr^{-1} (plastic)) based on measurements from the 1990s (Table 169 in Federal Environment Agency (2019)). Assuming ≈ 3000 km of pipelines in the targeted region, and further assuming that Hamburg's NGDN is representative of the national reported average (see qualifiers above), results in an estimated NGDN CH_4 emissions average of ≈ 870 t yr^{-1} (min = 155 t yr^{-1} and max = 1350 t yr^{-1}). While this study's estimate (220 – 350 t yr^{-1}) falls in the lower end of this range, the reported emissions variability factor of 9 (resulting from the variability in pipeline materials) highlights again the need for city-level specific activity data for a robust comparison. To put the national inventory comparison into perspective, it should be noted that GasNetz Hamburg detected and fixed leaks at 20 % of the fossil LIs in this study, which accounted for 50% of emissions. In Utrecht and Hamburg, the natural gas consumption in our target area were retrieved through communications with LDCs. In the Utrecht and Hamburg study areas, natural gas consumption is 0.16 bcm yr^{-1} (STEDIN, personal communication) and 0.75 bcm yr^{-1} (GasNetz Hamburg, personal communication) respectively. The estimated emissions from NGDNs in our study is between 0.10 – 0.12% in Utrecht and between 0.04 – 0.07% in Hamburg of total the annual natural gas consumptions in the same area. In the US, where the majority of natural gas consumption is from residential and commercial sectors, Weller et al. (2020) reported emissions of 0.69 Tg $year^{-1}$ (0.25 - 1.23 with 95% confidence interval), with a sum of ≈ 170 Tg $year^{-1}$ (U.S. EIA, 2019), showing 0.4% (0.15% - 0.7%) loss from NGDNs. The US NGDNs loss is about four times larger than our reported loss in Utrecht, and is about ten times larger than the loss for Hamburg. Considering the population of Utrecht (≈ 0.28 million) and Hamburg (≈ 1.45 million), the natural gas consumption densities in these study areas are ≈ 570 m^3 $capita^{-1}$ yr^{-1} and ≈ 520 m^3 $capita^{-1}$ yr^{-1}, where in the US (population ≈ 330 million (US Census Bureau, 2020)) the density is about ≈ 730 m^3 $capita^{-1}$ yr^{-1} (see SI, Sect. 2.S.3.2, Figure 2.S14). This shows that annual natural gas consumption per capita in the US is about 30% and 40% higher than in Utrecht and Hamburg respectively. The emission per km of pipeline in Utrecht is between 0.45 – 0.5 L min^{-1} km^{-1} and in Hamburg is between 0.2 – 0.32 L min^{-1} km^{-1}. In the US, based on 2,086,000 km km of local NGDN pipeline (Weller et al., 2020), this emission factor will be between 0.32 – 1.57 L min^{-1} km^{-1}. This shows higher emissions per km pipeline in the countrywide studies of US compared to just two European cities of Utrecht and Hamburg (see qualifiers above). This can be partly explained by pipeline material, maintenance protocols, and higher use of natural gas consumption in the US. However, the substantial variability in emission rates across US cities, as wells as the annual variability of gas consumption over the year, again restricts a direct comparison of two cities with a national average measured over multiple years.

Normalized LIs emissions per capita in Utrecht (0.54 ± 0.15 kg yr^{-1} $capita^{-1}$) are almost double the emission factor in Hamburg (0.31 ± 0.04 kg yr^{-1} $capita^{-1}$). This metric may be useful to compare cities, assuming that the emission quantification method is equally effective for different cities. CH_4 emissions can vary among different cities, depending on the age, management and material of NGDNs, and/or the management of local sewer systems. In our study, we only surveyed two cities, and the above number may not be adequate for extrapolation to the country scale (McKain et al., 2015).

2.4.4 Interaction with utilities

After the city surveys, locations with the highest emissions (high and medium categories) were shared with STEDIN Utrecht and all LI locations were reported to GasNetz Hamburg. The utilities repair teams were sent to check whether LIs could be detected as leaks from NGDN and fixed. The LDCs follow leak detection procedures based on country regulations (e.g., for GasNetz Hamburg in SI, Sect. 2.S.4.1, Table 2.S11). GasNetz Hamburg also co-located the coordinates of the detected reported LIs with the NGDN and prioritized repairs based on safety regulations mentioned in Table 2.S12 (see SI, Sect. 2.S.4.1). This interaction with the LDCs resulted in fixing major NGDN leaks in both cities. In Utrecht the only spot in the high emission category was reported to STEDIN, but the pipelines on this street had been replaced, which most likely fixed the leak, as it was not found later by the gas company nor in our later survey with the CH_4 - C_2H_6 analyzer. In Utrecht, half of the LIs in the medium category were found and repaired.

A routine leak survey (detection and repair) had been performed by GasNetz Hamburg between 1-5 months before the campaign, for the different regions (see SI, Sect. 2.S.4.1., Table 2.S11). The timing of any routine detection and repair likely influences the absolute number of LIs measured during independent mobile measurements, and the survey by GasNetz Hamburg thus likely has influenced the absolute number of LIs measured in our campaign. We then reported the LI latitude/longitude coordinates to GasNetz Hamburg about 4 months after our campaign. Additionally, we provided map images of the LIs immediately after the campaign. The comparison of the number of reported LIs (and emission rates) during our campaign with those identified by GasNetz Hamburg post-campaign assumes that the leaks continued to emit gas until they were detected and fixed by GasNetz Hamburg (if they were detected).

Depending on how close the gas leaks are located to a building, the LDCs prioritize the leaks into four classes from the highest to lowest priority: A1, A2, B, and C (see SI, Sect. 2.S.4.1, Table 2.S12). In Hamburg, both LIs in the high category were identified as A1 gas leaks and fixed by GasNetz Hamburg immediately. Most of the Hamburg LIs that were detected and identified as fossil are in close proximity to the natural gas distribution pipelines (see SI, Sect. 2.S.4.2, Table 2.S13). Investigation of the pipeline material shows that most of NGDN emissions are due to leaks from steel pipelines (see SI, Sect. 2.S.4.2, Table 2.S14), which are more prone to leakage because of pipeline corrosion (Zhao et al., 2018). Nevertheless, only 7 of the 30 LIs (23%) that were positively attributed to fossil CH_4 were detected and fixed by the LDC. If we assume that the fraction fossil / total LIs determined in Hamburg (≈ 35%) is representative for the entire population of LIs encountered (thus also for the ones that were not attributable), about 50 of the 145 LIs are likely due to fossil CH_4. The LDC found and fixed leaks at 10 of these locations (≈ 20%). A recent revisit (January 2020) to these locations confirmed that no LIs were detected at 9 out of these 10 locations. For the 10th location a smaller LI was detected in close proximity, and GasNetz Hamburg confirmed that this was a leak from a steel pipeline. The whole pipeline system on this street dates back to the 1930s and is targeted for replacement in the near future.

In summary, about 20 % of the LIs including the two largest LIs that were attributed to a fossil source were identified as NGDN gas leaks (see SI, Sect. 2.S.4.2, Figure 2.S18), and were repaired by GasNetz Hamburg, but these accounted for about 50 % of fossil CH_4 emissions of Hamburg, similar to what was observed in the US studies (Weller et al., 2018). Possibly, smaller leakages that can be detected with the high sensitivity instruments used in the mobile surveys cannot be detected with the less sensitive equipment of LDCs. Another possible explanation for the fact that the LDC did not detect more leaks may be that reported LI locations do not always coincide with the actual leak locations, although Weller et al. (2018) reported that the median distance of actual leak locations to the reported ones was 19 m. Combined measurements with GasNetz Hamburg are planned to investigate why the majority of the smaller LIs reported in mobile surveys is not detected in the regular surveys of the LDC.

The average C_2:C_1 ratio for LIs with a significant C_2H_6 signals across Hamburg was 5.6 ± 3.9%. For the spots where the LDC found and fixed leaks this ratio was 3.9 ± 2.6%. Thus, some of the locations where CH_4 enhancements were found were influenced by sources with an even higher C_2:C_1 ratio than the gas in the NGDN. One confirmed example is the very high ratio found in exhaust from a vehicle as shown in Figure 2.S12 (see SI, Sect. 2.S.2.6). The abnormal operation of this vehicle is confirmed by the very high CH_4:CO_2 ratio of 5.5 ppb:ppm (SI, section 2.S2). This is more than 20 times higher than CH_4:CO_2 ratios of 0.2 ± 0.1 ppb ppm^{-1} observed during passages through the Elbe tunnel, a ratio that agrees with previous studies (SI, section 2.S2).

Repairing gas leaks in a city has several benefits for safety (preventing explosions), sustainability (minimizing GHG emissions) and economics. Gas that is not lost via leaks can be sold for profit, but gas leak detection and repair is expensive and is usually associated with interruptions of the infrastructure (breaking up pavements and roads). Also, as reported above, and in agreement with the studies in US cities, for small LIs the underlying leaks are often not found by the LDCs, possibly because their equipment is less sensitive and aimed for finding leak rates that are potentially dangerous.

Our measurements in Hamburg demonstrate that in particular smaller LIs may originate from biogenic sources, e.g. the sewage system, and not necessarily from leaks in the NGDN. In this respect, attribution of LIs prior to reporting to the LDCs may be beneficial to facilitate effective repair. Figure 2.S19 (see SI, Sect. 2.S.5) illustrates how the individual measurement components can be efficiently combined in a city leak survey program.

2.4.5 Large facilities

The WWTP in Utrecht emits 160 ± 90 t yr^{-1}, which is similar to the total detected emissions (150 t yr^{-1}) inside the study area of Utrecht. The emissions reported for this facility from 2010 until 2017 are 130 ± 50 t yr^{-1} (Rijksoverheid, 2019), in good agreement with our measurements. CH_4 emission from a single well in Hamburg was estimated at 4.4 ± 3.5 t yr^{-1}, which is in the range of median emissions of 2.3 t yr^{-1} reported for gas production wells in Groningen, NL (Yacovitch et al., 2018), and average emissions of all US oil and gas production wells 7.9 ± 1.8 t yr^{-1} (Alvarez et al., 2018). In Hamburg, the emissions from a Compost and Soil Company amount to about 10% of the total emissions in the city target region, whereas a wellhead, a storage tank and a waste-oil separator contribute only about 1% each. This shows that individual facilities can contribute significantly to the total emissions of a city. The contribution of each source is dependent on infrastructure, urban planning and other conditions in the city (e.g. age and material of pipeline, maintenance programs, waste management, sewer system conditions, etc.), which may change the source mix from one city to another. For example, in Utrecht the WWTP is located within our domain of study. The wastewater treatment in Hamburg most likely causes CH_4 emissions elsewhere. Therefore, facility-scale CH_4 emissions should be reported on a more aggregated provincial or national level. For emissions from the NGDN, the urban scale is highly relevant, as the emission can only be mitigated at this scale.

2.5 Conclusions

Mobile measurements provide a fast and accurate technique for observing and identifying even relatively small CH_4 enhancements (i.e., tens of ppb) across cities and are useful for detecting potential gas leaks. During our intensive measurement campaigns, 81 LIs were observed in Utrecht (corresponding to emissions of ≈110 t CH_4 yr^{-1}) and 145 LIs (≈180 t CH_4 yr^{-1}) in Hamburg. These estimates, based on the streets covered, were then up-scaled to the total study area, using the road network map as a proxy for the length of the pipeline network which then yielded total emissions of 150 t yr^{-1} and 440 t yr^{-1} across the study area of Utrecht and Hamburg respectively. The isotopic signature of CH_4 in air samples and continuous mobile measurement of CO_2 and C_2H_6 mole fraction show that not all the LIs observed across the two cities have fossil origin. In Utrecht, C_2:C_1 and CH_4:CO_2 analyses show that 70 -90% of emissions were fossil. In Hamburg, C_2:C_1, CH_4:CO_2, and δ^{13}C-CH_4 and δD-CH_4 analyses suggests that 50 - 80% of emissions originate from natural gas pipelines. For the locations where samples for isotope analysis were collected, 80 % of emissions were identified as fossil. A large fraction of emissions in both cities originated from few high emitting locations. The LDC in Hamburg (GasNetz Hamburg) detected and fixed leaks at 20 % of the locations that likely due to fossil sources, but these accounted for 50% of emissions. Large LIs were generally confirmed as gas leaks from steel pipelines. The C_2:C_1 ratio at the locations where gas leaks were fixed by GasNetz Hamburg was 3.9 ± 2.6%. The mobile measurement technique is less labor and time intensive than conventional methods and can provide extensive coverage across a city in a short period. Based on our experience for the Netherlands and Germany a protocol could be developed that aids LDCs in guiding their leak detection and repair teams. The use of emission categories and source attribution can help target repair activities to the locations of large fossil emissions. Emission quantification from large facilities shows that these emissions may be equivalent to total CH_4 emissions from NGDN leaks in urban environments. In order to analyze discrepancies between spatial explicit measurement-based estimates as presented here with reported annual average national emissions by sectors a coordinated effort with

national agencies is necessary to address the lack of publicly available activity data (e.g., pipe material) disaggregated from the national-level (e.g., at the city-level).

Code availability

A MATLAB® code to analyze urban surveys is available on GitHub from Maazallahi et al. (2020a).

Data availability

The data including in-situ measurements, GPS data, and boundary of study areas are available on the Integrated Carbon Observation System (ICOS) portal from Maazallahi et al. (2020b).

Video supplement

A virtual tour of the measurements is available on the Leibniz Information Centre for Science and Technology and University Library (TIB) portal from Maazallahi et al. (2020c).

Author contributions

HM performed the mobile measurements, wrote the MATLAB® code, analyzed the data, and together with TR drafted the manuscript. JMF and MM contributed with air sampling and isotope analysis. DZ-A and SS contributed to the scientific interpretation and comparison between European and US cities. ZDW and JCvF facilitated comparison to US cities and contributed to the statistical analysis. HDvdG. and TR provided instruments, equipment, and supervised the measurements and data analysis. TR developed the research idea and coordinated the city campaigns. All authors contributed to the interpretation of the results and the improvement of the manuscript.

Acknowledgements

This work was supported by the Climate and Clean Air Coalition (CCAC) Oil and Gas Methane Science Studies (MMS) hosted by the United Nations Environment Programme. Funding was provided by the Environmental Defense Fund, the Oil and Gas Climate Initiative, the European Commission, and CCAC. This project received further support from the H2020 Marie Skłodowska-Curie project Methane goes Mobile – Measurements and Modelling (MEMO2; https://h2020-memo2.eu/, last access: 30 November 2020), grant number 722479. Daniel Zavala-Araiza and Stefan Schwietzke were funded by the Robertson Foundation. We thank Rebecca Fisher, who supervised the RHUL contribution to the isotopic analysis for the Hamburg campaign. Special thanks to Stefan Bühler from the Meteorological Institute of Hamburg University and Stefan Kinne from the Max Planck Institute for Meteorology for hosting our team during the Hamburg city measurement surveys. We would like to extend our appreciation to the anonymous referees for the insightful comments, which led to improvements of the paper. We appreciate continuous efforts from the executive and management board of GasNetz Hamburg along with Luise Westphal, Michael Dammann, Ralf Luy, and Christian Feickert, who facilitated productive communications, provided information on the gas infrastructure in Hamburg, and organized leak repairs with their teams in the study area in Hamburg. We also thank the asset manager of STEDIN Utrecht, Ricardo Verhoeve, who provided information and planned leak repairs by STEDIN in Utrecht. We thank Charlotte Große from DBI Gas and Environmental Technologies GmbH Leipzig (DBI GUT Leipzig), who helped with clarifying information on reported emission factors provided in national inventory reports. We thank the former MSc students of Utrecht University, Laurens Stoop and Tim van den Akker, who helped with the measurements in the Utrecht study area.

2.S Supplement

2.S.1) Data collection and instrumentation

2.S.1.1) Mobile measurements

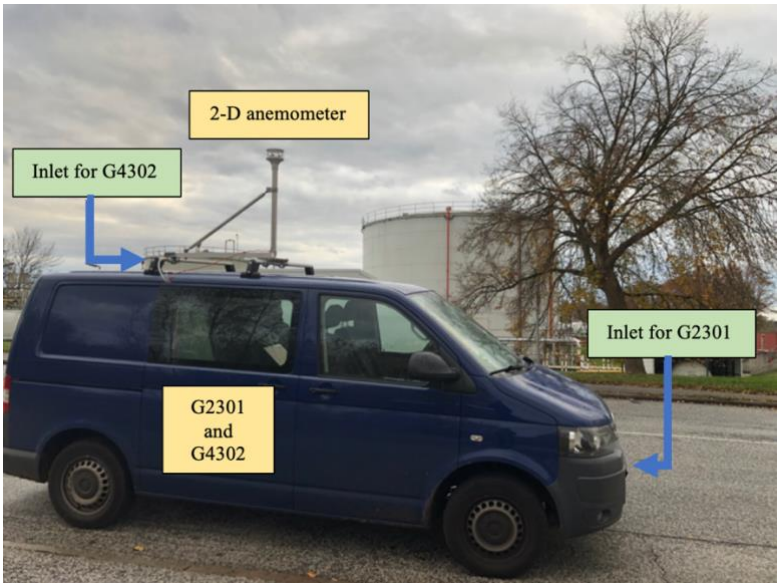

Figure 2.S1. Mobile measurement platform.

2.S.1.2) Target cities

Figure 2.S2a and Figure 2.S2b show total length of roads driven in Utrecht (≈ 1,300 km) and Hamburg (≈ 2,500 km). The areas outlined in black are the city areas where LIs from the NGDN were evaluated.

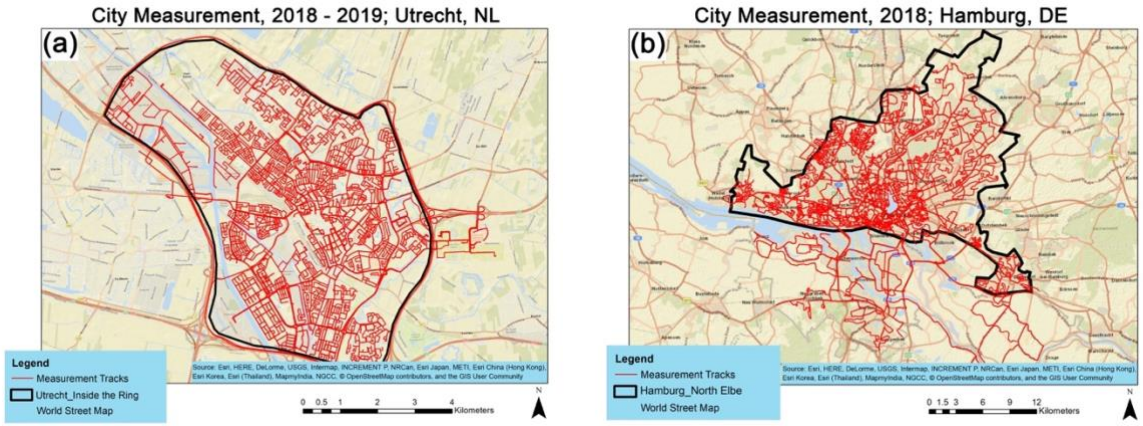

Figure 2.S2. Mobile measurement in (a) Utrecht and (b) Hamburg.

Table 2.S1 and Table 2.S2 provide information on each day's survey dates, districts targeted, instruments on-board, and duration of mobile measurements during each individual measurement days.

Table 2.S1. Information about each day's mobile measurement surveys in Utrecht.

Date dd.mm.yyyy	Picarro G2301		Picarro G4302		Target District	km driven	Km driven inside the ring
	Availability	Time correction	Availability	Time correction			
20.02.2018	Yes	14	-	-	Kanaleneiland	48.2	46.4
25.02.2018	Yes	14	-	-	Oud Hoograven, Hoograven, Lunette, and Hoograven,	53.2	50.5
26.02.2018	Yes	14	-	-	Tolsteeg	31.8	29.2

27.02.2018	Yes	14	-	-	Rivierenwijk	28.6	26.0
01.03.2018	Yes	14	-	-	Lombok, Nieuw Engeland, Oog in Al, and Halve Maan	72.2	69.8
12.03.2018	Yes	14	-	-	Rubenslaan, Schildersbuurt, Rijnsweerd, Tuindorp, and the Waste Water Treatment Plant	68.7	64.1
13.03.2018	Yes	14	-	-	Zeeheldenbuurt Hengeveldstraat, Rijnsweerd Noord, Wittevrouwen, Buiten Wittevrouwen, and Oudwijk	51	45.8
14.03.2018	Yes	14	-	-	Overvecht, Wolga- en Donaudreef, Taag- en Rubicondreef, Tigris- en Bostondreef, Schaakbuurt, and Geuzenwijk	123.9	119.6
15.03.2018	Yes	14	-	-	Lauwerecht, Pijlsweerd-Zuid, Tweede Daalsebuurt, Egelantierstraat-Mariëndaalstraat, Het Kleine Wijk, and Waste Water Treatment Plant	51.9	42.3
23.04.2018	Yes	14	-	-	Zuilen-Noord, Prins Bernhardplein, and Elinkwijk,	45.6	25.2
24.04.2018	Yes	14	-	-	Elinkwijk, Schepenbuurt bedrijvengebied Cartesiusweg, Dichterswijk, City Centre (Lange Nieuwstraat, Hooch Boulandt Moreelsepark, Wijk C, Breedstraatbuurt, Nobelstraat) and Waste Water Treatment Plant	204.4	117.1
25.04.2018	Yes	14	-	-	Blauwkapel and Voordorp en Voorveldsepolder	25.5	23.3
26.04.2018	Yes	14	-	-	Transwijk-Noord, Bedrijvengebied Kanaleneiland, and Bedrijventerrein De Wetering	100.5	94.0
29.04.2018	Yes	14	-	-	Bedrijventerrein Lageweide, Bedrijvengebied Overvecht, Wijk C, Rijnsweerd Noord, Waste Water Treatment Plant, and City Rings	36.3	33.9
09.05.2018	Yes	14	-	-	Hoograven-Zuid, Kanaleneiland, and Waste Water Treatment Plant	53.3	39.0
07.01.2019	Yes	28	-	-	Kanaleneiland and Waste Water Treatment Plant	38.4	30.4
14.02.2019	Yes	28	Yes	108	City Centre (Lange Nieuwstraat, Hooch Boulandt Moreelsepark, Wijk C, Breedstraatbuurt, Nobelstraat)	54.7	52.2
15.02.2019	Yes	28	Yes	108	Kanaleneiland	63.2	60.0
24.04.2019	Yes	28	Yes	220	City Centre, Kardinaal de Jongweg and Kanaleneiland	39.2	23.1
04.06.2019	Yes	21	Yes	220	Joseph Haydnlaan, Westbroek, and Waste Water Treatment Plant	68.1	18.8

Table 2.S2. Information about each day's mobile measurement surveys in Hamburg.

Date dd.mm.yyyy	Picarro G2301		Picarro G4302		Target District	km driven	Km driven north Elbe
	Availability	Time correction	Availability	Time correction			
18.10.2018	Yes	28	Yes	212	Harbor	50.9	13.7
19.10.2018	Yes	28	Yes	212	Harbor and oil extraction site	125.39	18.39
20.10.2018	Yes	28	Yes	212	Rotherbaum, Hoheluft-West, and Lokstedt	76.2	76.2
22.10.2018	Yes	28	Yes	217	Niendorf	89.3	89.3
24.10.2018	Yes	28	Yes	218	Schnelsen and Eidelstedt-West	98.8	91.6
25.10.2018	Yes	28	Yes	218	Harbor	122.6	12.6
26.10.2018	Yes	28	-	-	Groß Flottbek	47.1	47.1
27.10.2018	Yes	28	Yes	220	City Centre	74.2	72.3
28.10.2018	Yes	28	Yes	220	Altona	80.9	80.9
29.10.2018	Yes	28	Yes	220	Othmarschen-West, Nienstedten-East	66.8	66.8
30.10.2018	Yes	28	Yes	220	Blankenese, Sülldorf, and Rissen	137.6	132.4
31.10.2018	Yes	28	Yes	226	St. Georg, Hamburg-Hamm, Hohenfelde, Eilbek, and Barmbek-Süd	99.5	99.5
01.11.2018	Yes	28	Yes	227	Rahlstedt, Wandsbek, and Billstedt	156.5	154.8
02.11.2018	Yes	28	Yes	228	Sasel, Bergstedt, and Bramfeld,	111.3	111.3
03.11.2018	Yes	28	Yes	229	Barmbek-Süd, Winterhude, and Barmbek-Nord	82.7	82.7
04.11.2018	Yes	28	Yes	230	Hamburg-Nord, Hummelsbüttel, Langenhorn, Lemsahl-Mellingstedt, Duvenstedt, and Wohldorf-Ohlstedt	201.7	192.5
06.11.2018	Yes	28	Yes	236	Eimsbüttel, Lokstedt, Winterhude-North, Rotherbaum-West, and Schnelsen	114.6	114.6
07.11.2018	Yes	28	Yes	236	Harbor and Sampling	93.2	12.2
08.11.2018	Yes	28	Yes	236	Sampling	81.7	76.4
09.11.2018	Yes	28	Yes	236	Sampling	122.9	43.5
10.11.2018	Yes	28	Yes	236	Lurup, Groß Flottbek – NorthWest, Marmstorf, Neugraben-Fischbek, Harburg, and Ronneburg	171.6	78.7
11.11.2018	Yes	28	Yes	240	Bergedorf, Allermöhe, Lohbrügge,	175.1	88.5
14.11.2018	Yes	28	Yes	245	East-West Transects on the North Side of the Elbe River	87.4	72.6

2.S.1.3) Instruments comparison

In the Hamburg study, the two analyzers (G2301 and G4302) were operated in parallel. The Picarro G2301 instrument measures CH_4, CO_2, and water vapor (H_2O) and provides 0.3 Hz measurements at a flow rate of about 200 ml min^{-1} and the G4302 measures CH_4, C_2H_6, and H_2O with a frequency of 1 Hz and at a flow rate of about 2 L min^{-1}. The G4302 can be operated in CH_4 only mode, or in C_2H_6 – CH_4 mode, where the noise of CH_4 measurements increases by about one order of magnitude. The inlet for the Picarro G2301 instrument was from the bumper while the inlet for the G4302 was from the roof of the vehicle (Figure 2.S1). In Figure 2.S3c and Figure 2.S3d linear

correlation of CH_4 mole fractions shows a correlation of results from the G2301 and G4302 instruments, the latter in both C_2H_6 and CH_4-only mode, which show good linear correlation in both modes. In order to guarantee consistency with the von Fischer et al., (2017) and Weller et al., (2019) quantification algorithm which was developed for a G2301 instrument, in our study the data from this instrument are used for the CH_4 quantification and attribution through CH_4:CO_2 ratio, and the G4302 is primarily used for source attribution via the C_2:C_1 ratio.

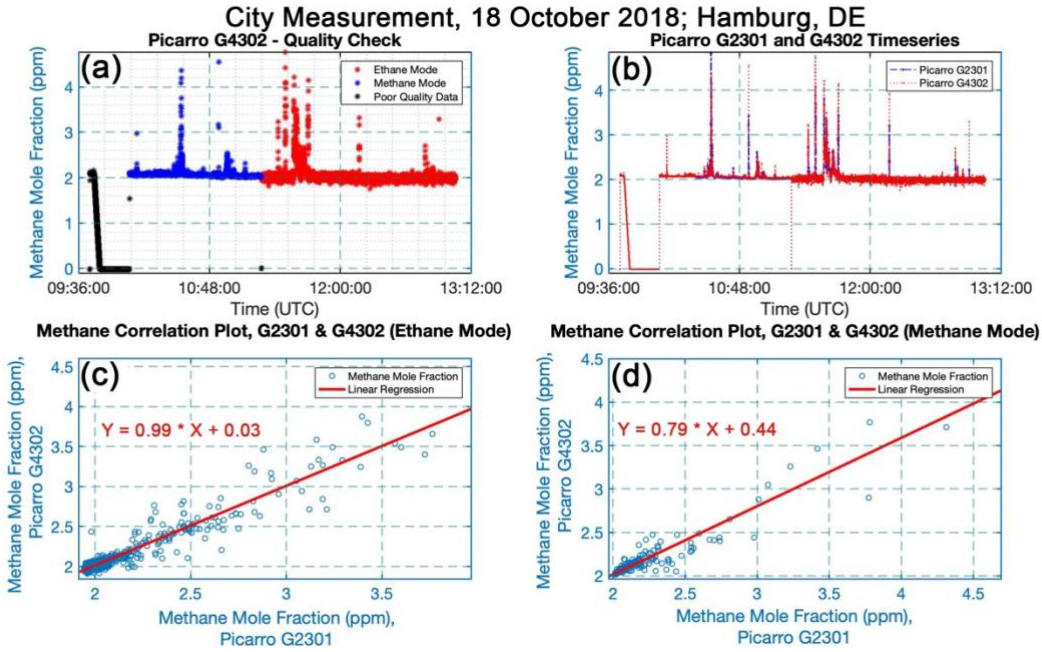

Figure 2.S3. (a) Example of raw data and data quality check of G4302, (b) timeseries of CH_4 mole fraction recorded by G2301 and G4302, (c) in-situ measurement correlation plot of G2301 and G4302 while the G4302 was in C_2H_6 mode, and (d) in-situ measurement correlation plot of G2301 and G4302 while the G4302 was in CH_4 mode.

Table 2.S3 shows a comparison between the different instruments and inlets for a selection of CH_4 enhancements where the G4302 operated in CH_4 mode. CH_4 enhancements above background level are referred to leak indications (LIs). All the LIs were observed by both instruments when both instruments were running together. In a few cases, the G4302 places an LI in a higher category (when using the Weller et al., (2019) algorithm). The largest difference between the two instruments was observed for the highest LI in Utrecht, where a CH_4 enhancement of 16.2 ppm (corresponding to 100 L min^{-1}) was recorded on the G2301 instrument, whereas an enhancement of 31.9 ppm (corresponding to 230 L min^{-1}) was recorded by the G4302. The difference may be due to the higher flow rate and sampling rate of the G4302, which reduces smoothing in the sample cell compared to the G2301 instrument. However, the difference may also be due to the two different inlets sampling different parts of the plume, because of the different inlet location. In principle, the expected behavior would then be opposite: Larger enhancements would be expected closer to the ground where the inlet of the G2301 instrument is located, but turbulent plume dispersion in on streets by driving cars can result in very irregularly shaped emission plumes.

Table 2.S3. Comparison of enhancements detected with the G2301 and G4302 instruments.

Instrument	Yellow category (0.5 – 6 L min^{-1} emissions)	Orange category (6 – 40 L min^{-1} emissions)	Red Category (>40 L min^{-1} emissions)	Total	Sum Emissions (L min^{-1})
Hamburg					
G2301	90	8	2	100	370
G4302	86	12	2	100	400
Utrecht					
G2301	22	3	1	26	180
G4302	20	5	1	26	370*

* The large difference is primarily due to the much higher CH4 elevation recorded with the G4302 for the LI in the "red" category, see text.

2.S.1.4) Road data from Open Street Map (OSM)

Information from the Open Street Map (OSM) (Figure 2.1) was used for several purposes. Firstly, it was investigated whether there is any correlation between type of roads and CH_4 enhancements. Therefore, the streets in both cities were categorized into level 1, 2, 3, residential, and unclassified streets based on the categories from the OSM (Table 2.S4). Secondly, not all streets across the cities were covered and data on the total road network from OSM were used to extrapolate the results from the roads covered to the entire natural gas distribution network in the cities. The OSM was also used to determine from the recorded GPS coordinates how many times each street was surveyed. As GPS coordinates may not perfectly sit on OSM data, 15m both-sided buffer zone was used for level 1, 2, and 3 and 10m both-sided buffer zone was used to extract driven streets out of OSM data. These distances are slightly smaller than used for the US cities, reflecting the denser infrastructure and street network in Utrecht and Hamburg.

2.S.1.5) Road visits

Table 2.S4. Road category visits.

	Inside the ring, Utrecht			North Elbe, Hamburg		
Road class	Total (km)	Once (km)	More than Once (km)	Total (km)	Once (km)	More than Once (km)
Level 1	37.4	9.0	28.4	160.5	92.5	68.0
Level 2	45.4	12.0	33.4	197.8	124.2	73.6
Level 3	43.5	14.8	28.7	194.3	142.5	51.8
Residential	246.8	146.8	100.0	619.6	509.6	110.0
Unclassified	81.7	48.7	33.0	50.5	35.7	14.8

2.S.1.6) Measurements from facilities

Table 2.S5. Measurement from the waste water treatment plant in Utrecht (52.109791° N, 5.107605° E).

No.	Date (dd.mm.yyyy)	Wind Direction (°)	Wind Speed (m s^{-1})
1	12.03.2018	200 ± 5	3.7 ± 1.1
2	24.04.2018	210 ± 5	4.0 ± 1.2
3	07.01.2019	178 ± 5	3.5 ± 1.1

Table 2.S6. CH_4 measurements from facilities in Hamburg.

Facility	Date dd.mm.yyyy	Lat (° N)	Lon (° E)	Time Start (UTC) hh:mm:ss	Time End (UTC) hh:mm:ss	Wind Direction (°)	Wind Speed (m s^{-1})
A) Tank Reserves	18.10.2018	53.493237	9.969307	11:25:43	12:10:46	342 ± 9.5	3.2 ± 1.0
B) Refinery	18.10.2018	Unknown	Unknown	11:00:01	11:11:48	328 ± 4.3	3.2 ± 1.0
B) Refinery	20.10.2018	Unknown	Unknown	13:47:00	13:49:21	289.8 ± 3.3	4.7 ± 1.4
C) Steel factory	25.10.2018	53.519042	9.906555	12:42:54	13:15:54	288.7 ± 3.3	7.0 ± 2.1
C) Steel factory	07.11.2018	53.519042	9.906555	11:44:46	12:31:04	153.7 ± 9.8	1.4 ± 0.4
C) Steel factory	09.11.2018	53.519042	9.906555	09:59:41	10:22:23	109.5 ± 6.4	1.8 ± 0.5
D1) Separator	19.10.2018	53.468829	10.184400	08:42:11	08:42:36	323.5 ± 25.4	1.0 ± 0.3
D2) Storage Tank	19.10.2018	53.468446	10.187410	08:41:44	10:04:36	323.5 ± 25.4	1.0 ± 0.3
D3) Extraction Well	19.10.2018	53.466709	10.180733	08:41:44	10:04:36	323.5 ± 25.4	1.0 ± 0.3
D2) Storage Tank	11.11.2018	53.468446	10.187410	14:02:53	14:28:08	175 ± 1.4	2.7 ± 0.8
E) Farm	11.11.2018	53.444276	10.226374	14:34:30	15:07:49	174 ± 1.6	2.5 ± 0.8
F) Compost and Soil Company	04.11.2018	53.680233	10.053751	14:44:34	15:29:26	112 ± 3.1	1.5 ± 0.5
G) Landfill	04.11.2018	53.690721	10.092599	09:42:58	10:00:52	124 ± 3.2	2.4 ± 0.7
H) Car manufacturing factory	07.11.2018	53.475618	9.925336	14:28:41	14:40:29	171.5 ± 3.8	0.8 ± 0.2

Figure 2.S4. Construction at the street level; (a) not possible to access the total width or (b) streets were completely blocked.

2.S.1.7) Revisits; example of Utrecht city centre

In Figure 2.S5, one of the revisit surveys across Utrecht is shown in which the city centre was revisited after about 10 months.

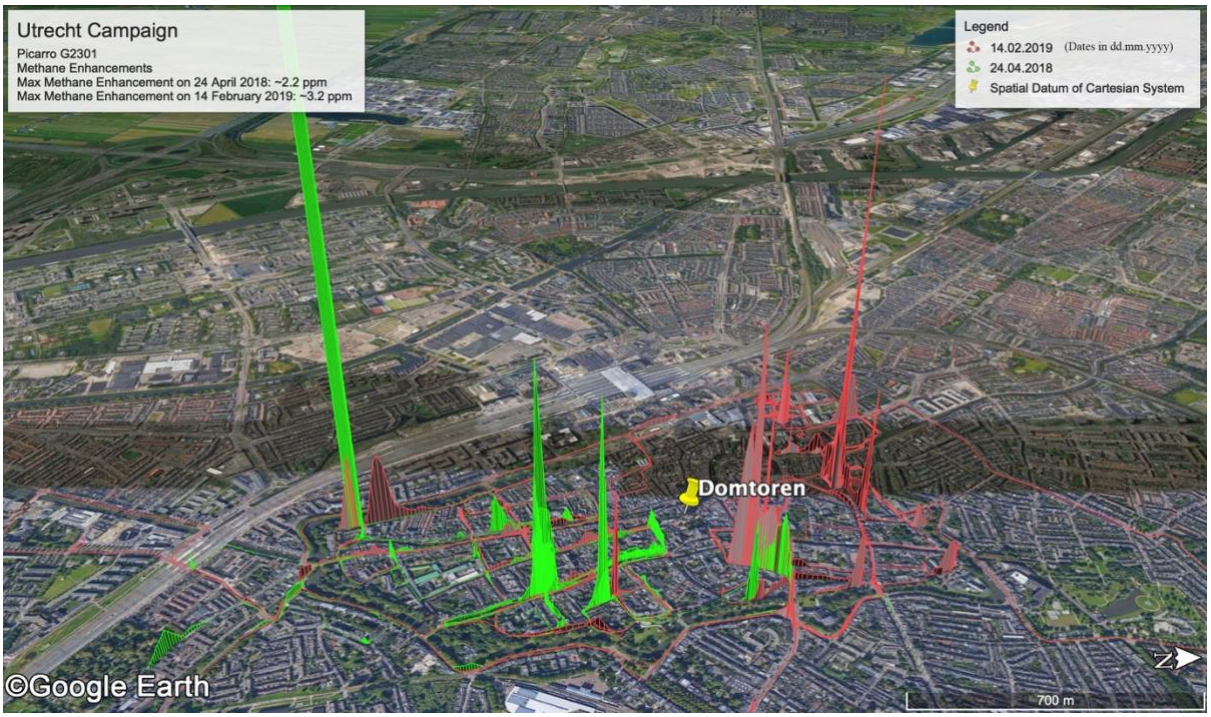

Figure 2.S5. Mobile measurement across city centre of Utrecht in February 2018 (red) and April 2019 (green).

2.S.1.8) Air sample collection

Samples were taken either inside the car or outside depending on road accessibility. Sampling locations were selected guided by the LIs observed during the untargeted surveys (Table 2.S1 and Table 2.S2). As the delay time of G4302 reading was lower and the analyzer is portable, it was more practical to use this instrument for sampling. In Figure 2.S6a, M. M. is taking samples at a location where the car could stop at the LI locations. In Figure 2.S6b, J. M. F. is walking with the G4302 analyzer to locate a source, in this case the source is shown in Figure 2.S15.

Figure 2.S6. Taking samples (a) inside the car or (a) outside.

2.S.2) Data evaluation procedures of CH_4 quantification

2.S.2.1) Background extraction

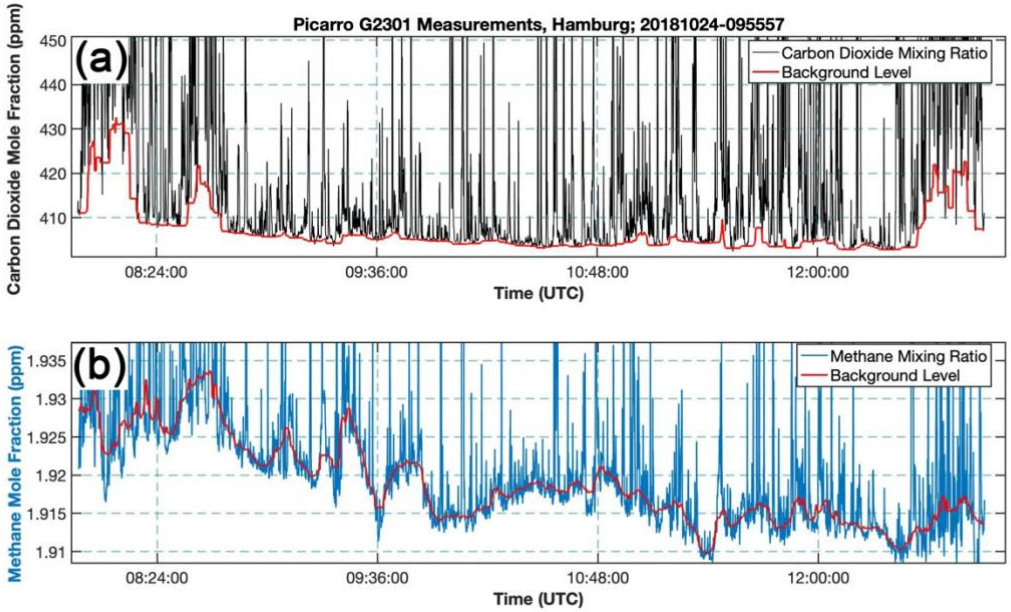

Figure 2.S7. Background extraction of (a) CO_2 and (b) CH_4; example of a survey in Hamburg.

2.S.2.2) Quantification of emissions from leak indications

The evaluation procedure was established by von Fischer et al. (2017) and Weller et al., (2019) for the G2301 instrument, so we used the dataset from G2301 for standard evaluation of LIs. Figure 2.S8 shows the overview of CH_4 emission quantification steps for emissions from the natural gas distribution network.

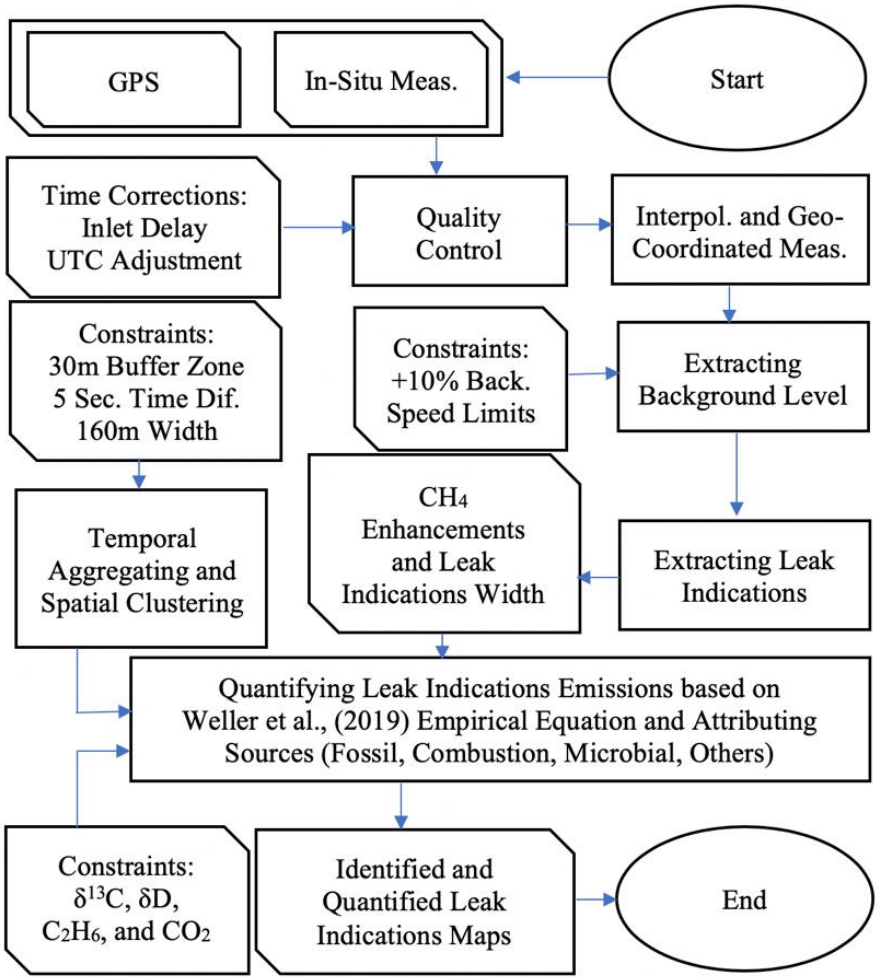

Figure 2.S8. Flow diagrams for the evaluating CH_4 emissions of leak indications.

2.S.2.3) Cartesian system and clustering

GPS records logged in decimal degrees were converted to a Cartesian coordinate system for further LI clustering using Eq. (2.S1). For this, local geographical datums were defined in both cities, in Utrecht it was the city cathedral (Domtoren) and in Hamburg the St. Nicholas' Church (Table 2.S7). The location of a point i relative to the reference point was calculated as:

$$X(i) = (\text{Longitude (i)} - \text{Longitude (Ref)}) * \frac{\pi}{180} * \cos\left(\frac{Latitude\ (Ref) * \pi}{180}\right) * R_e \quad (2.S1a)$$

$$Y(i) = (\text{Latitude (i)} - \text{Latitude (Ref)}) \frac{\pi}{180} * R_e \quad (2.S1b)$$

where Re = $6.378*10^6$ m is the radius of the Earth.

Table 2.S7. Local geographical datums in Utrecht and Hamburg.

City	Location	Latitude (° N)	Longitude (° E)
Utrecht	Domtoren	52.090628	5.121310
Hamburg	St. Nicholas' Church	53.547479	9.990709

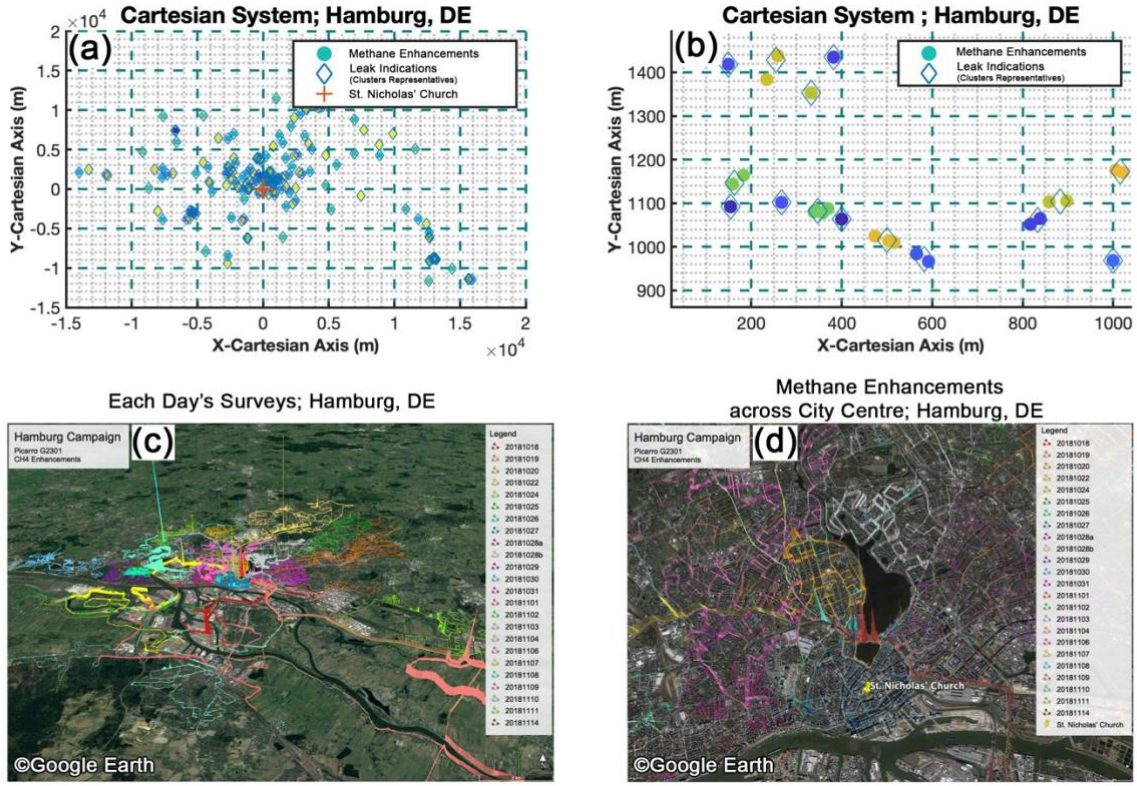

Figure 2.S9. Emission locations and clusters. (a) All LIs and clusters in the target area, (b) LIs and clusters in a smaller region, (c) complete view of each day's surveys across Hamburg, and (d) focus of each day's surveys across city centre of Hamburg.

2.S.2.4) Code comparison with CSU

Figure 2.S10 shows a comparison of results obtained with the MATLAB code from Utrecht University (UU) (Maazallahi et al., 2020a) with the code that was used by Colorado State University (CSU) for US cities. The two evaluation systems return basically very similar results.

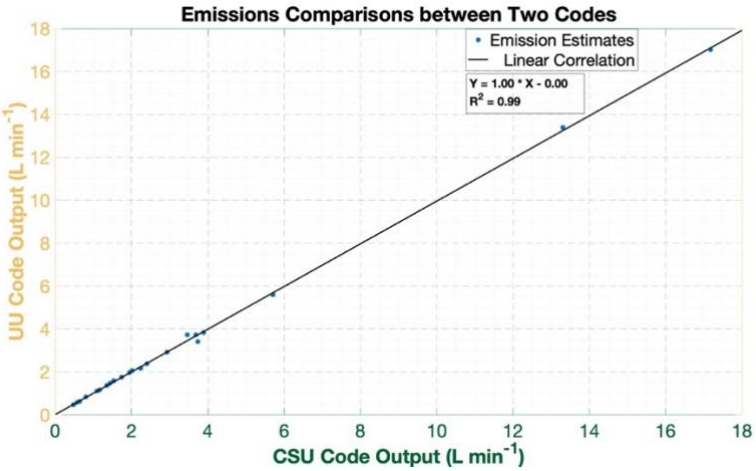

Figure 2.S10. Comparison of evaluation code from UU and CSU.

We adopt the distribution of observed CH_4 enhancements into different LI categories according to von Fischer et al., (2017).

2.S.2.5) Quantification of emissions from facilities

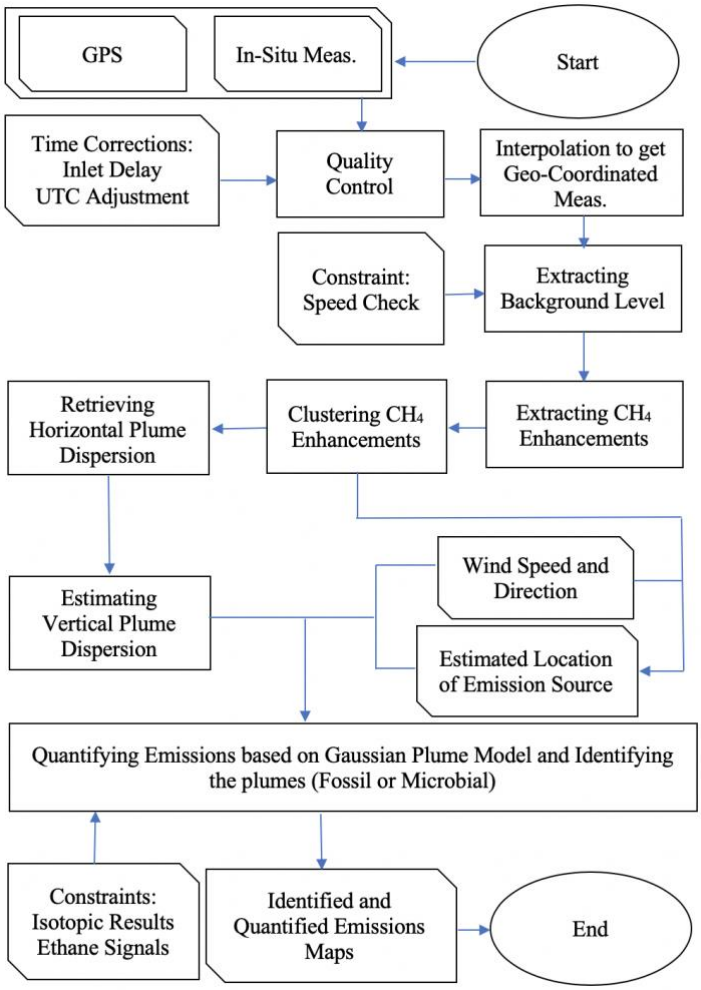

Figure 2.S11. Flow diagrams for the evaluating CH_4 emissions of facilities.

There are considerable difficulties and uncertainties in quantifying CH_4 emissions from facilities. Finding suitable roads that allow application of the Gaussian Plume Dispersion Model (GPDM) technique downwind of the source is often challenging. In addition, the characteristics of the sources are often complex. Waste water treatment plants like the one in Utrecht consist of several water tanks, but in the GPDM the whole plant was considered as one-point source. The same applies to the Compost and Soil Company and water-oil separator in Hamburg. Changing the distance from the source along the x-axis in GPDM analysis results in changes in σ_z, and for the case shown in Figure 2.7 $\sigma_z =$ 32.1 ± 14.2 m. Errors in wind speed are estimated to be ± 30% and for wind direction ± 5°. These errors are included in the total error estimate. The uncertainty in the height of the CH_4 emission is most relevant for the case of the storage tank in Hamburg. Most likely, emissions are from the top of tanks, but there can also be emissions at ground level. In addition, vertically stable atmospheric conditions or larger turbulences may lead to transport of air from a higher emission point to the ground level. In the simple GPDM, emission estimates rise exponentially when the point of emission is elevated. E.g. by changing source emission height from 0 - 10 m for the storage tank in Hamburg, the emission rate would change from 3.4 to 10.6 t yr^{-1}.

Emissions from facilities show significant contributions to the total emissions in both cities. This highlights the importance of considering emissions from all possible sources within a boundary of an study area. Hopkins et al. (2016b) showed that more than 30% of emissions from Los Angeles basin were not accounted in the emission inventory which are due to widely spread sources and mostly originate from fugitive fossil fuel emissions.

2.S.2.6) Unintended measurements

Figure 2.S12 shows measurements during a period when the measurement vehicle followed a car exhausting black smoke. Black smoke is an indication for incomplete internal combustion of the vehicle. In Figure 2.S12, the ratio of the area under the CH_4 enhancements along the driving track (in ppb*m) to the area of CO_2 enhancements along the driving track (in ppm*m) is 5.5 ppb ppm^{-1} which is much higher than reported in previous studies, possibly indicating incomplete combustion.

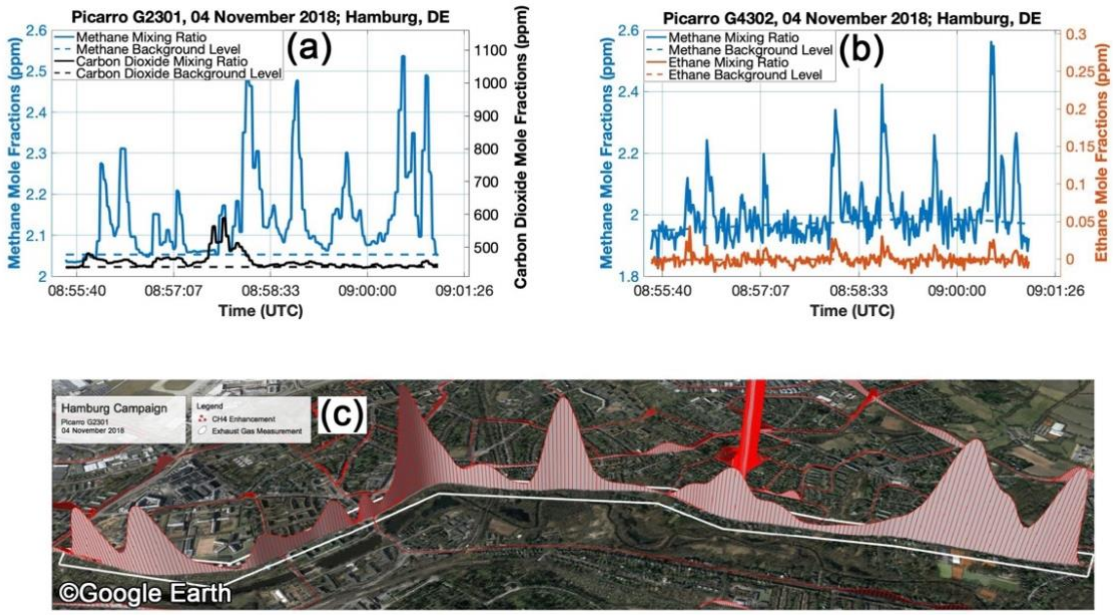

Figure 2.S12. Exhaust measurement from a car; (a) timeseries of CH_4 and CO_2 mole fractions from G2301, (b) timeseries of CH_4 and C_2H_6 mole fractions from G4302, and (c) the CH_4 excess track of measurement while following the car.

2.S.2.7) Data evaluation procedures of isotopic analysis

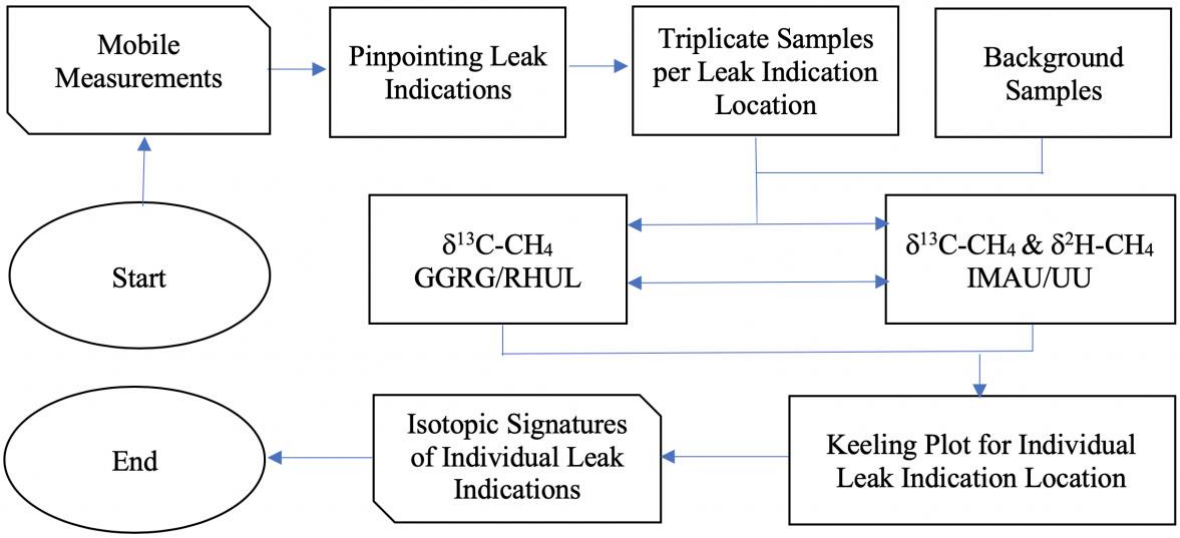

Figure 2.S13. Flow diagram for isotope analysis.

2.S.3) Evaluations outcomes

2.S.3.1) Methane emission distribution over different road categories

Table 2.S1. Statistics of observed LIs for different street categories in Hamburg and Utrecht. The three values per cell are the number of LIs, the total emission rate from all LIs in this category and the emission rate per LI.

		Total	Visited once	Visited more than once
Level 1				
Utrecht (Inside the Ring)	Number	6 LIs	----	6 LIs
	Emissions	4.6 L min^{-1}	----	4.6 L min^{-1}
	Emissions per LI	0.76 L/min/LI	----	0.76 L/min/LI
Hamburg (North Elbe)	Number	29 LIs	10 LIs	19 LIs
	Emissions	68.1 L min^{-1}	15.5 L min^{-1}	52.7 L min^{-1}
	Emissions per LI	2.3 L/min/LI	1.5 L/min/LI	2.8 L/min/LI
Level 2				
Utrecht (Inside the Ring)	Number	16 LIs	2 LIs	14 LIs
	Emissions	144.7 L min^{-1}	6.4 L min^{-1}	138.3 L min^{-1}
	Emissions per LI	9.0 L/min/LI	3.2 L/min/LI	9.9 L/min/LI
Hamburg (North Elbe)	Number	34 LIs	2 LIs	32 LIs
	Emissions	99.4 L min^{-1}	1.5 L/min	97.94 L min^{-1}
	Emissions per LI	2.9 L/min/LI	0.7 L/min/LI	3.1 L/min/LI
Level 3				
Utrecht (Inside the Ring)	Number	3 LIs	1 LI	2 LIs
	Emissions	10.2 L min^{-1}	1.6 L min^{-1}	8.6 L min^{-1}
	Emissions per LI	3.4 L min^{-1} LI^{-1}	1.6 L min^{-1} LI^{-1}	4.3 L min^{-1} LI^{-1}
Hamburg (North Elbe)	Number	23 LIs	8 LIs	15 LIs
	Emissions	43.0 L min^{-1}	7.6 L min^{-1}	35.4 L min^{-1}
	Emissions per LI	1.9 L min^{-1} LI^{-1}	1.0 L min^{-1} LI^{-1}	2.4 L min^{-1} LI^{-1}
Residential				
Utrecht (Inside the Ring)	Number	45 LIs	8 LIs	37 LIs
	Emissions	92.7 L min^{-1}	12.6 L min^{-1}	80.1 L min^{-1}
	Emissions per LI	2.1 L min^{-1} LI^{-1}	1.6 L min^{-1} LI^{-1}	2.2 L min^{-1} LI^{-1}
	Number	52 LIs	23 LIs	29 LIs
	Emissions	273.8 L min^{-1}	41.8 L min^{-1}	232.1 L min^{-1}
	Emissions per LI	5.3 L min^{-1} LI^{-1}	1.8 L min^{-1} LI^{-1}	8.0 L min^{-1} LI^{-1}
Unclassified				
Utrecht (Inside the Ring)	Number	11 LIs	5 LIs	6 LIs
	Emissions	37.8 L min^{-1}	13.4 L min^{-1}	24.4 L min^{-1}
	Emissions per LI	3.4 L min^{-1} LI^{-1}	2.7 L min^{-1} LI^{-1}	4.1 L min^{-1} LI^{-1}
Hamburg (North Elbe)	Number	7 LIs	2 LIs	5 LIs
	Emissions	5.9 L min^{-1}	1.5 L min^{-1}	4.4 L min^{-1}
	Emissions per LI	0.8 L min^{-1} LI^{-1}	0.8 L min^{-1} LI^{-1}	0.9 L min^{-1} LI^{-1}

2.S.3.2) Emission per capita

Per-capita emissions in both cities were based on the LandScan data, which use remote sensing imagery and analysis of nighttime lights, land cover and road proximity at ≈1 km^2 (30" * 30") spatial resolution (Bright et al., 2000) to estimate population density. The LandScan data yield 0.28 and 1.45 million inhabitants in the study area of Utrecht and Hamburg respectively (Figure 2.S14).

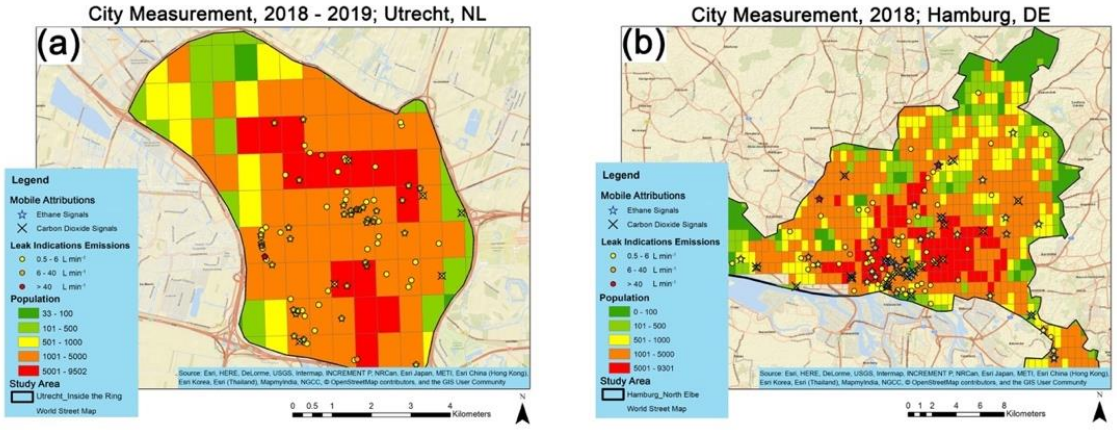

Figure 2.S14. Population distribution in (a) Utrecht and (b) Hamburg.

2.S.3.3) Isotopic signature and ethane-methane ratio

Table 2.S9. Isotopic signature and ethane-methane (C_2:C_1) ratio; North Elbe area in Hamburg

No.	Latitude (° N)	Longitude (° E)	Location	$\delta^{13}C$-CH_4	δD-CH_4	C_2:C_1 (%)	Emission (L min^{-1})
1	53.5605556	9.99483722	Warburgstrasse	-50.4	-278.5	0	7.6
2	53.577521	9.988869	Rothenbaumchaussee	-62.7	-258	0	1.9
3	53.567191	9.999819	Alte Rabenstrasse	-52.19	-317.9	0	7.5
4	53.557113	9.996773	Lombardsbrücke	-46.3	-344.6	0	11.4
5	53.548297	9.973536	Neumayerstrasse	-49.9	-315.6	0	15.0
6	53.558212	10.006785	An der Alster	-23.4	-152.5	0	1.8
7	53.582506	10.016915	Geibelstrasse	-40.7	-194.2	3.0 ± 1.0	1.6
8	53.63921	10.040574	Distelweg	-42.6	-206.8	1.5 ± 0.5	46.6
9	53.614763	9.892181	Halstenbekerweg	-43.3	-187	3.6 ± 1.5	1.7
10	53.61402	9.890026	Astweg	-41.9	-185.1	3.6 ± 1.5	98.1
11	53.5631395	9.9862702	Edmund-Siemers Allee	-41.2	-207.4	3.8 ± 0.7	19.5
12	53.5836695	9.9839906	Eppendorfer Baum	-51.1	-301.3	0	2.0
13	53.5431789	10.0255373	Amsinckstrasse+Süderstrasse	-53.6	-272.7	0	1.6

Table 2.S10. Isotopic signature and C_2:C_1 ratio from facilities in Hamburg.

No.	Date dd.mm.yyyy	Latitude (° N)	Longitude (° E)	Location	Wind Direction	$\delta^{13}C$-CH_4	δD-CH_4	C2:C1
1	04.11.2018	53.68281	10.046241	Hummelsbütteler Steindamm (F)	112 ± 3.1	-46.9	-265.4	0
2	10.11.2018	53.572974	9.898723	Luruper Chaussee; Sudden wide plume	155.9 ± 10.1	-62.6	-287.8	0
3	09.11.2018	53.541798	9.917605	The New Elbe Tunnel	111.7 ± 6.3	-28.6	-176.2	---
4	09.11.2018	53.51684	9.91380075	Steel factory; Dradenaustrasse (C)	109.5 ± 6.4	-50.1	-228.2	4.6 ± 1.9
	09.11.2018	53.5214485	9.90923915	Steel factory; Dradenaustrasse (C)	109.5 ± 6.4	-49.5	-269.9	---
5	18.10.2018	53.49147	9.97216	Oil storage tanks (A)	342 ± 9.5	-48.3	-421.7	0
6	07.11.2018	53.47645	9.924026	Mercedesstraße (H)	171.5 ± 3.8	-43.0	-207.3	2.4 ± 0.6
7	19.10.2018	53.40675	10.13535	Big Plume; Steller Chaussee	290 ± 29.5	-66.0	-101.9	---
8	11.11.2018	53.445221	10.228102	Farm; Neuengammer Hausdeich	174 ± 1.6	-57.0	-317.2	0
9	19.10.2018	53.46275	10.18198	Neuengammer	323.5 ± 25.4	-53.0	-235.8	-----
	19.10.2018	53.467774	10.19001	Oil Storage Tank; Randerseidet schleusendam (D2)	323.5 ± 25.4	-45.6	-164	6.6 ± 1.4
	11.11.2018	53.469045	10.188069	Oil Storage Tank; Neuengammer Hausdeich (D2)	175 ± 1.4	-44.8	-183.2	7.7 ± 1.5

Figure 2.S15. (a) CH_4 enhancements in the southern part of the Alster in Hamburg, the LIs inside the white polygon were attributed to a microbial source, and (b) the photograph shows an exhaust from the sewage system that was identified as strong CH_4 source.

2.S.3.4) Measurements inside the New Elbe Tunnel

During three surveys (07, 09, and 10 - November 2018), we drove inside the new Elbe tunnel to reach the south side of the Elbe river. Figure 2.S16a-c show the CO_2 and CH_4 measurement time series during these passages, and Figure 2.S16d shows a correlation of CO_2 and CH_4 enhancements above the background. The average CH_4:CO_2 enhancement ratio inside the tunnel was 0.2 ± 0.1 ppb:ppm which is in agreement with the ratio of 0.3 reported by Naus et al. (2018) for cars working under normal conditions.

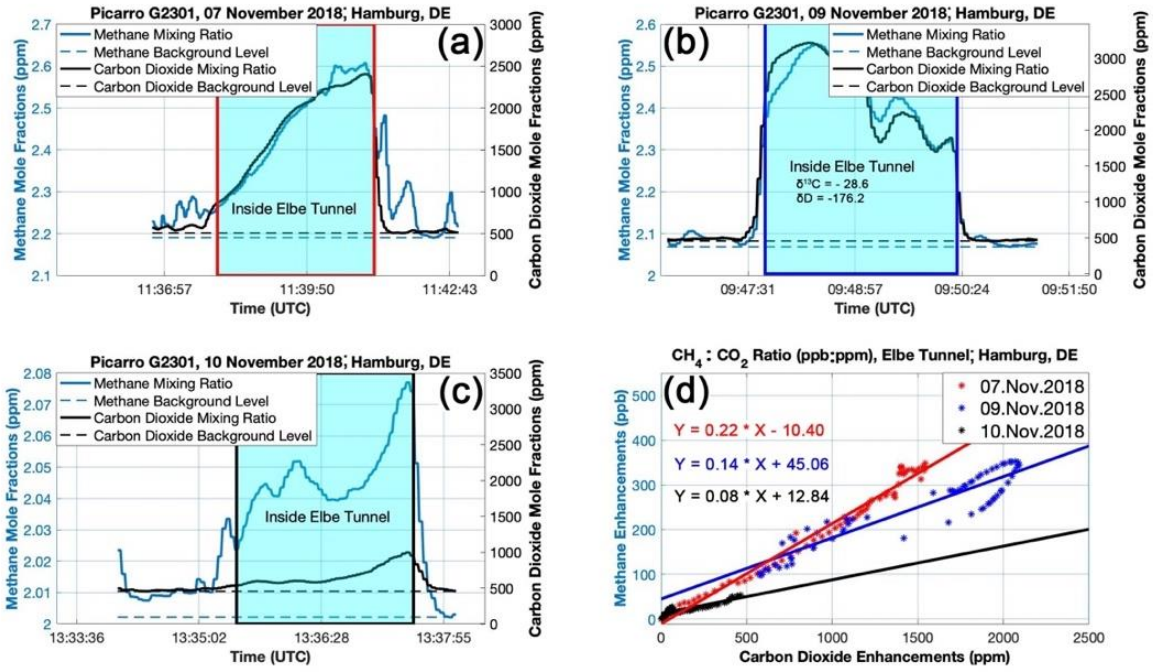

Figure 2.S16. In situ measurements from G2301 during driving inside the new Elbe tunnel; (a) on 07 November 2018, (b) on 09 November 2018 including signatures from isotopic sampling analysis, (c) on 10 November 2018, and (d) CH_4:CO_2 ratio of enhancements inside the tunnel.

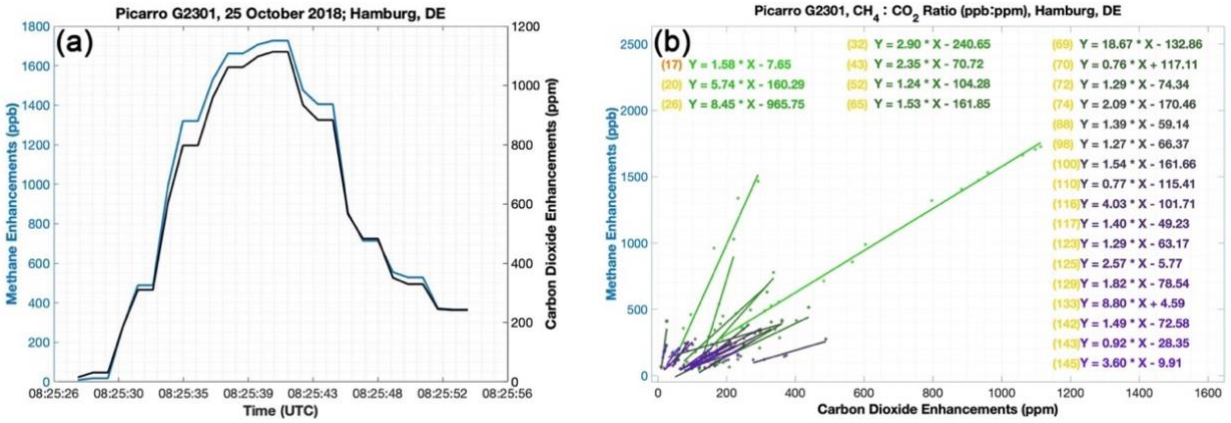

Figure 2.S17. (a) Example of concomitant CH_4 and CO_2 enhancements for a LI measured with the G2301 instrument and (b) CH_4 and CO_2 correlations for the LIs attributed to combustion sources in Hamburg.

2.S.4) Standards, regulations, and LDC leak detection

2.S.4.1) Standards and regulations for local gas companies in Germany

In this section, technical regulations on inspection of gas pipework systems with operation pressures up to 16 bar by Deutscher Verein des Gas- und Wasserfaches (DVGW) are provided

(document DVGW G 465-1 to 4 (DVGW, 2019b)). Inspections are carried out with measurement equipment (according to DVGW G 465-4 (DVGW, 2019b)) while walking along the street/areas with pipelines in the ground. Inspections of pipelines follow a fixed schedule (Table 2.S11).

Table 2.S11. Inspection intervals of gas pipes in the ground (Table 2 in DVGW G465-1 (DVGW, 2018))

Leak frequency (Number of detected leaks per km monitored / checked pipe	≤ 0.1	≤ 0.5	≤ 1
Operating pressure	Inspection interval in years		
≤ 1 bar	6 (only for PE-pipes and pipes with cathodic corrosion protection)	4	2
> 1 bar to ≤ 5 bar	4 (additional bimonthly track inspection)	2	1
> 5 bar to ≤ 16 bar	1 (depended on the material of the pipe)		

Leaks are classified into four categories based on proximity of the leaks to buildings, and each category requires certain actions to prevent incidents/accidents (DVGW, 2019a).

Table 2.S12. Leak classes and action required

Leak classification	Leak detection proximity to the building	Repairing actions
A1	Leak into a building	Immediate
A2	Leak very close to a building	Within a weak
B	Leak in bigger distance to a building	3 months
C	There is no danger of incoming gas in a building or cavity	According to recommended recovery plan

2.S.4.2) Measurement procedures by GasNetz Hamburg

GasNetz Hamburg uses gas detectors from Sewerin (e.g. portable Ex-Tec PM4, detection limit 1 ppm above background). The analyzer sucks in air close to the ground and a person pushes the analyzer forward while online readings are available on a screen (Figure 2.S18), while all the local gas distribution network pipelines are available and checked on site. All the 145 reported LIs where initially checked by GasNetz Hamburg by overlapping with the network map to see if the locations are in close proximity to pipeline from the NGDN. The LIs were prioritized in classes mentioned in Table 2.S12, and finally leak detection and repair practices were carried out. The company not only checked the reported locations by this study, but also the surrounding area including house connections, parks, gardens, etc., where pipelines are located close by.

Figure 2.S18. Leak detection operation by GasNetz Hamburg

Table 2.S13. Distances of observed LIs from the natural gas distribution network grid

Distance (m)	Red	Orange	Yellow
0	100 %	75 %	67 %
10	----------	25 %	21 %
20	----------	----------	5 %
30	----------	----------	3 %
40	----------	----------	1 %
50	----------	----------	2 %

Table 2.S14. Pipeline materials at the locations of observed LIs

Pipeline material	Red	Orange	Yellow
Steel	100 %	67 %	63 %
Polyethylene	----------	33 %	37 %

2.S.5) Gas Leak detection and repair

Mobile measurements provide enormous and valuable amount of data in a short period of time with an ability of large coverage in urban area for the purpose of detecting and quantifying leaks from NGDNs. This study shows that CH_4 mobile measurements associated with several attribution techniques are capable of distinguishing fossil LIs. In this study, we added source attribution techniques to an algorithm which was initially designed to detect and quantify leaks from pipeline. This algorithm was introduced in von Fischer et al. (2017), and later improved in Weller et al. (2019); Figure 2.S8 shows the steps we followed in this study to detect, quantify, and attribute CH_4 emissions in urban area. We concluded that the attribution techniques we used to distinguish fossil-related sources are effective. Mobile CO_2 and C_2H_6 enhancements to eliminate non-fossil LIs is effective in locating the most potential signals related which indicate leaks from pipelines. Analyzing isotopic samples ($\delta^{13}C$-CH_4 and δD-CH_4) provides detailed information on the origin of emission sources, however it is time-consuming effort and not possible to take samples from all locations where we observed CH_4 enhancements. In Figure 2.S19, we provide a flowchart based on the findings of this study and experiences we obtained by collaboration with GasNetz Hamburg and STEDIN Utrecht to locate NGDNs leaks. In this flowchart we suggest to combine mobile measurements and attribution (blue box) to report potential gas leaks to local utilities before current repair practice (green box).

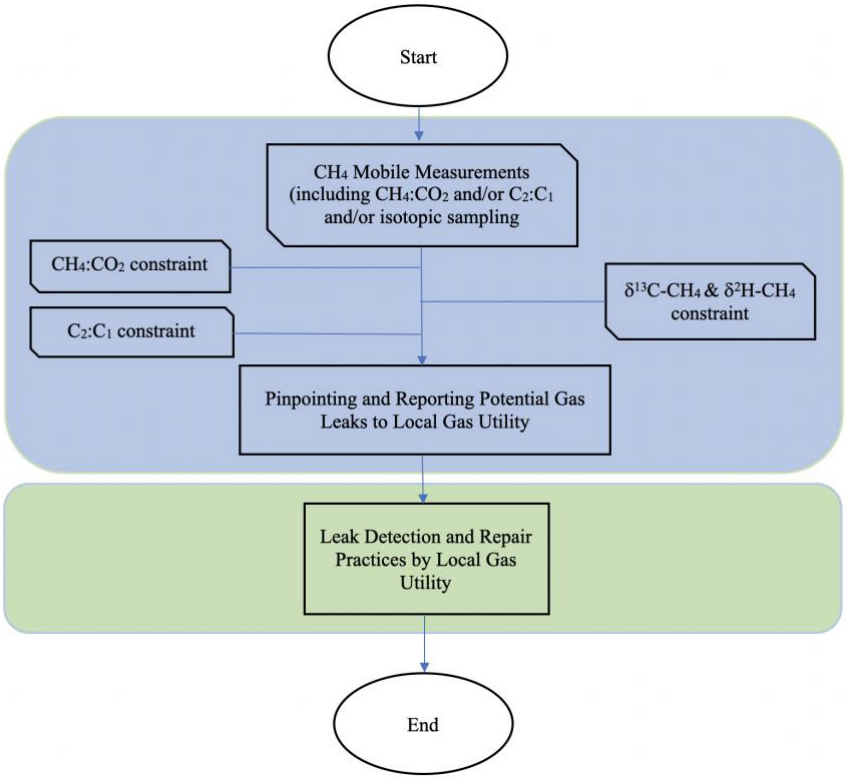

Figure 2.S19. Gas detection and repair practices flowchart

3 Street-level methane emissions of Bucharest, Romania and the dominance of urban wastewater

Julianne M. Fernandez[1], Hossein Maazallahi[2,3], James L. France[1,5], Malika Menoud[2], Marius Corbu[4], Magdalena Ardelean[4], Andrea Calcan[4], Amy Townsend-Small[6], Carina van der Veen[2], Rebecca E. Fisher[1], Dave Lowry[1], Euan G. Nisbet[1], and Thomas Röckmann[2]

[1]Department of Earth Sciences, Royal Holloway University of London, Egham, TW20 0EX, United Kingdom
[2]Institute for Marine and Atmospheric Research Utrecht, Utrecht University, Utrecht, The Netherlands
[3]Netherlands Organization for Applied Scientific Research (TNO), Utrecht, The Netherlands
[4]National Institute of Aerospace Research "ELIE CAROFOLI" - INCAS, Bucharest, 061126, Romania
[5]British Antarctic Survey, Natural Environment Research Council, Cambridge, CB3 0ET, United Kingdom
[6]Department of Geology, University of Cincinnati, Cincinnati, OH, 45221, United States of America

Abstract. Atmospheric CH_4 continues to increase, but there are multiple anthropogenic source categories that can be targeted for cost-effective emissions reduction. Cities emit CH_4 to the atmosphere from a mixture of anthropogenic CH_4 sources, which include, but are not limited to, fugitive emissions from natural gas distribution systems, wastewater treatment facilities, waste-and rainwater networks, and landfills. Therefore, to target mitigation measures, it is important to locate and quantify local urban emissions to prioritize mitigation opportunities in large cities. Using mobile measurement techniques, we located street-level CH_4 leak indications, measured flux rates, and determined potential source origins (using carbon and hydrogen stable isotopic composition along with C_2:C_1 ratios) of CH_4 in Bucharest, Romania. We found 969 confirmed CH_4 leak indication locations, where the maximum mole fraction elevation (above background) was 38.3 ppm (mean = 0.9 ppm ± 0.1 ppm s.e.; n = 2482). Individual leak indicator fluxes, derived using a previously established empirical relation, ranged up to around 15 metric tons CH_4 yr^{-1} (mean = 0.8 metric tons yr^{-1} ± 0.05, s.e.; n = 969). The total estimated city emission rate is 1832 tons CH_4 yr^{-1} (min = 1577 t yr^{-1} and max = 2113 t yr^{-1}). More than half (58% to 63%) of the CH_4 elevations were attributed to biogenic wastewater, mostly from venting storm grates and manholes connecting to sewer pipelines. Hydrogen isotopic composition of CH_4 and C_2:C_1 ratios were the most useful tracers of CH_4 sources, due to similarities in carbon isotope ratios between wastewater gas and natural gas. The annual city-wide CH_4 emission estimate of Bucharest exceeded emissions of Hamburg, Germany by 76% and Paris, France by 90%.

3.1 Introduction

CH_4 is a major greenhouse gas (GHG), with a global warming potential 28 times that of CO_2 over 100 years (IPCC AR5, Myhre et al., 2013). Shorter atmospheric lifetime of CH_4 compared to CO_2 of around a decade makes it an attractive target for rapid GHG reduction efforts. The atmospheric CH_4 burden has more than doubled over the past 200 years (Mischler et al., 2009; Saunois et al., 2020; Sowers et al., 2010), reaching a global annual average of 1877 ± 2 ppb in 2019 (WMO, 2020). Although we have a good qualitative understanding on various naturally produced (wetlands, freshwater, geological activity, etc.) and anthropogenically induced CH_4 sources (fossil fuel production, agricultural practices, waste management, etc.) (Kirschke et al., 2013), there still remain discrepancies on how these sources contribute to CH_4 budgets and isotopic balance locally and regionally (Miller et al. 2013; Saunois et al., 2020; Sherwood et al. 2017; Worden et al., 2017; Zazzeri et al., 2017). It is important to understand and discriminate between these source inputs at regional and local scales in order to identify mitigation opportunities, in order to halt the presently ongoing rapid global CH_4 increases (Dlugokencky et al., 2011; Nisbet et al., 2019) and bring the global CH_4 burden back to a pathway required to comply with the United Nations (UN) Paris Agreement (Nisbet et al. 2020). Over the past decade, there has been a growing research interest in identifying and quantifying fugitive CH_4 emissions from populated regions, specifically in urbanized areas. Studies of U.S. cities like Los Angeles, California and Boston, Massachusetts have shown that thermogenic natural gas emissions can be the major source of excess CH_4 in these urban areas (Brant et al., 2014; McKain et. al., 2015; Peischl et al., 2013; Philips et al., 2013; Townsend-Small et al., 2012; Wennberg et al., 2012). More broadly, CH_4 emissions in cities can also include combinations of multiple fossil fuel sources, as well as biological sources such as waste (landfills, sewers etc.), as seen in studies from Denver, Colorado and Indianapolis, Indiana (Chamberlain et al., 2016; Lamb et al., 2016; Townsend-Small et al., 2016b).

Various city studies have focused on detecting and quantifying emission rates from local natural gas distribution systems (Maazallahi et al., 2020d; von Fischer et al., 2017; Weller et al.,2018). Many of these studies have indicated city emission rates correlate with the state of infrastructure of the local natural gas distribution systems, for example depending on pipeline age and material (von Fischer et al., 2017; Hendrick et al., 2016; Gallagher et al., 2015). Such studies are useful in targeting infrastructure repairs and replacement plans of the local natural gas distribution systems. Though there are many studies on CH_4 emissions in urban areas, this field of research is still greatly dominated by investigations in U.S. cities. In Europe, studies have focused on only a few cities like London, U.K.

(Helfter et al., 2016; Lowry et al., 2001; O'Shea et al., 2014; Zazzeri et al., 2015; 2017), Paris, France (Defratyka et al., 2021; Xueref-Remy et al., 2020), Hamburg, Germany, Utrecht, Netherlands (Maazallahi, et al, 2020d), and Florence, Italy (Gioli et al., 2012). Less attention has been paid to emissions in eastern European cities (Kuc et al., 2002; Zimnoch et al., 2010; Zimnoch et al., 2018).

Urban CH_4 studies have indicated inconsistencies between measurements and regional inventory budgets. For example, in Boston, natural gas CH_4 emissions inferred from measurements were 2-3 times greater than the current inventory and industrial reports (McKain et. al., 2015). Importantly, most local and regional CH_4 inventories do not include top-down (TD) assessments, but instead rely on bottom up (BU) statistical emission estimates. TD methods use measurements of atmospheric CH_4, such as made by aircrafts, vehicles, walkers and tall fixed towers or monitoring stations. TD methods assess emissions integrated over large areas by a variety of techniques such as mass balance methods (Cambaliza et al., 2014; Mays et al., 2009) and inverse modeling. Continuous mobile measurement techniques and source tracers have been commonly used to investigate CH_4 emissions and identify the sources of these emissions (Defratyka et al., 2021; Lamb et al., 2016; Lowry et al., 2020; Maazallahi et al., 2020d; Philips et al., 2013).

Although, there are often disagreements between TD and BU observations (Saunois et al., 2020), detailed BU measurements can help reconciliate both approaches by detecting street-level emissions and appropriately allocating and quantifying them. This not only helps to reconcile TD and BU budgets, but improved inventories calculations also benefit local municipalities, gas consumers, local distribution companies, and supports resident safety (Han & Weng, 2010; Jackson et al., 2014; Ma et al., 2013). Recently, and currently still ongoing, significant mobile surveying efforts have been made to understand CH_4 sources in European cities. For example, there has been recent European Union and UN supported research in other cities including Paris (Defratyka et al., 2021), Hamburg, Germany & Utrecht, Netherlands (Maazallahi et al., 2020d).

Isotope measurements offer potent tools in discriminating between sources. In particular, mobile measurement techniques, in combination with various source tracers, have been efficient at separating emissions between waste sources and fossil fuel sources. Isotopic source signatures depend on the maturity / formation pathway of CH_4 (Schoell, 1984; Whiticar, 1990) (as seen in results section 4.3). Biogenic CH_4 is relatively depleted in ^{13}C and ^{2}H, whereas thermogenic CH_4, which is produced by the decomposition of ancient organic matter under elevated pressures and temperatures on a geological time scale (Coleman et al., 1981; Schoell, 1988), is often more enriched in ^{13}C and ^{2}H. CH_4 in air has commonly been analyzed for carbon 13 ($\delta^{13}C$-CH_4), as a tool in source apportionment. The analysis of δD-CH_4 is becoming more available as technology of analytical sample preparation systems advance, decreasing the need of large sample volumes and analysis time (Fisher et al., 2006; Jackson et al., 1999; Menoud et al., 2020; Röckmann et al., 2016; Yarnes, 2013). Research conducted on the Colorado Front Range in the U.S. has shown that δD-CH_4 was more powerful than $\delta^{13}C$-CH_4 at distinguishing waste, cattle husbandry, and fossil fuel sources (Townsend-Small et al., 2016b). Past studies that have utilized both carbon and hydrogen stable isotopes of CH_4 as source tracers have shown that δD-CH_4 is a more consistent tracer for characterizing natural gas sources (Townsend-Small et al., 2012; 2015; 2016b; Maazallahi et al., 2020d; Menoud et al.,2021).

The development of cavity ring-down spectroscopy (CRDS) and the capability of faster analysis (compared to isotopic analysis) has led to the utilization of C_2:C_1 (Lowry et al., 2020; Maazallahi et al., 2020d; Yacovitch et al., 2014), which allows for real-time determination of emission sources. C_2:C_1 ratios have been measured to identify gas leaks from natural gas distribution systems in cities (Lamb et al., 2016; Maazallahi et al., 2020d; Wunch et al., 2016), since biogenic sources do not contain C_2 higher alkanes, like C_2H_6, which are found only in thermogenic or combustion sources (Clayton 1991; James 1983). Past studies of pipeline material and age of a natural gas distribution network have shown that it is possible to model a network's "leak potential", with old cast iron and unprotected steel pipelines being most susceptible to corrosion, and thus with a greater frequency of leaks per unit of pipeline length (Harrison et al., 1993 Jackson et al., 2014; Lamb et al., 2015; Phillips et al., 2013; von Fischer

et al., 2017). These findings have also indicated that cities with aggressive pipeline repairs and replacement programs have fewer leaks per mile (90% less) when compared to cities without such maintenance programs (Gallagher et al., 2015).

Romania's long-standing oil and gas industry, the emergence of Bucharest as a major metropolis, and the lack of street-level measurements from Eastern European cities all make this region an interesting study site. Romania has a complex geological history resulting in an abundance of hydrocarbon-rich reservoirs within the Pannonian-Transylvanian Basin (Cranganu, 1996) and the Carpathian-Balkanian Basins (Amadori et al., 2012; Sclater et al., 1980). In 2019, Romania's natural gas production was 9.7 billion cubic meters, making Romania the 4th largest natural gas producer in Europe (BP, 2020). Romania's economy has long thrived from the petroleum industry due to the country's high producing reservoirs and was the first country to export gas in the 1900's (Nita, 2018). In 2016, Romania ranked within the top 20 countries globally for the reported highest gas-related CH_4 emissions globally (0.21 Tg a^{-1}) (Scarpelli et al., 2020).

This study aims to gain an understanding of urban street-level CH_4 emissions in Bucharest, Romania by answering the following questions:

1) What is the total annual CH_4 city-wide emission rate?

2) What are the dominant sources contributing to these emissions? and

3) How does the distribution of CH_4 sources in Bucharest compare with other measured cities?

To answer these questions, mobile surveys were conducted in the urban areas of Bucharest while continuously measuring CH_4 and C_2H_6 for locating enhanced CH_4 mole fractions above local atmospheric background, which are referred to as a leak indication (LI). The flux rates were determined for identified clusters of LIs. An annual city wide total emission estimate was calculated by scaling up the flux rates. Multiple locations, where CH_4 exceeded the daily atmospheric background mole fractions, were measured for $\delta^{13}C$-CH_4, δD-CH_4, and C_2:C_1 ratios for tracing contributing CH_4 sources. As Europe seeks to cut urban emissions, studies like this will be useful for identifying targets for mitigating emissions and for assessing future governmental regulation of greenhouse gas (GHG) emissions.

3.2 Study location

The focus location of this research is Romania's capital city, Bucharest. Romania has an area of 238,397 km^2 and a population of 19.4 million people in 2019 (NIS Romania, 2020). Bucharest is in the southeast of the country (44.4325° N, 26.1039° E). The metropolitan area covers 1,811 km^2, with a population of 2.2 million people in 2019 (NIS Romania, 2020). In addition to Bucharest, we also surveyed the nearby urban city of Ploiești, the historic center of Romania's oil industry, which is located in the county of Prahova, ≈60 km north of Bucharest (44.9333°N, 26.0333°E). Ploiești is much smaller by comparison, covering about 58 km^2 with a population of 225,000 (NIS Romania, 2020).

The total reported GHG emissions of Romania in 2018 were equivalent to 116,115 kt CO_2, which is made up of 66% CO_2, 24% CH_4 (28,184 kt CO_2 eq), 7% N_2O, and less than 2% fluorinated gases (Deaconu et al., 2020). The energy sector accounts for 66% (77,006 kt CO_2 eq) of the annual emissions, agriculture is 17%, industrial processes are 12%, and 5% is from the waste sector. These total relative GHG proportions are broadly similar to those from 1989, although the declared total fugitive CH_4 emissions from fossil fuels/distribution and livestock have decreased by 62% (UNFCCC, 2019). CH_4 emissions reported to the UNFCCC showed a 61.22% decrease between 1989 and 2017 (UNFCCC, 2019). From 1989 to 1992, decreased coal mining and lower energy consumption significantly reduced GHG emissions. The commissioning of Romania's Cernavodă Nuclear Power Plant 1996 has influenced a decrease in emission estimates from the energy sector.

Bucharest's industry, society, and landscape has been changing rapidly since the early 1990's and the city's economy has been growing since joining the EU framework (Nae and Turnock, 2010; Zolin, M.B., 2007). The 1989 Romanian Revolution and the resulting change of territorial governance practices had significant impacts on the management of Romania's urban GHG emissions (Kilkiș, Ș.,

2016), including the development of Bucharest's urban landscape and municipal planning (Ianoş et al., 2016; 2017; Nae and Turnock, 2010). During early 2004, Romania published its first National Waste Management Strategy (Orlescu and Costescu, 2013). Up until 2009, when the European model of integrated waste management was adopted, villages were storing waste in unofficial storage locations (Orlescu and Costescu, 2013). After the EU accession, Bucharest has closed 29 landfills (non-complying) and now has 3 major landfills (Chiajna-Rudeni, Glina and Vidra) located on the outskirts of the urbanized area (Orlescu and Costescu, 2013; Ianoş et al., 2012). Before the Glina Wastewater Treatment Plant was implemented in 2011, Bucharest did not have a designated wastewater treatment facility (Peptenatu et al., 2012; Veolia, 2013; Bojor, 2010), and raw wastewater was directly discharged into the local rivers (Arges, Dambovita and Colentia) (Peptenatu et al., 2012). The total simple length of sewage pipeline within Bucharest Municipality was 3,657 km in 2019 (NIS Romania, 2020), which collects both wastewater and storm water that discharges into a main conduit under the Dambovita River (Gogu et al., 2017). Both landfills and the sewage network are large potential contributors to the waste sector CH_4 emissions. Within the Bucharest municipality boundary, there was ≈2,124 km of gas pipeline contributing to the natural gas distribution network in 2019 (NIS Romania, 2020), which may be a large source of fossil fuel CH_4 emissions.

Although Romania does have a framework law on waste, Ianoş et al. (2016; 2017) suggest that Bucharest has lacked urban planning policies due to the passive urban management by local and central authorities. Measuring and monitoring GHG emissions in Bucharest may aid the local city governance to prioritize and enforce policies for the maintenance of municipality infrastructure such as natural gas distribution pipelines, residential and industrial sewage systems, and larger waste facilities like landfills (Iacoboaea and Petrescu 2013; Alamsi, 2013; Ianoş et al., 2012; Sandulescu, 2004).

3.3 Materials and methods

3.3.1 Mobile set-up

3.3.1.1 Continuous Instruments

Street-level emissions were measured using three vehicles and four different continuously measuring CRDS instruments. This included a Picarro G2301 (CH_4, CO_2, and H_2O) and a Picarro G2401 (CH_4, CO, CO_2, and H_2O) instrument. Both the G2301 and G2401 analyzers measure at a frequency of 0.33 Hz, and have a flow rate between 260 and 400 mL min^{-1} (Picarro, 2019; 2017a). Since C_2H_6 is a major component present in natural gas sources, two CRDS instruments were used to aid in source identification and attribution, measuring mole fractions of CH_4, C_2H_6, and H_2O; a Picarro Gas Scouter TM G4302 (Picarro, 2017b) and a Los Gatos Research Ultraportable CH_4/C_2H_6 Analyzer (LGRUMEA). The G4302 analyzer was measuring both CH_4 and C_2H_6 at 1 Hz at a flow rate of ≈2 L min^{-1}. The LGRUMEA has a standard flow rate of 1.7 L min^{-1} and was set to measure at 0.5 Hz. To ensure accuracy and comparability of the different continuous measurements, instruments measured gas standards, from MPI Jena, which were calibrated to the NOAA WMO X2004A CH_4 scale before and after the campaign. A cylinder tank containing 1 ppm C_2H_6 was also used for reliable C_2:C_1 measurements on the LGRMEA. The Picarro G4302 was cross calibrated using a 6.5 and 80 ppm CH_4 dilutions from a cylinder containing a 3.9% C_2:C_1 ratio, which was verified by the local gas company in Utrecht (STEDIN). A linear regression was produced from each of the instrument's calibration measurements vs. assigned mole fractions, and was applied to correct the raw data.

3.3.1.2 Sampling details

Non-electric vehicles were equipped as a mobile sampling kit. Supplied to each vehicle was an additional battery that was connected to the engine to power the instruments, an external sampling inlet, and equipment for recording location and wind parameters. The sampling inlet tube led from the vehicle's front bumper to the interior of the rear trunk, where it was connected to the intake valve of an instrument. If there were 2 instruments or a sampling pump in the car, a splitter was added for the instruments and the sampler pump to pull air from the same inlet. The sampling inlet was secured 60

cm from the ground level of each car. The average inlet delay for each instrument was as follows: G2301 at 17 s, G2401 at 5 s, G4302 at 5 s, and the LGRUMEA at 10 s. All vehicles had a GPS unit and an anemometer that recorded coordinates and wind speed and direction every second. Live data recordings were displayed either with a netbook, tablet, or monitor via internal Wi-Fi with ethernet or virtual network computing (VNC) connection.

Air samples were collected for analysis of stable carbon and hydrogen isotopic compositions of CH_4. A 12 V battery powered micro-diaphragm gas pump was attached to the sampling inlet via a splitter, or attached to an additional inlet that was in line with the instrument sampling inlet. A half-inch stainless steel dryer tube (magnesium perchlorate) was attached after the gas pump to limit the amount of moisture in the air sample. During the surveys, Flexfoil SKC and Supelco bags (3 L) were manually filled by a passenger within the vehicle. Each air sample took about 30 seconds to fill.

3.3.1.3 Survey strategies and sampling procedures

The main city campaigns for Bucharest and Ploiești were conducted in the late summer of 2019. A total of 27 surveys split between three vehicles were carried out in Bucharest between the 20th and 29th of August. The additional surveys of Ploiești were conducted (2nd – 5th September 2019), and utilized one car and only the G2401 analyzer. The equipment time clocks were synchronized to local time at the start of the day to facilitate matching of parameters between instruments. All surveys were about 6 to 8 hours in duration and were carried out during daylight hours.

Air samples for isotopic analysis were collected both downwind and upwind of plumes. Generally, spot sampling took place during the last 2 days of the main Bucharest campaign (28th – 29th Aug) and the last day of the Ploiești campaign (Sep 5th). During October of the same year, there were two additional days (16th and 18th) of sample collection from Bucharest and one day (15th) from Ploiești. Locations were targeted based on the August surveys and the presence of LIs, and by known local waste sources (landfills and sewage treatment plants). This was to collect samples for additional isotopic analysis. If time and locality allowed, the vehicle was parked to trace the exact locality of the source of a LI. This was done by attaching an extension tube (5 to 8 m) to the instrument intake inlet on the bumper, then walking around with a mobile device to read the measurements from the surrounding infrastructure (e.g. manholes, storm drains, residential gas meters, and above ground pipelines).

3.3.2 Data and sample processing

3.3.2.1 CH_4 leak indication quantification & emission calculations

CH_4 leak indication quantifications and flux rates were determined from the continuous CRDS measurements and data recorded within the city boundary. Here we utilized an algorithm that was initially developed by von Fischer et al. (2017), later improved by Weller et al. (2019) and modified by Maazallahi et al. (2020d). Von Fischer and Weller utilized this methodology to detect and quantify street level leaks from natural gas distribution networks from continuous mobile measurements. Maazallahi et al., (2020d) broadened this methodology to include additional street-level emissions from other non-fossil fuel sources, which was applied to two European cities studies (Hamburg, Germany, and Utrecht, Netherlands). Similarly, Defratyka et al., 2021 applied this methodology to 2018 and 2019 measurements of Paris, France.

For this study, the local atmospheric background CH_4 mole fraction is defined as the CH_4 mole fraction baseline. Specifically, we used a mean time frame of ± 2.5 minutes as an averaging moving window applied before and after each individual measurement. Subtracting the baseline mole fraction from the measurements allows us to determine where the CH_4 mole fraction exceeds the baseline (CH_4 excess). Here, we define any CH_4 excess ≥ 0.2 ppm above the CH_4 mole fraction baseline as a CH_4 leak indicator (LI).

Two speed limits were applied to exclude either unintended or unreliable measurements. All CH_4 LIs recorded at a speed of zero (mostly while stopped in traffic) were excluded to avoid any unintended signals from natural gas fueled vehicles and interference from general vehicle exhausts

(Maazallahi et al., 2020d). A past controlled release test verified that instrument performance at high speeds deviate outside of the recommended operation ranges, resulting in unreliable CH_4 measurements (von Fischer et al., 2017; Weller et al., 2019). Therefore, CH_4 LIs recorded at speeds >70 km h^{-1} were excluded from leak quantification. All CH_4 LIs were time aggregated (5 sec) and spatially clustered based on the algorithm constraints. Within this time window, the LIs are added and are treated as a single source leak. This defines the final CH_4 LI location of the cluster. CH_4 emission rates are quantified for each cluster using an empirical equation defined in Weller et al. (2019)

$$\overline{\ln(C)} = -0.988 + 0.817 * \ln(Q) \quad (3.1)$$

where C represents the maximum CH_4 LI (ppm) above the CH_4 mole fraction baseline, and Q is the estimated CH_4 emission rate in L min^{-1}. Where there were multiple passes for one location, the average *ln(C)*, based on the respective maximum CH_4 values of each pass, was used in the left side of equation 1 to calculate the emission rate (as in Weller et al., 2019).

To calculate a citywide CH_4 emission rate, the sum of the flux rates was converted from L min^{-1} to units of mass $time^{-1}$ using the relative density of CH_4 gas at 25°C, 1 atm. The emission factor (EF) for scaling up is the sum of all measured city emissions divided by the distance covered. This was then multiplied by the total length of streets within the metropolitan boundary of the study location, and then converted to metric tons of CH_4 per year for an annual city estimate. The uncertainty is calculated from a non-parametric bootstrap emission estimate that scales up the total number of LIs (after clustering) to account for the whole city. This process resamples the LIs 30,000 times. The mean of the iterated estimates is similar to the calculated annual city-wide emission rate, and the uncertainty is the range (min and max). Further details are described in Maazallahi et al., 2020d.

3.3.2.2 Isotopic measurements

Air samples were distributed either to Royal Holloway University of London (RHUL) or Utrecht University (UU) for CH_4 mole fraction and isotopic analyses. If enough sample air remained in a bag after analysis, then the sample was exchanged between the UU and RHUL for duplicate $\delta^{13}C$-CH_4 measurements. Samples measured at the RHUL department of Earth Sciences Greenhouse Gas Laboratory were first analyzed for CH_4 mole fractions using a Picarro G1301 CRDS analyzer, which logged data every 5 seconds for 2 minutes resulting in a precision ± 0.3 ppb (Lowry et al., 2020; France et al., 2016; Zazzeri et al., 2015). RHUL samples were then measured for stable isotopes ($\delta^{13}C$-CH_4) using a high precision (± 0.05 ‰) Elementar Trace Gas continuous-flow gas chromatograph isotope ratio mass spectrometer (CF GC-IRMS) system (Fisher et al., 2006). Each sample was measured 3 or 4 times for $\delta^{13}C$-CH_4 to achieve the desired precision. Both RHUL instruments are calibrated weekly to the WMO X2004A CH_4 scale using air-filled cylinders that were measured by the National Oceanic and Atmospheric Administration (NOAA), and cylinders that were calibrated against the NOAA scale by the Max-Planck Institute for Biogeochemistry (MPI-BGC) Jena (Lowry et al., 2020; France et al., 2016; Zazzeri et al., 2015; Fisher et al., 2006).

Air samples measured at the Institute for Marine and Atmospheric Research Utrecht (IMAU) at UU were analyzed for both $\delta^{13}C$-CH_4 and δD-CH_4 using a ThermoFinnigan MAT DeltaPlus XL, Thermo Scientific, coupled to a sample preparation system described previously (Brass and Röckmann, 2010). This IRMS system has a precision of 0.1‰ for $\delta^{13}C$-CH_4 and 2.0‰ for δD-CH_4 (Menoud et al, 2020; Röckmann et al., 2016). Each final isotopic value is an average of 2 to 4 measurements. The IMAU measurements are converted to international isotope scales using known reference air cylinders that were calibrated against standards from MPI-BGC, Jena, Germany (Sperlich et al., 2016).

3.3.2.3 $\delta^{13}C$-CH_4 and δD-CH_4 source signature calculations

$\delta^{13}C$-CH_4 and δD-CH_4 source signatures were calculated using the Keeling plot technique (Keeling, 1958, 1961). This calculates the linear regression between the measured delta value ($\delta^{13}C$-

CH_4 or $\delta D\text{-}CH_4$) and the inverse mole fraction ($[CH_4]^{-1}$) of the air samples, where the y-intercept represents the estimated source signature (Keeling, 1958, 1961; Pataki et al., 2003). This signature indicates the dominant CH_4 source that has increased the background CH_4 mole fraction. To calculate the y-intercept, we use the Bivariate Correlated Errors and intrinsic Scatter (BCES) regression to account for both the differences in the x and y axes, as well as accounting for the measurement errors (Akritas and Bershady, 1996). This technique has been utilized by many recent studies (Lowry et al., 2020; Xueref-Remy et al., 2020; Zazzeri et al., 2017; Zazzeri et al., 2016) and further details are described in Zazzeri et al. (2015) and France et al. (2016).

3.3.2.4 Ethane-methane ratio (C_2:C_1) source determination

The C_2:C_1 ratio is a useful diagnostic for gas leak attribution because C_2H_6 is present in measurable quantities in thermogenic gas, but not in biogenic gas (e.g. Plant et al., 2019). Knowledge of the C_2:C_1 ratio for the local gas supply allows emissions captured during the surveys to be compared to the expected signature for a local gas leak. For the two instruments with C_2H_6 measurements, the data were first smoothed using a 5 second moving average window for both C_2H_6 and CH_4 to reduce baseline noise. Data points with a CH_4 LI $\geq$ 0.5 ppm and $\geq$ 3 ppm (for the Picarro and LGR analyzers, respectively) were then selected, and the C_2:C_1 ratio calculated using a linear regression over a 10 second window centered around each CH_4 LI point. For these LIs, the corresponding C_2H_6 measurement would be above the baseline noise of the respective instrument at a C_2:C_1 ratio of 0.01, ensuring that thermogenic signals are not mis-classified as biogenic. This is further discussed in section 4.4.

3.4 Results

3.4.1 CH_4 mole fractions and leak indications

Figure 3.S1 displays the total roads driven and spatial coverage of CH_4 excess, indicating localities where CH_4 is greater than the atmospheric baseline. Figure 3.S3.1 shows that CH_4 LIs detected within the city area are mostly narrow plumes, but there were wide plumes identified just northwest of the Bucharest boundary, located close to Chiajna-Rudeni landfill site. Northeast of the city boundary, the largest CH_4 LIs were found on a residential road, Drumul Potcoavei (Horseshoe Road) (44.505°N, 26.133°E), 410 meters outside the Bucharest city border. The highest LGRUMEA reading at this location was around 650 ppm CH_4 and 30 ppm C_2H_6. Upon returning the next day with the local gas company, the G4203 recorded the highest mole fraction above background (around 2070 ppm CH_4 and 49 ppm C_2H_6). These extremely high values are above the instrument saturation point; therefore these are not necessarily accurate. The maximum was measured while trying to find the exact leak location on foot, therefore these data were at zero speed and not used for emission evaluations. This specific CH_4 leak indication was confirmed as a natural gas pipeline leak by the local utility company, which allowed for the characterization of the representative isotopic source signatures and C_2:C_1 ratio of the natural gas distribution network.

Table 3.1. Summary of emission quantifications and analysis. Survey distances (excludes multiple passes), CH_4 leak indications and clustered locations, CH_4 emission rates of measured leaks, standard errors (s.e.) for uncertainties, and emission categories.

		Statistic	Bucharest	Ploiești	Drumul Potcoavei
Distances	driven (km)	n	1845	240	-
	covered (km)	n	1359	233	-

CH_4 leak indications (LIs)	LIs	n	2482	87	89
	LI cluster locations	n	969	76	7
	density (locations km^{-1})	ρ	0.71	0.33	-
	CH_4 excess (ppm)	max	38.3	38.2	397.1
		mean	0.9	1.1	69.0
		median	0.4	0.4	15.9
		s.e.	0.1	0.5	54.8
CH_4 emissions	rates (L min^{-1})	sum	2124.0	138.8	532.6
		max	44.5	14.7	365.7
		mean	2.2	1.8	76.1
		median	1.1	1.0	17.4
		s.e.	0.1	0.3	50.1
	factor (L km^{-1} min^{-1})	EF	1.6	0.6	-
Emission category	LI locations	(n)	913	73	1
	small < 6 (L min^{-1})	emission sum	1322	106	5
	LI locations	(n)	54	3	2
	medium 6 – 40 (L min^{-1})	emission sum	713	33	56
	LI locations	(n)	2	-	5
	high > 40 (L min^{-1})	emission sum	89	-	5880

Note: reported max and min leak indications are for single passes, but the emission rates are estimated based on averaging the (LIs of multiple passes) as in equation 3.1. Driven distance is the total driven throughout the entire campaign, where the covered distance is only the distance driven within the Bucharest city boundary.

3.4.2 CH_4 leak indications and emission rates

Emission quantification and analysis is summarized in Table 3.1. The spatial distribution of the accepted CH_4 LI clusters can be seen in Figure 3.1. It should be reminded that these locations represent CH_4 emissions from any source, not just gas pipelines. From the distance covered in Bucharest, 2482 CH_4 LIs were identified which were clustered into 969 LI locations, where the maximum CH_4 excess was 38 ppm (mean = 1 ppm ± 0.1 s.e.) (Table 3.1). Of these locations, the maximum inferred emission rate was 45 L min^{-1} (mean = of 2 L min^{-1} ± 0.1 s.e.; n = 969). Dividing the number of clustered LI

locations in Bucharest by the road coverage determines a CH_4 LI density of 0.7 (LIs per km covered). Using the same distance, the final emission factor calculated was 1.6 L km^{-1} min^{-1} (Table 3.1).

In Ploieşti, 87 CH_4 LIs were detected within the 233 km of road covered, which account for 76 CH_4 LI cluster locations (Table 3.1). Similar to Bucharest, maximum excess of measured leaks in Ploieşti was also 38 ppm CH_4 (1 ppm ± 1 s.e; n = 76). Ploieşti's maximum averaged emission rate found was 15 L min^{-1} (mean = 2 L min^{-1} ± 0.3 s.e.). Taking the total number of clustered CH_4 LIs to the total road distance covered, calculates a CH_4 LI density of 0.3 (LIs km^{-1}) and an emission factor of 0.6 L km^{-1} min^{-1}.

On Drumul Potcoavei (the road mentioned above, outside Bucharest city limits, with a large gas pipeline leak), CH_4 LIs were observed near continuously over a distance of 0.7 km. A total of 89 CH_4 LIs were detected and contribute to the 7 LI cluster locations. The maximum CH_4 excess was 397 ppm (mean = 69 ppm ± 55 s.e.; n = 7). Along this transect, the largest averaged emission rate found on this single road was 366 L min^{-1} (mean = 76 L min^{-1} ± 50 s.e.; n = 7), and the total sum of all the averaged emissions was 533 ± 50 L min^{-1}.

To categorize the CH_4 LI emission rates, we utilize the emission magnitude categories defined in von Fisher et al., 2017, which defines a "small" leak rate as < 6 L min^{-1}, a "medium" leak is between 6 to 40 L min^{-1}, and any leak ≥ 40 L min^{-1} is considered "high" (Figure 3.1, Table 3.1). The total emissions from Bucharest are defined as 62% small, 34% medium, and 4% large, and Ploiesti's total emissions were 76% small and 24% medium (Figure 3.S2). For Drumul Potcoavei, 1% of the emissions were small, 11% were medium and 89% were large (Figure 3.S2).

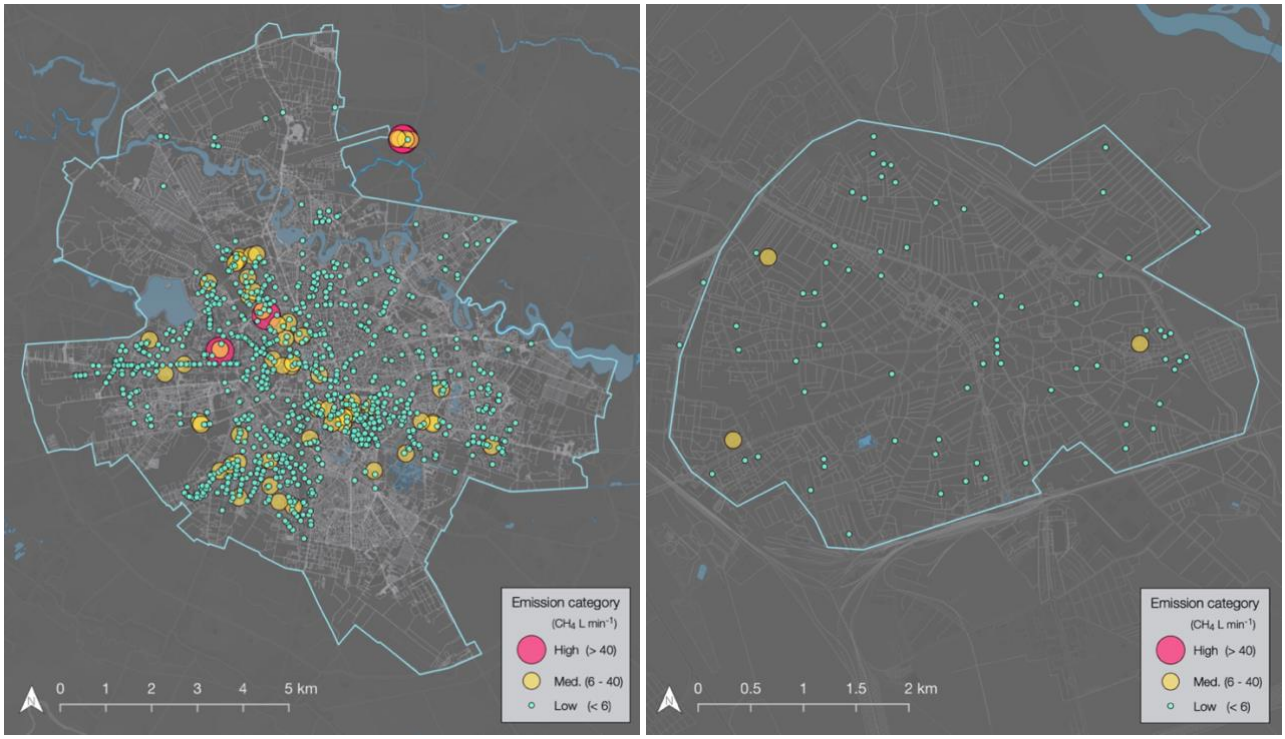

Figure 3.1. CH_4 emission rate categories of Bucharest and Ploieşti. Bucharest (left) has 969 CH_4 LI localities that were identified through clustering a total of 2482 CH_4 LIs. The major Drumul Potcoavei leaks (northeast of the Bucharest boundary) include 7 LI locations which were clustered from 89 CH_4 indicators. Ploieşti (right) includes CH_4 76 LI locations, clustered from 87 CH_4 LIs. Within the city borders (solid blue line), the maximum averaged emission rate was 45 L min^{-1} for Bucharest and 15 L min^{-1} for Ploieşti. Magnitude categories defined as in von Fisher et al., 2017. The corresponding data are summarized in Table 3.1.

3.4.3 Isotopic source signatures

Isotopic measurements between the RHUL and UU laboratories are in good agreement, indicated by an average difference of duplicate $\delta^{13}C\text{-}CH_4$ source signature calculations of ± 0.32 ‰ (n =11) (Figure 3.S5). For Bucharest, a total of 45 locations were sampled for the stable isotopic composition of CH_4 ($\delta D\text{-}CH_4$ and $\delta^{13}C\text{-}CH_4$), and 8 locations were sampled in Ploiești. For both cities, two of the locations were sampled more than once. The results summaries of isotopic source signatures are shown in Tables 3.S1 and 3.S2. Since our sample set of Ploiești is 20% smaller than the sample size of Bucharest, we combine the city data for a general isotopic urban analysis. To minimize potential skewing of analysis from the offset of the number of $\delta^{13}C\text{-}CH_4$ (n = 58) and $\delta D\text{-}CH_4$ (n = 56) source signatures, only one $\delta^{13}C\text{-}CH_4$ source signature was used for each sampled location.

$\delta^{13}C\text{-}CH_4$ source signatures ranged from -61‰ to -36‰ (mean = -49 ± 6‰ s.d.; n = 55), and $\delta D\text{-}CH_4$ ranged from -388‰ to -157‰ (mean = 274 ± 69‰ s.d.; n = 55). The known source type signatures are indicated by an asterisk in Tables 3.S2 and 3 and displayed in Figure 3.2. Sources falling under an 'unknown' type have either ambiguous signatures where $\delta^{13}C\text{-}CH_4$ and $\delta D\text{-}CH_4$ are not in agreement of source type or the signature falls in the overlapping range between thermogenic and biogenic, and the exact location of the source could not be found.

For known thermogenic natural gas signatures, our end member sample was confirmed by the local natural gas company. This was the leak found on Drumul Potcoavei which was sampled with the assistance of the natural gas company by opening up a utility access panel (manhole) (Figure 3.S3). The $\delta^{13}C\text{-}CH_4$ source signatures of this leak ranged from -51‰ to -47‰ (mean = -49‰ ± 2 s.d., n = 4) and $\delta D\text{-}CH_4$ signatures ranged from -175‰ to -132‰ (mean = -154‰ ± 31 s.d.; n = 2). All known fossil fuel source signatures have a $\delta^{13}C\text{-}CH_4$ mean of -50‰ ± 5 s.d. (n = 8) and a $\delta D\text{-}CH_4$ mean of -188‰ ± 40 s.d. (n = 8). The most depleted $\delta^{13}C\text{-}CH_4$ fossil fuel signature was -60‰, which was directly sampled from a domestic gas supply box (Figure 3.S4) in Ploiești and had a $\delta D\text{-}CH_4$ signature of -198.4‰ (Table 3.3, source P-9c). The $\delta^{13}C\text{-}CH_4$ values are much more depleted compared to other natural gas leaks we found in Bucharest.

For biogenic waste signatures, Vidra-Sinteşti landfill and Glina-Popeşti-Leordeni landfill in southern and eastern Bucharest were sampled downwind. These measurements resulted in a known landfill signature of $\delta^{13}C\text{-}CH_4$ = -58‰ ± 1 s.d. (n = 2) and $\delta D\text{-}CH_4$ = -280‰ ± 6 s.d. (n = 2). For a known wastewater signature, Glina water treatment plant was targeted and sampled downwind which resulted in a $\delta^{13}C\text{-}CH_4$ of -50‰ and a $\delta D\text{-}CH_4$ of -335‰ (Table 3.S1).

The spatial distribution of the city samples, analyzed for both $\delta^{13}C\text{-}CH_4$ and $\delta D\text{-}CH_4$, are shown in Figure 3.3. There is an overlap in $\delta^{13}C\text{-}CH_4$ isotopic signatures for the known gas and wastewater samples, but better separation of the $\delta D\text{-}CH_4$ signatures, indicated by more color variability (Figure 3.3). This is further supported by the bi-modal $\delta D\text{-}CH_4$ distribution vs the normal distribution of the carbon signatures (Figure 3.4). There is a large cluster of biogenic $\delta D\text{-}CH_4$ signatures, implying that local wastewater emissions may be responsible for many of the CH_4 LIs identified.

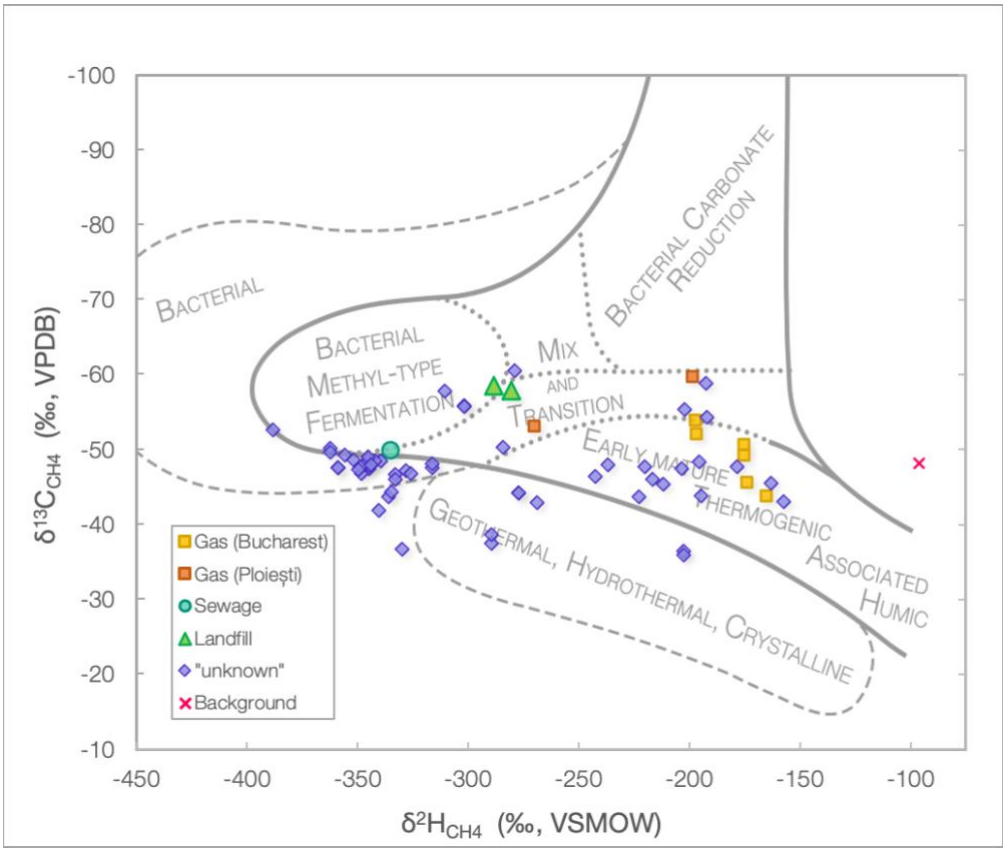

Figure 3.2. Isotopic source signatures of enhanced CH_4 where bag samples were collected. Comparison between 11 identified and 55 unknown (purple diamond) source signatures. Known $\delta^{13}C$-CH_4 source signature ranges: gas -60 to -44 ‰ (yellow & orange, n=5), landfill -59 to 58 ‰ (green triangle, n = 2), and wastewater is -50 ‰ (circle). Known δD-CH_4 source signature ranges: natural gas -270 to -166 ‰, landfill -288 to -280 ‰, and wastewater is -335 ‰. Points overlay bacterial and thermogenic classifications from Whiticar, 1999.

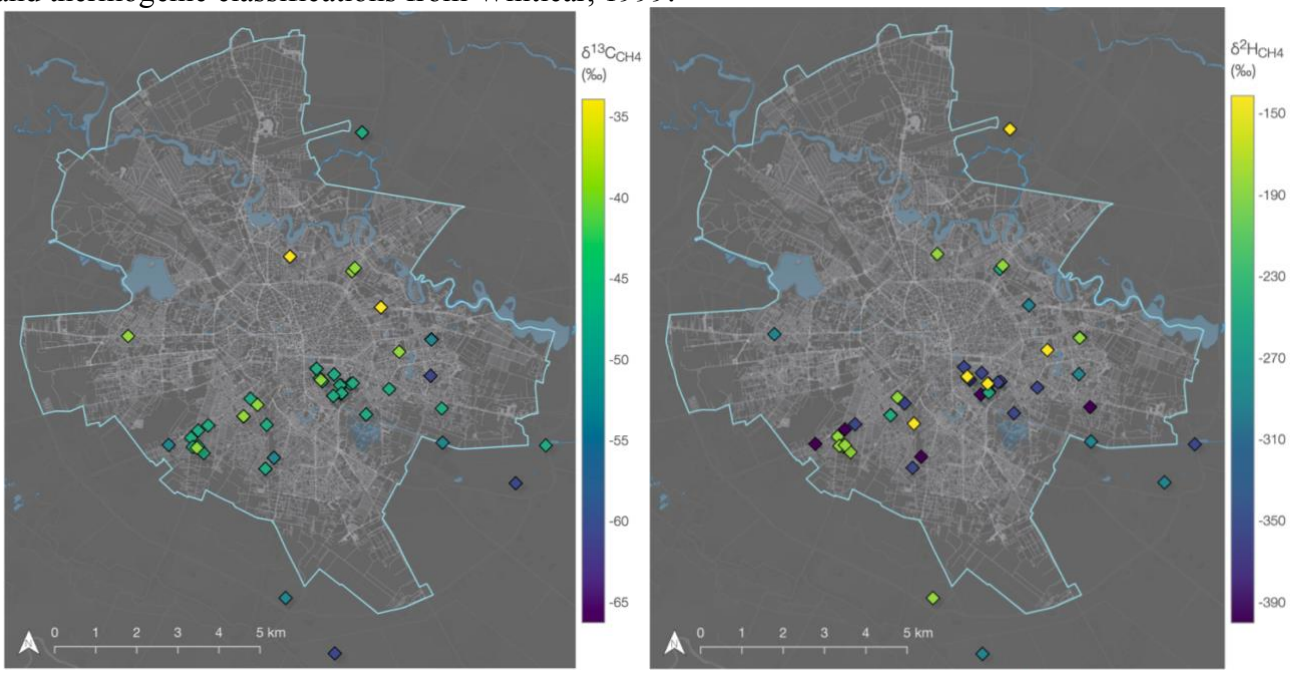

Figure 3.3. Spatial distribution of $\delta^{13}C$-CH_4 and δD-CH_4 source signatures. Combined RHUL and UU $\delta^{13}C$-CH_4 signatures (left), yellow colors indicate sources of ^{13}C enrichment and blue colors show ^{13}C

depletion. δD-CH_4 signatures (right), yellow colors are more enriched and are indicative of thermogenic sources, and purple darker shades indicate ^2H depletion and are more likely to be biogenic sources. Signatures correlate to values and locations listed in Table 3.S1. Less source signature overlap for δD-CH_4 is indicated by the greater color variability.

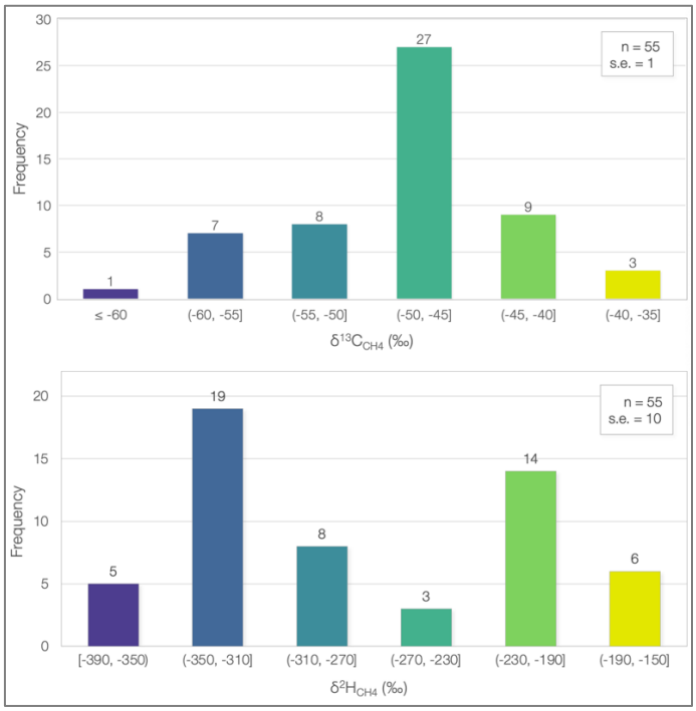

Figure 3.4. City source signature population distribution (δ^{13}C-CH_4 and δD-CH_4). Combined source signatures of both Bucharest and Ploiești. Histogram showing a unimodal distribution of δ^{13}C-CH_4 (top) signatures ranging from -65‰ to -37‰. δD-CH_4 source signatures (bottom) show a bimodal distribution ranging from -388‰ to -157‰. 6% of LIs were attributed to sources using δD-CH_4 source signatures. Colors correspond to the color scale in Figure 3.3.

3.4.4 Ethane:methane (C_2:C_1) ratios

C_2:C_1 ratios were calculated as an additional source tracer. Ratios were calculated where CH_4 leak indications were > 0.5 ppm (for the Picarro G4302 analyzer) and >3ppm (for the LGR UMEA analyzer) above the local CH_4 baseline. In total 11% of the LIs could be attributed to sources using this technique and may not be representative of the smaller LIs which fall below the detection limits. The spatial distribution and locations of Bucharest C_2:C_1 ratios is shown in Figure 3.5, where the maximum C_2:C_1 ratio was 0.300 (mean = 0.02 ± 0.004 s.e.; n = 111). This shows a larger dataset and more uniform spread of measurements than the isotopic data. The light yellow colored points are expected to represent biogenic CH_4 emissions (mainly wastewater) and those with C_2:C_1 ratios above 0.01 are representative of gas pipeline or combustion emissions (orange and darker colors). The leak on Drumul Potcoavei road had measured C_2:C_1 ratios of 0.016, 0.018, and 0.022, which are in agreement with a fossil fuel origin. Within the plume near Chiajna-Rudeni landfill site there was no C_2H_6, as expected from biogenic waste sources.

Figure 3.6 is a histogram showing the population distribution of the calculated C_2:C_1 ratios. The maximum C_2:C_1 ratio was 0.300 (mean = 0.02 ± 0.004 s.e.; n = 111). For this study we define our C_2:C_1 source type ratios based on past studies, where biogenic sources ratios range from anything < 0.005, thermogenic sources range from > 0.005 to < 0.09, and a ratios > 0.10 are considered pyrogenic or combustion (Defratyka et al., 2021; Kort et al., 2016; Lowry et al., 2020; Yacovitch et al., 2014; 2020; Sherwood et al., 2017). Using these ranges, our C_2:C_1 dataset is 63% biogenic (wastewater), 32% identify as thermogenic (fossil fuel), and 5% indicate other/pyrogenic origins (Table 3.2). From

Figure 3.6, gives us a visual of the of how the C_2:C_1 dataset is dominantly more biogenic, which are most likely from wastewater. Some plumes were traced back to manholes or storm grates that expose the sewage pipelines to the atmosphere. Landfills were outside of the city boundaries and were not included in this apportionment. Due to instrument limitations, Ploiești surveys were conducted without an C_2H_6 analyzer.

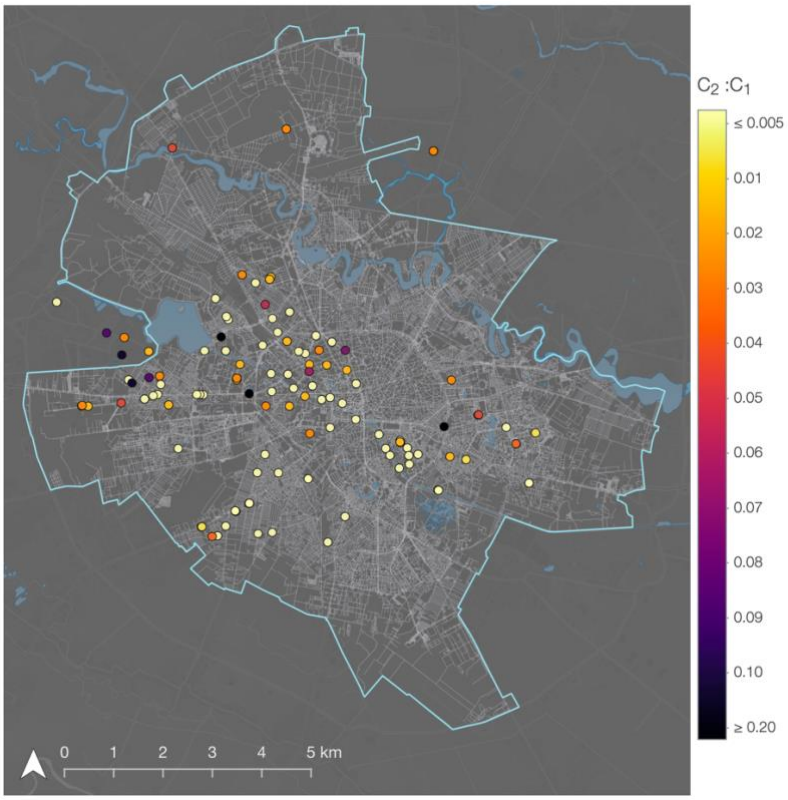

Figure 3.5. Bucharest C_2:C_1 spatial distribution. C_2:C_1 ratios calculated, where peaks of > 0.5 ppm and > 3 ppm CH_4 excess over background (for the Picarro G4302 and LGR UMEA analyzers, respectively) were recorded. Lighter colors indicate a relatively low abundance of C_2H_6 and darker shades a relatively high abundance.

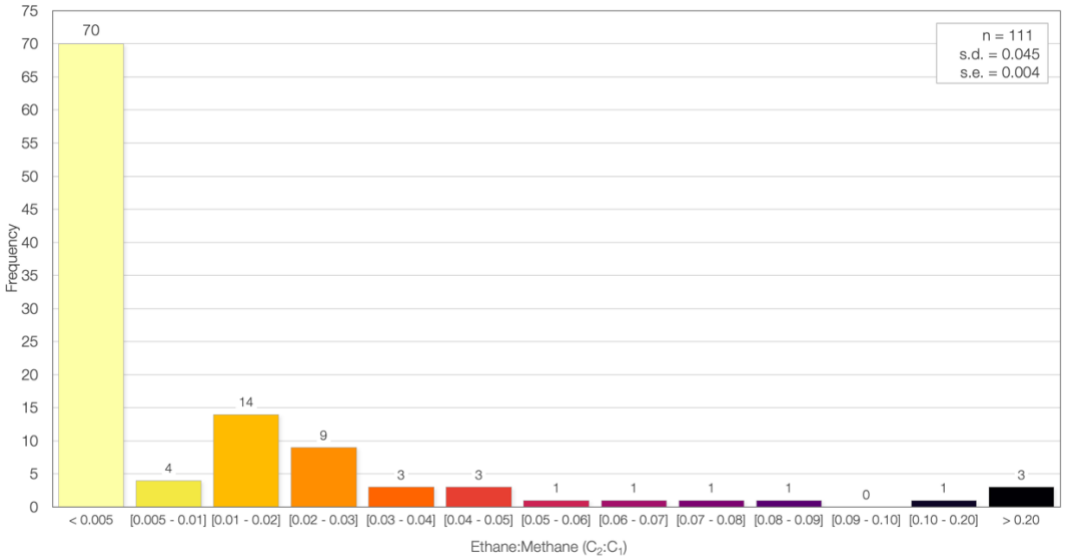

Figure 3.6. Population distribution of C_2:C_1 ratios. Histogram showing the distribution of determined C_2:C_1 ratios from locations of enhanced CH_4 mole fractions from Bucharest, Romania. 11% of total

LIs were attributed to sources using this technique. Colors correlate to ratios on Figure 3.5. Biogenic sources are <0.005, thermogenic ranges from > 0.005 to < 0.09 and anything > 0.10 is considered pyrogenic (Defratyka et al., 2021; Kort et al., 2016; Lowry et al., 2020; Yacovitch et al., 2014; 2020; Sherwood et al., 2017

Table 3.2. Source tracers of locations of enhanced CH_4. Source categories are defined by $\delta D\text{-}CH_4$ and $C_2{:}C_1$. Biogenic sources (< -270‰, < 0.005) are assumed to be from wastewater and thermogenic sources (≥ -270‰; ≥ 0.005 to < 0.090) are assumed to be from the natural gas distribution system. $\delta^{13}C\text{-}CH_4$ source apportionment is not utilized because observed signatures strongly overlap between biogenic (-58 to - 49‰) and thermogenic (-60 to -43‰).

Source tracer		Biogenic (wastewater)	Thermogenic (fossil fuel)	Other (Pyrogenic)
$\delta D\text{-}CH_4$ (‰)	n	31	24	-
	Percent	58%	42%	-
$C_2{:}C_1$	n	70	37	4
	Percent	63%	32%	5%

3.5 Discussion

3.5.1 City wide methane emissions estimations

We calculated an annual city-wide emission rate for both Bucharest and Ploiești. To scale-up the city emissions, we used an emission factor of 1.6 L min^{-1} km^{-1} for Bucharest and 0.6 L min^{-1} km^{-1} for Ploiești, respectively (Table 3.1). By scaling-up Bucharest's emissions to the entire road network (3399 km) (NIS Romania, 2020) within the Bucharest city boundary, we estimated an annual emission of 1832 tons CH_4 yr^{-1} (min = 1577 t yr^{-1} and max = 2113 t yr^{-1}) (assuming this is representative of emissions throughout the year) or ≈45,800 tons CO_2 – equivalent (CO_2-e), using a CH_4 GWP of 25 (US EPA, 2020). Ploiești's emission rate scaled-up to 324 km of city roads is 67 tons CH_4 yr^{-1} (min = 43 t yr^{-1} and max = 110 t yr^{-1}) or ≈1,675 tons CO_2-e (US EPA, 2020).

The annual emission rate of Bucharest is much larger than recently surveyed European cities. A study conducted in 2018 by Maazallahi et al. (2020d) estimated an annual emission rate (440 ± 70 tons CH_4 yr^{-1}) for Hamburg, Germany (≈1.45 million people) that is 24% of the estimated emissions of Bucharest. Defratyka et al., 2021 surveyed the city of Paris, France (≈2 million people) between autumn 2018 – summer 2019 and estimated an annual emission of 140 - 190 tons CH_4 yr^{-1}, which is 8 – 10% of the annual estimates of Bucharest. The empirical method used for these studies is associated with large errors for surveys conducted in both rural and urban areas, but maybe even larger in urban environments. CH_4 enhancements can have high temporal variability, and Luetschwager et al. (2021) suggest 5-8 repeat target surveys help reduce the uncertainty of leak frequency, enhancement, and magnitude. Repeat surveys were conducted in detail for Paris and Hamburg, but were limited for the Bucharest study due to time, which may lead to an overestimation of Bucharest emissions. Measurement conditions could also pose an influence on the difference in emissions observed between cities, but all cities were measured over many days with varying wind conditions, so this should not exert as much influence as the differences in the city utility infrastructure and maintenance, where Bucharest has very different waste management protocols. Since the Hamburg and Paris studies used similar methodologies, the difference of these two cities compared to the total annual CH_4 emissions of Bucharest is probably not an artifact of the methods used. It is most likely related to differences in city leak densities and emission factors used for scaling-up.

The CH_4 LI frequency for Bucharest (Table 3.1) was 83% - 85% larger than the leak densities used for Paris (0.11 leaks km^{-1}) and Hamburg (0.12 leaks km^{-1}). Hamburg had an emission factor that is 0.4 L min^{-1} km^{-1}, and Paris had an emission factor of 0.3 L min^{-1} km^{-1} which is only 25% and 19% of the emission factor calculated for Bucharest (1.6 L min^{-1} km^{-1}, Table 3.1). Downscaling the annual

city-wide emissions by population, Hamburg has a CH_4 emission of 0.31 kg yr^{-1} per capita (Maazallahi et al., 2020d), where in this study, the per capita emission of Bucharest is 0.83 kg yr^{-1} per capita, 63% more than Hamburg. This may indicate CH_4 emission estimations scaled by population could result in an underestimation.

Using C_2:C_1 ratios, CH_4:CO_2 ratio, and $\delta^{13}C$-CH_4 and δD-CH_4, just half (0.19 L min^{-1} km^{-1}) of the Hamburg's total emissions are from fossil fuels. Just under half of Bucharest total emission are from fossil fuels (32% - 42%) resulting in a fossil fuel emission factor of 0.50 – 0.66 L min^{-1} km^{-1}).

3.5.2 Source apportionment

Figure 3.S6 shows no correlation between isotopic signature type and flux magnitude. For a more defined source type apportionment, we look at the individual C_2:C_1 distribution of each emission magnitude category (Figure 3.7). These skewed categorial distributions show that biogenic C_2:C_1 ratios dominate all emission categories, where biogenic ratios contribute to 57% of small,61% of medium, and 77% of high emission flux rates (Table 3.5). Of all the calculated LI C_2:C_1 ratio emission estimations, 63% of the total LIs are biogenic (Table 3.5). Scaling our Bucharest total city-wide emission estimates (2124 L min^{-1}, Table 3.1) to these total source percentages, biogenic sources (wastewater) account for ≈1155 ± 42 tons CH_4 yr^{-1}, thermogenic sources (natural gas) account for ≈587 ± 21 tons CH_4 yr^{-1}, and pyrogenic sources contribute to ≈92 ± 3 tons CH_4 yr^{-1}. Although we see that the smallest LI's add up and contribute to the majority of the total emissions (Table 3.3), which is similar to previously sampled cities in the U.S. (von Fischer et al., 2017), applying the correlation between C_2:C_1 ratios indicates a biogenic dominance which is different from most surveyed cities. If we did not have the capability of attribution, natural gas leaks would drastically be overestimated.

Studies in other European studies, attributed more than half of the observed total city emissions to fossil fuels, Hamburg (50-80%), Utrecht (70-90%), and Paris (56%) (Maazallahi et al., 2020d; Defratyka et al., 2021). Similarly, in the US, Gallagher et al., 2013 showed that emissions found in Durham, North Carolina, Manhattan, and Cincinnati, Ohio were primarily from thermogenic sources as opposed to biogenic sources. Fries et al., 2018 followed up on Gallagher's Cincinnati study (a city with an NGND pipeline replacement plan) applying source tracer measurements (N_2O, $\delta^{13}C$-CH_4, and δD-CH_4). Of the reduced city-wide emissions, Fries et al. found that the emission sources were mostly biogenic than thermogenic, indicating that fossil fuels may have been reduced by the pipeline replacements. Both the US and European studies, as well as others, indicated that the NGDN emissions are dependent on pipeline material, age, and or maintenance practices, and demonstrate that cities with natural gas pipeline replacement plans have less leaks per distance than cities such priorities (Gallagher et al., 2015; Lamb et al., 2015; von Fischer et al., 2017).

We assume that the dominance of wastewater emissions vs fossil fuel emissions may be a result of poor sewage infrastructure and a lack of urban city utility maintenance prioritization (Ianoş et al. 2016; 2017; Kilkiş, 2016; Orlescu and Costescu, 2013; Peptenatu et al., 2012; Gogu et al., 2017). Underground sewage networks are direct sources of CH_4 to the atmosphere (Guisasola et al., 2008; Liu et al., 2015). This biological dominance can potentially be affected by seasonality as biogenic CH_4 produced by anaerobic digestion correlates with temperature (Lin et al., 2016), so the result only represents a snapshot of the late summer measurements. There is a lack of research focusing on CH_4 emissions from sewage network mains, especially in heavily urbanized cities like Bucharest. Therefore, more research is needed to see how much these wastewater emissions reduce during cooler and winter seasons.

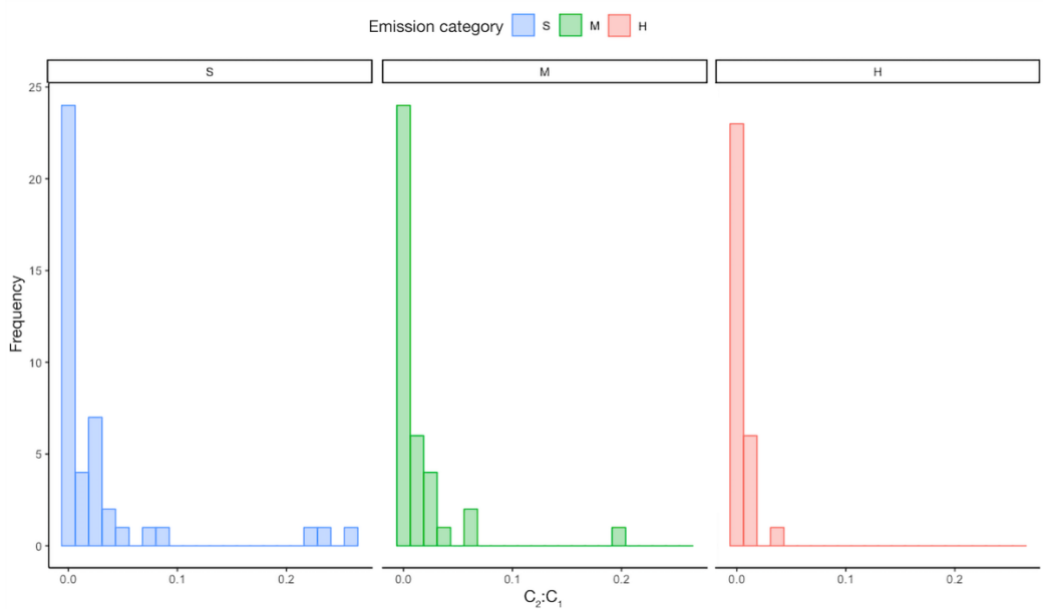

Figure 3.7. Distribution of C_2:C_1 ratios for each emission flux category type. Histogram of C_2:C_1 emission flux rates (n = 111) defined by emission type, S (small) = 6 L min^{-1}, M (medium) = 6 to 40 L min^{-1}, H (high) = ≥ 40 L min^{-1}.

Table 3.3. C_2:C_1 source type attributions by emission size category. Amount of calculated C_2:C_1 ratios that contribute to each category type. C_2:C_1 was used to define a source type for the individual emission flux rates. These rates were then assigned a category type (small, medium, high) depending on the emission rate.

		Small	Medium	High	totals	source
Source type	stat.	< 6 L min^{-1}	6 – 40 L min^{-1}	>40 L min^{-1}	(n)	percent
Biogenic (wastewater)	N	24	23	23	70	63%
Thermogenic (natural gas)	N	15	14	7	36	32%
Pyrogenic (combustion)	N	3	1	0	5	5%
C_2:C_1	N	42	38	30	111	100%

3.5.3 Source tracer reliability

This work shows that δD-CH_4 and C_2:C_1 are more valuable tracers compared to δ^{13}C-CH_4 for urban CH_4 sources in a city like Bucharest, Romania. It was difficult to assign specific source types using δ^{13}C-CH_4 due to the close similarity between signatures of background air (δ^{13}C-CH_4 -48‰ ± 1‰ s.d. (n = 14)), and ^{13}C depleted natural gas sources (50‰ ± 2 s.e. (n = 8)), with the latter overlapping with biogenic source signatures. Unlike δ^{13}C-CH_4, atmospheric background δD-CH_4 (-96‰ ± 7‰ s.d.; n = 12) was relatively far from δD-CH_4 signatures found for natural gas (-196‰ ± 13‰ s.e.; n =7) and the Drumul Potcoavei leaks (-175‰ ± 2‰; n = 5). Other work also indicates that δ^{13}C-CH_4 can be an ambiguous tracer of urban CH_4 sources due to the high variability of δ^{13}C-CH_4 of natural gas which in some regions overlaps with the signatures of other sources (Townsend-Small et al., 2012; 2015; 2016b; Maazallahi et al., 2020d; Menoud et a., 2021). Use of δ^{13}C-CH_4 to distinguish urban sources is more successful in regions with a distinctly enriched δ^{13}C-CH_4 signature in the gas network, such as in UK

cities (Zazzeri et al., 2015; Lowry et al., 2020) or the Netherlands (Röckmann et al., 2016; Menoud et al., 2020).

3.6 Conclusions

This study estimated a city emission rate of about 1832 tons CH_4 yr^{-1} (min = 1577 t yr^{-1} and max = 2113 t yr^{-1} for Bucharest and 67 tons CH_4 yr^{-1} (min = 43 t yr^{-1} and max = 110 t yr^{-1}) for Ploiesti. C_2:C_1 and δD-CH_4 tracers attributed our total emissions to 58% - 63% wastewater, 32% - 42% natural gas, and 0 - 5% pyrogenic CH_4 sources (Table 3.4, 3.5). Measurements were made only during the summer and early autumn of 2019 and it is unknown how emissions differ during other seasons. We suspect that the large contributions of biogenic (wastewater) emission are directly related to the city sewage and wastewater infrastructure. Landfill emissions were not included in the analysis as they were outside of the city boundaries.

We found that δD-CH_4 and C_2:C_1 are more useful for CH_4 source apportionment in the Bucharest area compared to $\delta^{13}C$-CH_4. In regions of NW Europe , $\delta^{13}C$-CH_4 is a successful source tracer (Dlugokencky et al., 2011; Maazallahi et al., 2020d; Menoud et a., 2021) due to $\delta^{13}C$-CH_4 enriched natural gas sources of that locality, which is not the case in Bucharest. The measured CH_4 emissions in Bucharest are higher than those published in recent surveys of other European cities such as Paris (190 tons CH_4 yr^{-1}) and Hamburg (440 ± 70 tons CH_4 yr^{-1}) with large emissions both from gas leaks and wastewater. In terms of liters per minute per km, emissions from Bucharest are 4 times greater than Hamburg, Germany and 6 times greater than emissions reported from Paris, France. The proportion of emissions from sewage/wastewater was higher in Bucharest than in Hamburg and Paris. These results show the need for local governance to assess and prioritize specific city utility infrastructure maintenance.

Supplementary data availability

The data, including in situ measurements, GPS data, and boundaries of study areas, are available on the Inte- grated Carbon Observation System (ICOS) portal from Fernandez et al., (2021).

Author contributions

JMF: Writing – original draft, Visualization, Methodology, Validation, Isotopic, Formal analysis, Data curation, Investigation. HM: Project administration, Methodology, Software, Validation, Emission, Formal analysis, Data curation, Investigation, Writing – review & editing. JLF: Conceptualization, Methodology, Software, Validation, C_2:C_1, Formal analysis, Data curation, Investigation, Writing – review & editing. MM: Methodology, Validation, Investigation, Writing – review & editing. MC: Project administration, Investigation. MA: Project administration, Resources. AC: Project administration, Conceptualization, Resources. AT-S: Writing – review & editing. CvdV: Methodology, Resources. REF: Supervision, Conceptualization, Methodology, Validation, Resources, Writing – review & editing. DL: Supervision, Conceptualization, Methodology, Validation, Resources, Writing – review & editing. EGN: Writing – review & editing. TR: Supervision, Project administration, Funding acquisition, Conceptualization, Methodology, Resources, Writing – review & editing.

Acknowledgements

This study was supported by the Romanian Methane Emissions from Oil & gas (ROMEO) project funded by the Climate and Clean Air Coalition (CCAC) Oil & Gas Methane Science Studies (MSS) of the United Nations Environment Programme (UNEP) under grant number PCA/CCAC/UU/DTIE19-EN652. Additional funding is from the European Union's Horizon 2020 Research and Innovation Program under the Marie Sklodowska-Curie Grant Agreement 722479 ($MEMO^2$). Royal Holloway University of London Greenhouse Gas Research Laboratory lab has been supported by grants from NERC including NE/N016238/1 MOYA The Global Methane Budget (2016–2021).

3.S Supplement

Table 3.S1. Bucharest air sample analysis. Results of air samples collected via mobile inlet, air pump and Flexfoil bags. List of street locations, coordinates, source type, and mole fractions of calculated source signatures from Bucharest, Romania. All signatures represented had CH_4 mole fractions ≥ 200 ppb above background levels. C_2:C_1 ratios are calculated from continuous CRDS instrument measurements reading simultaneously during air sample collection. The uncertainty in the isotope source signature is calculated from the Keeling plot regression. Where there is no uncertainty given there were just 2 points used to calculate the signature.

Source ID	Collection Date	Location	Coordinates		Type	CH_4 (ppm)	Isotopic signatures			Emission rates		
			Latitude	Longitude			RHUL $\delta^{13}C$-CH_4 (‰)	UU $\delta^{13}C$-CH_4 (‰)	UU δD-CH_4 (‰)	C_2:C_1	Flux (L min^{-1})	LIs (n)
B-1	2019-08-22	Drumul Potcoavei	44.5054	26.1327	Gas*	37.2	-47.9	-47.0	-131.9	0.04	98.8	3
B-2	2019-08-23	Drumul Potcoavei	44.5054	26.1327	Gas*	290.0	-49.3	-50.7 ± 0.1	-175.3 ± 1.7	0.02	225.7	9
B-4	2019-08-27	Aleea Lacob Andrei	44.3872	26.0851	Unknown	2.3	-47.7	-48.1	-316.2	0.00	-	-
B-5	2019-08-27	St Zâbrâutului	44.4026	26.0858	Gas	2.4	-	-45.5	-163.1	0.06	-	-
B-6	2019-08-27	St Gardeniei (mh)	44.3956	26.0376	Wastewater	10.0	-	-52.7 ± 0.1	-388.1 ± 1.1	0.00	14.7	4
B-7	2019-08-27	Aleea Posada (mh)	44.4006	26.0521	Wastewater	69.0	-	-49.3 ± 0.0	-355.9 ± 0.9	0.00	29.4	16
B-8	2019-08-27	St Garoafei (mh)	44.4024	26.0570	Wastewater	9.1	-	-48.5 ± 0.4	-339.4 ± 0.6	0.00	290.6	19
B-9	2019-08-28	Splaiul Unirii	44.4224	26.1103	Wastewater	4.0	-47.2	-48.8	-328.2	0.00	46.4	10
B-10	2019-08-28	St Vlad Dracu (mh)	44.4204	26.1189	Wastewater	41.5	-47.4 ± 0.2	-47.9 ± 0.2	-344.9 ± 1.4	0.02	178.4	12
B-11	2019-08-28	St Foișorului & Zizin (mh)	44.4165	26.1225	Wastewater	13.8	-	-48.5	-342.1 ± 0.4	0.00	9.1	17
B-12	2019-08-28	St Foișorului (mh)	44.4138	26.1226	Wastewater	13.8	-46.7	-46.0	-332.8	0.00	8.2	7
B-13	2019-08-28	St Zizin (sd)	44.4173	26.1281	Wastewater	15.0	-46.8	-	-325.8	0.00	-	-
B-14	2019-08-28	Intrarea Dumitru-Drăgan (mh)	44.4152	26.1460	Wastewater	9.6	-	-46.9	-348.1	0.01	11.1	14
B-15	2019-08-28	St Trapezului (mh)	44.4084	26.1718	Wastewater	32.0	-	-48.6	-351.9	0.00	-	-
B-16	2019-08-28	St Drumețului (sd)	44.4063	26.1347	Wastewater	148.0	-48.7	-49.0	-345.0	0.00	187.1	8
B-17	2019-08-28	Splaiul Unirii	44.4128	26.1185	Wastewater	25.6	-47.6	-47.6	-358.6	0.00	-	-
B-18	2019-08-28	St Balomir (sd)	44.3910	26.0893	Wastewater	7.8	-50.2	-49.6	-362.3	0.00	10.4	5
B-19	2019-08-28	St Doina (sd)	44.4097	26.0812	Wastewater	9.0	-	-41.9	-340.3	0.00	17.2	5
B-20	2019-08-29	St Prisaca Dornei	44.4199	26.1663	Unknown	7.2	-55.8 ± 0.4	-55.8 ± 0.3	-301.8 ± 2.4	0.00	10.8	14
B-22	2019-08-29	St Țărăncuței	44.4283	26.1509	Gas	3.0	-43.1	-	-157.3	0.00	5.8	26
B-24	2019-08-29	St Sublocotenent Dima Cristescu	44.4440	26.1419	Unknown	2.4	-37.5	-38.7	-289.3	0.00	3.5	4
B-25	2019-08-29	St Mașina de Pâine (mh)	44.4567	26.1278	Unknown	9.0	-42.9	-	-268.7	0.00	8.4	6
B-26	2019-08-29	St Ion Berindei (mh)	44.4578	26.1291	Gas	3.4	-43.7	-	-222.9	0.08	5.5	4
B-27	2019-08-29	St George Călinescu (mh)	44.4618	26.0972	Gas	3.2	-36.5	-35.9	-202.5	0.00	-	-
B-28	2019-08-29	Bd Iuliu Maniu (mh)	44.4339	26.0177	Unknown	3.5	-44.2	-	-277.0	0.00	5.7	1
B-29	2019-10-16	St Bârsei	44.4328	26.1668	Gas	2.3	-	-55.4	-202.1	-	-	-
B-30	2019-10-16	St Bârsei, gas supply	44.4326	26.1667	Gas*	2.7	-	-52.1	-196.5	-	-	-
B-31	2019-10-16	St Zizin (mh)	44.4170	26.1268	Wastewater	12.7	-	-48.0	-346.8	0.00	7.8	3
B-32	2019-10-16	St Mugur Mugurel	44.4166	26.1218	Gas	3.6	-	-47.8	-178.3	-	-	-
B-33	2019-10-16	St Foișorului	44.4135	26.1223	Gas	2.4	-	-48.0	-236.8	-	-	-
B-34	2019-10-16	Bd Mircea Vodă (mh)	44.4179	26.1132	Wastewater	86.8	-	-47.8	-348.8	-	-	-
B-35	2019-10-16	Splaiul Unirii	44.4185	26.1124	Wastewater	3.8	-	-43.7 ± 0.0	-335.9 ± 1.4	-	-	-

B-36	2019-10-16	Splaiul Unirii, gas supply	44.4191	26.1118	Gas*	6.8	-	-45.6	-173.6	-	-	-
B-37	2019-10-16	St Vedea	44.4118	26.0778	Gas	2.5	-	-45.4	-211.7	-	-	-
B-38a	2019-10-16	Soseaua Salaj (mh)	44.4056	26.0743	Unknown	30.0	-	-46.4	-242.5	-	-	-
B-38b	2019-10-16	Soseaua Salaj (mh)	44.4057	26.0744	Unknown	3.7	-	-44.3	-334.6	-	-	-
B-39	2019-10-16	Șoseaua București-Măgurele	44.3981	26.0486	Gas	2.5	-	-46.0 ± 0.0	-216.7 ± 0.3	-	2.3	3
B-40	2019-10-16	St Brătila	44.3946	26.0514	Gas	2.7	-	-43.9 ± 0.2	-194.5 ± 0.6	-	-	-
B-41	2019-10-16	St Caracal	44.3949	26.0494	Gas	4.0	-	-47.7 ± 0.2	-219.9 ± 1.1	-	-	-
B-42	2019-10-16	St Iași	44.3927	26.0548	Gas	3.2	-	-48.4	-195.3	-	-	-
B-43	2019-10-16	Câmpia Mierlei	44.3951	26.0521	Gas	3.0	-	-47.5	-203.3	-	-	-
B-44	2019-10-18	Jilava oil storage, N	44.3417	26.0951	Gas*	2.7	-	-53.9 ± 0.1	-197.2 ± 0.4	-	-	-
B-45	2019-10-18	Vidra landfill, W	44.3222	26.1192	Landfill*	4.3	-	-57.8 ± 0.1	-280.3 ± 0.1	-	-	-
B-46	2019-10-18	Glina water treatment plant, W	44.3954	26.2230	Wastewater*	3.0	-	-49.9	-335.0	-	-	-
B-47	2019-10-18	Glina landfill, W	44.3821	26.2081	Landfill*	5.3	-	-58.5 ± 0.1	-288.1 ± 1.4	-	-	-
B-48b	2019-10-18	Glina oil park, gas comp.	44.3770	26.2709	Gas*	4.1	-	-43.7	-164.9	-	-	-
B-49	2019-10-18	Splaiul Unrii	44.3964	26.1722	Biogenic	2.6	-	-50.3	-284.1	-	-	-

- *Known source identified during sampling, and those sources labeled without an asterisk are identified though the source signatures.
- mh = manhole
- sd = storm drain

Table 3.S3. Ploiești air sample analysis. Results of air samples collected via mobile inlet, air pump and Flexfoil bags. List of street locations, coordinates, source type, mole fractions, calculated source signatures, and emission rates from Ploiești, Romania. All signatures represented have CH_4 LIs ≥ 200 ppb above background levels. Correlating emission rates were paired by location. The uncertainty in the source signature is calculated from the Keeling plot regression. Where there is no uncertainty given there were just 2 points used to calculate the signature.

Source ID	Collection Date	Location	Coordinates		Type	CH_4 (ppm)	Isotopic signatures			Emission rates	
			Latitude	Longitude			RHUL $\delta^{13}C$-CH_4 (‰)	UU $\delta^{13}C$-CH_4 (‰)	UU δD-CH_4 (‰)	Flux (L min^{-1})	LI (n)
P-2	2019-10-15	St Curcubeului	44.9392	26.0078	Unknown	2.3	-	-57.8	-310.7	-	-
P-4	2019-10-15	St Baiului	44.9286	26.0075	Wastewater	2.2	-	-48.0	-344.0	3.0	2
P-9a	2019-10-15	St Meșterul x Pielari (mh)	44.9433	26.0450	Gas	2.6	-	-54.4 ± 0.0	-192.0 ± 0.2	-	-
P-9b	2019-10-15	St Meșterul x Pielari (mh)	44.9433	26.0450	Wastewater	122.8	-	-47.3	-349.4	-	-
P-9c	2019-10-15	St Pielari, gas supply	44.9434	26.0451	Gas*	357.3	-	-59.7	-198.4	-	-
P-11a	2019-10-15	St Nucilor	44.9512	26.0210	Unknown	2.2	-	-60.5 ± 0.1	-278.9 ± 0.2	0.7	1
P-11b	2019-10-15	St Nucilor (mh)	44.9512	26.0211	Unknown	57.0	-	-36.8	-329.7	-	-
P-11c	2019-10-15	St Nucilor, gas supply	44.9512	26.0210	Gas*	2.3	-	-53.1	-270.1	-	-
P-12	2019-10-15	St Principala, Strejnicu	44.9214	25.9694	Gas	22.0	-	-58.9 ± 0.0	-192.4 ± 0.0	-	-
P-15	2019-09-05	St Petrochimistilor	44.9392	26.0455	Unknown	2.1	-64.8	-	-	-	-
P-16	2019-09-05	St Pelinului	44.9487	26.0524	Unknown	2.3	-53.0	-	-	-	-

- *Known source identified during sampling, and those sources labeled without an asterisk are identified though the source signatures.
- mh = manhole
- *sd = storm drain*

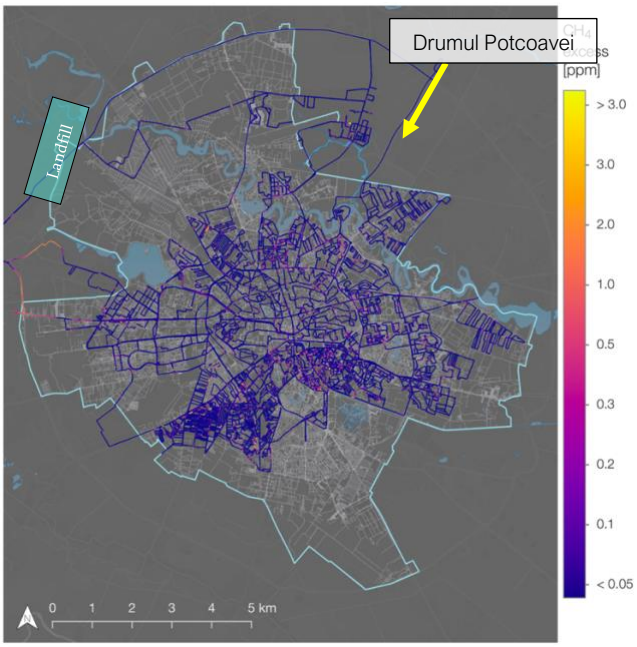

Figure 3.S1. Bucharest street-level CH_4 mixing ratio excess. Combined street level measurements from the four CRDS instruments of CH_4 excess (ppm) above background levels. Lighter shades indicate greater mole fractions of CH_4 excess whereas darker shades are closer to background level (blue). The Bucharest city boundary is indicated by the solid pale blue outline and roads are indicated by light grey. Chiajna-Rudeni landfill is highlighted by the green box and the yellow arrow points to the largest LI detected during the campaign.

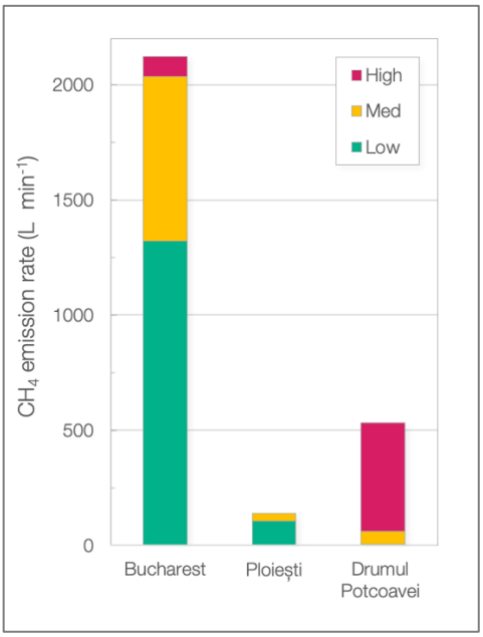

Figure 3.S2. City CH_4 emission totals divided by the category type. Emission rates by magnitude category where High = >40 L min^{-1}, Med = 6 to 40 L min^{-1}, and Low = <6 L min^{-1}. Bucharest's total emissions amount to 2124 ± 0.1 L min^{-1}. Ploieşti emissions totaled to 139 ± 0.3 L min^{-1}. Emissions on Drumul Potcoavei Road totaled to 533 ± 503 L min^{-1}.

Figure 3.S3. Sampling a known pipeline leak for source signatures. Residential utility manhole on Drumul Potcoavei (Horseshoe Road) (44.505°N, 26.133°E), 410 meters from the Bucharest city border. Manhole was opened with the assistance of the local gas company, and confirmed a pipeline leak. Fernandez, J.M. collects air samples for the analysis of CH_4 mixing ratios, $\delta D\text{-}CH_4$, and $\delta^{13}C\text{-}CH_4$ (via bag pump and FlexFoil sample bags). Maazallahi, H. measures real-time CH_4 and C_2H_6 mixing ratios for C_2:C_1 ratios using a Picarro backpack Gas Scouter TM G4302.

Figure 3.S4. Domestic gas supply utilities. Residential gas utility components for maintaining and monitoring domestic natural gas usage for homes in Bucharest and Ploieşti. Consealed box contains meter, regulator, and valves. Measurements from these utilities are considered as known natural gas source.

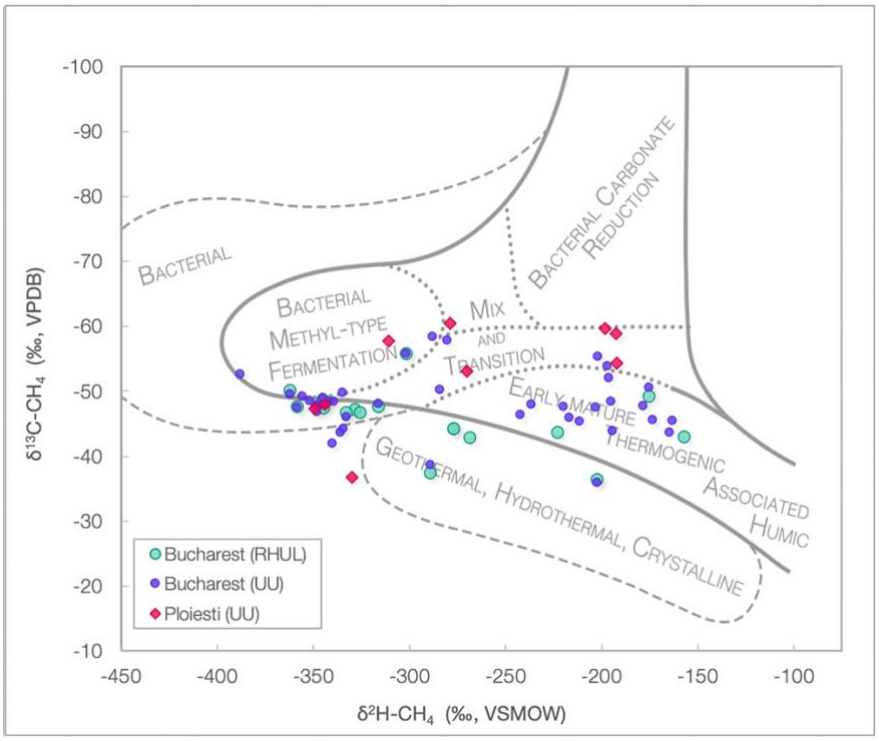

Figure 3.S5. Isotopic source signatures of CH_4 emissions. Comparison between laboratory measurements from RHUL (n = 17) vs. UU (n = 40) and Bucharest (n = 57) vs. Ploiesti (n = 9) samples. Average difference of $\delta^{13}C$-CH_4 source signature calculations between the labs is 0.32 ‰ (n = 11). Points overlay bacterial and thermogenic classifications from Whiticar, 1999.

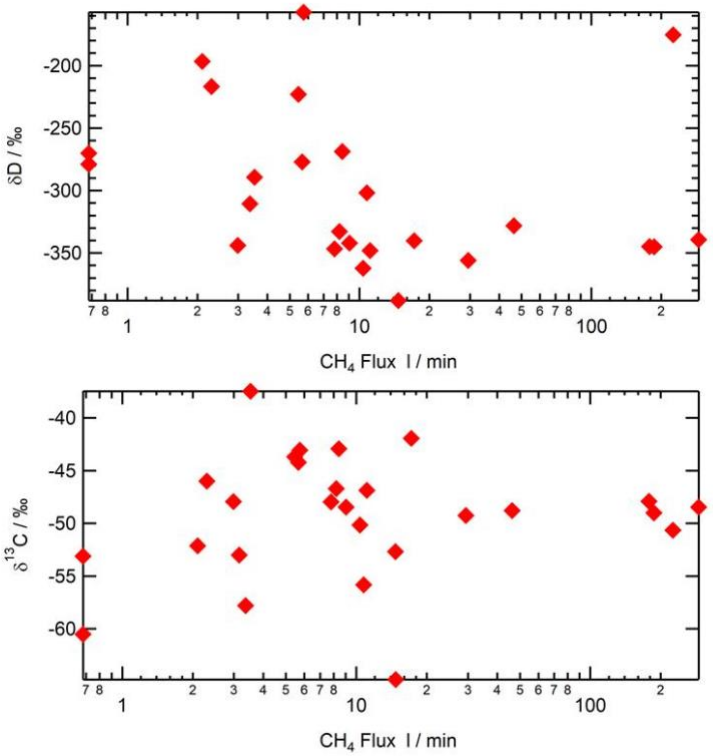

Figure 3.S6. Bucharest source tracers type compared to CH_4 flux and CH_4 leak indication mole fraction. δ^2H-CH_4 vs. CH_4 flux (top) and $\delta^{13}C$-CH_4 vs. CH_4 flux (bottom) show that there is no correlation between source signature type.

4 Intercomparison of detection and quantification methods for methane emissions from the natural gas distribution network in Hamburg, Germany

Hossein Maazallahi[1 2], Antonio Delre[3], Charlotte Scheutz[3], Anders M. Fredenslund[3], Stefan Schwietzke[4], Hugo Denier van der Gon[2], Thomas Röckmann[1]

[1]Institute for Marine and Atmospheric research Utrecht (IMAU), Utrecht University (UU), Utrecht, The Netherlands
[2]Netherlands Organisation for Applied Scientific Research (TNO), Utrecht, the Netherlands
[3]Department of Environmental Engineering, Technical University of Denmark (DTU), Lyngby, Denmark
[4]Environmental Defense Fund (EDF), Berlin, Germany

Abstract. In August and September 2020, three different measurement methods for quantifying CH_4 emission from leaks in urban gas distribution networks were applied and compared in Hamburg, Germany: the "mobile", "tracer release" and "suction" methods. The mobile and tracer release methods determine emission rates to the atmosphere from measurements of CH_4 mole fractions in the ambient air, and the tracer release method also includes measurement of a gaseous tracer. The suction method determines emission rates by pumping air out of the ground using soil probes that are placed above the suspected leak location. The quantitative intercomparison of the emission rates from the three methods at a small number of locations is challenging because of limitations of the different methods at different types of leak locations.

The mobile method was designed to rapidly quantify the average or total emission rate of many gas leaks in a city, but it yields a large emission rate uncertainty for individual leak locations. Emission rates determined for individual leak locations with the tracer release technique are more precise because the simultaneous measurement of the tracer released at a known rate at the emission source eliminates many of the uncertainties encountered with the mobile method. Nevertheless, care must be taken to properly collocate the tracer release and the leak emission points to avoid biases in emission rate estimates. The suction method could not be completed or applied at locations with widespread subsurface CH_4 accumulation, or due to safety measures, and this sampling bias may be associated with a bias towards leak locations with low emission rates. The leak locations where the suction method could not be applied were the biggest emitters as confirmed by the emission rate quantifications using mobile and tracer methods and an engineering method based on leak's diameter, pipeline overpressure and depth at which the pipeline is buried. The corresponding sampling bias for the suction technique led to a low bias in derived emission rates in this study. It is important that future studies using the suction method account for any leaks not quantifiable with this method in order to avoid biases, especially when used to inform emission inventories.

4.1 Introduction

Natural gas combustion has a lower carbon footprint than combustion of other fossil fuel sources for the same thermal output (EIA, 2021). However, fugitive CH_4 emissions can significantly turn the balance in terms of climate impact (Alvarez et al., 2012) because the global warming potential of CH_4 over a 20-year time scale is 84 times higher than that of CO_2 (Myhre et al., 2013). The atmospheric abundance of CH_4 has increased about 2.5-fold since the pre-industrial era (Bousquet et al., 2006). Following a short period of stable levels after the year 2000, atmospheric CH_4 has continued to increase since 2006. Worden et al (2017) concluded that about 50 to 80% of the post-2006 increase originated from fossil sources and Jackson et al. (2020) attributed the accelerated increase of 6 – 13 ppb yr^{-1} from 2014 to 2017 (Nisbet et al., 2019), equally to the emission increase from fossil and agriculture sectors.

Gas distribution networks in cities are subject to maintenance programs by the operators to detect and fix leakages that occur, as CH_4 is an incendiary gas and can be explosive at concentrations between 4 and 16% in ambient air (DVGW, 2022). Since the safe operation of the distribution network and leak repair is the primary objective of this maintenance, quantification of emissions from leakages is rarely performed. The absence of regulations on CH_4 emissions is another reason why leak rates are not routinely quantified, however CH_4 emissions from the energy sector needs to be addressed properly within the EU CH_4 strategy by 2050 (EC, 2020). Nevertheless, from the perspective of climate change and possible mitigation options, it is important that emissions from gas leakages are (i) quickly detected and fixed and (ii) well quantified. Weller et al. (2020) and Alvarez et al. (2018) respectively reported 5 and 1.6 times higher CH_4 emissions from leaks in the US gas distribution network based on such observations compared to the national inventory reports.

Leaks from buried pipelines can be due to corrosion or failure/defects in joints or materials (EPA, 1996). When a leak occurs on a buried urban gas pipeline, the gas will generally accumulate in the air space below the surface and then find its path to the atmosphere through a single or several surface outlets. The outlets can be either unpaved soil surfaces, cracks in the road or pavements, or

associated with different types of cavities (manholes, communication covers, rain drains, etc.). The major outlet is generally the one with the highest overall permeability for gas released from the buried natural gas pipeline. On the way from the leak location on a buried pipeline to the atmosphere through outlets, CH_4 may be oxidized by methanotrophs in the soil and/or merge with CH_4 from other sources, e.g. biogenic CH_4 emissions from sewage system.

Routine leak surveys in Germany are conducted by walking with handheld CH_4 sensors above buried pipelines, referred to as the carpet method (DVGW, 2019c). The success of leak detection with the carpet method depends primarily on soil permeability (Ulrich et al., 2019), which is influenced by soil moisture, texture, soil organic content and the location of the groundwater table (Wiesner et al., 2016). Based on risk of explosion, gas leaks are classified into four types: A1, A2, B and C (DVGW, 2019c). This classification is based on the accumulation of CH_4 in cavities (e.g. manholes, rain drains, etc.) or buildings and the distance of gas leaks to buildings and cavities. If natural gas leaks into buildings or cavities, the leak classifies as A1, and it must be repaired immediately to minimize explosion risk. If the gas leak has a distance up to 1 m to buildings and does not fill cavities, it is classified as A2, and it must be fixed within a week. If the distance is between 1 to 4 m to buildings, the leak is classified as B and the repair time window is three months, and if the distance is more than 4 m then, the leak is considered as C category and can be fixed according to the scheduled repair plan. Gas pipelines in a city with the scale of Hamburg are monitored every 5 years with the carpet method. The leak emission rate is not quantified and thus also not a parameter affecting the course of action.

In recent years, mobile measurement methods using vehicles with fast and high-precision laser instrumentation have been established for leak detection and emission quantification in numerous cities (Fernandez et al., 2022; Defratyka et al., 2021; Luetschwager et al., 2021; Keyes et al., 2020; Maazallahi et al., 2020d; Ars et al., 2020; Weller et al., 2018; von Fischer et al., 2017; Jackson et al., 2014). In-situ measurements of atmospheric CH_4 from mobile vehicles are used to pinpoint and quantify CH_4 emission sources at street level in urban areas. The mobile method was calibrated using above-ground controlled release experiments, in which known amounts of CH_4 were released from gas cylinders (Weller et al., 2019). Simultaneous measurements of CO_2 and C_2H_6 can provide valuable additional information for attributing CH_4 sources (Maazallahi et al., 2020d). A characteristic of the resulting emissions distribution from gas distribution grids in cities is the existence of a few leak locations with very high leak rates, up to 100 L min^{-1}, resulting in a right-skewed leak emission rate distribution (Weller et al., 2020). Usually about 10% of the leaks are responsible for between 30% to 70% of the emissions (Weller et al., 2019; Maazallahi et al., 2020d). Therefore, the CH_4 emission from the gas distribution system can be reduced very effectively if the largest leaks can be found and fixed quickly, thus augmenting the routine leak detection (carpet method) and repair programs with the mobile method.

The tracer dispersion method is another method to quantify CH_4 emissions from point and area sources. In this method, a tracer gas is released at a known rate close to the outlet of the gas leak, and both tracer and target gas concentrations are measured downwind. From these measurements and the known tracer gas release rate, the target gas emission rate can be determined with an uncertainty of ± 15% (Lamb et al., 1995) or less than 20% (Fredenslund et al., 2019). Lamb et al. (2015) applied the tracer method to quantify leaks from urban underground pipelines where they reported moderate agreement (± 50%) to excellent agreement (± 5%) between the tracer and high-flow sampler method.

Another approach to quantify underground leak rates from buried gas pipelines is the so-called suction method. In this method air is pumped out of the ground at a known rate via probes surrounding the underground leaks until an equilibrium CH_4 mixing ratio is reached in air out-flow, from which the CH_4 leak rate can be calculated. In Germany, this approach is applied to a limited number of leak locations, which do not have to be repaired immediately or within 1 week. Suction measurements normally find leak rates that are < 2 L min^{-1} (E.ON, personal communication, 2020). The reported uncertainty range of this method is ± 10% based on 23 measurements in the 1990s (E.ON, personal communication, 2020). The discrepancy between these rather low leak rates compared to leak rates

inferred with the mobile method calls for further investigation, since the suction method is also employed to derive network-wide emission factors for the German country-wide gas distribution network (Federal Environment Agency, 2020).

Hendrick et al. (2016) used surface flux chamber measurements carried out between 2012 and 2014 to estimate gas leak rates from 100 leak locations in the Boston area that were detected using mobile measurements (n = 45) in 2011 from Phillips et al. (2013) and additional locations from later mobile surveys (n = 55). They reported CH_4 emission rates from gas leaks ranging from 0.003 g min^{-1} to 16 g min^{-1}, corresponding to roughly 0.0 – 24.4 L min^{-1}. They also reported that their estimate using chamber measurements underestimated total CH_4 emissions, likely because the chambers didn't capture the total CH_4 emitted from the leak. This is similar to the enclosure measurements results from Weller et al. (2018).

The flow through a hole in a pipeline can also be calculated theoretically and empirically from the physical properties of the hole, mainly the ratio of hole to pipeline diameter and the overpressure in the pipeline. There are three different engineering model types to estimate emissions from gas leaks: the hole model, the rupture model and modified models to bridge the gap between hole and rupture models (Hu et al., 2020; Moloudi and Esfahani, 2014; Yuhua et al., 2002; Arnaldos et al., 1998). These types of models are either to estimate leak strength from a pipeline in open space or a buried pipeline. A leak on a buried pipeline has higher surrounding resistance depending on soil conditions compared to a situation where the pipeline is in open space. Such models have been used to quantify emissions from holes in pipelines in open space (Hou et al., 2020; Manda and Morshed, 2017; Moloudi and Esfahani, 2014; Mahgerefteh, Oke and Atti, 2005; Yuhua et al., 2003; Kayser and Shambaugh, 1991) but also from buried pipelines (Liu et al., 2021; Ebrahimi-Moghadam et al., 2018; Okamoto and Gomi, 2011; Yan, Dong and Li, 2015). Cho et al. (2021) introduced a model, which takes into account soil properties including absolute and relative permeability and porosity, the underground spread of the leak, surface CH_4 mole fractions and depth of the buried pipeline based on experiments with a controlled release rate. This model was calibrated based on release rates ranging from 1.3 g min^{-1} to 5.7 g min^{-1}, corresponding to roughly 2.0 – 8.7 L min^{-1}.

In this study, we present results from measurements with the mobile, the tracer release and the suction methods in Hamburg, Germany, in August and September 2020. We present the quantitative emission estimates as well as a qualitative intercomparison of the three methods, in particular related to the applicability and the strengths and weaknesses of the different methods at different leak locations. We investigate differences between the leaks detected from mobile measurements and leak locations reported from the routine leak detection surveys performed by the local gas utility (hereinafter LDC (Local Distribution Company)). Finally, we discuss implications of our study for national emission inventories.

4.2 Materials and Methods

4.2.1 Campaign preparation and general overview

As a preparation for the intercomparison campaign, all partners contributed to the preparation of an "intercomparison matrix" where the characteristics and deployment details of the different methods were specified. This matrix is provided in section 4.S.1 of the Supplemental Information (SI). The matrix includes descriptions related to the identification of gas leaks, the quantification of gas leaks, adjustments of the method to the intercomparison exercise and upscaling. It also laid out an initial plan for the intercomparison in terms of identification of suitable locations and deployment of the different methods.

According to this plan (Fig. 4.1), we first applied the mobile method to identify potential gas leak locations, namely leak indications (LIs). When the mobile method had detected one or more emission outlets (See Sect. 4.S.2 in SI) and classified them as a potential gas leak location, the carpet method was applied to confirm the leak and determine the confine leak location. Some additional locations that

had previously been identified by the carpet method (leak categories B and C) were added to the list of target locations.

Following leak detection, the mobile quantification method (multiple transects) was applied on all the locations and the tracer and suction methods were applied at the confirmed leak locations, and with some restrictions regarding safety and method capacities. The release location for the tracer quantification method was confirmed based on surface screening using a handheld CH_4 analyzer. For comparison of the mobile and tracer release methods with the suction and hole methods we assumed that (i) a steady state between pipeline leakage under-ground CH_4 accumulation and emission to the atmosphere had been reached (Kirchgessner et al., 1997) and (ii) methanotrophs and methanogens have negligible impact on quantification of gas leak emissions. Thus, the total emission rate of all outlets in the vicinity of a leak location is equal to the natural gas emission rate from the pipeline leak. We will discuss implications of the above assumptions for selected cases. After leak repair, the LDC reported leak hole sizes, pipeline diameters and pipeline operational pressures, allowing leak rate estimation with the hole method.

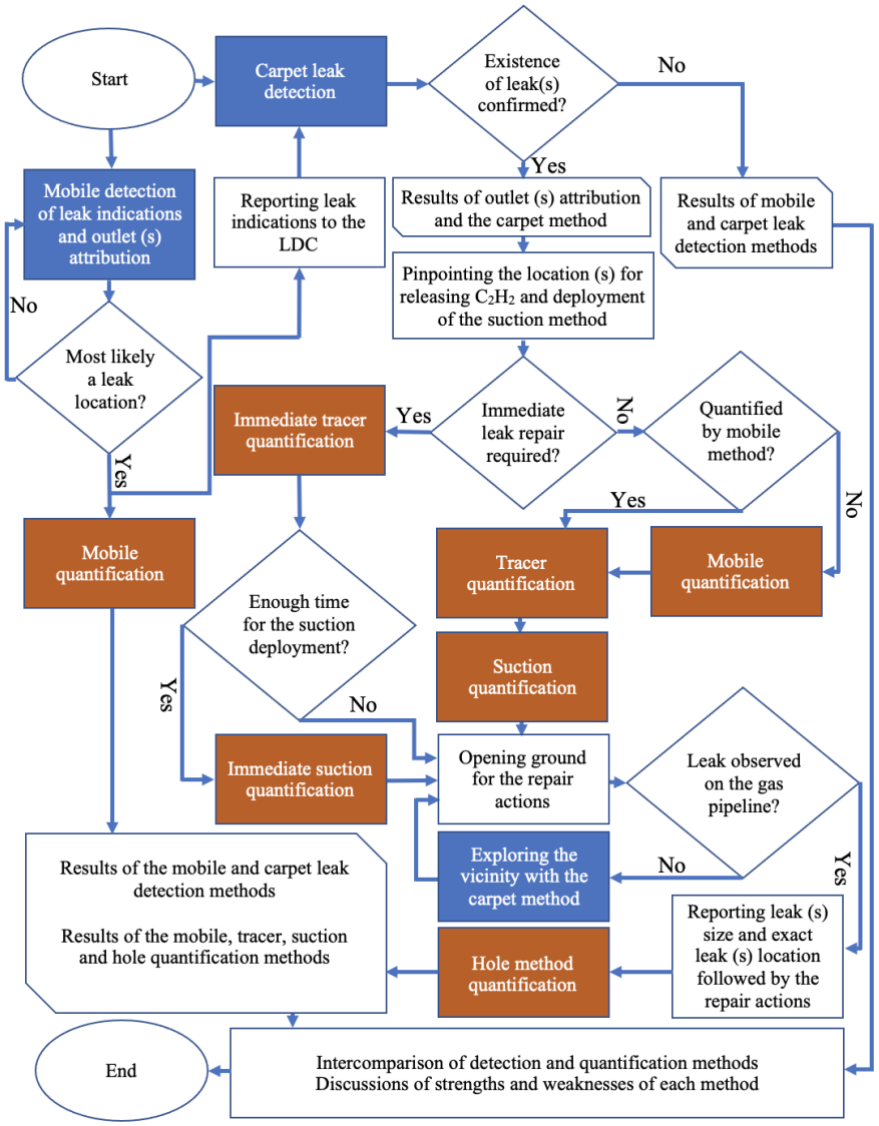

Figure 4.1. Flowchart of application of leak detection methods (blue colors) and quantification methods (red colors) followed by repair actions and intercomparison of the detection and quantification methods.

4.2.2 Measurements setups

4.2.2.1 Mobile measurement setup

Onboard the measurement vehicle (VW Transporter) we operated two cavity ring-down spectrometers (CRDS), model G2301 and model G4302 (Picarro, Santa Clara, California, USA). The G2301 measures CH_4, CO_2 and water vapor (H_2O) at a flow rate of ≈ 0.2 L min^{-1} and 0.3 Hz frequency. The G4302 has a flow rate of ≈ 2.2 L min^{-1} and sampling frequency of about 1 Hz for CH_4, C_2H_6 and H_2O. The air intake for both instruments was from the same tubing attached to the front bumper. This setup allowed us to directly compare the enhancements observed from the two instruments during surveys. The G4302, which is in a shape of a backpack, was also used in attribution of outlets emissions in walking surveys to check presence of C_2H_6 in emission outlets.

4.2.2.2 Tracer release measurement setup

The tracer release method was applied by releasing acetylene (C_2H_2) at the emission outlet identified by the mobile leak detection and confirmed by the carpet method. The tracer gas was released at the main emission outlet, which was confirmed by surface screening using a handheld CH_4 analyzer. Tracer release rates between 1.3 and 2.6 L min^{-1} from a gas cylinder. A Picarro CRDS, G2203 instrument was used to measure CH_4 and C_2H_2 mole fractions continuously with ≈ 0.3 Hz frequency. The instrument was installed in a measurement vehicle (VW Caddy), and air was sampled from the atmosphere through an inlet on the roof about 2m above ground. The tracer method was applied either in static mode, where air was sampled in one or a few locations downwind from the outlets and tracer release locations (n = 11) or mobile mode (n = 5), where the plumes were transected while measuring concentrations of CH_4 and C_2H_2. The choice of mode depended on the site conditions including road accessibility and wind direction. The tracer release setup including instrumentation used as well as mobile mode is described in detail in Mønster et al (2014), and the principle of the static mode is described in Fredenslund et al (2010).

4.2.2.3 Suction measurement setup

In the suction method, 12 probes were used to insert in the soil around the confirmed gas leak location by the LDC. The probes are connected to a pump to extract accumulated subsurface CH_4 from the leak. CH_4 mole fraction at the outflow is measured with a Flame Ionization Detector (GERG, 2018).

4.2.2.4 Carpet method setup

Leak detection experts from the LDC operate a CH_4 detector (Sewerin instruments, Gütersloh, Germany) on a rolling device, where a plastic cover (the carpet) moves over the ground and provides a loose seal to the surrounding atmosphere, facilitating preferential analysis of air emanating from the surface right below the carpet. The instrument gives an acoustic signal when a high CH_4 from a potential leak has been detected. The instrument can detect C_2H_6 with a gas chromatograph, which take about couple of minutes per outlet location.

4.2.3 Detection, confirmation and attribution of emissions at gas leak locations

4.2.3.1 Mobile detection of possible leak location

For leak detection with the mobile method, we first evaluated CH_4, C_2H_6 and CO_2 signals during mobile surveys. If (i) CH_4 and C_2H_6 signals were observed with a ratio of less than 10% with no CO_2 signal or (ii) CH_4 was observed (< 500 ppb enhancement on G4302) with no C_2H_6 and CO_2 signals, then we parked the mobile measurement car, detached the G4302 analyzer from the system and searched for gas outlets on foot with the G4302. This detailed search for outlets was performed to (i) confirm the presence of both CH_4 and C_2H_6 signals (ii) map the spatial spread of outlets and (iii) spatially constrain the possible gas leak location. The reported possible gas leak locations from the mobile method were then reported to the LDC for confirmation and localization of the leak with the carpet method and subsequent underground measurements.

4.2.3.2 Attribution of leak indication signals from mobile measurements

To attribute an observed leak indication (LI) from mobile measurements to a source category, namely fossil, microbial and combustion, we used CO_2 and C_2H_6 signals, which were continuously measured along with CH_4. We quantitatively evaluated C_2:C_1 ratios (%) when (i) the CH_4 enhancements were larger than 0.5 ppm (ii) C_2H_6 enhancements were also larger than 15 ppb and (iii) the determination coefficient (R^2) of the linear regression between CH_4 and C_2H_6 was larger than 0.7. If CH_4 signals in mobile measurements were associated with CO_2 and high C_2H_6 mole fractions (C_2:C_1 > 10%), we attributed those emissions to combustion (Maazallahi et al., 2020d). When we repeatedly observed CH_4 enhancements, no CO_2 enhancements and C_2:C_1 ratios between 1 and 10%, or we observed persistent CH_4 signals in several passes we did further on-foot inspection of the outlets. If the emissions from the outlets clearly pointed to a fossil origin based on the CH_4 and C_2H_6 signals, we labeled the locations as potential gas leak locations and reported them to the LDC for confirmation. We only considered a location as a gas leak for further investigation if the LDC confirmed the existence of a gas leak.

If at a particular location, we observed several CH_4 maxima, for example from different outlets, we considered the "strongest" outlet as the main emission point. The "strongest" emission point refers to a point where we observed the highest CH_4 mole fraction when the G4302 intake inlet was put at a distance of ≈ 2 - 5 cm above the surface or outlet. When several emission outlets with similar mole fractions were found, we considered the spatial average of the coordinates as the main emission point. The tracer method then released C_2H_2 at the main outlet emission point.

The LDC reported a C_2:C_1 ratio of 3.0% (96.20 ± 0.02 mol % CH_4 and 2.88 ± 0.00 mol % C_2H_6, GNH personal communication) for the gas composition in the grid for the period of August and September 2020 in Hamburg. This ratio was reported 3.5% (95.09 mol % CH_4 and 3.37 mol %, GNH personal communication) in April 2020.

4.2.3.3 LDC leak detection and confirmation

Since the pipeline locations are known to the LDC, the method can be applied precisely above the pipelines, including visible cracks and cavity outlets in the close vicinity, increasing the possibility of leak detection. Once the carpet method detects a CH_4 source, a second measurement is performed above the location with the highest signal, where air is accumulated and analyzed for the presence of C_2H_6. The C_2H_6 detection in the carpet method is not online with higher detection threshold and in batch mode (gas chromatography), which takes time, 5 – 10 minutes per location. If sufficiently high CH_4 and C_2H_6 levels are found, the leak is categorized in one of safety categories of A1, A2, B or C.

4.2.3.4 Precise underground leak localization

When a leak has been confirmed with the carpet method, a precise localization of the leak is performed by drilling holes about 20-40 cm into the ground along the pipeline track and measuring the sub-surface CH_4 concentration. The location with the maximum sub-surface reading is assigned the most likely leak location where the repair teams open the road and attempt repair of the leak. The final exact leak location is reported after opening ground for the repair reactions. Mostly the locations reported from the carpet method matches the locations reported from the leak repair team, which depends on the transport pathways of emission undersurface and surface coverage.

4.2.4 Emission quantification

4.2.4.1 Mobile measurements quantifications

After the detection of the target locations, we performed additional transects at these locations on different days. We accepted a mobile measurement transect of a leak location for further analysis if (i) the GPS signals of transects were logged correctly along the street track and (ii) at least one of the two instruments, G2301 (for quantification and attribution) and / or G4302 (for attribution), were running during the transect and (iii) the transect track included at least one GPS coordinate less than 50

m from the leak location. The start and end point of the accepted transects were determined as the locations where the driving tracks intersected with a circle with radius of 100 m centered at the gas leak location reported by the LDC, or a reported outlet location from the mobile method, for the locations where the LDC did not confirm a leak. The segments between the start and end points were evaluated one by one (See an example in Sect. S.4.1 in SI) to determine various parameters, e.g., the maximum CH_4 enhancements, plume area, driving speed, distance to the actual leak locations, etc. The plume area is the integral of the CH_4 enhancements above background along the driving track from the location where the CH_4 enhancement exceeds > 10 ppb until the location where it falls again below the 10 ppb threshold.

Gas leak quantification from mobile measurements is based on an empirical equation derived from controlled release experiments reported by von Fischer et al., (2017) and reevaluated in Weller et al., (2019) (Eq. 4.1).

$$Q = \exp\left(\left(\overline{Ln\ (C_{max})} + 0.988\right) / 0.817\right) \quad (4.1)$$

In Eq. 4.1, C_{max} is the maximum CH_4 enhancement (ppm) observed during each transect next to the leak location. The maximum CH_4 enhancement should be more than 10% above CH_4 background level to be considered for the quantification algorithm. The emission rate is denoted by Q and it is in L min^{-1}. $\overline{Ln\ (C_{max})}$ is the mean of the logarithm of the maximum mole fraction enhancements for all accepted transects.

The standard quantification method only uses transects where CH_4 enhancements are more than 10% or ≈ 200 ppb above background level. This 10% enhancement threshold corresponds to about 0.5 L min^{-1} emission rate in Eq. 4.1. Thus, ≈ 0.5 L min^{-1} is the minimum emission rate that can be quantified with Eq. 1 and leaks with smaller emission rates are ignored by design of the method. Below we investigate the effect of relaxing the enhancement threshold. The application of the tracer release technique in mobile mode allowed us to use the known C_2H_2 release rate and the measured C_2H_2 plumes to independently validate the mobile approach, including the effect of the enhancement threshold. We also investigated the effect of distance between CH_4 maxima to gas leak locations, which is not a parameter in Eq. 4.1.

The uncertainty of the emission rate for each location in the mobile method was calculated using standard error and t-factor (95% confidence) for the locations with at least three CH_4 enhancements greater than the 10% threshold.

In addition to evaluating the maximum CH_4 enhancement from each transect we also derived the plume area (mixing ratio times distance and in unit of ppm m) for comparison between the instruments. In principle, the plume area should provide a more robust quantification of an ambient CH_4 plume than the maximum enhancement: When a plume spreads out, individual realizations of the plume can be sharper and higher, or wider and lower, depending on meteorological conditions, but the plume area should be less affected. In addition, when an instantaneous plume is sampled with two instruments with different gas flow rates, instruments with a lower flow rate will be affected by mixing of air in the measurement cell. This will lead to a lower maximum enhancement but a wider peak, and thus the peak area should lead to a better comparison between the instruments.

4.2.4.2 Tracer measurements quantifications

The tracer method uses Eq. 4.2a to quantify CH_4 emissions in mobile mode (integral over space dimension) and Eq. 4.2b in the static mode (integral over time dimension). Parameters relevant for the evaluation with the tracer method are provided in Sect. 4.S.4.2.

$$Q_{CH_4} = Q_{C_2H_2} \cdot \frac{\int_{start}^{end} C_{CH_4} dx}{\int_{start}^{end} C_{C_2H_2} dx} \cdot \frac{MW_{CH_4}}{MW_{C_2H_2}} \quad (4.2a)$$

$$Q_{CH_4} = Q_{C_2H_2} \cdot \frac{\int_{start}^{end} C_{CH_4} dt}{\int_{start}^{end} C_{C_2H_2} dt} \cdot \frac{MW_{CH_4}}{MW_{C_2H_2}} \quad (4.2b)$$

Here C is the mole fraction (ppm) and MW is the molecular weight of the species, 16 g mol^{-1} for CH_4 and 26 g mol^{-1} for C_2H_2. Q_{CH_4} is the CH_4 emission rate estimate for CH_4 (g s^{-1}) and $Q_{C_2H_2}$ is the controlled release rate of C_2H_2 (g s^{-1}). The C_2H_2 flow rate was controlled and measured with a flow controller (Brooks Sho-Rate). In addition, the mass of C_2H_2 released at each location was measured by weighing the release cylinder before and after the tracer release with a precise scale (KERN DE60K5A). The change in mass was then converted to a mass flow rate using the release time. To convert the emission rate from mass (g s^{-1}) to volume (L min^{-1}) we used normal temperature and pressure (NTP) conditions, T = 293.15 K, p = 1.01325 bar. The locations of tracer release (C_2H_2) at the confirmed gas locations were determined with the combined information from the mobile and the carpet methods.

The tracer gas can also be used to pinpoint and confirm the emission source location. Prior to quantification, it is important that the emission outlet is located for proper tracer release (see Fig. 4.1) and source simulation and that other potential interfering emission sources can be ruled out. This is secured by performance of upwind and downwind CH_4 mole fraction screening. During transecting of the CH_4 and tracer plumes, the two plumes should match, if this is not the case, the tracer release should be relocated until a proper plume match is obtained. If an emission source consists of multiple outlets, the combined emission from all outlets can be measured by releasing the tracer at the main outlet and increasing the measuring distance until one confined overlapping plume of CH_4 and tracer gas is obtained. If the distance cannot be increased to access limitations, tracer should be released at each single emission outlet.

4.2.4.3 Suction measurements quantifications

The quantification of a leak with suction method is possible after pumping accumulated air out of soil and reaching CH_4 mole fraction equilibrium in the outflow. With the equilibrium CH_4 reached and the known pumping rate through the probes, it is then possible to calculate emission rate (See Sect. 4.S.4.3 in SI).

4.2.4.4 Hole method, based on leak and pipeline properties

The LDC reported the physical properties of gas leaks and pipeline conditions. These include leak area, pipeline diameter and pipeline operational pressure. In order to get an estimate of the upper physical limits of gas leakage through a hole with the given properties, we used the empirical model by Liu et al., (2021), which was designed to quantify emissions from buried natural gas pipelines to estimate emission rates from the leaks (Eq. 4.3), hereinafter "hole" method.

$$Q = 0.567 \cdot [(h + 139.592)^{-0.1} - 0.542] \cdot d^{1.5} \cdot p^{0.7} \quad (4.3)$$

Here, Q is the gas leak rate in $m^3\ h^{-1}$ (at standard atmospheric conditions and converted to NTP), h is the depth of the buried pipeline in cm, d is the gas leak hole diameter in mm and p is the pipeline overpressure in kPa. We used 150 cm as pipeline depth for all the locations in Hamburg to estimate emission rate. We note that the model that we employed is for buried pipelines not pipelines in open space, and emission estimates for the gas leak emission rate in open space would be even higher (See Sect. 4.S.4 in SI). Ebrahimi-Moghadam et al. (2018) showed that CH_4 emission from a pipeline hole area can be between 7 to 10 times higher in open space relative to the subsurface conditions.

4.3 Results

4.3.1 Leak Detection

15 possible leak locations were detected by the mobile method in the initial surveys, (labeled as HH001 – HH015). At 13 out of these 15 locations, leaks were confirmed by the LDC, HH007 and

HH012 locations were not confirmed as gas leak locations. In addition, the LDC identified 5 other leak locations (labeled as HH100 – HH104) that had not yet been fixed (category B and C). The overview of the measurements (detection and quantification) is provided in the SI (See Sect. 4.S.5 in SI). At some locations we also observed that vegetation was impacted negatively by the presence of leaks in their vicinities, a known phenomenon as high levels of CH_4 cause harmful anoxic conditions for the plant roots (See Sect. 4.S.6 in SI). At several locations the outlet identification was straightforward, because we only observed one outlet, but at 5 locations we observed numerous outlets spread over a large area. Figure 4.2 shows the spread of emission outlets at one of the locations (Fig. 4.2a), with correlations of CH_4 and C_2H_6 at the "strongest" outlet (Fig 4.2b). Fig. 4.2c shows precise gas leak location practice of the LDC at one of the other locations.

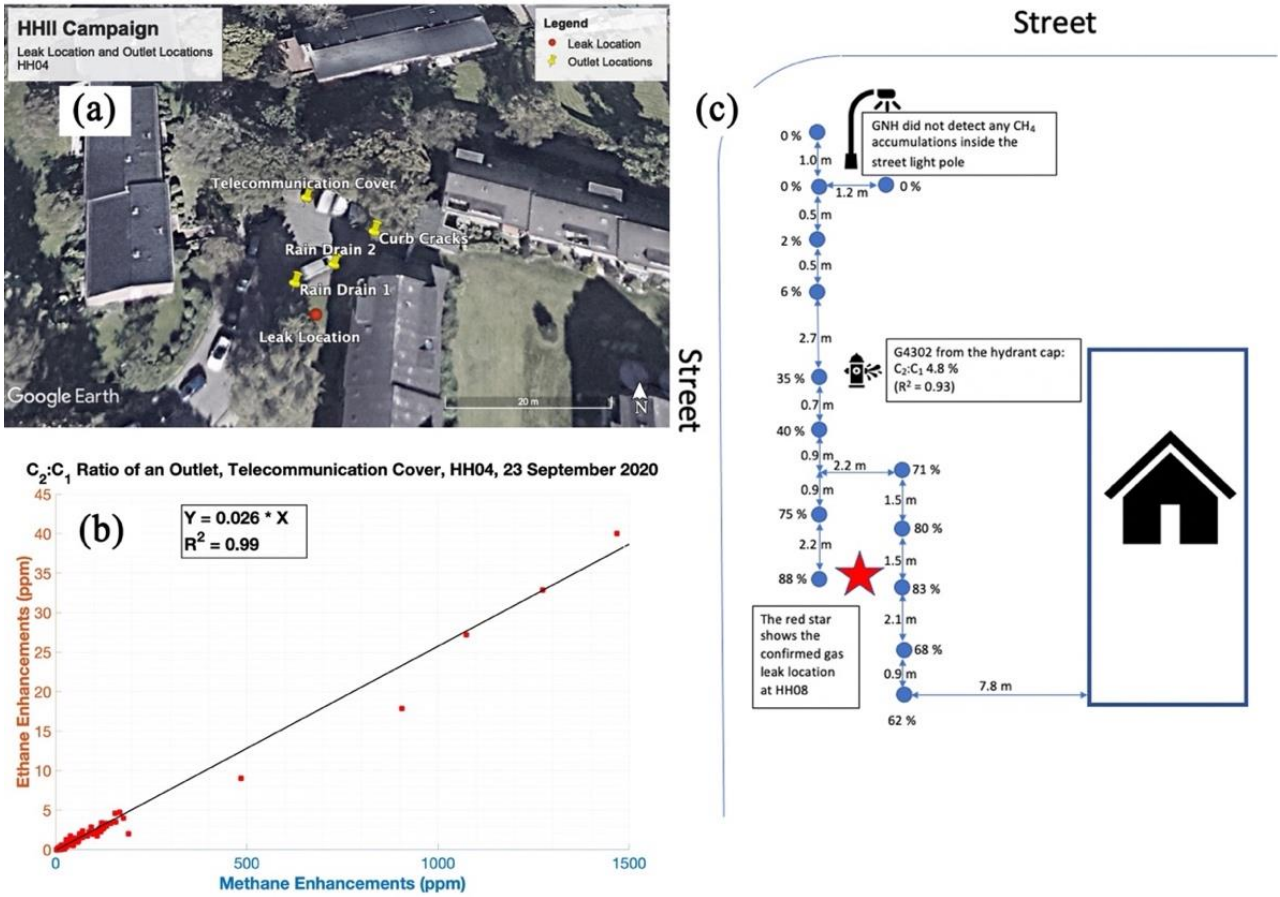

Figure 4.2. (a) aerial image of location HH004 (© Google Maps). Yellow pins show surface emission outlet locations, and the red point shows the actual pipeline leak location reported by the LDC; (b) correlation between CH_4 and C_2H_6 measured from a telecommunication cover; (c) Map (not to scale) of drilled holes (blue dots) to locate the pipeline gas leak at HH008. The red star shows the actual pipeline gas leak location as indicated by the undersurface CH_4 mole fractions (See Sect. 4.S.3, Fig. 4.S3).

4.3.2 Leak Quantification

Table 4.1 shows the results of the leak emission rate quantifications from the four methods. All these locations were quantified by the mobile method, although for 6 of them the 10% enhancement threshold was not reached. 16 locations were quantified by the tracer release method and 8 by the suction method. A complete overview of key parameters for all measurements (detection and quantification) is provided in Sect. 4.S.5.

Table 4.1. Results of gas leak quantification with different methods in Hamburg, Germany.

	ID	Leak quantification methods (L min^{-1})							Info. from the LDC			
		Mobile (measurements from G2301)			Tracer (L min^{-1})	Suction		Hole (L min^{-1})	Pipeline buried year	Leak size (cm^2)	Leak type; Safety considerations	Pipeline Size and Material[#]
		Transect (s) w/ CH_4 Enh. > 10% threshold	Emission average	Emission range; 95% confidence		Emission (L min^{-1})	Status					
Detected by mobile method	HH001	n=1(10%)	0.7	-	0.06	<1.8	INC	39	1935	2.5	C	DN80ST
	HH002	n=5(50%)	4.9	0.7 – 36.0	0.22	<0.7	INC	45	1935	3.0	A2	DN80ST
	HH003	n=6(86%)	7.5	1.1 – 53.0	1.37	-	-	-	1963	-	A1	DN100ST
	HH004	n=4(100%)	7.8	1.8 – 34.5	5.33	-	-	-	1959	-	A1	DN80ST
	HH005[+]	n=19(51%)	1.8	0.9 – 3.6	0.21	-	-	-	1935	-	A2	DN80ST
	HH006[*]	n=11(39%)	1.2	0.8 – 1.8	0.02	0.3	CPLT	33	1934	0.5	B	DN80ST
	HH007[°]	n=0(0%)	-	-	-	-	-	-	-	-	-	-
	HH008	n=6(26%)	1.5	0.4 – 6.4	0.32	<1.3	INC	-	1934	-	C	DN80ST
	HH009[×]	n=9(38%)	3.9	1.5 – 9.8	4.86	<3	INC	-	1928	-	A1	DN80ST
	HH010	n=3(38%)	1.6	0.2 – 13.7	0.51	<0.7	INC	-	1937	-	C	DN200ST
	HH011[^×]	n=4(50%)	1.9	0.2 – 18.6	0.37	-		150	1963	15	A1	DN300ST
	HH012[°]	n=0(0%)	-	-	-	-	-	-	-	-	-	-
	HH013[^]	n=2(40%)	1.8	-	-	-		65	1939	5	A1	DN80ST
	HH014	n=24 (55%)	1.6	1.1 – 2.5	1.41	-	-	65	1950	5	A1	DN100ST
	HH015	n=1(50%)	1.0	-	0.38	<0.9	INC	19	1935	1	A1	DN80ST
Reported	HH100	n=1(13%)	0.7	-	0.14	-	-	-	1994	-	C	d225Pe
	HH101	n=0(0%)	-	-	0.07	<0.7	INC	-	1960	-	C	DN80ST
	HH102	n=0(0%)	-	-	0.01	-	-	-	1928	-	C	DN125ST
	HH103	n=0(0%)	-	-	0.03	-	-	-	1963	-	B	DN150ST
	HH104	n=0(0%)	-	-	-	-	-	-	1930	-	C	DN100ST

[+] The LDC reported three leak locations, ≈ 30 m distance between the two ends, for this location: two leaks with area of 5 cm^2 and one leak with area of 1 cm^2

***** Complete measurements for the suction method and used for averaging

^ Leak size reported as sum of total hole area of all the leaks on the pipeline

[×] Large difference between leak location and the tracer release location

[°] The LDC did not confirm a gas leak

[#] Pipeline materials, steel (ST) or Polyethylene (Pe), pipeline Diameter Nominal (DN), which is close to the inner pipeline diameter in mm

4.3.2.1 Mobile method

The mobile method was applied at all the 20 locations (18 confirmed and 2 unconfirmed gas leak locations). At 14 (all confirmed gas leak locations) out of the 20 locations, CH_4 enhancements above the 10% threshold were observed and could be evaluated with the standard algorithm. The emission rate estimates for these 14 gas leak locations ranged from 0.7 to 7.8 L min^{-1}. At the 6 other locations we didn't observe any CH_4 enhancements above the 10% threshold. When we lowered the enhancement threshold to 10 ppb, the emission rates were 0.07 (HH007; not confirmed gas leak location), 0.1 (HH012; not confirmed gas leak location), 0.04 (HH101), 0.02 (HH102), 0.05 (HH103) and 0.02 L min^{-1} (HH104). Of the 5 leak locations reported by the LDC, 4 did not show any enhancement maximum above the 10% threshold, i.e., these locations would not have been identified with the default algorithm (Weller et al., 2018) and would thus not produce an emission estimate.

Fig. 4.2 shows a summary of all individual observed enhancement maxima with the G2301 analyzer from all transects with the mobile vehicle, which were used for the quantification of emission rates with Eq. 1. The figure illustrates the large spread in enhancement maxima for multiple passes at each location, similar to Luetschwager et al (2019), leading to large uncertainties in emission estimates of individual locations. Fig. 4.2 also shows the diversity of the various locations, where at some locations most or all of the observed enhancement maxima are above the 10% threshold (e.g. HH003 and HH004), at several locations none of the enhancement maxima was above the threshold (e.g. HH101 and HH104) and at other locations many transects showed enhancement maxima both above and below the threshold (e.g. HH006, HH008, HH009, HH014).

As shown in Fig. 4.3, there is a wide range of CH_4 enhancement observations per location. This depends on wind conditions, distance of the observed plume maximum to the emission outlet location, the superposition of emissions from several outlets and likely other variables such as soil water content. The mean relative uncertainty from the mean emission rate values for the mobile method is ≈ 70% for lower and 400% fort the upper ends for the locations with at least 3 transects (n = 10) which pass the 10% enhancement threshold (significant signals) in this study. The lower and upper ranges go down to 60% and 275% for the locations with at least 5 transects (n = 7) with significant CH_4 enhancements.

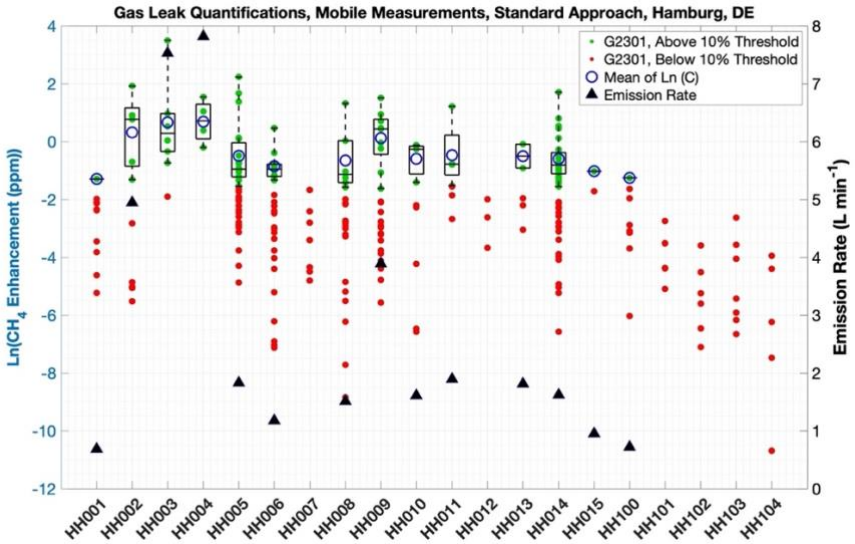

Figure 4.3. CH_4 enhancement maxima from all individual transects for each location using G2301. Red points show CH_4 enhancement maxima below the 10% threshold, green points show CH_4 enhancement maxima above the 10% threshold, thus used for the standard quantification. Blue circles show the $\overline{\text{Ln}\ (C_{max})}$ of all the green points for each location, and black triangles show the derived mean emission rate (based on all green points) using Eq. 4.1 for the location with at least one green point (right y-axis).

4.3.2.2 Tracer method

The tracer method performed emission rate quantification at 16 gas locations out of 20 locations. The derived emission rates range from 0.03 to 5.3 L min^{-1} (Table 4.1). For 4 locations the tracer method was not applied because (i) the emissions were not persistently observable and the LDC also didn't confirm existence of gas leaks at these locations (n = 2; HH007 and HH012) or (ii) the leak had already been repaired (n = 1; HH013) or (iii) no emission was detectable during the visit of the tracer team (n = 1; HH104). For two of the locations (HH11 and HH09), where leaks were confirmed and the tracer method was successfully deployed, later investigations during repair actions (see Fig. 4.1) showed that the surface emission outlets were located far (15 to 60 m) from the actual gas pipeline leak location indicating underground gas migration. It is evident from Table 4.2 that the tracer technique can also quantify very small emission rates, below the cut-off of the mobile technique of 0.5 L min^{-1}. Emission

rate estimates derived from the tracer technique were in general lower than the ones derived from the mobile technique, except for three sites where they were comparable (HH004, HH009 and H014).

4.3.2.3 Suction method

Due to the time-consuming nature of the suction measurements, initially 10 gas leak locations had been planned for deployment of the suction method in this campaign. The goal was to cover a wide range of expected emission rates, as stated in the intercomparison matrix. The suction method was applied at 8 gas leak locations (see Table 4.1) out of which the suction quantification was complete (HH006) according to protocol where an equilibrium concentration has to be reached. This was at HH006, with a derived emission rate of 0.3 L min^{-1}. At several of the locations where the mobile method had indicated high emission rates, subsurface accumulation was widespread, and the suction method was either not deployed (n = 3; HH003, HH04, HH011) or the measurements were incomplete (n = 7; HH001, HH002, HH008, HH009, HH010, HH015 and HH101) because of either safety reasons or because the suction team estimated that they would be unable to complete the measurements within a day. For the 7 locations with incomplete suction measurements, the emission rates were reported ranging from 0.7 to 3 L min^{-1}. These can be regarded as upper limit estimates because suction was not yet completed and CH_4 concentrations would have supposedly dropped further.

4.3.2.4 Hole method

For 5 locations where the leak area of a single gas pipeline leak was reported, the corresponding emission rates are between 19 to 65 L min^{-1}. For locations HH011 and HH013, the hole area was reported as the sum of several holes and the total hole area for these two locations resulted in an emission rate of 150 and 65 L min^{-1}, respectively. The quantification from the hole method is higher than from the mobile, tracer and suction methods by at least an order of magnitude.

4.3.3 Leak categories

The 20 (18 confirmed + 2 not confirmed) locations can be divided into four main categories related to measurement challenges of the various methods. These categories may overlap.

(i) Large subsurface CH_4 accumulation
(ii) Insufficient CH_4 enhancements for mobile quantification
(iii) Large CH_4 enhancement variability for mobile quantification
(iv) Several outlets and / or leaks or atmospheric turbulence

In this section we present the overall results and discuss in detail one selected location for each of these categories. The remaining locations (with similar characteristics) are presented in the SI.

4.3.3.1 Location type I – Large subsurface CH_4 accumulation and multiple outlets

The spatial spread of surface emission outlet locations identified with the G4302 instrument as part of the mobile method provides an indicator for the extent of the subsurface accumulation of CH_4. For 5 locations, emission outlets were found at great distance from each other, in order of tens of meters. The total emission of a gas leak is equal to the sum of emissions from all the surface outlets at a location, thus it is necessary to quantify each outlet separately to get the total emission.

HH011 (Fig. 4.4) is an example where very widespread CH_4 accumulation and migration was observed. During the initial mobile gas leak detection, leaks were located at the intersection of streets 1 and 2, close to a subsurface vent and a rain drain, ≈ 2 m far apart, (the yellow pin in Fig. 4.4a) based on clear signals from these outlets and a sign next to the road indicating presence of gas pipelines. The vent showed a C_2:C_1 ratio of 2% (R^2 of 0.8 and max CH_4 mole fraction of 31 ppm) and we observed C_2:C_1 ratio of 2.8% with R^2 of 0.96 and max CH_4 mole fraction of ≈ 70 ppm from the rain drain, clearly indicating a large / dominant contribution from fossil CH_4. However, after quantifying the emission from these two leaks using the mobile and the tracer release methods, the LDC found the actual gas pipeline leak, during the repair actions, on the south side of the intersection, far from the vent and the

rain drain, at the intersection of street no. 3 and no. 2 indicating that the gas had travelled about 60 m underground. It is possible that the leak resulted in several gas emission outlets, likely closer to the gas pipeline leak location. The emission rate measured using the mobile method was 1.6 L min^{-1} based on 5 plume transects and is likely underestimated because some emission outlets potentially were not included in the performed plume transect. It should also be noted that the distance from the gas pipeline leak location to the plume transect is larger than the distances applied during the controlled release calibrations (average 15 m) (Weller et al., 2019).

The tracer was released at the vent and the rain drain and thus measured the combined emission from these two outlets to be 0.4 L min^{-1}. If the gas pipeline leak gave rise to multiple unidentified surface emission outlets, the emission from the gas pipeline is underestimated. In fact, Fig. 4.4 shows that a CH_4 plume without C_2H_2 was observed during the tracer release measurements at HH011, confirming that at least one other source of CH_4 emission was present nearby.

Based on the previous experience at locations with widespread subsurface accumulation it was concluded that the suction method could not be applied at this location. The other case in this category was HH009.

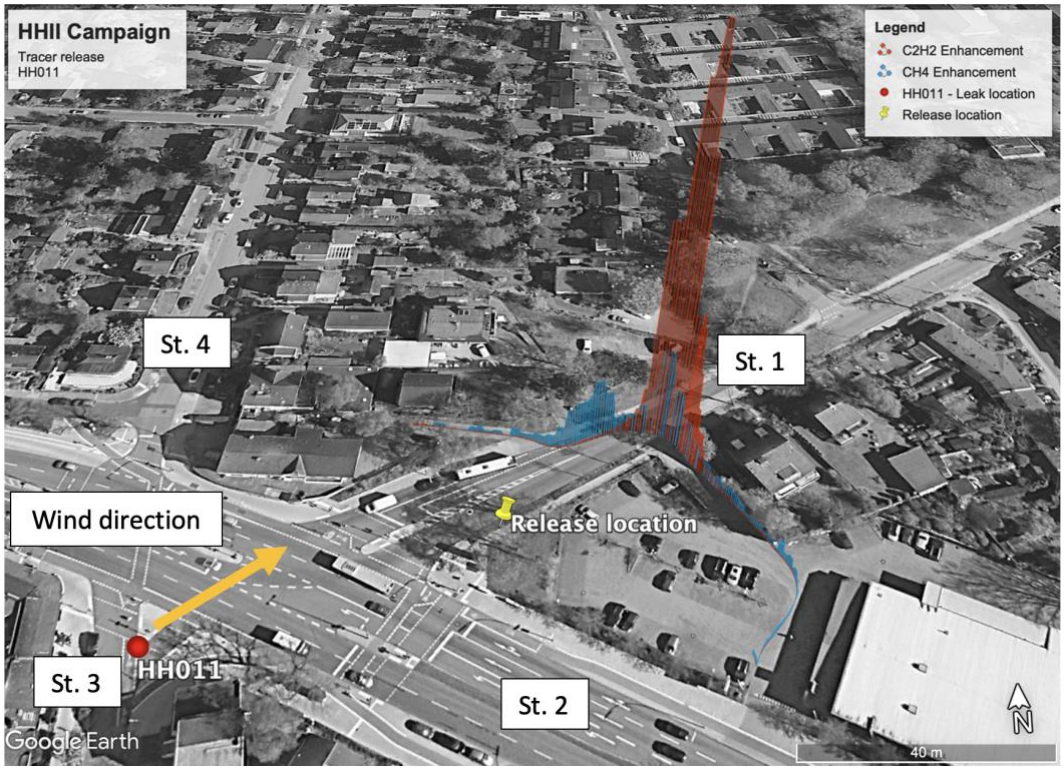

Figure 4.4. Aerial image of HH011 (© Google Maps). A gas leak location with widespread undersurface CH_4 accumulation. The yellow pin shows the assumed leak location and location of tracer release, which was very different from the actual leak location as identified by the LDC (red circle). St. 1-4 are added to identify streets that are discussed in the text. General wind direction during tracer release deployment is shown with an orange arrow. CH_4 (in blue) and C_2H_2 (in red) levels measured at a plume transect. One of the CH_4 plume is proportional to the C_2H_2 plume while the other CH_4 plume lacks the C_2H_2 signals suggesting existence of at least another emission outlet.

The LDC reported the total area of several holes in the pipeline as 15 cm^2 for HH011, which is the largest leak size among all the locations. If we assume that there was one hole with this size, then the emission rate estimated by Eq. 4.3 will be 150 L min^{-1}, a hole of 5 cm^2 gives emission rate of 65 L min^{-1}. The pipeline for this location was DN300ST and has been in operation since 1963.

4.3.3.2 Location type II – Insufficient CH_4 enhancements for mobile quantification

At HH101, on a narrow (≈ 3 m wide) street, which had about 1 m wide bare soil pavement on one side, the LDC reported a gas leak location based on their routine surveys. On both sides of the street there were about ≈ 1.5 m tall bushes and some trees. All three methods (mobile, tracer and suction method) were deployed at this location. Gas emissions found their way to the atmosphere through cracks in the asphalt with C_2:C_1 ratio of 2.5% (R^2 of 0.93) with max CH_4 mole fraction of ≈ 25 ppm. None of the CH_4 enhancement maxima observed during the mobile surveys at this location were above the 10% enhancement threshold with the G2301 instrument, thus this location would not be labeled as LI and no quantification would be reported from mobile method as implemented in Weller et al (2019) and Maazallahi et al. (2020d). The tracer method was applied in static mode at a distance of ≈ 15 m and reported an emission rate of 0.1 L min^{-1}, which is compatible with the emission strength being below the "detection limit" defined by the 10% cut-off of the standard algorithm (0.5 L min^{-1}). When the emission strength is evaluated using the CH_4 enhancements below the cut-off, the value is 0.04 L min^{-1}. The suction method was applied at this location but an equilibrium was not achieved after 9 hr, i.e. incomplete suction measurements, and an upper limit for the emission rate of ≈ 0.7 L min^{-1} was reported. The fact that the suction measurement was incomplete at this location with a small emission rate shows that subsurface accumulation can also be large for smaller leaks.

Three of the leak locations in this study only showed one CH_4 enhancement above threshold. The 10% threshold is a constraint, which removes enhancements less than about 200 ppb. This means for the locations where we only have one transect with CH_4 enhancements more than the 10% threshold, the minimum emission rate estimated is about 0.5 L min^{-1}, no matter how many transects we had with CH_4 enhancements less than the 10% threshold. This situation was observed for HH001, HH015 and HH100 (Fig. 4.5). In this case, the mobile method likely overestimates the total leak rate, because only the maximum enhancement is used for quantification. The tracer method reported low emission rates for these three sites 0.12 L min^{-1} on average (n = 6).

For the two locations (HH007 and HH012) where the LDC didn't confirm gas leaks (despite periodic observation of C_2H_6 at outlets during the mobile surveys) none of the transects showed CH_4 enhancement maxima above the 10% threshold. At HH007, the outlet was through cracks in the pavement but at HH012 the outlets were from manholes. At HH007 the outlet location had shifted by about 2 m for two different days (4-week gap). We note that the correlation coefficients between CH_4 and C_2H_6 at these locations were between 0.4 and 0.6, so less than 0.7, which is the threshold correlation we accepted for the outlets. As a leak was not confirmed for these locations, the tracer and suction methods were not applied.

4.3.3.3 Location type III – Large CH_4 enhancement variability for mobile quantification

For several locations, we observed a large variability of CH_4 enhancements from different transects. One example is HH008, where only 6 of the 23 transects exceeded the 10% threshold, i.e. the leak was only observed in about every 4th transect. The leak location of HH008 is an example where CH_4 enhancements from several transects cover a wide range. Based on the 6 transects, which showed enhancement maxima above the 10% threshold, a leak rate of 1.5 L min^{-1} is derived. This may be an overestimate since many transects with maxima below the threshold were not considered. For this location the mobile tracer method was applied, which resulted in a leak rate quantification of 0.3 L min^{-1}.

The suction method derived an upper emission estimate of 1.3 L min^{-1} from incomplete measurements at HH008. The LDC reported a C category leak for this location from a DN80ST pipeline, which was installed in 1934.

4.3.3.4 Location type IV – Several outlets and / or leaks or atmospheric turbulence

On a ≈ 5 m wide street, we detected two leaks about 80 m away from each other, HH001 and HH002 (Fig. 4.5a). It was a cobblestone street and there were bushes and few trees planted, mostly on

one side of the street. The mobile method performed 10 transects at both locations and all the transects were accepted for the evaluation. The tracer team could quantify both locations using static measurements. The suction team began to quantify HH002 and HH001, but during quantification of HH001, there was a small accident (fire due to contact of drilling head with electric cable) and the leak had to be fixed immediately. The plumes on this street were sufficiently separated to positively identify two different leaks on the same street. In contrast, at location HH005, we observed several maxima for the same transect, but because the maxima were close to each other, those were clustered together in the mobile measurement algorithm (Fig. 4.5b). Later the LDC reported even three individual pipeline leaks on this street. In another example (HH010), some transects showed several plume maxima although only one emission outlet and later on only one gas pipeline leak was found (Fig. 4.5c). However, the release of the tracer resulted in several matching CH_4 and tracer gas plumes confirming that the emission indeed occurred form a single outlet and that the multiple plumes at this location were due to inhomogeneous plume dispersion. This illustrates that the existence of several maxima in one transect does not necessary correspond to presence of several leaks and/or outlets, but it can also be related to a spatially heterogeneous/disturbed plume. This shows that the signals from the mobile detection method are not sufficient to allow determining the number of leaks at a location with several plume at a close distance from each other in a single transect.

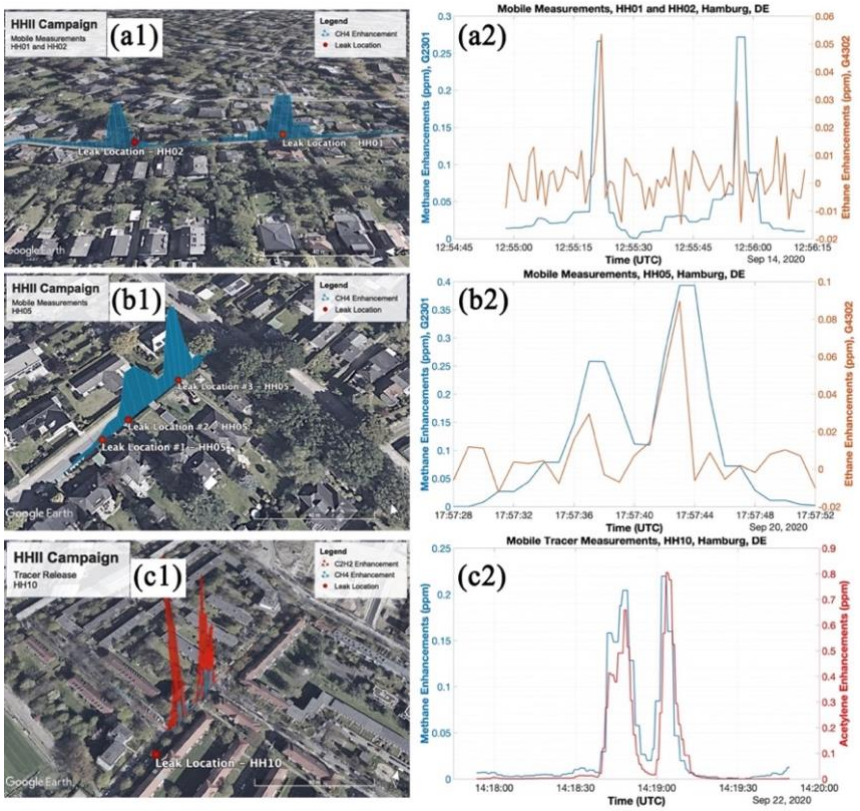

Figure 4.5. Several maxima observed during a single transect on one street showing different situations: two well isolated leaks with about 80 m distance from each other (a1 and a2, HH001 and HH002), three pipeline leaks close to each other with several emission outlets (b1 and b2, HH005) and one leak and one outlet but several CH_4 enhancement maxima due to turbulence (c1 and c2, HH010), aerial images: © Google Maps.

After detection by mobile measurements, emissions out of the ground were detected at HH001 and HH002 with the G4302 backpack within 3 m distance from the gas pipeline leak locations, which was later reported by the LDC. For the single transect with a maximum above the 10% threshold observed with the mobile method, the derived emission rate at HH001 was 0.8 L min^{-1} (n = 1). For HH002, the derived emission estimate for the transects with maxima above the threshold is 5.2 L min-

^{1} (n = 5) from the mobile method. At HH002, individual derivation of emission from separate CH_4 enhancement gives a wide range between 0.7 and 36.0 L min^{-1} (95% confidence) from the mobile method (see category III above). For HH001, the tracer method was applied in static mode at ≈ 30 m distance to the release point and ≈ 40 m far from HH002. The derived emission rate for HH001 is 0.06 L min^{-1} and for HH002 0.22 L min^{-1} from the tracer method. For HH001, after about 5 hr of pumping, the suction quantification had to be stopped due to the incident described above. Based on the incomplete suction measurement an upper limit for emission rate of ≈ 1.8 L min^{-1} for HH01 was estimated. An emission estimate of ≈ 0.7 L min^{-1} was derived for HH002 from an incomplete suction measurement. The LDC reported leak size of ≈ 2.5 cm^2 for HH001 and for ≈ 3 cm^2 for HH002 which then give emission rate of 39 and 45 L min^{-1} respectively from the hole method. For both locations, leaks were due to pipeline corrosion.

4.3.4 Emission rates of different leak safety types

The 18 confirmed gas leak locations that were investigated in the campaign were categorized into the four safety categories, A1 (n = 7), A2 (n = 2), B (n = 2) and C (n = 7). The mobile method quantified all the A1 and A2 leaks (n = 9) with an average emission rate of 3.6 L min^{-1}. 5 out of 9 leaks in categories of B and C leaks were quantified with the mobile technique including the 10% threshold with average emission rate of 1.1 L min^{-1} (n = 5). Apart from one location, which had to be fixed before the measurements, the tracer method quantified the A1 and A2 leaks (n = 8) and reported an average emission rate of 1.8 L min^{-1}. The tracer method also quantified all the B and C leaks (n = 9) with an average emission rate of 0.1 L min^{-1}. Mostly due to the safety and time constraints and medium to large underground accumulations of CH_4, the suction method could provide incomplete measurements at only 3 locations of A1 and A2 leaks with an average emission rate of 1.5 L min^{-1} (n = 3). The suction method measured at 5 out of 9 B and C locations, one of the measurements was complete and the others were incomplete, with an average emission rate of 1.0 L min^{-1} (n = 5). Although the number of quantified leaks is limited, all the three methods show that the emission rates from category A1 and A2 leaks are higher than category B and C leaks (Fig. 4.6). This indicates that the site selection bias of measurements for the suction method due to safety concerns (see qualifier above), can lead to a bias in the emission rate in this method.

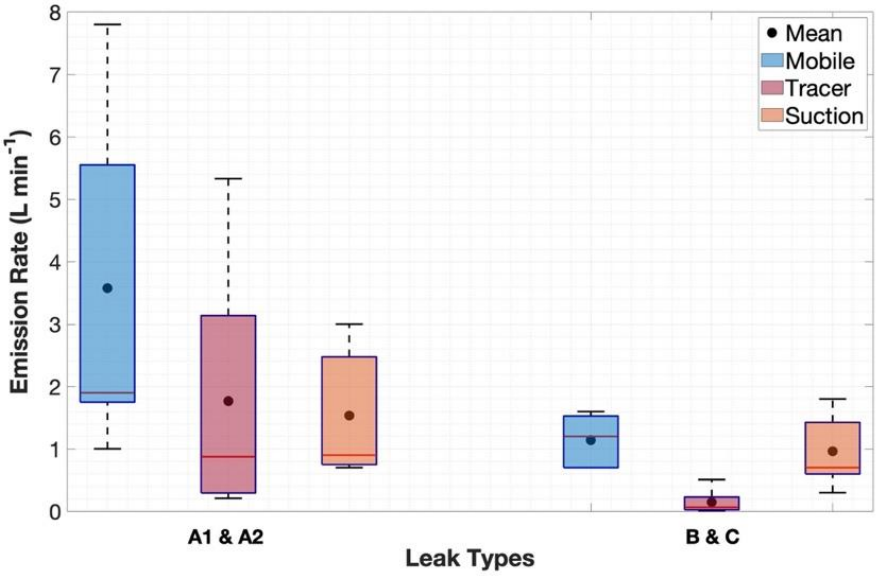

Figure 4.6. Emission rate differences between different gas leak categories.

4.4 Discussion

4.4.1 Leak detection methods

4.4.1.1 Leak location vs outlet location

There is a difference between the location of the leak in the gas pipeline (leak location; See Sect. 4.S.7 in SI) and the location where the gas is emitted to the atmosphere (outlet locations; See Sect. 4.S.2 in SI). Furthermore, a single leak in the gas pipeline can result in multiple emission outlets at the surface. In this campaign we observed that in most cases, the emission outlet at the surface occurred only a few m (sometimes < 1 m) from the location of the leak in the gas pipeline. However, in one case, an emission outlet was detected about 60 m away from the leak location indicating significant underground gas accumulation and migration (see Fig. 4.4).

4.4.1.2 Intercomparison of the gas leak detection methods

The mobile method detects atmospheric CH_4 enhancements while measuring continuously with ppb precision from an inlet installed at the front bumper of the car while LDCs apply the carpet method with an instrument precision at the ppm level. High precision for the carpet method is not needed as the inlet to their instruments is connected to a carpet, which is attached to the ground. The mobile method can cover larger areas in shorter times, but not all roads, walkways, or other surface areas where pipelines are buried are accessible with a vehicle. The advantage of the carpet method is that it can precisely follow the pipeline map, which also means that it can locate leaks more precisely. The mobile method use a 10% threshold to neglect unreliable gas leak sources, which sometimes results in neglecting actual signals from small leaks. Also the mobile measurements do not detect all leaks due to the dependence on the wind direction (only downwind sources leaks can be detected). Luetschwager et al. (2021) suggested that 5 to 8 plume transects give > 90% probability of gas leak detection at a given location, so if all the streets in an urban area are covered 5 to 8 times, > 90% of the leaks can be detected by mobile measurements.

Both the mobile and the carpet method use C_2H_6 signals for distinguishing between fossil and microbial CH_4 emissions, and as for C_2H_6, the instrument used in the mobile method is more sensitive, and faster. In the carpet method, the laboratory analysis of C_2H_6 is slow and with higher detection threshold compared to the mobile method, where C_2H_6 is measured in real-time during the surveys, and also on foot from the emission outlet. The CRDS instrument provides real-time measurements of CH_4 and C_2H_6 at 1 Hz frequency so checking various outlets at a possible gas leak location is faster.

At 14 out of the 20 locations in this study, gas leaks were detected (CH_4 signals passing the 10% threshold) and quantified with the mobile method. However, we observed that 4 out of 5 locations reported by the LDC would not have been detected in mobile surveys without prior information on existence of the leaks because the maximum enhancement was below the mobile detection threshold. At the only location (HH100) from the list of the LDC, where mobile method could quantify the emissions, the outlets were located on the road and the vehicle was driving on top of the outlet. For this location only one of the transects passed the 10% enhancement threshold, and the quantification for this location was ≈ 0.7 L min^{-1}, close to the detection threshold of this method, ≈ 0.5 L min^{-1}. One of the other locations, HH101, reported by the LDC had similar surrounding conditions (e.g. presence of buildings, road conditions, etc.) as the other leaks detected by the mobile method, but still the mobile method was not able to detect a gas leak at this location without a priori information from the utility. The quantifications made by the tracer method suggest that the emission rates of the locations provided by the LDC were much lower than the locations detected by mobile measurements (Table 4.2). The 10% threshold in the mobile method precludes the identification of small leaks (< 0.5 L min^{-1}), which would only be identified by the carpet method.

4.4.2 Signal attribution in mobile detection method

4.4.2.1 Attribution during mobile survey in car

During the mobile measurements we used two approaches to find correlation between CH_4 and C_2H_6. When we compare the online measurements point by point, the probability of detecting a fossil signal is high, as only one single significant reading is sufficient to indicate a fossil signal. When we use the R^2 of the linear correlation between CH_4 and C_2H_6 enhancements above the cut-off, the attribution is more reliable. In a large dataset without a priori information on the existence of a gas leak at different locations, the correlation method is more trustworthy as the point-by-point method could be affected by instrument noise and/or spikes.

We also used CO_2 signals and their correlation with CH_4 signals to investigate interference from combustion or microbial processes. For only 7 plumes at 6 locations, we detected correlations between CO_2 and CH_4, which could indicate either oxidation of CH_4 to CO_2 or mixture of microbial CH_4 emissions from e.g. the sewer system with the emissions from natural gas leaks. The number of these possible co-emissions is low compared to the number of total transects (only ≈ 7% of the plumes with CH_4 enhancements greater than 10%), thus such an admixture of microbial CH_4 should not impact the quantification from mobile method significantly.

4.4.2.2 Plume attribution to emission outlets

The outlet attribution was performed using the G4302 CRDS instrument which is portable like a backpack. We checked the outlets (See Sect. 4.S.2, Fig. 4.S1) around the locations of interest and evaluated the correlation between CH_4 and C_2H_6 and the persistence of the emissions on different days. In theory, it is possible to estimate contributions of fossil and microbial CH_4 in a plume using the C_2H_6 signals during the mobile measurements with the vehicle and the reference C_2:C_1 ratio provided by the LDC. However, due to the low C_2H_6 signals in ambient air, it was not feasible to quantify the possible contribution of microbial CH_4 emissions. Nevertheless, the C_2H_6 signals of the G4302 CRDS instrument were still very useful to identify a location as a possible gas leak location or not. For all the 15 locations, which were initially detected by the mobile method we observed detectable C_2H_6 signals, including the two locations which later were not confirmed as a gas leak location by the LDC. This suggests that either the leak is at a greater distance and depending on the transport of the emission we periodically can see the signals at the detected outlets or that there are sources that produce both CH_4 and C_2H_6 in the vicinity of the location.

4.4.3 Leak quantification methods

4.4.3.1 Mobile method

If the outlets are close to each other, we may observe several CH_4 enhancements close to each other or overlapping when a single transect is performed at a close distance. If we assume that the number of CH_4 maxima is equivalent to the number of real outlets that exist on a road and only use the maximum enhancements from the most pronounced plume to calculate the emission rate, the total emission will be underestimated with the mobile method.

Emission rate estimates with the mobile method from individual transects are associated with high uncertainty, related to variabilities in either above-ground or under-ground conditions. For example, an unfavorable wind direction (above ground condition) can result in missing a plume from a gas leak. The mobile measurement van itself may also affect the measurement, e.g., by creating pressure fluctuations. Luetschwager et al. (2021) showed that the quantifications from the same leak in individual mobile transects can vary by more than an order of magnitude. In Hamburg, we found that the range can be even a factor 50 or 100 in exceptional cases (Table 4.2). This high variability illustrates that if we perform only one transect per location, the estimated leak emission rate can result in high under / overestimation in emission estimate for the single location, as was also reported by Maazallahi et al. (2020d). This large uncertainty for individual locations is less severe when the results are

extrapolated to the city-level, where the sample size is also large, including over- and underestimates (Brandt et al., 2016).

In our previous study in Hamburg (Maazallahi et al., 2020d) the overall average emission rate for all the LIs was estimated 3.4 L min^{-1} LI^{-1} (n = 145) while for the fossil-attributed locations it was 5.2 L min^{-1} LI^{-1} (n = 45; standard error of 3.1). This showed that the biggest emitters were among the fossil categories. In the present study, the average emission rate from mobile measurements for the gas leak locations is 2.7 L min^{-1} LI^{-1} (n = 14; standard error of 0.6). The higher average emission rate per fossil location in the first campaign may have been caused by the fact that in that campaign only a smaller number of transects performed per location (on average 1.1 in the precious study versus 6.9 transects with CH_4 > 10% threshold per location in the present study). Luetschwager et al. (2021) stated that after 6 transects with CH_4 exceeding the 10% threshold per location the average overestimation of leak size estimates will be less than 10%. In addition, the differences in sample size and locations in these two studies (45 versus 14 locations in the first and second studies respectively) may partially explain the difference in average. This is because the probability of detecting large emitters, which increase the average emission rate of all leaks, increases with sample size.

The two CH_4 sensors onboard the mobile van play specific roles in the detection and quantification of leaks. CH_4 enhancements on the G2301 are 3.8 times lower than the G4302. This is an artefact of the G2301, which smoothes the signal compared to the G4302 because of the slower pump and sampling rate (See Sect. 4.S.8.1 in SI). On the other hand, this results in more signals passing the 10% threshold on G4302. This then also leads to higher detection probabilities using G4302 (See Sect. 4.S.8.2 in SI). Higher record of CH_4 enhancements then also results in higher emission rate quantification using Eq. 1 (See Sect. 4.S.8.3 in SI). We use the G2301 for quantification, since this is the instrument that was also used for introduction of the mobile equation quantification in Weller et al. (2017). The quantification of the gas leak locations using Eq. 1 depends only on the CH_4 enhancements. This gives about a factor 2 higher emission rates from G4302 than from G2301 for the same plumes. When we evaluate the plume areas from the two instruments, they are much closer to the 1:1 line (See Sect. 4.S.8.3 in SI). This agrees with findings from another study using two different in-situ instruments onboard a mobile car (See Sect. 4.S1.5, Fig. 4.S6 from Ars et al. (2020)). They also found that the plume area is closer to the 1:1 line in mobile measurements even if the air intakes are not at the same location of the vehicle. This suggests that the plume area is a more robust parameter than maximum enhancement for emission rate quantification and a leak rate quantification equation using the plume area should be developed.

In general, the closer the air intake is to the emission point the higher the CH_4 mole fraction reading is (See Sect. S.9 in SI), but when several outlets are present at one location it is not possible to uniquely determine the distance to the emission point, and also determine which plume belongs to which outlet. Eq. 1 from Weller et al. (2019) only uses the maximum CH_4 enhancements above the 10% threshold from each pass. In their controlled release experiments the average distance between the leak and measurement was 15.75 m. Analysis of our results (Table 4.S4, Sect. 4.S.5 in SI) shows that higher maximum concentrations are encountered more often when the distances of the transect to the leak location are small. For example, at HH002 the transect was very close to the main emission point, which likely leads to the substantially higher emission rate estimate derived from the mobile method (4.9 L min^{-1}) compared to the tracer method (0.22 L min^{-1}). On the other hand, at HH011 the mobile method underestimates the emission rate (See Sect. 4.3.3.1), as at this location the measurement distance to the leak was larger than reference distance of 15.75 m applied by Weller et al. (2019). This suggests that to reduce the quantification error for individual leak locations, distance should also be included in an improved transfer equation.

The effect of neglecting or retaining the transects with enhancement maxima below the 10% threshold was quantitatively investigated for 5 locations where the tracer team conducted mobile measurements (See Sect. 4.S.10 in SI). These measurements were evaluated as “controlled release” experiments for C_2H_2, because the actual C_2H_2 release rate is known, and measurements were made in

mobile mode. The standard mobile quantification algorithm with the 10% threshold yields emission estimates that are in relatively good agreement with the released quantities, whereas the estimates are biased considerably low when measurements with maxima below the threshold are retained. This supports the use of the original method, which removes transects with an improper realization of the plume. Relating to section 4.5, it must be noted, however that in these measurements the distances of the C_2H_2 maxima to the release points were between 30 to 45 m, thus larger than the normal distance of mobile CH_4 measurement to the emission outlets (from few meters up to 30 m).

4.4.3.2 Tracer method

The tracer method is more labor intensive than the mobile method. However, the strength of the method is the application of a tracer gas providing the plume dilution and avoiding the use of atmospheric dispersion models and weather information. If the tracer release location does not reflect the sum of all the outlet emissions at a gas leak location, or misses some of the outlets, then the total emission quantification from the gas leaks will be underestimated. An example of such a case is site HH011 in this study where the leak location in the gas pipeline (after quantification; see Fig. 4.1) was found to be located about 60 m upwind the targeted emission outlet. During tracer quantification, an additional CH_4 plume (not defined by the tracer gas) was observed indicating more than one emission outlet (Fig. 4.4). The confirmation for this is the finding of gas leak location by the carpet method. The emission rate of the targeted emission source (the vent and the drain) is thus not representing the combined emission from the gas leak in the pipeline located 60 m upwind the emission source. Further surface screening and leak detection would have been needed to identify and quantify all emission outlets.

4.4.3.3 Suction method

The suction method is the most labor-intensive quantification method. Following a strict, safety first, protocol the gas utilities fix leaks in the A1 safety category immediately upon detection and A2 leaks within a week. Given logistical constraints, the suction method therefore mainly or exclusively quantifies B or C leaks (50% of confirmed gas leak location in this study). We investigated whether such a site selection bias could lead to a bias in the average quantified emission rate in the inventory report. In this study, we observed that the leaks detected from the mobile methods were mostly in the A1 and A2 category and the biggest emitters (based on the mobile and tracer release measurements) had soil CH_4 accumulation of a magnitude that prevented successful application of the suction method. Further research is needed to identify the physical mechanism(s) to explain the observed correlation between A1 and A2 leaks and high emission rates. As a hypothesis, the presence of soil cavities associated with leak category A1 may result in higher permeability, i.e. lower underground resistance, which then leads to higher emission rate for the same pipeline hole size compared to locations with no cavity.

The suction method was intended to be deployed right before the repair actions. For some of these locations, the suction method was in operation for more than 10 hours, but due to the high soil CH_4 accumulation, the measurements were stopped and labeled as incomplete in this study. For the other locations with high soil CH_4 accumulation, the suction method was not attempted, given the expectation (based on experience at the incomplete locations) that completion of measurements for leak rate quantification at those locations was unlikely.

4.4.3.4 Hole method

Based on the leak size, pipeline depth and overpressure, the average emission rate was estimated at 40 L min^{-1} (n = 5). We note that these estimated should be regarded as upper limits since flow restrictions outside the pipe are not included. The emission range of individual gas leaks based on the hole method is between 19 to 150 L min^{-1} for 1 cm^2 to 15 cm^2 hole sizes respectively, larger than any of the measurement-based quantification methods. This method requires information about the

overpressure of the gas pipeline, depth of buried pipeline and size of a leak and it does not include the information about soil properties, which can impact the emission rate.

4.4.3.5 Intercomparison of methods

In this study, a reliable quantitative intercomparison of the three methods (mobile, tracer and suction methods) was attempted. A complete comparison of all three methods was possible at only one out of 20 locations (18 confirmed gas leak locations) because of the long time (>8-10 hrs) needed for full equilibrium of the suction method, whereby emission rates for 7 out of the 8 leaks quantified by the suction method were reported as maxima rather than absolute values (Table 4.1). At these 7 locations the emission was thus overestimated.

In total, the average CH_4 emissions from natural gas pipeline leaks for the same locations where we have quantifications from mobile and tracer methods (n = 13) are 2.8 and 1.2 L min^{-1} respectively. The suction method could only be completed at one location. The average emission rate reported for all the locations from the suction method (high bias due to incomplete measurement) is 1.2 L min^{-1} (n = 8).

The higher emission rates derived with the mobile method are in qualitative agreement with previous studies. Weller et al. (2018) compared quantifications from the mobile measurements described in von Fischer et al. (2017) with the tracer method and surface enclosure method in four US cities. They reported that mobile measurement estimates were ≈ 2.3 L min^{-1} greater than the tracer method mean estimates of ≈ 3.2 L min^{-1} (n = 59). This was attributed to the overestimation of small leaks (< 2.4 L min^{-1}) in the mobile measurements method, which we have also discussed above for our dataset. In addition, performance of only a few transects at individual locations also lead to systematically high biased emission rate estimates for higher emission rates (Luetschwager et al., 2021). Indeed, at the locations where we only have one transects with CH_4 enhancements above the 10% threshold, there is an overestimation from mobile method compared to the tracer method. For example, at HH001 (n=1), HH015 (n=1) and HH100 (n=1) the mobile method estimated emissions of a factor 4 higher in comparison to the tracer method. The analysis of Luetschwager (2019) clearly shows that this high bias is reduced when numerous transects are performed. Therefore, we carried out multiple transects to reduce this systematic bias. We note that there are also large differences between the mobile and tracer methods, e.g. HH002 and HH006. We suspect that the very short gas leak location distance to the mobile driving transects can explain partially the difference. Moreover, existence of another leak in the category of A1 at the HH006 location which had to be fixed prior to the tracer method could explain the difference in emission rate magnitude at this location. Nevertheless, the limited number of transects and the 10% threshold can contribute to an overestimation of the average leak rate with the mobile method at an individual location. At the same time, however, the mobile method fails to detect leaks entirely when the leak outlet is located downwind of the mobile van. The fact that the mobile method misses downwind emissions constitutes a method specific factor towards biasing city-wide emissions low, which qualitatively counteracts the high bias above.

4.4.4 Possible suction method sampling bias with implications for emission inventories

The national inventory for CH_4 leakage from the gas distribution network in Germany is based on measurements with the suction technique (Umweltbundesamt, 2021). An ongoing project is underway to refine these emission estimates (MEEM, 2022). The utilities choose leak locations for application of the suction method where there are no safety concerns and/or immediate leak closure is compulsory. This implies that this method is not applied at locations of the A1 category, which demand immediate repair (P. 27 in GERG, 2018). Due to logistic constraints and the time-consuming nature of the suction measurements, they are likely also not (or rarely) applied at locations in the A2 category, which require repair within a week. Thus, suction measurements have a location sampling bias towards leaks in the B and C category. This is supported by the fact that the leak locations that were contributed by the LDC to the intercomparison campaign were locations in the B and C category. This study

investigated whether this location sampling bias could result in an emission rate bias, which could contribute to the fact that the suction method did not report leaks with emission rates as high as they have been reported by the mobile method in this study or during previous measurements in the same city (Maazallahi et al., 2020d).

In this study, emission rates from A1 and A2 category leaks were larger compared to those from B and C category leaks (Figure 4.6). The emission rate differences vary by measurement method: a factor 2 for the mobile method (n = 9 for A1&A2, n = 4 for B&C), a factor 11 for the tracer method (n = 8 for A1&A2, n = 8 for B&C) and a factor 1.6 for the suction method (n=3 for A1&A2, n = 5 B&C). For the mobile method, there is a clear separation between the A1&A2 versus the B&C categories. The highest emission estimate for the B&C group (HH010) is similar to the lowest emission rate estimate for the A1&A2 group (HH014). Furthermore, HH011 in the A1 category was very likely biased low because of the wrongly assumed leak location.

For the tracer method, the difference between the two groups is largest, an order of magnitude, and we know that emissions are underestimated at least at one location of the A1 category (HH011). The uncertainty of the tracer method is much smaller than the difference between the two groups. The tracer method also illustrates that 4 of the 5 leaks that were contributed by the LDC to the intercomparison campaign were extremely small. If these would be representative for locations where the suction method is usually applied, it would indeed indicate a severe emission rate bias for the suction method, not because the measurements themselves are biased, but because locations with low emission rates are targeted with this method. In the intercomparison campaign, we attempted to apply the suction method also at locations of the A categories, but at 8 out of 9 locations from the A category, the suction measurements could not be applied for safety reasons, or suction could not be completed, because of the widespread subsurface accumulation (Table 4.2). At the other A location (HH014), the suction method could not be applied as the ground had been already opened for the repair.

4.5 Conclusion

In summer 2020, we compared three gas leak rate quantification methods, namely the mobile, tracer, and suction methods, in Hamburg, Germany. While the mobile and tracer methods have been evaluated previously, this is the first peer-reviewed study that includes the suction method.

The mobile method can cover large areas in a short time, but some of the smaller leaks (< 0.5 L min^{-1}) are not identified as a gas leak location due to the 10% enhancement threshold in the standard mobile quantification algorithm. While the mobile method quantification algorithm is designed to accurately report city-level total gas distribution leak rates (i.e., considering a large sample size), it has large (known) uncertainties for individual leaks. The tracer method has a smaller uncertainty, but it is labor intensive in comparison to the mobile method. On average, CH_4 emissions from natural gas pipeline leaks were higher from mobile quantifications in comparison to tracer quantifications. For many locations, we encountered several outlets and with widespread underground gas accumulations. At one location, after deployment of the mobile and the tracer quantification and during the repair actions, it was found out that the actual leak in the gas pipeline was located ≈ 60 m away from the identified emission outlet indicating significant underground gas migration. It is possible that this leak had several emission outlets that were not identified and the emission quantified from the single outlet is thus not representative for the whole emission from this leak.

The suction method has a low reported uncertainty, but it is even more labor and time intensive than the tracer method. Due to the time and effort needed to plan and execute the measurements, the suction method is likely never applied in routine operation at A1 or A2 safety category leaks that mandate immediate or near-time repair. In our study, it was also not feasible to apply the suction method at locations with large subsurface CH_4 accumulations. Our results thus indicate a systematic difference between A1 and A2 (high emissions) versus B and C (low emissions) category locations, and generally larger emission rates are inferred with the mobile and tracer methods for sites with widespread subsurface accumulation.

This study did not allow a direct, quantitative comparison of emission rates estimated with all three different methods because of the inability to quantify the same leak locations with all methods. However, this inability illuminates the importance of site selection for deriving representative emission factors based on empirical measurements. Specifically, the results suggest that a significant emission rate bias could exist for measurements that are carried out with the suction method. Our results therefore stipulate that representative site selection includes sampling at all leak safety categories (GERG, 2020). Otherwise, this could lead to a sampling and emission rate bias in the national inventory of gas leak CH_4 emission in Germany.

Authors contributions

TR, HM and SS conceived and designed the study. TR coordinated the campaign in collaboration with DBI, Technical University of Denmark (DTU), Environmental Defense Fund (EDF), E.On and Gasnetz Hamburg (GNH) teams. HM carried out the mobile measurements, emission outlet attribution, performed the analyses of mobile data and collectively with TR analyzed the intercomparison results. AD, CS and AMF performed the tracer method and reported the emission rates from the tracer dataset. HDvdG and TR made instruments and equipment available for the mobile method and CS provided those for the tracer method. HM wrote the paper, and all co-authors supported the interpretation of the results and contributed to improving the paper.

Acknowledgement

This study was carried out with the financial support from the Environmental Defense Fund. Extra financial supports were provided by the H2020 Marie Skłodowska-Curie actions through Methane goes Mobile – Measurements and Modelling project (MEMO^2; https://h2020-memo2.eu/, last access: 20 April 2022), grant number 722479. In this study, Robertson Foundation supported contribution of Stefan Schwietzke. We appreciate efforts from Luise Westphal, Michael Dammann, Ralf Luy, Christian Feickert, Volker Krell, Turhan Ulas, Dieter Bruhns and Sönke Graumann, from GasNetz Hamburg GmbH who facilitated this study by hosting the teams, arranging and applying the carpet method leak detection and confirmation procedures, making information on gas leaks and pipelines available for the data analysis and applying leak repair protocols. We extend our appreciation to Andre Lennartz, Stefan Gollanek and Dieter Wolf from E.On-for their contribution in the planning of the campaign, deploying the suction method at the locations, and exchanging their knowledge and experiences from their previous campaigns. We thank the team from DBI Gas and Environmental Technologies GmbH Leipzig (DBI GUT Leipzig) including Charlotte Große, who contributed in providing information for structuring the campaign planning.

4.S Supplement

4.S.1) Measurement intercomparison planning

In this intercomparison campaign, participating teams from Utrecht University (UU), Technical University of Denmark (DTU) and EON joined the local host of Gasnetz Hambug (GNH). UU applied the mobile detection and quantification methods, DTU the tracer release method and EON deployed the suction method, and GNH contributed to the leak detection or confirmation and applied gas leak repair protocols. In total, the four teams spent about 6 weeks to first detect and then quantify gas leaks. In the process of planning the intercomparison campaign, all participants contributed to a method intercomparison matrix, where the characteristics of the different measurement approaches were compared (Table 4.S1). The matrix includes descriptions related to the identification of gas leaks, the quantification of gas leaks, adjustments of the method to the intercomparison exercise and upscaling. It also laid out an initial plan for the intercomparison project in terms of identification of suitable locations and deployment of the different methods. This plan was based on the expectation that we would ideally be able to locate 50 leak locations in preparatory mobile surveys from UU, supplemented with locations from routine leak detection surveys by the Local Distribution Company (LDC). Out of 50 leak locations, 10 leak locations would be selected for the intercomparison, ideally including at least 3 locations from each of the three emission categories (low/medium/high) as used by the mobile evaluations (von Fischer et al., 2017; Maazallahi et al., 2020d). Emissions at these locations would subsequently be quantified by the tracer release and suction teams. This approach failed for two reasons: (i) it was not possible to locate 50 leak indications (LIs) in the preparatory surveys in August 2020 and (ii) several of the leak locations had to be fixed immediately or within a week of detection (A1 or A2 category). In one example, gas leak emission rate was estimated about 5.0 L min^{-1} from the mobile method. Therefore, in a second attempt in September 2020, all the three teams were in Hamburg at the same time to immediately quantify any confirmed locations just before repair.

Table 4.S1. Measurement matrix of method intercomparison campaign in Hamburg.

		Mobile Method
Site Selection	**Approach**	• Random sampling of leak indications • Extensive coverage of large fraction of the street network (potentially in target areas within city) • Partial (or complete in the US) re-sampling for verification So far usually one-time, multi-week intensive field campaign
	Adjustment for inter-comparison	• Stratified random sampling of LIs • For the intercomparison it would be good if we observe a larger number (≈ 50) of LIs with a "representative" distribution, i.e. including LIs from three categories (low/med/high leak rate). Possible to include LIs indicated by the carpet method during previous service walks (this would not be random, but an additional targeted survey to increase database) • Based on the population of LIs found, select 10 LIs for intercomparison with the suction method, including three per category (low/med/high leak rate) ◦ Low leak rates are those below 6 L min^{-1} (= 360 L h^{-1}), medium between 6 and 40 L min^{-1} (= between 360 and 2.400 L h^{-1}) and high is everything above 40 L min^{-1} (2.400 L h^{-1}). • If not enough LIs from all categories are found: select 10 sites with a variation of assumed leak sizes from the 'collection' found. • Further identification of leak locations using carpet method (part of the standard leak survey) and portable Picarro instrument if needed • Possibility to prioritize locations previously identified by carpet method

Air Sampling	Site preparation	n/a
	Measurement process	• Air inlet at front bumper or roof of vehicle • Methane concentration measurement in instrument inside the vehicle • GPS determines location where methane plume entered inlet (inlet/instrument delay accounted for)
	Further Conditions	• Quantification is not reliable under no wind or stormy conditions. There are no formal thresholds on when the method can be applied, so decisions will be taken based on scientific judgement during the campaign. During poor wind conditions we would still attempt to identify LIs for creating our population, to be quantified later during more suitable conditions. • Fresh rain fills the soil pores and will block methane diffusion out of the soil, so mobile surveys will not be carried out during/shortly after mid to strong rain events.
Leak-level analysis	Flux quantification	• Conversion of methane concentrations to flux using regression model based on controlled release field experiments
	Flux interpretation	• Estimates for individual locations have considerable flux uncertainties • This necessitates large sample size to reduce city-level flux uncertainties • Quantified flux at a given LI location are from plumes released to atmosphere
	Identification of location	• Localization of approximate leak expression (within 30 m)
Spatial extrapolation		• Method produces information about LIs per km, leak rates per km, taking into account repeats and spatial aggregation • Can be extrapolated to total length of road network within city boundaries • Extrapolation to other cities or country scale possible, but has high uncertainties (very big differences between different cities in US) • Extrapolation to country scale may require more measurements in different cities and/or identification of suitable parameter (activity value) for upscaling
	Interpretation	• Accuracy of extrapolation depends on the representativity of surveyed city section (in terms of pipeline age, material, etc.) to the extrapolated area. Accuracy increases with knowledge of pipeline infrastructure in the surveyed and extrapolated area (and accounting for this knowledge in the model).

Tracer Method		
Site Selection	**Approach**	• Not a typical method for gas distribution leak emission quantification, thus approach will be designed specifically for inter-comparison project (see below)
	Adjustment for inter-comparison	• Same sites that will also be quantified using suction / carpet method. • Note possible interference of other nearby CH_4 sources.
Air Sampling	Site preparation	• Need access downwind at moderate distance (e.g., more than 10 m, less than 100 m) • Need to be able to safely release tracer gas at leak expression location
	Measurement process	• Tracer gas released at known rate at outlet(s) • Methane concentration and tracer gas measurements measured downwind of source with vehicle-mounted instruments
	Further Conditions	• Quantification with the tracer method requires adequate meteorological conditions. The expert group from DTU will assess this during the surveys.
Leak-level analysis	Flux quantification	• Flux estimation based on ratio of tracer gas to CH_4 and the known tracer gas release rate
	Flux interpretation	• Uncertainty: < 20% (Fredenslund et al., 2019) under normal operating conditions • Quantified flux at a given LI location are from tracer released to atmosphere
	Identification of location	• n/a (location was known before)
Spatial extrapolation		• Tracer method not meant to be spatially extrapolated to city-level • For inter-comparison project, objective of tracer method is to provide comparison for emission quantification from individual leak locations
	Interpretation	See above

Suction Method		
Site Selection	**Approach**	• No selection of an existing "leak pool" since leaks are repaired after they were detected by the operator → cooperation with the grid operators is necessary to intervene the process and make the measurement possible • Leaks from underground pipes found during standard leak survey are being reported using an initial protocol. Leaks reported this way are being measured 'as they come', as finding leaks takes time and leaks found soon need to be repaired with respect to DVGW rules. Thus, it is not possible to collect a larger number of leaks to choose from first. • Standard leak survey in Germany follows technical rulebook G465 of the DVGW in which both periods of time are specified with respect to pipeline pressure, material and history of leak rate per km as well as the actual survey procedure. Basically, a fraction of a DSO's grid is surveyed every year and the areas to be covered are planned in advance for every year. Then specialized employees or a service provider (both have to be certified/trained with respect to G465; today having a service provider do the survey is very common) are walking along the pipes using maps with documentation of the pipeline positions. To trace natural gas emissions from the ground both a visual inspection (for example checking for faded vegetation along the pipeline trace) and concentration measurements using equipment allowed/specified by G465 are applied. Equipment used for concentration measurements with a ppm resolution are either FIDs (flame ionization detector) or semiconductor detectors. Indications found must be reported using standardized templates the DSO uses later on to decide on further actions. If a leak of category AI or AII is found the DSO is informed immediately to start repairs asap (refer to annex for explanation on risk categories). • After accessing the suitability for measurement (enough time for preparation – i.e. a leak that does not have to be repaired immediately, accessible surroundings – e.g. not in the middle of a heavy traffic road or on private property the DSO lacks permission to enter, enough space for equipment, project wise to make sure that different types of leak situations – like pressure level, pipeline material, rural vs. urban environment, pipe diameter, location distribution across Germany – are being reflected) a measurement is scheduled. • Any interested DSO can report a leak for examination. In this regard there is a certain level of randomness.
	Adjustment for inter-comparison	• If possible: minimum 3 sites per category (low/med/high leak rate) defined by mobile measurements (definition ref. column right) • If not possible: 10 sites with a variation of assumed leak sizes from the 'collection' found, maybe not covering all leak size categories. • General site areas determined by mobile method stratified sampling • Further identification of leak locations using carpet method (part of the standard leak survey) and portable Picarro instrument if needed (i.e., if carpet is unable to detect the leak)

Air Sampling	Site preparation	• Need to be able to bring measurement equipment to site (by car); enough space to place equipment. • Localization of leaks has taken place upfront. • If leak is close to a street there needs to be barriers
	Measurement process	• Freeing soil above assumed leak location from potential excess methane accumulations by sucking air from the soil through up to 12 probes at approx. 35 cm depth until methane concentration equilibrium is reached in the soil. • Measurement of air flow rate (via flow meter) and methane concentration (via FID).
	Further conditions	• Rain dependency: not possible when soil is soaked with rain • Wind dependency: none • Temperature dependency: not possible when soil is frozen
Leak-level analysis	Flux quantification	• Calculation of leak rate from pipe to soil by combining measured values for both methane concentration and volume flow in air-gas-mixture sucked through the soil after equilibrium is reached.
	Flux interpretation	• Measurement of flux into the soil at specific location(s) where leaks were previously identified using the standard leak survey. • Since information of the location of the pipeline is available and additional probing holes will be drilled to specify the leak site along other quality assurance measures it is seen as unlikely to measure a false-positive this way. • Uncertainties range at ± 10% based on 23 measurement points on two independent test sites with artificial leaks allowing to create controlled release rates at E.ON Ruhrgas and Gaz de France as part of a GERG project conducted in the mid-1990s.
	Identification of location	• n/a (location was known before) • Nevertheless, localization is checked at the beginning of the measurements based on above-ground methane concentrations measured via carpet/bell probe at drilling holes.

Spatial extrapolation		• Spot sample is extrapolated to national/country-specific emission factors for leaks of underground pipes • Knowing the pipeline material and operation pressure of each spot sample, when applied at sufficiently large sample size (N >> 10), statistical analysis will tell if emission factors can be differentiated by e.g. pipeline material or operation pressure. Emission factors are being derived from full measurement campaign within DVGW's ME-DSO project, NOT based on measurements in Hamburg alone! • Aggregation of emissions is done via MEEM method (ref. link) • MEEM distinguishes in detail between several different leak sources with corresponding ways to access and accumulate data. (Please refer to annex for a tree diagram illustrating all different source paths covered by MEEM. These include leaks detected by survey, incidents and operational emissions as well as leaks reported by third parties for both pipelines and facilities. In the Hamburg campaign only the path "leaks detected by survey" is being investigated.) • For underground leaks an event-based approach is foreseen • DVGW is collecting data on leaks found through survey from all national gas grid operators (GaWaS) – these are categorized by safety risks (A1, A2, B, C – for definitions see below) • Principal formula: E_CH4 = EF * n * t, where EF is the emission factor for underground leaks [l_CH4/h], n is the number of leaks this EF applies to and t is the assumed average lifetime [h] of such a leak • Category-specific lifetimes of leaks/incidents: Average lifetimes for leaks found in a survey are retrieved via t = (t_period + t_repair)/2, where t_period is the timespan in which a respective segment of pipe (depending on material, pressure, leak frequency history) needs to be surveyed and t_repair is the maximum time needed to repair a leak of the respective category. The calculation is a naïve statistical average as the leak might occur immediately after the last time the respective pipe segment has been surveyed or just before the survey takes place. • Conservative lifetime estimate: Maximum repair times for each category can be found via the DVGW rulebook while many DSOs will repair most leaks a lot quicker • More realistic approach: average repair time per category is known by operator and used in calculation • As regular surveys in a year will not cover the entire pipeline length a rolling horizon over a survey period needs to be considered (average leak lifetimes are in the range of 2,25 years for leaks checked every four years for example, hence calculations over four years should be averaged)
	Interpretation	• Accuracy of aggregation depends on quality of EF and completeness of leak identification through surveys • In Germany, the spatial extrapolation assumes that the vast majority of all existing leaks will be found through survey • The EF is being derived from spot sampling where all kinds of circumstances existing in the national distribution grid is supposed to be represented. As it is intended to split emission factors by statistically relevant parameters such as e.g. pipeline material changes in the structure of the grid can be accounted for. • This can also be applied if aggregated emission values for a single DSO or grid are wanted. The respective structure of the grid under consideration can be mimicked by separating number of leaks with respect to parameters different EFs apply for. • The MEEM method comprises of a lot more categories (other intrinsic emissions such as permeation from plastic pipes, operational emissions from maintenance, repair, construction and dismantling and incident emissions e.g. from digging accidents) than just underground pipes to compile a complete emission value that can be retrieved on different levels (single grid, entire grid of a DSO, national view).

4.S.2) Emission outlets

Figure 4.S1 shows example of outlets that were identified in this study. A manhole next to a tree (a, HH009), a manhole in the middle of street (b, HH005), asphalt cracks (c, HH101), rain drains (d, HH009), a hydrant (e, HH010), a vent (f, HH011), bare soil surface next to a street (g, HH012), bare soil surface next to a tree (h, HH003), a cobble stone street (i, HH001), gaps between street curbs (j, HH006), surface gas caps on top of gas pipelines (k, HH100), telecommunication cover on streets (l, HH004), open ground before repair (m, HH014). Fig. 4.S1n shows one of the examples when a leak had to fixed before quantification could be applied (black pipeline).

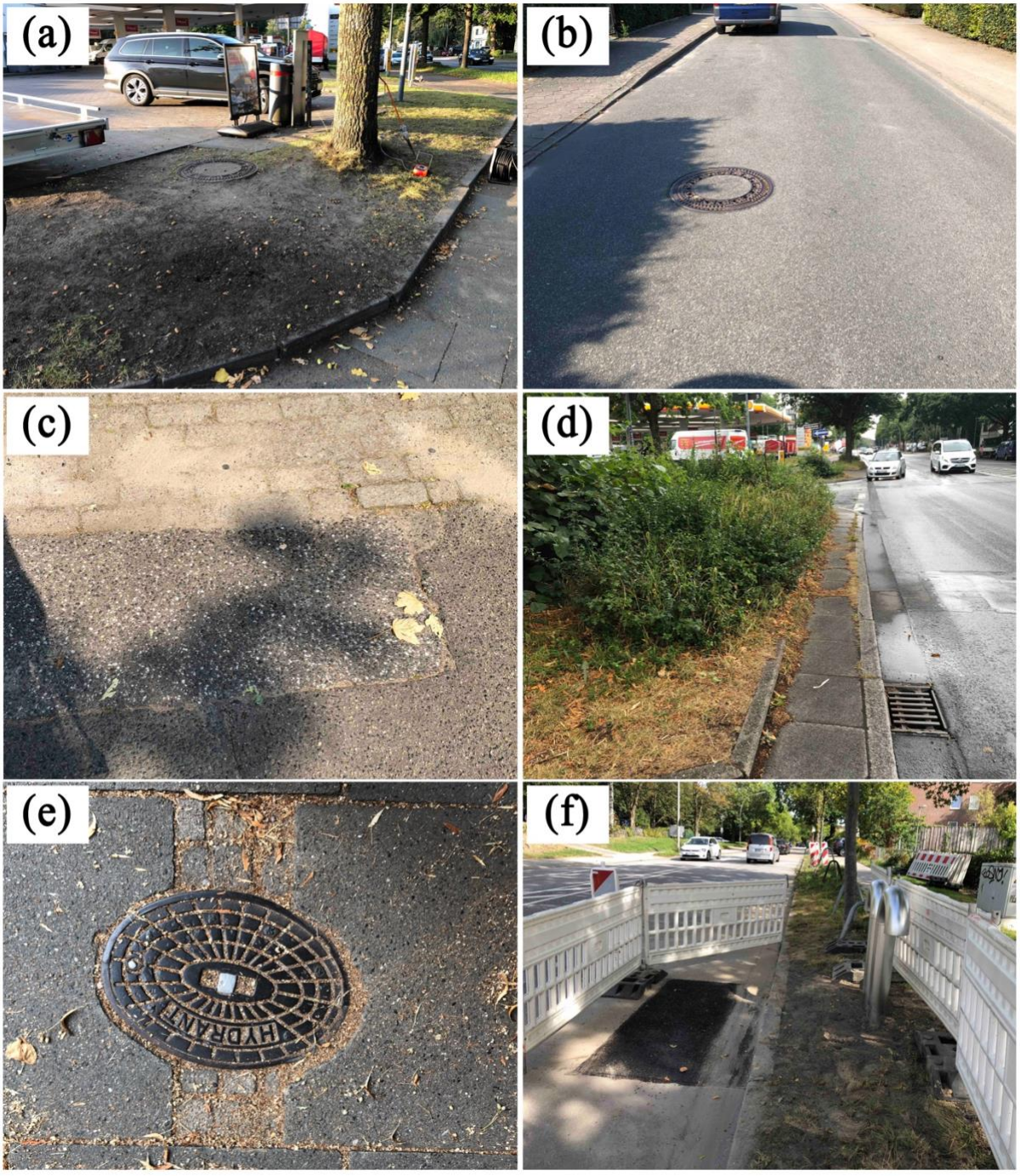

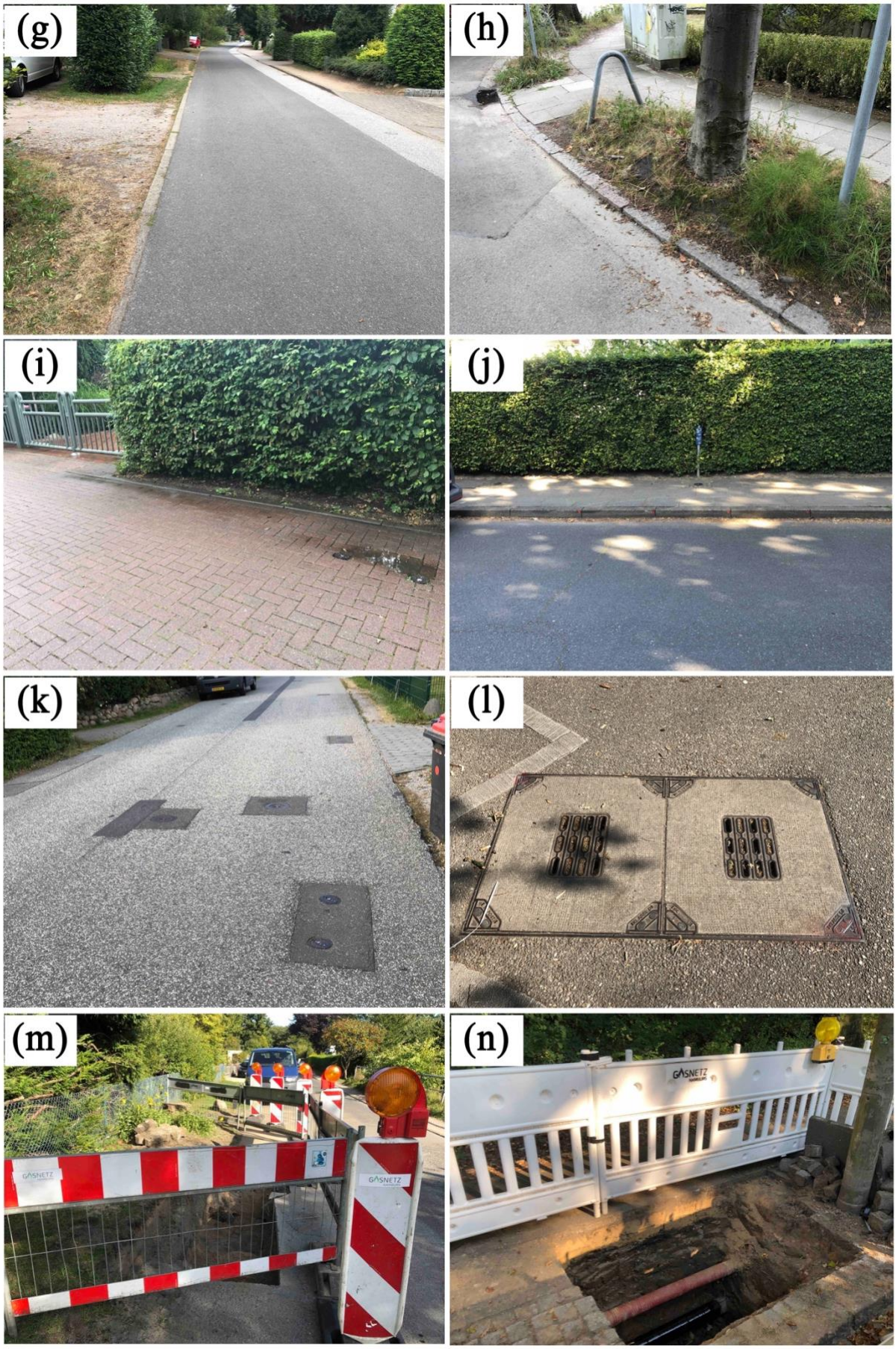

Figure 4.S1. Variety of emission outlets detected in Hamburg

4.S.3) Leak detection, confirmation and attribution

In this campaign we focused on 15 locations which were initially detected by mobile surveys and later confirmed as gas leaks by the LDC, except for 2 locations, plus 5 more locations which had been already detected by the LDC leak detection surveys. After sharing the locations with the LDC we visited the locations with the leak searching experts from the LDC (Fig. 4.S2). When a leak had been confirmed, the LDC leak searchers drilled holes (Fig. 4.S3a) and measured subsurface CH_4 volume mole fraction for each hole (Fig. 4.S3b).

For the mobile measurements, we used CO_2 and C_2H_6 signals to attribute CH_4 signals. From our past experiments (Maazallahi et al., 2020d), we concluded that combustion signals in Hamburg are mostly related to engine combustion. Microbial emissions were sometimes, but not always, also associated with CO_2 signals. We considered a microbial contribution to the observed CH_4 enhancement if the linear regression of CH_4 and CO_2 enhancements had $R^2 > 0.8$. To evaluate the CO_2:CH_4 ratio, the start and end point of CH_4 enhancements were defined when the mole fraction increased 20 ppb above background level until it dropped below the 20-ppb enhancement again. If we observed CO_2 signals associated with CH_4 and with C_2:C_1 ratio less than 10% we attributed those signals a to mixed plume of fossil and microbial emissions.

Figure 4.S2. Example of a visit at one of the locations, HH008, together with the LDC.

Figure 4.S3. Drilling holes around the surface-projected track of gas pipeline (a) and measuring the CH4 mole percentage (b) to find the gas leak location, HH008.

4.S.4) Leak quantification methods

4.S.4.1) Mobile method

Figure 4.S4. Mobile measurements vehicle.

Table 4.S2 shows an example of a location, HH001, where we performed 10 transects. For this location all the transects were accepted for the quantification (1 for accepted and 0 for denied), and on all the transects the status of the two instruments indicated proper operation (1 for running properly and 0 for malfunctions).

Table 4.S2. Example of mobile measurements transects at one of the locations.

ID	Transect No.	Transect	G2301 status	G4302 status	Date (dd.mm.yyyy)	Start_UTC (hh:mm:ss)	End_UTC (hh:mm:ss)
HH001	1	1	1	1	21.08.2020	09:24:10	09:24:35
HH001	2	1	1	1	21.08.2020	09:29:45	09:30:54
HH001	3	1	1	1	21.08.2020	09:54:43	09:55:21
HH001	4	1	1	1	21.08.2020	09:59:01	09:59:33
HH001	5	1	1	1	22.08.2020	11:44:17	11:44:47
HH001	6	1	1	1	22.08.2020	11:45:31	11:45:59
HH001	7	1	1	1	13.09.2020	13:11:34	13:12:10
HH001	8	1	1	1	13.09.2020	13:39:10	13:39:54
HH001	9	1	1	1	14.09.2020	12:52:09	12:52:39

4.S.4.2) Tracer method

Table 4.S3. Overview of all measurements performed with the tracer release method

ID	Tracer method; Mobile (M), Static (S)	Date (dd.mm.yyyy)	Time_Start (hh:mm:ss)	Time_End (hh:mm:ss)	Distance between CH_4 maxima and release point (m)	Distance of release to the leak location (m)	Wind Speed (m s^{-1})
HH001	S	23.092020	15:01:09	15:43:28	≈ 30	< 1	0.3
HH002	S	23.09.2021	13:58:42	14:30:24	≈ 40	≈ 6	0.5
HH003	S	22.09.2020	08:27:57	09:14:30	≈ 25	≈ 5	0.3
HH004	S	23.09.2020	11:53:00	12:24:05	≈ 40	≈ 5	0.6
HH005	S	20.09.2020	17:11:40	18:09:17	≈ 40	-	-
HH006	S	25.09.2020	11:22:07	11:49:41	≈ 15	≈ 3	0.5
HH007	-	-	-	-	-	-	-
HH008	M	21.09.2020	09:28:00	10:33:00	≈ 35	≈ 1	-
HH009	M	21.09.2020	13:58:00	15:56:00	≈ 43	≈ 20	0.5
HH010	M	22.09.2020	13:16:00	14:56:00	≈ 44	≈ 4	0.6
HH011	M	24.09.2020	07:54:00	08:50:00	≈ 35	≈ 64	1.95
HH012	-	-	-	-	-	-	-
HH013	-	-	-	-	-	-	-
HH014	M	20.09.2020	14:24:00	15:08:00	-	< 1	-
HH015	S	25.09.2020	09:37:33	10:18:52	≈ 20	≈ 3	0.9
HH100	S	24.09.2020	10:55:13	11:26:33	≈ 30	≈ 2	2.5
HH101	S	25.09.2020	13:55:06	14:33:36	≈ 15	≈ 4	0.6
HH102	S	24.09.2020	15:19:37	16:07:41	≈ 20	≈ 3	-
HH103	S	24.09.2020	12:19:30	13:10:51	≈ 18	< 1	-
HH104	-	-	-	-	-	-	-

Figure 4.S5. Tracer method in static mode (a) at HH004 and in mobile mode (b) at HH014.

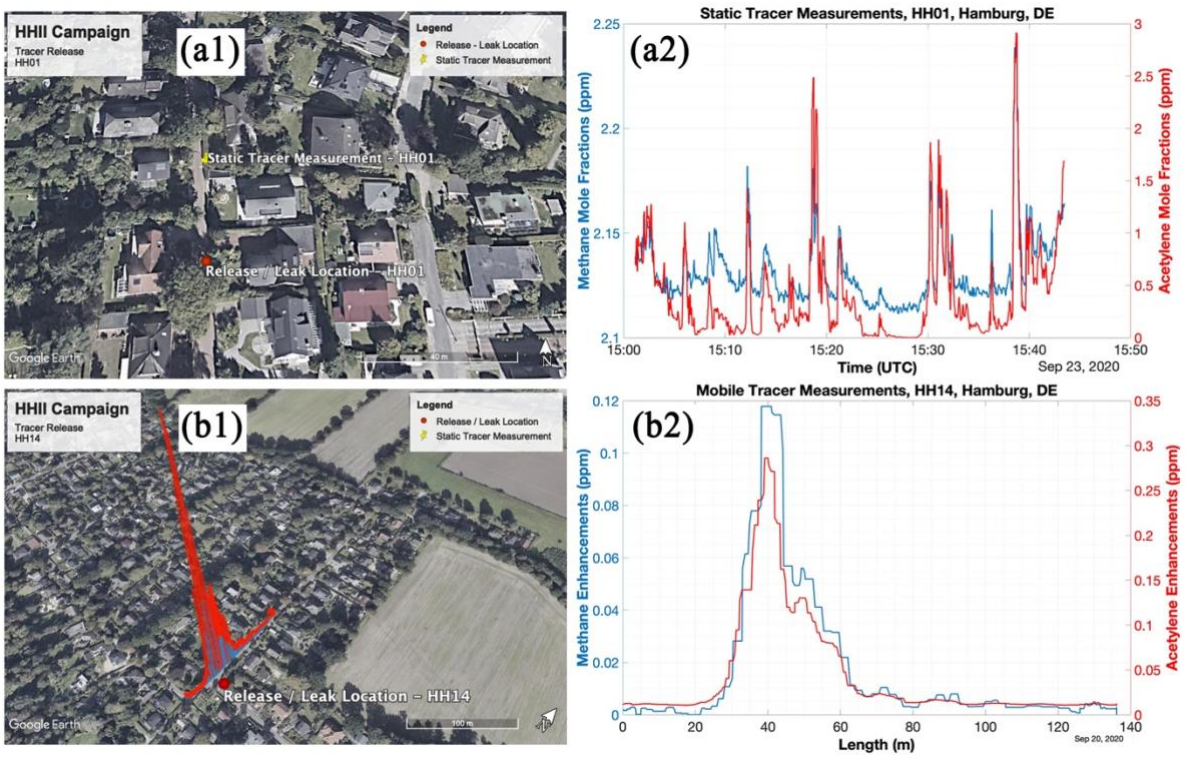

Figure 4.S6. Results from the tracer method applied in static (top panel, HH001) and mobile (bottom panel, HH014) modes, aerial images: © Google Maps.

4.S.4.3) Suction method

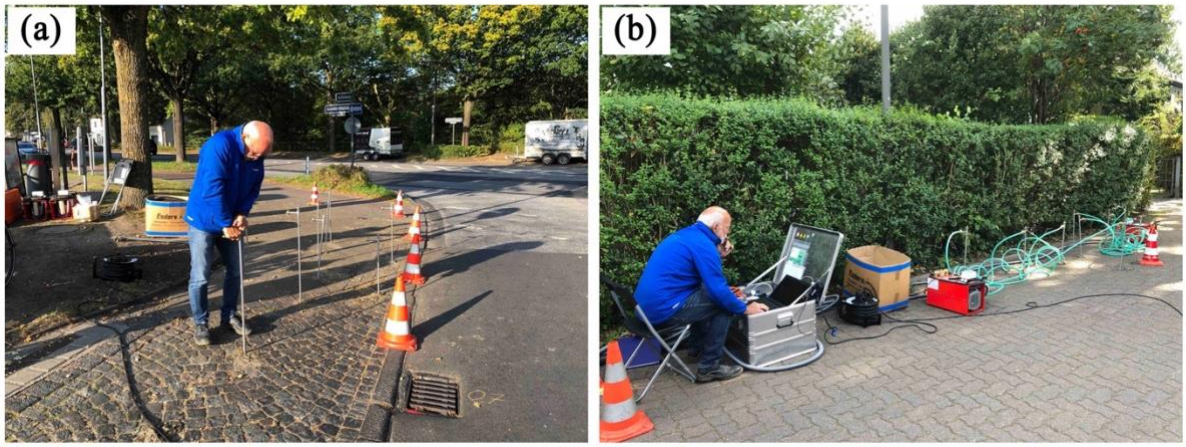

Figure 4.S7. Inserting suction probes into holes drilled above the pipeline at location HH009 (a), and quantification in action at location HH002 (b).

4.S.4.4) Gas leak quantification based on hole models

There are several models to quantify CH_4 emissions from a pipeline in open space or underground. Equation 4.S1 was developed by Ebrahimi-Moghadam either for the pipeline leaks in open space (Eq. 4.S1a) or for buried pipelines (Eq. 4.S1b). In this model, β is the ratio of hole diameter to pipeline diameter, d is the hole diameter in mm, and p is the pipeline absolute pressure in bar and Q is in $m^3\ hr^{-1}$.

$$\boldsymbol{Q} = \begin{cases} \boldsymbol{0.808 * \left(1 + \beta^4\right) * d^2 * p,} & \boldsymbol{d \leq 15\ mm} \\ \boldsymbol{0.708 * \left(1 + \beta^4\right) * d^2 * p,} & \boldsymbol{15 < d \leq 80\ mm} \end{cases} \quad \textbf{(4.S1a)}$$

$$\boldsymbol{Q} = \begin{cases} \boldsymbol{0.117 * \left(1 + \beta^4\right) * d^2 * p,} & \boldsymbol{d \leq 15\ mm} \\ \boldsymbol{0.0677 * \left(1 + \beta^4\right) * d^2 * p,} & \boldsymbol{15 < d \leq 80\ mm} \end{cases} \quad \textbf{(4.S1b)}$$

In the model from Cho et al. (2020), gas leak emission rates depend on soil properties, which vary spatially and temporally due to weather conditions. Importantly, precipitation increases soil water content and blocks gas pathways through the soil, which results in decreasing gas leak emissions to the atmosphere. On the other hand, emissions from a pipeline leak can dry the above soil layer and generate cavities and gas transport channels, which result in temporarily higher emission rates to the surface compared to rates at the leak (Bonnaud et al., 2018). When comparing results from the suction method, which quantifies underground pipeline leakages, to the mobile and tracer methods, which quantify the emissions into the atmosphere, we make the implicit assumption that the emission is in steady state. With this assumption, the different methods can be compared without considering impact of soil conditions. Note that in this study, the weather was mostly dry with few rainy days in August 2020.

4.S.5) Gas leak detection and quantification methods overview

In theory, emissions from different sources can occur at the same surface location, e.g., at a manhole, and overlap. For combination of fossil and microbial sources, the mixture of fossil with microbial gas would lead to a reduction in the C_2:C_1 ratio which also leads to an overestimate of fossil emissions if the mixture was exclusively attributed to gas leak sources. We attempted to use the C_2:C_1 ratio for a possible correction, but the G4302 instrument showed day-to-day variability even when measuring gas from a cylinder on different days, so we consider this approach not reliable. This is because for the purpose of separating a possible contribution of emission from a microbial source at a

specific location in mobile method, it is necessary to quantify reliably small percentage differences from the ratio reported by the LDC in the analysis.

4.S.5.1) Detection and attribution of locations

We used two methods to report the C_2:C_1 ratio, the single point and the linear method. The single point method calculates the C_2:C_1 ratio from only the maximum of C_2H_6 and CH_4, while the linear method determines the correlation of multiple points of C_2H_6 and CH_4 in a plume. The distance to the leak locations were determined using the location of CH_4 enhancement maxima during the mobile method to the leak location reported by the LDC.

Table 4.S4. Attribution of individual plumes from mobile measurements using C_2H_6 and CO_2 signals.

ID	Leak observation probability (%) from the car based on C_2:C_1 (%)		Attribution at outlet			Leak confirmed by the LDC; Yes (Y), No (N)	CO_2 attribution for transects with CH_4 enhancements > 10%		
	Point method	Linear method	C_2:C_1 (%)	Distance to the leak (m)	Max CH_4 (ppm) (Outlet type)		Transects with CO_2 observ.	CH_4:CO_2 (ppb ppm^{-1})	CO_2 Enhance. (ppm)
HH001	30	0	4.0 – 5.8	≈ 3	≈ 25 (Straight from ground)	Y	0 out of 1	-	-
HH002	60	50	3.4 – 5.3	≈ 3	≈ 230 (Straight from ground)	Y	1 out of 5	240	11
HH003	83	50	2.3 – 3.1	3 - 20	>> 1000 (Tele. cover)	Y	2 out of 6	275 and 180	113 and 8
HH004	75	75	1.5 – 3.5	4 - 17	>> 1000 (Tele. cover)	Y	0 out of 4	-	-
HH005	60	30	1.4 – 5.9	5 - 27	≈ 870 (manhole)	Y	1 out of 19	0.8	260
HH006	40	17	3.0 – 5.2	4 - 33	435 (Curb cracks)	Y	1 out of 11	370	3
HH007	14	0	- ($R^2 < 0.7$)	- (Not confirmed)	4.4 (Pavement cracks)	N	-	-	-
HH008	44	9	4.8 – 6.2	≈ 4	≈ 930 (Hydrant cap)	Y	0 out of 6	-	-
HH009	38	13	1.3 – 4.5	2 - 35	≈ 800 (Rain drain)	Y	1 out of 9	19	235
HH010	38	0	2.3 – 2.4	≈ 2	≈ 65 (Hydrant cap)	Y	0 out of 3	-	-
HH011	38	0	1.9 – 2.8	≈ 60	≈ 70 (Rain drain)	Y	0 out of 4	-	-
HH012	0	0	4.2	- (Not confirmed)	7.3 (Manhole)	N	-	-	-
HH013	40	20	2.6 – 5.0	≈ 15	11.5 (Straight from ground)	Y	0 out of 2	-	-
HH014	55	41	2.3 – 7.2	0 - 11	>> 1000 (Asphalt holes; LDC)	Y	1 out of 24	4000	1.5
HH015	83	33	6.0 – 6.9	≈ 5	> 1000 (Curb cracks)	Y	0 out of 1	-	-
HH100	13	0	1.3 – 2.0	≈ 8	15 (Gas cap)	Y	0 out of 1	-	-

HH101	33	0	2.5	≈ 3	25 (Asphalt holes; LDC)	Y	-	-	-
HH102	33	0	2.2	≈ 1	55 (Asphalt holes; LDC)	Y	-	-	-
HH103	43	0	- ($R^2 < 0.7$)	≈ 1	8 (Asphalt holes; LDC)	Y	-	-	-
HH104	40	0	- ($R^2 < 0.7$)	≈ 1	45 (Asphalt holes; LDC)	Y	-	-	-

4.S.5.1) Quantifications of locations

Table 4.S5. Measurement overview of the mobile, tracer and suction methods.

ID	Mobile method						Tracer method			Suction method	
	Measurements status; Complete (CPLT)	Number of Transects			Driving Speed (m s^{-1})	Min. driv. track dist. to leak loc. (m)	Measurements status Complete (CPLT)	Release location Right (R), Wrong (W), Questionable (Q)	Acetylene release rate (L min^{-1})	Measurements status; Complete (CPLT), Incomplete (INC)	Pumping rate (L min^{-1}) - time (hr)
		All	Accepted								
			with G2301	with G4302							
HH001	CPLT	10	10	10	3.5±0.8	2.7±1.8	CPLT	R	1.8	INC	-
HH002	CPLT	10	10	10	3.7±0.8	2.4±2.2	CPLT	R	1.8	INC	380 - 6
HH003	CPLT	7	7	6	2.5±2.0	3.0±1.3	CPLT	R	1.6	-	-
HH004	CPLT	4	4	4	1.3±1.1	5.7±2.3	CPLT	Q	1.5	-	-
HH005	CPLT	40	37	37	1.3±1.0	5.5±6.2	CPLT	R	1.5	-	-
HH006	CPLT	31	28	30	3.9±2.0	7.8±7.8	CPLT	Q	2.1	CPLT	345 - 7
HH007	CPLT	8	7	7	2.2±0.7	7.3±3.9	-	-	-	-	-
HH008	CPLT	23	23	23	5.1±3.0	9.3±8.2	CPLT	R	1.3	INC	370 - 10
HH009	CPLT	25	24	24	8.4±4.0	30±14	CPLT	W	1.8	INC	-
HH010	CPLT	8	8	8	3.3±2.0	12±9.7	CPLT	R	1.6	INC	400 - 7
HH011	CPLT	8	8	8	5.9±2.0	25±6.3	CPLT	W	1.4	-	-
HH012	CPLT	4	3	3	5.6±3.0	2.8±1.2	-	-	-	-	-
HH013	CPLT	5	5	5	3.9±2.0	3.2±1.8	-	-	-	-	-
HH014	CPLT	44	44	44	2.7±1.0	13±5.9	CPLT	R	2.3	-	-
HH015	CPLT	6	2	6	3.4±0.8	2.9±1.6	CPLT	R	1.4	INC	380 - 9.5
HH100	CPLT	8	8	8	3.4±3.0	3.3±4.1	CPLT	R	2.6	-	-
HH101	CPLT	6	6	6	3.1±2.0	2.8±1.0	CPLT	R	2.1	INC	240 - 9
HH102	CPLT	6	6	6	8.7±1.0	3.3±1.8	CPLT	R	2.6	-	-
HH103	CPLT	7	7	7	2.3±1.0	3.4±1.0	CPLT	R	1.3	-	-
HH104	CPLT	5	5	5	1.8±1.0	2.4±2.2	-	-	-	-	-

4.S.6) Gas leak influence on urban vegetation

Increased soil CH_4 content can also adversely influence vegetation. Methanotrophs oxidize CH_4 which lowers the soil oxygen content and consequently impacts soil quality and urban vegetation health (Schollaert et al., 2020). We observed on several occasions that the vegetation, especially trees, next to the leak locations were affected by the presence of a gas leak in proximity. Fig. 4.S12 shows two examples from HH004 and HH010 where trees were affected by gas leaks.

Figure 4.S8. Example of unhealthy trees (red box) affected by gas leaks in close vicinity, HH004 (a) and HH010 (b)

4.S.7) Leak localization

Figure 4.S9. The LDC reported 6 leaks on the pipeline at this location with total leak area of 5 cm^2, HH013.

4.S.8) Comparison of two CRDS instruments, G2301 and G4302

4.S.8.1) Comparison of maximum CH_4 enhancements and plume area

Fig. 4.S10 shows the comparison of the maximum CH_4 enhancement recorded during individual transects (Fig. 4.S10a) and the integrated peak area (Fig. 4.S10b) between the two different instruments, G2301 and G4302, which both sampled air from the same inlet at the front bumper.

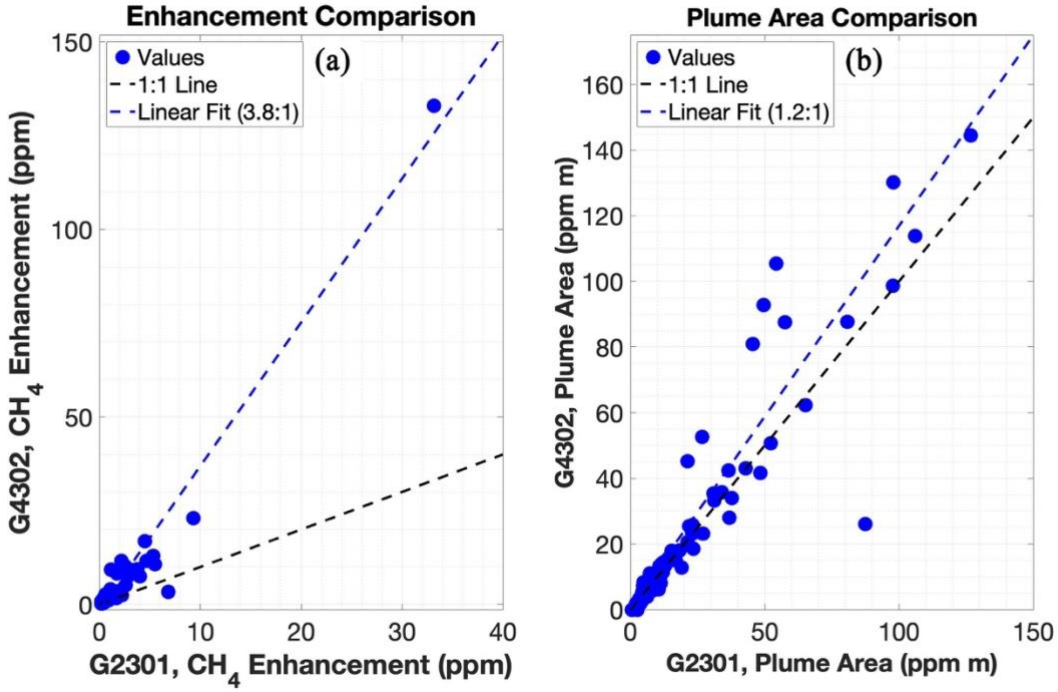

Figure 4.S10. Comparison between maximum CH4 enhancements (a) and plume areas (b) from two different instruments, G2301 and G4302.

4.S.8.2) Detection of leak indications with two instruments

In Table 4.S6, observations carried out with the G2301 and G4302 instruments are compared. It is shown that the probability of identifying a CH_4 leak indication with the G4302 is generally higher than for the G2301. This is because CH_4 enhancements on the G4302 is 3.8 times higher than enhancements on the G2301 (Fig. 4.S10a).

Table 4.S6. Observation comparison of CH_4 enhancements from G2301 and G4302.

	ID	**G2301** flowrate of ≈ 0.2 L min^{-1} Sampling frequency of ≈ 0.3 Hz Cell size of 35 mL		**G4302** flowrate of ≈ 2.2 L min^{-1} Sampling frequency of ≈ 1 Hz Cell size of 35 mL	
		Transect (s) w/ CH_4 Enh. > 10% threshold	Transects where the G2301 was in operation	Transect (s) w/ CH_4 Enh. > 10% threshold	Transects where the G4302 was in operation
Detected by mobile method	HH001	n = 1 (10%)	n = 10	n = 6 (60%)	n = 10
	HH002	n = 5 (50%)	n = 10	n = 5 (50%)	n = 10
	HH003	n = 6 (86%)	n = 7	n = 6 (100%)	n = 6
	HH004	n = 4 (100%)	n = 4	n = 4 (100%)	n = 4
	HH005	n = 19 (51%)	n = 37	n = 25 (68%)	n = 37
	HH006	n = 11 (39%)	n = 28	n = 17 (57%)	n = 30

	HH007	n = 0 (0%)	n = 7	n = 1 (14%)	n = 7
	HH008	n = 6 (26%)	n = 23	n = 9 (39%)	n = 23
	HH009	n = 9 (38%)	n = 24	n = 10 (42%)	n = 24
	HH010	n = 3 (38%)	n = 8	n = 3 (38%)	n = 8
	HH011	n = 4 (50%)	n = 8	n = 7 (88%)	n = 8
	HH012	n = 0 (0%)	n = 3	n = 1 (33%)	n = 3
	HH013	n = 2 (40%)	n = 5	n = 4 (80%)	n = 5
	HH014	n = 24 (55%)	n = 44	n = 27 (61%)	n = 44
	HH015	n = 1 (50%)	n = 2	n = 6 (100%)	n = 6
Reported by LDC	HH100	n = 1 (13%)	n = 8	n = 4 (50%)	n = 8
	HH101	n = 0 (0%)	n = 6	n = 0 (0%)	n = 6
	HH102	n = 0 (0%)	n = 6	n = 1 (17%)	n = 6
	HH103	n = 0 (0%)	n = 7	n = 2 (29%)	n = 7
	HH104	n = 0 (0%)	n = 5	n = 0 (0%)	n = 5

4.S.8.3) Emission quantification comparisons

Table 4.S7. Emission quantification comparison with two different instruments. The G2301 is similar to the instrument that was used to derive the conversion equation (Eq. 4.1 in the main manuscript, Weller et al, 2019). The G4302 has a much shorter sample exchange time of the measurement cell, therefore, higher enhancements, which translate to higher emission rates if the same conversion equation (Eq. 4.1) is used for quantification.

	ID	**G2301** flowrate ≈ 0.2 L min^{-1} Sampling frequency of ≈ 0.3 Hz Cell size of 35 mL		**G4302** flowrate ≈ 2.2 L min^{-1} Sampling frequency of ≈ 1 Hz Cell size of 35 mL	
		Emission ave. (L min^{-1})	Emission range (L min^{-1})	Emission ave. (L min^{-1})	Emission range (L min^{-1})
Detected by mobile method	HH001	0.7	-	0.8	0.5 – 1.3
	HH002	4.9	0.7 – 35.1	14.8	3.3 – 67.6
	HH003	7.5	1.4 – 243.5	9.4	0.9 - 1300
	HH004	7.8	2.6 – 22.1	18.1	5.9 – 67.8
	HH005	1.8	0.5 – 51.5	3.3	0.5 – 155.8
	HH006	1.2	0.7 – 5.9	1.7	0.6 – 12.2
	HH007	-	-	0.6	-
	HH008	1.5	0.5 – 16.9	2.5	0.6 – 52.1
	HH009	3.9	0.5 – 21.2	5.9	0.6 – 106.6
	HH010	1.6	0.6 – 2.9	2.8	1.6 – 3.8
	HH011	1.9	0.5 – 14.8	2.0	0.8 – 50.4
	HH012	-	-	0.9	-
	HH013	1.8	1.1 – 3.0	2.6	0.8 – 12.8
	HH014	1.6	0.5 – 27.0	3.1	0.5 – 61.5
	HH015	1.0	-	1.6	0.9 – 3.3
Reported by GNH	HH100	0.7	-	1.0	0.7 – 1.2
	HH101	-	-	-	-
	HH102	-	-	0.5	-
	HH103	-	-	0.8	0.7 – 0.9
	HH104	-	-	-	-

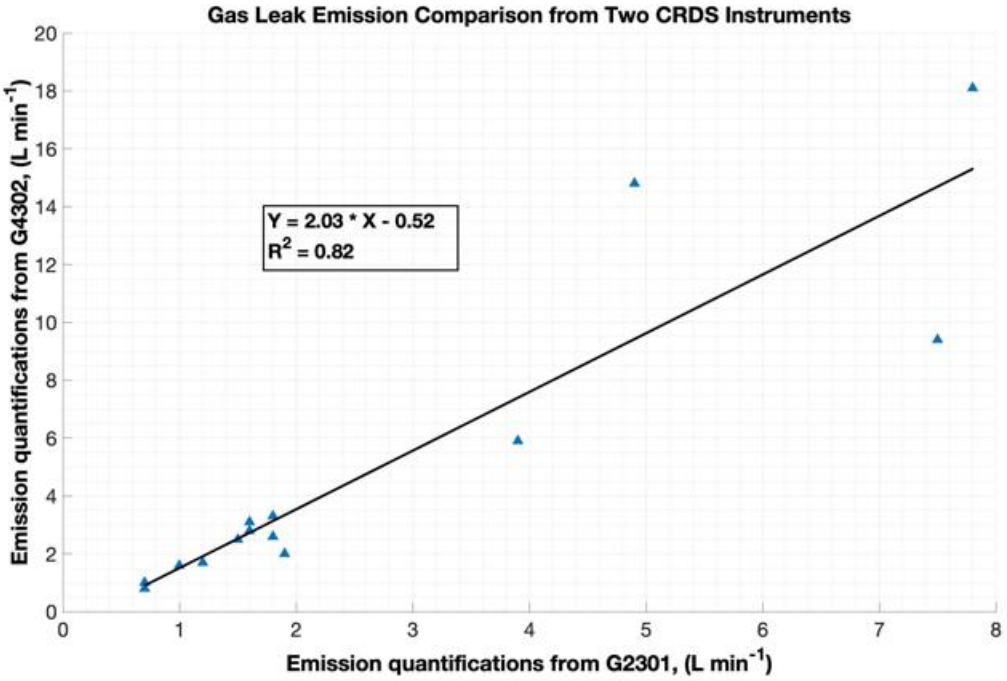

Figure 4.S11. Emission comparison between the two CRDS instruments, G2301 and G4302, onboard the mobile measurement vehicle.

4.S.9) Impact of distance on the enhancements

Since emission plumes dilute as they disperse through the atmosphere, we expected that the closer the air intake is to the emission point the higher CH_4 enhancements are recorded. Fig. 4.S12 shows the maximum enhancement of individual transects as a function of distance from the actual leak location. The highest CH_4 maxima are observed within 15 to 20 m to the leak locations.

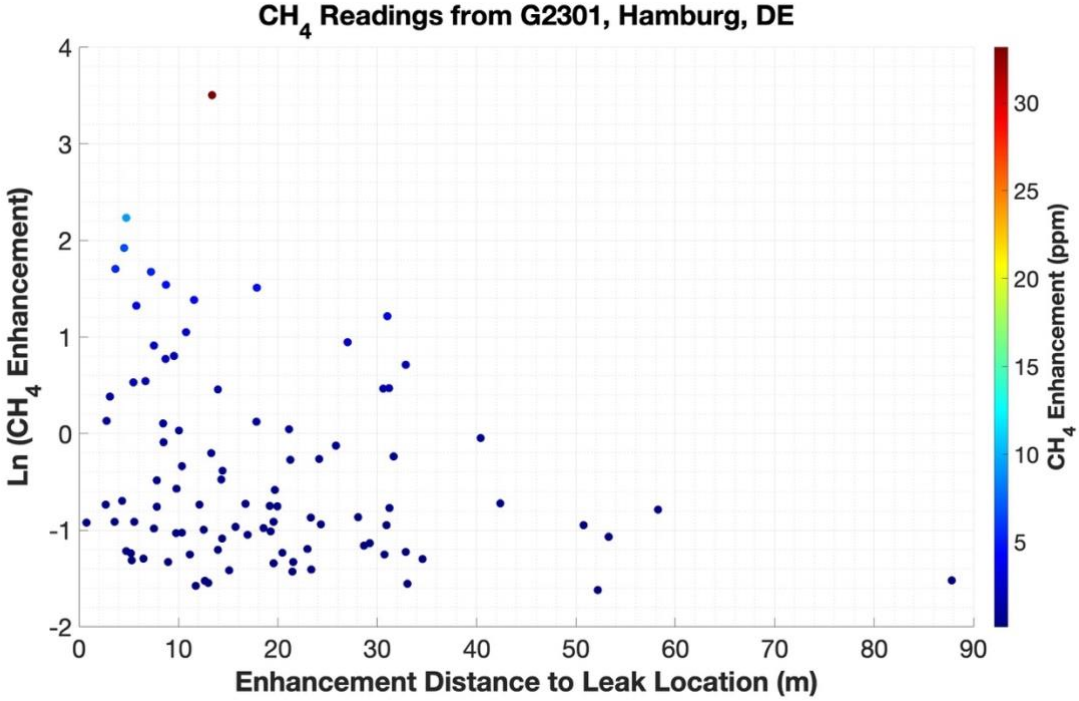

Figure 4.S12. Impact of distance on the measurements during mobile measurements.

4.S.10) Use of 10% or 10 ppb threshold

Table 4.S8. Emission estimate for the C_2H_2 release rate from 5 mobile quantifications in the tracer release technique. These were evaluated a) with the original 10% (≈ 200 ppb) threshold and b) with a 10 ppb threshold. The lower threshold was still applied in order to exclude transects where the plume is completely missed.

ID	10% threshold		10 ppb threshold		C_2H_2 actual release rate (L min^{-1})
	C_2H_2 release estimate (L min^{-1})	Distance (m)	C_2H_2 release estimate (L min^{-1})	Distance (m)	
HH008	0.88 (n = 4)	35.5 ± 7.1	0.30 (n = 14)	33.6 ± 4.9	1.29
HH009	0.71 (n = 1)	43.4 ± 30.0	0.05 (n = 16)	49.9 ± 30.0	1.78
HH010	1.51 (n = 10)	44.3 ± 19.7	0.06 (n = 26)	48.0 ± 17.7	1.55
HH011	0.64 (n = 5)	34.5 ± 7.2	0.15 (n = 22)	36.9 ± 9.4	1.38
HH014	2.42 (n = 10)	-	0.86 (n = 16)	-	2.29

4.S.11) Descriptions of locations that were not described in detail in the main text

4.S.11.1) HH003

HH003 was at a T-junction of two streets, each of them was about 6 m wide. We detected several outlets with CH_4 signals from which we could also observe C_2H_6 signals. The street cover on this location was asphalt. A ≈ 1.5 m stroke with trees separated pavements from streets on both sides. We accepted 7 transects from the mobile measurements for the quantification. The tracer team quantified this location using in static mode ≈ 25 m downwind the release point. The leak had to be fixed immediately after confirmation by the LDC and the suction method could not be applied.

On-foot measurements across the T-junction with the G4302 instrument indicated that emissions from gas leak (s) were mostly released out of four major outlets, including direct emissions from the soil next to a tree, from a manhole, asphalt cracks in the middle of the T-junction and a telecommunication cover. The C_2:C_1 ratio was highest at the telecommunication cover (3.1%, R^2 = 0.91 and max CH_4 reading of >1000 ppm). The ratio of C_2:C_1 next to the tree was 2.4% (R^2 of 0.92 and max CH4 reading of ≈ 22 ppm) with air intake of ≈ 5 cm distance from the soil. The air intake from the asphalt cracks in the middle of the T-junction showed a C_2:C_1 ratio of 2.3% (R^2 of 0.85 and maximum CH_4 reading of ≈ 17 ppm). From the manhole, C_2H_6 signals were observable but the R^2 of the C_2:C_1 linear regression was below 0.7, however CH_4 mole fraction reading went up to of ≈ 27 ppm.

Emission quantification for this location from the mobile measurement method based on the 6 transects with CH_4 enhancement maxima above the 10% threshold on the G2301 was 7.5 L min^{-1}. For HH003, based on the first field assessment, the leak location was assumed to be next to a tree at the T-junction, and the C_2H_2 release was performed with a release rate of 1.55 L min^{-1}. HH003 was listed as type A1 leak by the LDC. The pipeline was DN100ST and in operation since 1963, and the latest inspection of this pipeline was in 2019. The pipeline at this location was replaced completely, 34 m.

4.S.11.2) HH004

At the end of an almost circular dead-end, 15 m diameter turning bay covered with asphalt, we detected numerous outlets with clear fossil C_2:C_1 ratio (Fig. 4.1). The turning bay was surrounded by grass and trees and then residential buildings. We found CH_4 and C_2H_6 signals in numerous manholes, rain drains, telecommunication covers, curb cracks and asphalt cracks. As this location was located at a dead-end location, normal driving conditions could not be applied, and after data quality check we considered 4 transects for quantification.

We identified numerous outlets in a circular area with diameter of ≈ 30 m. The maximum CH_4 mole fractions were observed at the telecommunication cover (>> 1000 ppm) which was ≈ 17 m away from the leak location and showed C_2:C_1 ratios of 2.6% (R^2 of 0.99) and 3.3% (R^2 of 0.90) on two different days. Two rain drains which were about 3.8 m and 6.9 m far from the leak location showed C_2:C_1 ratios of 1.5% (R^2 of 0.97, CH_4 maximum 69 ppm) and 2.2% (R^2 of 0.98, CH_4 maximum 110 ppm). The closest outlets with the highest C_2:C_1 ratios of 3.5% (R^2 of 0.99) were several curb cracks, ≈ 5.9 m away from the leak location, and the maximum CH_4 mole fraction at 2-5 cm distance from these cracks was ≈ 30 ppm.

All of the four transects showed CH_4 enhancement higher than 10% above background level. The emission rate derived from mobile measurements was 7.8 L min^{-1} (95% confidence range: 1.8 – 34.5 L min^{-1}). At HH004, the static tracer method was applied ≈ 50 m downwind the release point and an emission rate of 5.3 L min^{-1} was derived. We note that the application of the tracer method is uncertain at this location due to the presence of several outlets, which would qualify the emission rate estimate as a lower limit. Nevertheless, despite the challenging location, at HH004 there was a good agreement of the two "above ground" emission rate estimates, confirming the existence of a relatively large leak. Unfortunately, the suction method could not be applied at HH004 because of the widespread CH_4 soil accumulation in close vicinity to residential buildings, so this leak (category A1) had to be fixed immediately.

4.S.11.3) HH005

In the beginning of a ≈ 4.5 m wide street, we observed CH_4 and C_2H_6 signals on several days. In total we had 37 accepted transects for this location from the mobile measurement. The street cover was asphalt with two soil-covered pavements on each side, one was ≈ 2.5 m wide and the other one was ≈ 1 m wide. The houses at this location had front yards, some were separated from street with bushes but there were not big trees around the leak area. Comparing to other locations like HH003, this location was not very confined with buildings. The LDC reported three leaks over a ≈ 30 m distance of the street, and we used the average latitude and longitude coordinates as the representative location for this location. We identified several outlets at this location and considered the "strongest" outlet as the main emission point. The tracer team applied static quantification and due to time constraint, suction team could not be deployed at this location.

Several outlets along about 30 m segment of the street were identified as fossil emitting points including two manholes rain drains and curb cracks. There was a manhole in the middle and another one at the pavement. The manhole in the middle of the road which was ≈ 5.5 m far from the representative location of the leak showed C_2:C_1 ratios of 2.0% (R^2 of 0.8, max CH_4 of ≈ 29 ppm), 3.1% (R^2 of 0.88 and max CH_4 of ≈ 890 ppm), 4.6% (R^2 of 0.99 and max CH_4 of ≈ 20 ppm) and 3.3% (R^2 of 0.92 and max CH_4 of ≈ 16 ppm) on different days. The other manhole located on the pavement which was ≈ 9.5 m far from representative leak location showed C_2:C_1 ratios of 3.6% (R^2 of 0.98 and max CH_4 of ≈ 67 ppm) and 2.4% (R^2 of 0.98 and max CH_4 of ≈ 9 ppm) on two different days. There were many different curb cracks. Some examples: At 9.5 m distance to the representative leak location with C_2:C_1 of 4.1% (R^2 of 0.91, max CH_4 of ≈ 60 ppm), 7 m far from the representative location with C_2:C_1 ratio of 1.4% (R^2 of 0.85 and max CH_4 of ≈ 100 ppm), at a distance of ≈ 5 m with C_2:C_1 ratio of 4.8% (R^2 of 0.97 and max CH_4 of ≈ 320 ppm) and the other location at distance of ≈ 6 m and C_2:C_1 ratio of 5.9% (R^2 of 0.96 and max CH_4 of ≈ 170 ppm). Fossil emissions were also observed from three rain drains with C_2:C_1 ratios of 4.6% (R^2 of 0.98, distance of 26 m and max CH_4 of ≈ 110 ppm) 5.6% (R^2 of 0.99, distance of 12 m and max CH_4 of ≈ 100 ppm) and 5.3% (R^2 of 0.98 distance of 23 m and max CH_4 of ≈ 720 ppm).

From the 20 transects, out of 37 transects, which showed CH_4 mole fraction more than 10% above background level on G2301, the leak rate was estimated 1.8 L min^{-1} from mobile method. The tracer method was applied for this location with C_2H_2 at the "strongest" emission location. CH_4 and

C_2H_6 plumes were measured in static mode at 40 m. The emission rate derived for this location from the tracer method was 0.2 L min^{-1} from the tracer method. All the three leaks found at this location were categorized as A2, on DN80ST pipeline, and happened due to corrosion. The reported leak areas were ≈ 1 cm^2 for one and ≈ 5 cm^2 for the other two leaks. For the two leaks with leak area of ≈ 5 cm^2, 6 - 7 m segments of the pipeline were replaced. The emission estimates for the smaller hole were 19 L min^{-1} and 39 L min^{-1} for the bigger holes from the hole model.

4.S.11.4) HH006

About 25 m from a T-junction, we found strong signals mainly coming out of street curbs and also from some of the gaps between pavement bricks. The asphalt street was ≈ 5 m wide with a ≈ 1 m pavement on one side and several trees close to each other on the other side. For this location the LDC reported two leaks, one of the leaks was in the middle of the T-junction and the other one was ≈ 25 m far away. The first one was repaired during the campaign, but we could still detect signals after the repair. After revisits with the LDC, we detected the second leak, and we assume that the second leak was there for the whole period. Bush walls existed on both side of the street. Mobile measurements performed 28 transects on this location. The tracer method was applied in static mode for this location. The suction method could quantify this location completely. Both tracer and suction methods were applied to the second leak as the first leak had been already fixed.

The highest CH_4 mole fraction was observed from the street curbs with ratio of 5.2% (R^2 of 0.92 and max CH_4 of ≈ 440 ppm). C_2:C_1 ratio from the pavement cracks with air inlet of 2-5 cm above ground level was 4.9% (R^2 of 0.78 and max CH_4 reading of ≈ 110 ppm). We also observed C_2:C_1 ratio of 3.3% (R^2 of 0.9 and max CH_4 reading of 3.8 ppm) from two manholes very close to each other (≈ 1 m) but about 25 m far from the leak location. The manholes were closer to the first leak location, but we could still observe C_2H_6 and CH_4 signals even after repair of the first leak.

The emission rate estimate from the mobile measurements at this location was 1.2 L min^{-1}. This includes signals from 11 transects (out of 28) which showed CH_4 mole fraction maxima above the 10% threshold on the G2301 instrument. The tracer method was applied in static mode at ≈ 15 m distance from the leak location. The emission rate of 0.02 L min^{-1} was derived from the tracer method. The suction method was applied for this location successfully and the emission estimated emission rate was ≈ 0.3 L min^{-1}.

The first leak was classified as A1 and had to be repaired immediately and the second leak was classified as B. The pipeline of the first leak was documented as DN80ST while the pipeline of the second leak was bigger with code DN100ST. Both pipelines were steel and dated back to 1934. The leaks on both locations were due to corrosion. The first leak had ≈ 0.5 cm^2 area while the second leak had ≈ 2 cm^2 leak area, which respectively were translated to 12 L min^{-1} and 33 L min^{-1} from the hole method.

4.S.11.5) HH009

On a T-junction of a 6 m wide street and a bigger road next to a fuel station we found several outlets. On both sides of the smaller street, there were ≈ 2 m wide pavements. Based on the visit together with the LDC, initially "two" leak locations were indicated with ≈ 20 m distance from each other, but later after opening the ground no leak evidence was found at one of the locations. So, for this location the actual leak location was about 20 m north of the T-junction into the smaller road. The bigger road was ≈ 15 m wide at the T-junction and it was a two-way street with heavier traffic than the one-way and smaller street. Both streets had an asphalt surface. In the southeast corner of the T-junction there was a gas station and on the northwest corner of the T-junction there were some shops and a 3 - 4 m wide pavement. Next to the leak, there was a tree and no vegetation was present. We detected emissions mainly from two rain drains, a manhole and pavement cracks next to the wrongly assigned leak location. At this location, the mobile measurement was applied, the tracer method was also applied at the initially assumed leak location and the suction method was applied for one day at the first location but in the

second day on the second location (≈ 20 m far from the first location) where the LDC found the actual leak location. As this location showed several outlets far from each other, similar to one other location (HH011), we included all CH_4 enhancements within 100 m radius of the leak location.

On-foot measurements of outlets at this location showed that major emissions were released to the atmosphere through two gullies, ≈ 11 m apart, on two sides of smaller street, a manhole and some cracks on pavement. The C_2:C_1 ratio from the gully closest to the leak (≈ 2 m) was 4.5% (R^2 of 0.93 with max CH_4 of ≈ 800 ppm) and 3.3% (R^2 of 0.31 and max CH4 of ≈ 360 ppm) on two different days. The C_2:C_1 ratio from the other gully (≈ 13.5 m far from the leak) was 2.4% (R^2 of 0.92 and max CH_4 of 18 ppm) and 2.5% (R^2 of 0.92 with max CH_4 of ≈ 280 ppm) on two different days. The C_2:C_1 ratio from the manhole with ≈ 4.5 m distance to the leak was 3.1% (R^2 of 0.84 and max CH_4 of ≈ 730 ppm). The C_2:C_1 ratio from the pavement cracks was 1.3% (R^2 of 0.7 with max CH_4 of ≈ 16 ppm).

Based on the CH_4 enhancements from 9 transects which showed enhancements more than 10% above background level on the G2301 instrument, the emission rate estimate from the mobile method was 3.9 L min^{-1}. For HH009, the tracer method was applied in mobile mode, and the CH_4 emission rate estimate for this location from the tracer method was 4.9 L min^{-1}. The suction method estimated an upper-limit emission rate of 3 L min^{-1} for this location based on incomplete measurements. The LDC classified the leak at this location as A1 category from a DN80ST pipeline which was installed in 1928.

4.S.11.6) HH010

On a ≈ 4.5 m wide one way street, we detected signals of gas leak (s). On both side of the street there were about 2 – 3 m wide pavements with trees on both sides. Buildings were separated by small gardens from the pavements. On the east side of the street, there was no gap between side-to-side houses, while on the west side of the street, there was a recreational area with a line of trees. The fossil signals were detected mainly from a hydrant cap and bare soil next to a tree. The street cover was asphalt and pavement the was covered with cobblestones. The hydrant and tree were about ≈ 1 m far apart.

Emissions from the hydrant showed signals with C_2:C_1 ratio of 2.4% (R^2 of 0.77 and max CH_4 mole fraction of 20 ppm) and signals from bare soil next to a tree, ≈ 1m far from the hydrant cap, showed a C_2:C_1 ratio of 2.3% (R^2 of 0.94 and max CH_4 mole fraction of 65 ppm).

Based on the three CH_4 enhancements which were more than 10% above background level on the G2301, the CH_4 emission rate for this location was estimated 1.6 L min^{-1}. The tracer method was applied in mobile mode and estimated an emission rate of 0.5 L min^{-1}. The suction method reported an emission rate of 0.7 L min^{-1} for this location. This location was classified as type C leak location. The pipeline was DN200ST and dated back to 1937. Pipeline overpressure is 30 – 60 mbar. Due to presence of a large tree it was not possible to dig at the assumed leak location and 30 m of pipeline was replaced.

4.S.11.7) HH012

On a 6-m wide and two-way street, we found a manhole which showed CH_4 and C_2H_6 signals on some days but not on the other days. The leak detection expert from the LDC didn't confirm any leak in the vicinity of this outlet which was similar to the situation of HH007. We had 3 accepted transects for this location from mobile measurements, but we didn't apply the tracer and suction methods as the gas leak on this location was not confirmed.

On-foot measurements with G4302 showed C_2:C_1 ratio of 4.2% (R^2 of 0.82) with max CH_4 mole fraction of 7.3 ppm from the manhole.

None of the CH_4 signals from G2301 were above the 10% threshold, so it is not possible to quantify the emission rate for this location from mobile measurements with the standard approach. The tracer and suction methods were not applied at this location as no gas leak was confirmed from the LDC surveys.

4.S.11.8) HH013

On a ≈ 3-m wide street we detected signals of gas leak emissions. On both sides of the street there were pavements with bare soil, and on the side where we also detected signals there were some shallow canals (≈ 0.5 m deep). Very few trees grew on each side of the street and houses were separated by short bushes from the street.

We performed several transects at this location, but before applying the tracer or suction method the gas leak had been found by routine surveys of the LDC independently and was fixed before applying suction or tracer methods.

On-foot surveys of the area with the G4302 showed a C_2:C_1 ratio of 5.0% (R^2 of 0.85 and max CH_4 mole fraction of 5.8 ppm) at 2-5 cm distance from ground.

Based on the two CH_4 enhancements, which were more than 10% above background level on G2301, the emission rate 1.8 L min^{-1} was derived for this location. The leak was classified as A1 leak from a DN80ST pipeline which dated back to 1939 with overpressure of 30 – 60 mbar. The total leak area, 6 holes (See Sect. S.7) next to each other, was estimated ≈ 5 cm^2 which was due to corrosion.

4.S.11.9) HH014

During mobile surveys, at a T-junction of two streets, we passed a location that had been already detected by the LDC and was under repair procedures. The ground was already open with safety fences around the location. Both streets were ≈ 5 m wide and on both sides, there were strokes with about 1 m wide bare soil. There were trees and bushes on both sides of the streets, including a tree ≈ 2 m away from the leak location. There were dispersed houses with private gardens around this location and buildings were less dense compared to most of other locations, e.g. HH003. We performed mobile measurements and tracer release at this location, but as the ground was already open, it was not possible to apply the suction method.

The recorded C_2:C_1 ratio from the open ground area with some soil on top of the pipeline was 7.2% (R^2 of 0.95 and max CH_4 enhancement of 94 ppm). The C_2:C_1 ratio from two holes in asphalt with distance of ≈ 9 and ≈ 11 m to the leak location were 2.3% (R^2 of 0.93 and max CH_4 of ≈ 330 ppm) and 3.2% (R^2 of 0.99 and max CH_4 of >>1000 ppm).

Out of the 44 transects, CH_4 enhancements from 24 transects exceeded the 10% threshold on the G2301 instrument, which then were used to quantify the emission rate, yielding an emission rate estimate of 1.5 L min^{-1}. The tracer method was applied for this location in mobile mode and estimated an emission rate of 1.4 L min^{-1}.

This leak was categorized as A1 leak on a DN100St pipeline, which had been in operation since 1950, the leak area was estimated as ≈ 5 cm^2 as a result of corrosion. For this location, 12 m of gas pipeline were subsequently replaced by the LDC. Previous inspection for this location was in 2016. Gas overpressure of this pipeline, like other locations, was between 30 – 60 mbar.

4.S.11.10) HH015

On a ≈ 4.5-m wide street, we detected signals of fossil CH_4, which then was confirmed as a gas leak location by the LDC. The street cover was asphalt and on both sides of the street, there were ≈ 2 m wide pavements. Emissions were coming mainly from two manholes close to each other in the middle of the street and several curb cracks along ≈ 5 m length of pavement on one side of the street. For this location, we had 6 transects but due to technical issues, the G2301 instrument was not in operation for 4 transects, however the G4302 was available in all of the 6 transects. For the quantification, we only used the measurement from the two transects when G2301 was running, while for the attribution we report measurements during all transects (n = 6) from G4302.

Two manholes, ≈ 1 m apart from each other were identified as outlets, and also the curb cracks of the pavement above the leaky pipeline. The C_2:C_1 ratios measured from the manholes were similar with values of 6.0% (R^2 of 0.99 and max CH_4 of ≈ 270 ppm) and the C_2:C_1 ratio from the cracks was 6.9% (R^2 of 0.91 and max CH_4 of >1000 ppm).

Based on the only two transects for this location from mobile measurements when the G2301 was in operation, the emission estimate for this location was 0.6 L min^{-1}. The tracer method was applied in static mode at ≈ 20 m downwind the release location. The emission rate estimate from the tracer method for was 0.4 L min^{-1}. The suction method was applied for this location, and based on the incomplete measurements, the emission rate estimate was estimated ≈ 0.9 L min^{-1}. This leak was classified as an A1 leak from a DN80ST pipeline dated back to 1935. For this location, two of the connections were leaking and a corrosion leak area of ≈ 1 cm^2 was reported by the LDC. To repair this location, ≈ 10 m of pipeline was replaced.

4.S.11.11) HH100

This location was one of the five leak locations reported by the LDC. The emissions were coming through several gas cap outlets located in asphalt. The road was a bit elevated relative to the surrounding area with dispersed houses and open agricultural fields around. Compared to most of the first 15 locations (HH001 – HH015), this location had very open surroundings. For this location, we had quantification from mobile measurements and tracer method.

On-foot measurements of the surrounding area with the G4302 instrument resulted in finding 4 gas caps next to each other as the emission source. The C_2:C_1 ratios measured at two of these caps were 2.0% (R^2 of 0.83 with max CH_4 mole fraction of 14.9 ppm) and 1.3% (R^2 of 0.81 with max CH_4 mole fraction of 11.4 ppm). For the other two, the linear regression between C_2H_6 and CH_4 was insufficient to derive a reliable estimate.

Only two of the transects at this location showed CH_4 enhancements above the 10% threshold, and an emission rate of 0.6 L min^{-1} was derived from mobile measurements. The static measurements of released C_2H_2 and CH_4 plumes were performed ≈ 30 m downwind C_2H_2 release point, the center of the gas caps, with release rate of 2.6 L min^{-1}. The emission rate estimate of the tracer method for this location was 0.14 L min^{-1}. Due to time constraints, the suction method was not deployed at this location. This location was classified as C category and the leak was a d225Pe pipeline dated back to 1994. The latest inspection of this area was in 2016.

4.S.11.12) HH102

On one side of the two-lane asphalt road, the LDC reported a gas leak. This was a ≈ 6 m wide road with a narrow, ≈ 1 m wide, pavement on one side. On the both sides of the leak location there were trees and bushes, but beyond the vegetation line there were open fields and few scattered houses one the south side of the road.

The LDC had already drilled holes in the ground on top of the pipeline during their routine surveys and these holes were identified as the only emission outlets with C_2:C_1 ratio of 2.2% (R^2 of 0.91) and max CH_4 mole fraction of 55 ppm.

None of the CH_4 enhancements on G2301 were above the 10% threshold, thus no quantification could be derived from the mobile measurement technique using the "standard algorithm". The tracer method was applied at this location in static mode at ≈ 20 m distance from the release location and the estimated emission rate was 0.01 L min^{-1}. The suction method was not performed due to time constraints. The leak at this location was classified as C category from a DN125ST pipeline which was operational since in 1928. The overpressure at this location was 30 – 60 mbar, similar to the other location.

4.S.11.13) HH103

This leak was found by the LDC on a ≈ 4.5 m wide cobblestone street. On the east side of the street, there was a ≈ 2 m wide bare soil pavement and on the other side there was a narrow, ≈ 1 m wide, asphalt pavement. The leak was located on the east side of the street, where in about 3 m distance there were some bushes. The location was widely open and there were not dense buildings around.

The C_2H_6 signals from the location didn't give a good correlation with CH_4 so no C_2:C_1 ratio could be derived for this location.

As none of the CH_4 enhancements on G2301 was greater than the 10% threshold, we couldn't report gas emission for this location from mobile measurement "standard" method. The tracer method quantified this location in static mode at ≈ 18 m distance from the release location and estimated an emission rate of 0.03 L min^{-1}. Due to time constraints, the suction method was not applied at this location.
This location was classified as B category from a DN150ST pipeline which was connected to the distribution network in 1963.

4.S.11.14) HH104

On a 5-m wide asphalt covered street south-east of Hamburg municipality with about 1 m pavement on both sides, the LDC reported another leak location. The were some houses around the street but beyond the houses there were agricultural fields. There were private open spaces between houses.
None of CH_4 enhancements from any of the transects exceeded the 10% threshold, so based on the mobile measurements it's not possible to report emission rate for this location. At the time of applying the tracer method, CH_4 emission signals could not be detected at the reported location, thus tracer release was not applied. The suction method was also not applied due to time limitation.

The leak was categorized as C category from a DN100ST pipeline which was installed and connected to gas network in 1930. The pipeline overpressure for this location was 30 – 60 mbar.

5 Conclusions and outlook

5.1 Conclusions

Within the climate change framework greenhouse gas emissions from cities are an important component of national total emissions. It is therefore important to better understand the (urban) sources of emissions and their granularity. In this thesis the focus was on CH_4, the 2nd most important greenhouse gas. Results of mobile measurement campaigns in Hamburg (DE), Utrecht (NL) and Bucharest (RO) have been discussed and evaluated in detail. The measurements were performed at the street level aiming to understand the distribution, contribution and total emissions from very localized CH_4 sources, e.g. fossil CH_4 emissions from natural gas pipeline leaks, or microbial biogenic CH_4 emissions from the sewage network escaping mainly through street manholes. We used mobile measurements of CO_2 and C_2H_6 to attribute mobile CH_4 signals into fossil, microbial and combustion categories. To quantify CH_4 emissions from these measurements, we used an empirical equation that had been previously developed specifically for this purpose by Weller et a., (2018) (See Sect. 1.7.2). We also performed air sampling in small bags for further isotopic analysis of $\delta^{13}C$-CH_4, $\delta^{2}H$-CH_4 at some locations where we observed enhanced CH_4 signals. In addition to measurement of emissions from very localized sources at urban streets, we also performed mobile measurements downwind larger facilities, e.g. a waste water treatment plant in Utrecht and oil production facilities in Hamburg. The results from CH_4 emission quantification from facilities enable a comparison with the sources located in the urban area and together complement the picture of the city. This may provide a scientific basis for prioritizing the emission mitigations. Moreover, the gas leak locations have safety priority because of potential explosion danger in addition to the emission priority.

Different methods exist to quantify urban CH_4 emissions. A detailed discussion about CH_4 emissions quantification from gas leaks in urban natural gas pipeline infrastructure using three different measurement methods (mobile, tracer and suction methods) was presented. It is important to understand any potential differences between such methods to be able to compare results from different studies and /or cities. The mobile urban survey quantifications showed that emission rates reported at individual urban gas leak locations in Hamburg were higher than what is usually observed with the suction method. The latter is also used to provide data for the German national emission inventory. In order to understand discrepancies, we designed a campaign in Hamburg to compare emission rate estimates derived from three measurements methods in more detail. The tracer method uses an independent tracer to improve the emission quantification and was deployed because it has a lower uncertainty associated with the emission quantification compared to the mobile method.

5.1.1 Urban CH_4 emissions in Hamburg (DE) and Utrecht (NL) (Chapter 2)

Based on the campaigns executed in 2018 and 2019, we reported total emission rates of 440±70 t yr^{-1} and 150±50 t yr^{-1} in the selected urban areas of Hamburg and Utrecht, respectively (Fig. 2.1). These emission rates include emissions from pipeline leaks, sewer system and combustion. With the help of the attribution analysis, we estimated that the majority of the emissions in each city (70% to 90% in Utrecht and 50% to 80% in Hamburg) originates from gas pipeline leaks and is thus of fossil origin. We attributed 8% and 35% of emissions to microbial sources in Utrecht and Hamburg, respectively. Combustion emissions only contribute 2% (Utrecht) and 10% (Hamburg) to the total emissions in these two cities. After accounting for the contribution of natural gas leaks to total emissions in both cities, we could derive CH_4 emission rates per km of natural gas pipeline of 0.47±0.14 L min^{-1} km^{-1} in Utrecht and 0.19±0.03 L min^{-1} km^{-1} in Hamburg. The emission losses through the natural gas pipeline networks in Utrecht and Hamburg constitute 0.10 – 0.12% and 0.04 – 0.07% of the total natural gas consumption respectively, which needs to be taken account when reporting total emission loss in natural gas use. Similar to studies in other cities, we found that on average 50% of emissions in each city could be attributed to about 10% of the locations, i.e. a skewed distribution of emission rates. This means that by detecting and fixing a few bigger pipeline gas leaks, it is possible to reduce a significant part of total city emissions.

5.1.2 Urban methane emissions in Bucharest (RO) (Chapter 3)

Using our experience with emission detection and quantification in Utrecht and Hamburg, a similar approach was deployed in Bucharest, Romania. It is important to obtain data from a larger number of cities in Europe because previous work in the US had shown that differences between cities can be large due to differences in age and maintenance of the gas infrastructure. We estimated a total CH_4 emission rate of 1832 t CH_4 yr^{-1} for the city of Bucharest and found that the majority of emissions could be attributed to biogenic sources, most likely emissions from the sewage and wastewater system (Fig. 3.1). Out of the total CH_4 emissions, we attributed 58% to 63% to biogenic sources, 32% to 42% to leaks from the natural gas system and 0% to 5% of total emissions to pyrogenic emissions. The majority of the microbial emissions were related to the open outlets connected to the sewer system. We reported fossil CH_4 emission per km pipeline of natural gas in Bucharest as 0.5 to 0.7 L min^{-1} km^{-1} which is higher than this emission factor in Utrecht and Hamburg. The greater contribution of CH_4 emissions from the sewer system in Bucharest suggests that this is an attractive target for emission mitigation policies in Bucharest.

5.1.3 Urban methane emissions in Toronto (CA) and Paris (FR)

Ars et al. (2020) performed mobile surveys in Toronto, Canada where they installed mobile CRDS sensors on a car and a bike platformes and carried out the measurements in the Greater Toronto Area (GTA). They attributed 60 to 1395 kg CH_4 d^{-1} to the leaks from natural gas distribution network. This value cannot be compared directly to the FLAME-GTA inventory report, 9600 kg CH_4 d^{-1}, which also includes emissions from compressors in the GTA. Ars et al. (2020) reported that the main emissions in the GTA are related to the waste sector which might be an interesting sector for mitigation in the GTA. However, their emissions estimates from the facilities are lower than the reports in the FLAME-GTA inventory, and they might have missed or mis-attributed some of the emissions from the natural gas distribution network.

Defratyka et al. (2021) used $\delta^{13}C$-CH_4 for source attribution in Paris, France. They performed mobile surveys with CRDS technology onboard a car on the streets of Paris. They reported emissions of 190 t CH_4 yr^{-1} and attributed them to 56% from gas pipeline leaks, 34% from microbial sources and 10% from furnaces. This study shows that repairing gas leaks in Paris should be a priority within the framework of mitigation strategy, which shows a different mitigation pathway from the study in Bucharest (Fernandez et al., 2022).

5.1.4 Unreported CH_4 emissions from urban sources in inventories

Chen et al. (2020) performed mobile walking and cycling surveys around Theresienwiese in Munich, Germany, where Oktoberfest, the world largest folk festival, happens every year. Their analysis shows emissions of 6.7 ± 0.6 µg-CH_4 m^{-2} s^{-1} which is about 11 times higher than the emission rate per unit of area in Boston (0.6 ± 0.1 µg-CH_4 m^{-2} s^{-1} in McKain et al., 2015). However the emission from Oktoberfest is temporary, and from a small area, while this is not the case in Boston. Chen et al. (2020) reported that this festival is an example of a source that is not included in the inventories, despite the magnitude of emission. The analysis of gas loss during the festival compared to the gas use shows 1.1% loss, which is significant, but lower than the loss ratio in Boston or a report from the US gas system (2.3% in Alvarez et al., 2018).

CH_4 can also escape at the very end-use point in urban area, e.g. during the use of natural gas for cooking, Lebel et al. (2022) estimated that 0.8 to 1.3 % of natural gas escapes unburned from the use of stoves in the US. They quantified CH_4 emissions from unburned natural gas stoves in the US in order of 28.1 Gg CH_4 $year^{-1}$ (18.5 to 41.2 Gg CH_4 $year^{-1}$ with 95% confidence interval). They estimated that the yearly CH_4 emission from incomplete combustion of stoves in the US is equivalent to the annual CO_2 emissions of 0.5 million cars; this analysis was based on the 20 year time horizon GWP of CH_4. Emissions from the home appliances can range differently in different states compared to the natural gas consumed, e.g. 0.04% in Boston and Indianapolis (Merrin and Francisco, 2019) or 0.5% in

California (Fischer et al., 2018). This shows that these escapes can also be influential regarding the climate benefit of natural gas while they may not be included in the inventory of some countries.

5.1.5 Intercomparison of measurement methods (Chapter 4)

In the intercomparison campaign we had in Hamburg it was not possible to do a one-to-one comparison between emission rate estimates derived from the different locations, due to limitations of different methods (mobile, tracer and suction) at the different locations. For example, some of the identified locations were, according to German regulation, safety category A1 or A2. Such leaks need to be repaired as soon as possible which did not allow planning and setting up of some of the more time-consuming methods, like the suction method. However, we noted that the locations with safety concerns (i.e. the locations where immediate or within one week repair actions are required; safety category of A1&A2) show significantly higher emission rates than locations that have less safety concerns (category B and C) with all the three measurement methods. In particular, gas leak locations with high subsurface CH_4 accumulations were only among the A1&A2 safety categories. The suction method is relatively time consuming and logistically challenging, thus this method is most likely never applied at this type of locations. This suggest that the suction method, which provides data for the official German inventories, may have a low emission rate bias due to this site selection bias that excludes the sites with the highest emission rates.

5.1.6 Importance of attribution

There are three main diffuse CH_4 emission sources in urban areas (i) gas pipeline leaks (ii) microbial emissions mainly from sewer system and (iii) emissions from incomplete combustion. Attribution of CH_4 signals is the key to determine the contribution of each source to the total emission of an urban area. Moreover, attributing CH_4 signals to leaks from the natural gas distribution network is important in terms of safety reasons, i.e. identifying gas leaks with confidence, and reporting to the local gas utility. In order to separate these CH_4 sources, applying mobile attribution through the simultaneous measurements of other co-emitted species like C_2H_6 and CO_2 is crucial.

The natural gas composition is known by each country authority and gas distribution company. The main component is CH_4 (80-95%) with smaller shares of C_2H_6 and other hydrocarbons. CO_2 is either not present or only in a very small portion. The added value of CO_2 is that it indicates combustion sources or biogenic respiration. Thus, atmospheric observations of CH_4 and C_2H_6 with a ratio similar to the gas transported in the pipelines, in combination with an absence of CO_2 signals implies existence of gas leaks from a pipeline in the vicinity of the mobile measurement.

Microbial CH_4 emissions from sewer systems may include concurrent emissions of CO_2, while C_2H_6 signals are lacking. Thus, if during mobile measurements significant CH_4 plumes are detected without a concurrent C_2H_6 plume, and/or CO_2 signals are observable, these plumes can be attributed to emissions from the sewer system. The CH_4:CO_2 ratio for the observed microbial emissions were greater or far greater than 20 ppb ppm^{-1} (R^2 >0.8).

During incomplete combustion, part of the CH_4 and C_2H_6 from the natural gas escapes combustion, while CO_2 is the primary product of the combustion process. We can therefore attribute CH_4 plumes which include CO_2 and C_2H_6 signals to the combustion process. We observed that these plumes showed a C_2:C_1 ratio above 10% which is higher than the typical C_2:C_1 in the urban natural gas pipeline (Fig. 2.S17.). We used CH_4:CO_2 ratio of 0.02 to 20 ppb ppm^{-1} (R^2 > 0.8) to attribute the CH_4 signals to combustion. Thus, using these constraints, we attributed some of the fossil CH_4 signals to incomplete combustion emissions.

In the work presented in this thesis, we added the attribution of mobile CH_4 signals using both C_2H_6 and CO_2 measurement as a routine component to mobile city surveys, which previously were often carried out without such direct attribution techniques.

Although the mobile continuous measurements of co-emitted gases (C_2H_6 and CO_2) are beneficial to attribute the mobile CH_4 signals to their source origin, the mobile attributions have a

limitation when the CH_4 signals are low (<500 ppb). In those cases, implementing the attribution analysis of CO_2 and specifically C_2H_6 is challenging. Thus, high-precision analysis of isotopic lab measurement helps attributing these CH_4 signals. The mobile isotopic analysis cannot yet be performed at very high precision from mobile platforms. Instead, this analysis requires collection of samples in the plumes and subsequent laboratory measurements. However, the advantage is that these data can help attribute CH_4 elevations that are only 100 or 200 ppb above the background level, which is not yet possible for the online CH_4 – C_2H_6 analyzers. Moreover, in our studies, we found out that δ^2H-CH_4 provide more distinct signature for natural gas leaks than δ^{13}C-CH_4.

The improved attribution using all the above-mentioned techniques enabled us to split up the total emissions into the different categories and identify differences between the different cities.

5.1.7 Strengths and limitations of the mobile detection method

The mobile measurement method provides a possibility for a large coverage of gas leak detection across an urban area in a shorter time-period compared to the conventional walking detection method of the local gas utilities. For example, in Hamburg the whole urban area is monitored with the walking method every 1-5 years while we covered the city with the mobile in few weeks. This can dramatically improve the monitoring intervals, with the benefit of detecting leaks quickly after they appear.

An advantage of the walking method is that the survey teams can follow the exact map of buried pipelines of the natural gas distribution network and the inlet to the detector collects air from the ground surface. Thus, if a leak occurs subsurface, CH_4 emissions can be detected during one walking survey. The mobile method detects leaks in the ambient air, so it is dependent on the meteorological conditions, primarily on the wind direction. Therefore, several transects on each street are required to properly and locate a gas leak. Although several coverages are required, the mobile method is still 5 to 10 times faster than the walking method.

In our studies in urban areas, we used a detection threshold to remove very small CH_4 enhancements to avoid false positives. This threshold is defined as 10% of CH_4 background during the mobile surveys. However, we noticed that the small leaks can show CH_4 signals lower than the 10% threshold, thus some minor leaks will be overlooked in the mobile detection surveys.

Results from the mobile detection method can be beneficial to understand patterns and distribution of CH_4 emissions from other sources. For example, how microbial emissions from sewer systems are distributed throughout a city. The method is also sensitive to other CH_4 sources within the urban boundary, such as certain facilities. These are attractive by-products of mobile surveys.

In Vogel et al. (in press) mobile transects from 11 European cities, including the cities evaluated in this thesis, were reevaluated with a lower detection threshold. This results in many more leak indications. In chapter 2 and 3 we reported 145, 81 and 969 leak indications for Hamburg, Utrecht and Bucharest respectively. With a lower threshold these numbers increased to 253, 187 and 1312 for these three cities accordingly. It should be investigated which threshold is the most useful one in still detecting real leaks but avoiding too many false positives.

5.1.8 Strengths and Limitations of the mobile quantification method

The mobile quantification method is easy to implement and uses a rather simple empirical formula to calculate the emission rate from the observed enhancement. In the present version, the emission rate is only dependent on the maximum CH_4 enhancement within a plume observed at each leak location. We used this equation throughout the work reported in this thesis, with the main goal and advantage to remain consistent with previous studies.

However, we identified several important missing components in the quantification method and showed how they introduced different biases in the emission rate estimates.

a) Emission rates are instrument type dependent: We have shown that different instruments with different cavity size, sampling rate and flush rate report clearly different maximum CH_4 enhancement from the same gas leak plume. For example, in chapter 4, we have shown that with the use of two different CRDS instrument with the same inlet, the maximum CH_4 enhancement from each transect can be about 3.8 times higher on one instrument than the other This then results in higher or lower maximum emission rates. In this example, the emission quantification would be about two times higher on the instrument with higher maximum CH_4 enhancement.
b) The enhancement observed from a mobile vehicle shows a large variability between different transects at the same gas leak location. This results in a large uncertainty in gas leak quantification. It is, however, possible to perform several transect at a gas leak location and use averages to reduce this error.
c) Important parameters that should affect the results are not included in the conversion equation from Weller et al. (2018). One important parameter is distance. For example, if the measurement vehicle passes close to a small gas leak, the derived emission quantification rate can be reported higher than that for a larger gas leak that is passed at a greater distance. However, in our measurements reported in chapter 4 we clearly showed for multiple transects along the same leak, that higher emission rates are derived when the distance to the leak location is smaller, as expected from theory.
d) The application of the 10% detection threshold in the conversion equation means that especially for smaller leaks just above or below threshold, only a small percentage of the transects are used for quantification. This may result in an overestimate for these smaller leaks. For larger leaks, the threshold is likely useful, since it removes transects in which the plume is not captured in representative way. Including the transects would lead to a low bias and a larger spread of the estimates.

Measurements from the mobile surveys can also be used to quantify other CH_4 emissions sources within urban areas, e.g. from facilities. This then enables comparison of the strengths of different sources which can be useful for prioritizing CH_4 mitigation policies.

5.2 Outlook

5.2.1 Improvement of mobile detection method

The attribution part of the mobile method is meant to distinguish between source categories, however, attribution of small CH_4 enhancement signals can become challenging. With the instruments used in this thesis, online attribution was generally only possible when the CH_4 enhancement was larger than 500 ppb. This can be improved with instruments that have a higher sensitivity, or lower noise level for C_2H_6.

The wind direction is also not included in the mobile detection method. In principle, the mobile measurement car should be downwind of a possible source to detect CH_4 emission from the source. In the dense urban area, this can be addressed by performing several transects, thus increasing the possibility as well as the certainty of detecting gas leaks. However, in an open urban area if all the mobile transects are performed upwind of the gas pipeline, then it is not possible to be conclusive on presence or absence of gas leaks.

5.2.2 Improvement of mobile quantification method

As discussed above, the mobile quantification equation is instrument dependent. This can be improved by using plume area (integration of CH_4 enhancement across driving distance) instead of the use of the maximum CH_4 enhancement from each transect. We showed that the plume area is a more robust indicator and independent of the instrument type (Fig. 4.S10.).

Distance should preferable also be included in the emission quantification. One complication is that the distance is not known a priori. But if this technique is used by local gas utilities in the future, it will be easy to routinely determine the distance between plume and leak or main outlet. This should help in providing more reliable emission rate estimates

In addition, plume dispersion is clearly dependent on wind speed. Von Fischer et al (2017) reported that the inclusion of wind speed did not improve their emission rate estimates, but conceptually it should be able to improve the results. Future studies should investigate this aspect further. Of course, this also requires operating a reliable wind sensor on the measurement vehicle. This can also improve the assessment of reliable detection (see previous paragraph) because it will allow to determine which parts of cities or streets have ben surveyed downwind of gas pipelines.

5.2.3 Ground-based mobile measurements to support flight in-situ measurements

In the last years, CH_4 emissions from the 1.B.1.a category (coal mining activities) in Poland account for about 60% of total EU27+UK emissions in this category but few independent quantifications had been carried out previously. The Carbon Dioxide and Methane (CoMet) aimed to quantify CH_4 emissions in major coal mining region in Poland (Bovensmann et al., 2019). From the MEMO^2 project, we contributed to this campaign with the CRDS mobile measurements.

Fiehn et al. (2020) used mass balance method using in-situ measurements onboard flights during the CoMet campaign to estimate CH_4, CO_2 and CO emissions from the coal mining activities in Upper Silesian Coal Basin (USCB). The flight measurements were supported with in-situ mobile measurements vehicles upwind and downwind. The combination of flight and ground-based in-situ measurements then gave a better altitude profile of CH_4 mixing ratio. Measurements from the two flights resulted in CH_4 emission rate of 436 ± 135 and 477 ± 126 kt-CH_4 yr^{-1}, CO_2 emission rate of 38.3 ± 23.6 and 35.2 ± 11.9 Mt-CH_4 yr^{-1} and CO emission rate of 317 ± 114 and 339 ± 139 kt-CO yr^{-1}. Although their measurements are based on only two flights, they covers a large fraction of the coal mining activities, about 35 mine shafts. Their annual CH_4 emission rate estimates were in the range of reports from inventories, while estimates for CO_2 emissions were at the lower end of the reports and their derived emissions for CO were at the high end of inventories reports. For this study, they used various inventories, Scarpelli et al. (2020), European Pollutant Release and Transfer Register (E-PRTR), CAMS, EDGAR and GESAPU.

Luther et al. (2020) quantified CH_4 emissions from either individual mine shafts or a sub region of the USCB using a mobile Fourier transform spectrometer which was also part of the CoMet campaign in 2018. Their analyses resulted in an emission rate of 6 ± 1 kt-CH_4 yr^{-1} for an individual shaft and 109 ± 33 kt-CH_4 yr^{-1} of emission for a subregion of the UCSB. In a later publication using the same instruments and techniques, Luther et al. (2021) estimated 414 to 790 kt-CH_4 yr^{-1} of emission for the USCB. The lower end of this range agrees with the 440 kt CH_4 yr^{-1} report from the inventories. Tu et al. (2022) used satellite imageries from the TROPOspheric Monitoring Instrument (TROPOMI) and Infrared Atmospheric Sounding Interferometer (IASI) to quantify CH_4 emissions from coal mining activities in the UCSB and reported 1.5 ± 0.1 kg-CH_4 s^{-1} using TROPOMI alone and with the use of both datasets (TROPOMI and IASI) they estimated 1.4 ± 0.6 kg-CH_4 s^{-1}.

5.2.4 Real-life application of the mobile method and a potential business model

After the rigorous testing described in this thesis and several other studies, the mobile method is mature enough to be implemented in real-life for speeding up detection of gas leaks from urban gas pipeline networks. This higher speed of gas leak detection then results not only in a safer urban environment, but also CH_4 emission mitigation. Leaks can be detected and repaired faster, which is an easy and rather straightforward way to help reducing greenhouse gas emissions. Thus, the already published findings of peer-reviewed articles can be applied in the real-life day to day practices.

In chapter 2 we have provided an open-source code that was used to evaluate our mobile measurements. This code can be implemented by any user who has a mobile measurement setup and would like to detect significant CH_4 signals which can point to potential gas leak location. This code can be further improved in the future by coupling it directly with the attribution constrains we introduced in the work presented in this thesis. Moreover, further interfaces and other functionalities can be added. Thus, the mobile method can be brought to the market together with authorities and gas

utilities to (i) repair gas leaks in a shorter period of time (ii) address the urge for CH_4 emissions reduction, (iii) use the measurement to better understand the CH_4 emission patterns in different cities and (iv) quantify the urban gas facility CH_4 emissions for further mitigation strategies.

These services can be performed through start-ups. The author of this thesis has recently started the company Maaz Maps. It intends to bridge the gap between academic findings and industrial needs. The CRDS instrument manufacturers Picarro and ABB also offer gas leak detection services, but the market is potentially large and may provide new business opportunities.

5.2.5 General outlook on the use of mobile methods to mitigate emissions from natural gas distribution, natural gas end use and other urban sources

The cumulative emission distributions from different cities showed that in each city a small number of gas leak locations contributes a lot to the total CH_4 emissions from urban gas pipeline distribution networks. Generally, fixing about 10% of the gas leak locations could reduce the total emissions from urban gas leaks by 30% - 70% (Fig. 2.4). As more data for different cities will become available we will be able to say with more certainty if cumulative distributions for all cities are similar, even in cities where more repeat surveys were performed.

In the future green gas may become more important than fossil natural gas but CH_4 leakage of green gas has a comparable climate impact and should also be minimized. The spatially explicit mobile detection, attribution and quantification methods will help in getting CH_4 emission from cities mapped in more detail and understand the contributions from other sources, e.g. biogenic diffuse sources, or larger urban facilities like waste management treatment plants. Hence there is a broader need for implementation of the methodologies studied in this thesis.

The mobile method can be easily deployed, and its use can be extended to other urban areas, within or outside Europe, in the commercial market or for further research. In the near future, we are going to implement this method in collaboration with the Seoul National University to investigate urban CH_4 emission in Seoul, South Korea.

5.2.6 Possible CH_4 emission measurement campaign in Iran

CH_4 mitigation policies for the fossil fuel related emissions in different regions or countries should be target-specific depending on the emission contribution of oil, gas and coal related activities. In Europe coal mining activities contribute significantly in the total emissions from the European energy sector while in Iran, CH_4 emissions from oil and gas activities are dominant.

Iran stands as the second largest natural gas reserves holder in the world after Russia. In the third national report submitted to the UNFCCC, the energy sector was the main contributor to total anthropogenic CH_4 emission of the country (63%, ≈4,000 kt-CH_4 yr^{-1}) followed by the waste (≈21%, ≈1,300 kt-CH_4 yr^{-1}) and agriculture sectors (≈16%, ≈1000 ktCH_4 yr^{-1}) in 2010 (UNFCCC, 2017). Almost all the CH_4 emissions in the energy sectors were related to fugitive emissions.

Maazallahi et al. (2017) used the Hyperion sensor onboard the EO-1 satellite to detect CH_4 emissions from oil and gas facilities in Iran. Ghadaksaz and Saboohi (2020) stated that the energy policy of Iran should be focused on improving energy efficiency in the country to meet the goals of Paris Agreement. Energy transition toward lower GHG emission in countries with high oil and gas production is challenging due to the low cost of energy. Noorollahi et al. (2021) provided a BU model for the energy transition in Iran and stated that efficiency improvements in electricity generation will reduce CO_2 emission in the country. CH_4 emission detection and quantification methods have not been deployed in Iran so far. Inventory based BU estimates should be compared to TD estimates derived from atmospheric measurements to constrain the emission rate from oil and gas activities in Iran. This could have implications for CH_4 emission reduction policies, similar to the methods applied in the ROMEO and CoMet campaigns. Within the framework of UNEP methane emission studies, we have started initial discussions with the National Iranian Oil Company (NIOC) and National Iranian Gas

Company (NIGC) to explore the possibilities of performing a CH_4 emission measurement campaign related oil and gas activities in Iran.

Bibliography

ACM: Authority for Consumers and Markets in the Netherlands, Low NOx Burgners (LNBs) gas code, [online] Available from: https://wetten.overheid.nl/BWBR0037935/2018-05-26, 2018.

Akritas, M.G., Bershady, M.A., 1996. Linear Regression for Astronomical Data with Measurement Errors and Intrinsic Scatter. Astrophys. J. 470, 706. https://doi.org/10.1086/177901.

Alamsi, A.M., 2013. Municipal Waste Management in Romania.

Allen, D. T., Torres, V. M., Thomas, J., Sullivan, D. W., Harrison, M., Hendler, A., Herndon, S. C., Kolb, C. E., Fraser, M. P., Hill, A. D., Lamb, B. K., Miskimins, J., Sawyer, R. F. and Seinfeld, J. H.: Measurements of methane emissions at natural gas production sites in the United States, Proc. Natl. Acad. Sci., 110(44), 17768–17773, https://doi.org/10.1073/pnas.1304880110, 2013.

Allen, D. T.: Methane emissions from natural gas production and use: reconciling bottom-up and top-down measurements, Current Opinion in Chemical Engineering, 5, 78-83, https://doi.org/10.1016/j.coche.2014.05.004, 2014.

Allwine G., Lamb B., Westberg H., Application of Atmospheric Tracer Techniques for Determining Biogenic Hydrocarbon Fluxes from an Oak Forest. In: Hutchison B.A., Hicks B.B. (eds) The Forest-Atmosphere Interaction. Springer, Dordrecht. https://doi.org/10.1007/978-94-009-5305-5_23, 1985.

Alvarez, R. A., Pacala, S. W., Winebrake, J. J., Chameides, W. L., Hamburg, S. P.: Greater focus needed on methane leakage from natural gas infrastructure, PNAS, 109 (17) 6435-6440, https://doi.org/10.1073/pnas.1202407109, 2012.

Alvarez, R. A., Zavala-Araiza, D., Lyon, D. R., Allen, D. T., Barkley, Z. R., Brandt, A. R., Davis, K. J., Herndon, S. C., Jacob, D. J., Karion, A., Kort, E. A., Lamb, B. K., Lauvaux, T., Maasakkers, J. D., Marchese, A. J., Omara, M., Pacala, S. W., Peischl, J., Robinson, A. L., Shepson, P. B., Sweeney, C., Townsend-Small, A., Wofsy, S. C., and Hamburg, S. P.: Assessment of methane emissions from the U.S. oil and gas supply chain, Science, 361, 186–188, https://doi.org/10.1126/science.aar7204, 2018.

Amadori, M.L., Belayouni, H., Guerrera, F., Martín-Martín, M., Martin-Rojas, I., Miclăuş, C., Raffaelli, G., 2012. New data on the Vrancea Nappe (Moldavidian Basin, Outer Carpathian Domain, Romania): Paleogeographic and geodynamic reconstructions. Int. J. Earth Sci. 101, 1599–1623. https://doi.org/10.1007/s00531-011-0744-1.

Arnaldos, J., Casal, J., Montiel, H., Sánchez-Carricondo, M., Vílchez, J.A., Design of a computer tool for the evaluation of the consequences of accidental natural gas releases in distribution pipes, Journal of Loss Prevention in the Process Industries, https://doi.org/10.1016/S0950-4230(97)00041-7, 1998.

Ars, S., Vogel, F., Arrowsmith, C., Heerah, S., Knuckey, E., Lavoie, J., Lee, C., Mostafavi Pak, N., Phillips, J. L., and Wunch, D., Investigation of the Spatial Distribution of Methane Sources in the Greater Toronto Area Using Mobile Gas Monitoring Systems, Environ. Sci. Technol., 54, 24, 15671–15679, https://doi.org/10.1021/acs.est.0c05386, 2020.

Bojor, J., 2010. Water and Wastewater Sectors in Romania DEMO Market Brief 2010.

Bonnaud, C., Cluzel, V., Corcoles, P., Dubois, J. P., Louvet, V., Maury, M., Narbonne, A., Orefice, H., Perez, A., Ranty, J., Salim, R., Zeller, L. M., Foissac, A., Poenou, J., Experimental study and modelling of the consequences of small leaks on buried transmission gas pipeline, Journal of Loss Prevention in the Process Industries, 55, 303-312, https://doi.org/10.1016/j.jlp.2018.06.010, 2018.

Bousquet, P., Ciais, P., Miller, J. B., Dlugokencky, E. J., Hauglustaine, D. A., Prigent, C., Van der Werf, G. R., Peylin, P., Brunke, E. G., Carouge, C., Langenfelds, R. L., Lathière, J., Papa, F., Ramonet, M., Schmidt, M., Steele, L. P., Tyler, S. C., White, J., Contribution of anthropogenic and natural sources to atmospheric methane variability. Nature.; 443(7110):439-43. https://doi.org/10.1038/nature05132, 2006.

Bovensmann, H., Krautwurst, S., Fiehn, A., Roiger, A., Gerilowski, K., Borchardt, J., Meyer, S. L., Fix, A., Necki, J., Swolkie´n, J., Amediek, A., Jöckel, P., Gałkowski, M., Gerbig, C., and the CoMet Team.: Combining airborne remote sensing (lidar, spectrometer) of CH_4 as well as in-situ data to determine CH4 emissions of a European CH_4 emission hot spot area – initial results from the CoMet campaign, EGU General Assembly 2019, Vienna, 4–8 May 2020, EGU2019-15249-2, 2019. BP, 2020. Statistical Review of World Energy, 2020 68th edition 66.

Brandt, A. R., Heath, G. A. and Cooley, D.: Methane Leaks from Natural Gas Systems Follow Extreme Distributions, Environ. Sci. Technol., 50(22), 12512–12520, https://doi.org/10.1021/acs.est.6b04303, 2016.

Brantley, H. L., Hagler, G. S. W., Kimbrough, E. S., Williams, R. W., Mukerjee, S. and Neas, L. M.: Mobile air monitoring data-processing strategies and effects on spatial air pollution trends, Atmos. Meas. Tech., 7(7), 2169–2183, https://doi.org/10.5194/amt-7-2169-2014, 2014.

Brass, M. and Röckmann, T.: Continuous-flow isotope ratio mass spectrometry method for carbon and hydrogen isotope measurements on atmospheric methane, Atmos. Meas. Tech., 3(6), 1707–1721, https://doi.org/10.5194/amt-3-1707-2010, 2010.

Bright, E. A., Coleman, P. R. and Dobson, J. E.: LandScan : A Global Population database for estimating populations at risk, [online] Available from: https://www.semanticscholar.org/paper/LandScan-%3A-A-Global-Population-database-for-at-risk-Bright-Coleman/17e6076b6761788684434d1e14e85e8877fc0146 (Accessed 23 September 2019), 2000.

Brümmer, B., Lange, I. and Konow, H.: Atmospheric boundary layer measurements at the 280 m high Hamburg weather mast 1995-2011: mean annual and diurnal cycles, Meteorol. Zeitschrift, 21(4), 319–335, https://doi.org/10.1127/0941-2948/2012/0338, 2012.

Buendia, E. C., Guendehou, S., Limmeechokchai, B., Pipatti, R., Rojas, Y., Sturgiss, R., Tanabe, K., Wirth, T., Romano, D., Witi, J., Garg, A., Weitz, M. M., Cai, B., Ottinger, D. A., Dong, H., MacDonald, J. D., Ogle, S. M., Rocha, M. T., Sanchez, M. J. S., Bartram, D. M. and Towprayoon, S.: 2019 refinement to the 2006 IPCC guidelines for national greenhouse gas inventories. [online] Available from: https://www.ipcc.ch/report/2019-refinement-to-the-2006-ipcc-guidelines-for-national-greenhouse-gas-inventories/, 2019.

Bukowiecki, N., Dommen, J., Prévôt, A. S. H., Richter, R., Weingartner, E. and Baltensperger, U.: A mobile pollutant measurement laboratory - Measuring gas phase and aerosol ambient concentrations with high spatial and temporal resolution, Atmos. Environ., 36(36–37), 5569–5579, https://doi.org/10.1016/S1352-2310(02)00694-5, 2002.

Cambaliza, M.O.L., Shepson, P.B., Caulton, D.R., Stirm, B., Samarov, D., Gurney, K.R., Turnbull, J., Davis, K.J., Possolo, A., Karion, A., Sweeney, C., Moser, B., Hendricks, A., Lauvaux, T., Mays, K., Whetstone, J., Huang, J., Razlivanov, I., Miles, N.L., Richardson, S.J., 2014. Assessment of uncertainties of an aircraft-based mass balance approach for quantifying urban greenhouse gas emissions. Atmos. Chem. Phys. 14, 9029–9050. https://doi.org/10.5194/acp-14-9029-2014.

Caulton, D. R., Li, Q., Bou-Zeid, E., Fitts, J. P., Golston, L. M., Pan, D., Lu, J., Lane, H. M., Buchholz, B., Guo, X., McSpiritt, J., Wendt, L. and Zondlo, M. A.: Quantifying uncertainties from mobile-laboratory-derived emissions of well pads using inverse Gaussian methods, Atmos. Chem. Phys., 18(20), 15145–15168, https://doi.org/10.5194/acp-18-15145-2018, 2018.

Chamberlain, S. D., Ingraffea, A. R. and Sparks, J. P.: Sourcing methane and carbon dioxide emissions from a small city: Influence of natural gas leakage and combustion, Environ. Pollut., 218, 102–110, https://doi.org/10.1016/J.ENVPOL.2016.08.036, 2016.

Chen, J., Dietrich, F., Maazallahi, H., Forstmaier, A., Winkler, D., Hofmann, M. E. G., Denier van der Gon, H., and Röckmann, T.: Methane emissions from the Munich Oktoberfest, Atmos. Chem. Phys., 20, 3683–3696, https://doi.org/10.5194/acp-20-3683-2020, 2020.

Cho, Y., Ulrich, B. A., Zimmerle, D. J., Smits, K. M., Estimating natural gas emissions from underground pipelines using surface concentration measurements, Environmental Pollution, https://doi.org/10.1016/j.envpol.2020.115514, 2020.

Christensen, T. R., Arora, V. K., Gauss, M., Höglund-Isaksson, L., Parmentier, F-J W., Tracing the climate signal: mitigation of anthropogenic methane emissions can outweigh a large Arctic natural emission increase. *Sci Rep* **9,** 1146. https://doi.org/10.1038/s41598-018-37719-9, 2019.

Clayton, C., 1991. Carbon isotope fractionation during natural gas generation from kerogen. Mar. Pet. Geol. 8, 232–240. https://doi.org/10.1016/0264-8172(91)90010-X.

Coleman, D.D., Risatti, J.B., Schoell, M., 1981. Fractionation of carbon and hydrogen isotopes by methane-oxidizing bacteria. Geochim. Cosmochim. Acta 45, 1033–1037. https://doi.org/10.1016/0016-7037(81)90129-0.

Cranganu, C., Deming, D., 1996. Heat flow and hydrocarbon generation in the Transylvanian Basin, Romania. Am. Assoc. Pet. Geol. Bull. 80, 1641–1653. https://doi.org/10.1306/64eda0e6-1724-11d7-8645000102c1865d.

Curran, S. J., Wagner, R. M., Graves, R. L., Keller, M. and Green, J. B.: Well-to-wheel analysis of direct and indirect use of natural gas in passenger vehicles, Energy, 75, 194–203, https://doi.org/10.1016/j.energy.2014.07.035, 2014.

Dalsøren, S. B., Myhre, C. L., Myhre, G., Gomez-Pelaez, A. J., Søvde, O. A., Isaksen, I. S. A., Weiss, R. F., and Harth, C. M.: Atmospheric methane evolution the last 40 years, Atmos. Chem. Phys., 16, 3099–3126, https://doi.org/10.5194/acp-16-3099-2016, 2016.

Davis, J. B. and Squires, R. M.: Detection of Microbially Produced Gaseous Hydrocarbons Other than Methane., Science, 119(3090), 381–2, https://doi.org/10.1126/science.119.3090.381, 1954.

Deaconu, S., 2020. Romania's Greenhouse Gas Inventory 1989-2018, National Inventory Report, Ministry of Environment, Waters and Forests National Environmental Protection Agency. Romania.

Dean, J. F., Middelburg, J. J., Röckmann, T., Aerts, R., Blauw, L. G., Egger, M., Jetten, M. S. M., de Jong, A. E. E., Meisel, O. H., Rasigraf, O., Slomp, C. P., in't Zandt, M. H., Dolman, A. J.: Methane feedbacks to the global climate system in a warmer world. Reviews of Geophysics, 56. https://doi.org/10.1002/2017RG000559, 2018

Defratyka, S. M., Paris, J. D., Yver-Kwok, C., Fernandez, J. M., Korben, P., and Bousquet, P., Environmental Science & Technology Article ASAP, https://doi.org/10.1021/acs.est.1c00859, 2021.

Delre, A., Greenhouse gas emissions from wastewater treatment plants: measurements and carbon footprint assessment, Ph.D. Thesis, Department of Environmental Engineering, Technical University of Denmark (DTU), Copenhagen, Available at: https://orbit.dtu.dk/en/publications/greenhouse-gas-emissions-from-wastewater-treatment-plants-measure (last accessed: 15 June 2021), 2018.

DelSontro, T., Beaulieu, J. J. and Downing, J. A.: Greenhouse gas emissions from lakes and impoundments: Upscaling in the face of global change, Limnol. Oceanogr. Lett., 3(3), 64–75, https://doi.org/10.1002/lol2.10073, 2018.

Dlugokencky E. J., Nisbet, E. G., Fisher, R. and Lowry, D.: Global atmospheric methane: budget, changes and dangersPhil. Trans. R. Soc. A.3692058–2072, http://doi.org/10.1098/rsta.2010.0341, 2011

Dlugokencky, E. J., Masarie, K., Lang, P. *et al.* Continuing decline in the growth rate of the atmospheric methane burden. Nature 393**,** 447–450. https://doi.org/10.1038/30934, 1998.

DVGW: Technische Regel – ArbeitsblattDVGW G 260 (A), Bonn. [online] Available from: https://shop.wvgw.de/var/assets/leseprobe/508866_lp G 260.pdf, 2013.

DVGW: Technische Regel-Arbeitsblatt; DVGW G465-1 (A). [online] Available from: https://shop.wvgw.de/var/assets/leseprobe//510544_lp_G 465-1_2019_05.pdf, 2018.

DVGW: Technische Mitteilungen Hinweis; DVGW G 465-3. [online] Available from: https://shop.wvgw.de/var/assets/leseprobe//510545_lp_G 465-3_2019_05.pdf, 2019a.

DVGW: Technischer Hinweis - Merkblatt; DVGW G465-4 (M). [online] Available from: https://shop.wvgw.de/var/assets/leseprobe//510546_lp_G 465-4_2019_05.pdf, 2019b.

DVGW: Technische Regel-Arbeitsblatt; DVGW G465-1 (A). [online] Available from: https://shop.wvgw.de/var/assets/leseprobe//510544_lp_G 465-1_2019_05.pdf. (last access: 15 December 2021), 2019c.

DVGW: High-performing infrastructure. [online] Available from https://www.dvgw.de/english-pages/topics/safety-and-security/technical-safety-gas, (last access: 25 January 2022), 2022.

Ebrahimi-Moghadam, A., Farzaneh-Gord, M., Arabkoohsar, A., Jabari Moghadam, A., CFD analysis of natural gas emission from damaged pipelines: Correlation development for leakage estimation, Cleaner Production, https://doi.org/10.1016/j.jclepro.2018.07.127, 2018.

EC: EU strategy to reduce methane emissionsavailable at: https://eur-lex.europa.eu/legal-content/EN/TXT/?uri=CELEX%3A52020DC0663&qid=1644853088591, (last access: 28 March 2022), 2020

EC: European Commission, EU strategy to reduce methane emissions, available from: https://ec.europa.eu/energy/sites/ener/files/eu_methane_strategy.pdf, last access: 08 April 2022, 2020.

EDF: Local leaks impact global climate, [online] Available from: https://www.edf.org/climate/methanemaps (Accessed 5 November 2019), 2019.

Efron, B.: Bootstrap Methods: Another Look at the Jackknife, Ann. Stat., 7(1), 1–26, https://doi.org/10.1214/aos/1176344552, 1979.

Efron, B.: The Jackknife, the Bootstrap and Other Resampling Plans, Society for Industrial and Applied Mathematics., 1982.

Efron, B. and Tibshirani, R. J.: An Introduction to the Bootstrap, Champman & Hall, London., 1993.

Ehhalt, D.H., Schmidt, U. Sources and sinks of atmospheric methane. *PAGEOPH* **116,** 452–464. https://doi.org/10.1007/BF01636899, 1978.

Ehhalt, D. H., and M. Prather, Atmospheric chemistry and greenhouse gases, in Climate Change 2001: The Scientific Basis, pp. 245–287, Cambridge Univ. Press, New York., 2001.

Ehhalt, D., Prather, M., Dentener, F., Derwent, R., Dlugokencky, E., Holland, E., Isaksen, I., Katima, J., Kirchhoff, V., Matson, P., Midgley, P., Wang, M., Berntsen, T., Bey, I., Brasseur, G., Buja, L., Collins, W.J., Daniel, J., DeMore, W.B., Derek, N., Dickerson, R., Etheridge, D., Feichter, J., Fraser, P., Friedl, R., Fuglestvedt, J., Gauss, M., Grenfell, L., Grübler, A., Harris, N., Hauglustaine, D., Horowitz, L., Jackman, C., Jacob, D., Jaeglé, L., Jain, A., Kanakidou, M., Karlsdottir, S., Ko, M., Kurylo, M., Lawrence, M., Logan, J. A., Manning, M., Mauzerall, D., McConnell, J., Mickley, L., Montzka, S., Müller, J. F., Olivier, J., Pickering, K., Pitari, G., Roelofs, G. J., Rogers, H., Rognerud, B., Smith, S., Solomon, S., Staehelin, J., Steele, P., Stevenson, D., Sundet, J., Thompson, A., van Weele, M., von Kuhlmann, R., Wang, Y., Weisenstein, D., Wigley, T., Wild, O., Wuebbles, D., Yantosca, R., Atmospheric Chemistry and Greenhouse Gases, [online], Available from: https://www.ipcc.ch/site/assets/uploads/2018/03/TAR-04.pdf, 2018.

EIA, Carbon Dioxide Emissions Coefficients , available at: https://www.eia.gov/environment/emissions/co2_vol_mass.php, (last access: 28 March 2022), 2021.

EPA, Methane emissions from the natural gas industry: underground pipelines, https://www.epa.gov/sites/production/files/2016-08/documents/9_underground.pdf, 1996.

EPA: Draft Inventory of US greenhouse gas emissions and sinks, Available from: https://www.epa.gov/system/files/documents/2022-02/us-ghg-inventory-2022-main-text.pdf, last access: 11 April 2022, 2022.

EPA: Inventory of US Greenhouse Gas Emissions and Sinks: 1990–2018, U.S. Environmental Protection Agency (EPA), available at: https://www.epa.gov/ghgemissions/inventory-us-greenhouse-gas-emissions-and-sinks-1990-2018, 2020.

EPA: User's guide for the industrial source guide complex (ISC3) dispersion models, volume II - Description of model algorithms., 1995.

Etheridge, D. M., Steele, L. P., Francey, R. J. and Langenfeld, R. L.: Atmospheric methane between 1000 A.D. and present: Evidence of anthropogenic emissions and climatic variability, J. Geophys. Res., 103, 979–993, https://doi.org/0148-0227/98/98JD-00923, 1998.

Etminan, M., Myhre, G., Highwood, E. J., and Shine, K. P., Radiative forcing of carbon dioxide, methane, and nitrous oxide: A significant revision of the methane radiative forcing, *Geophys. Res. Lett.*, 43, 12,614– 12,623, doi:10.1002/2016GL071930, 2016.

Evans, M., Roshchanka, V.: Russian policy on methane emissions in the oil and gas sector: A case study in opportunities and challenges in reducing short-lived forcers, Atmospheric Environment, 92, 199-206, https://doi.org/10.1016/j.atmosenv.2014.04.026, 2014

Federal Environment Agency: National Inventory Report for the German Greenhouse Gas Inventory 1990 – 2017. [online] Available from: https://unfccc.int/documents/194930, 2019.

Federal Environment Agency: National Inventory Report for the German Greenhouse Gas Inventory 1990 – 2018, available at: https://unfccc.int/documents/226313 (last access: 30 March 2022), 2020.

Fernandez, J. M., Maazallahi, H., France, J. L., Menoud, M., Corbu, M., Ardelean, M., Calcan, A., Townsend-Small, A., van der Veen, C., Fisher, R. E., Lowry, D., Nisbet, E.G., Röckmann, T.: Street-level methane emissions of Bucharest, Romania and the dominance of urban wastewater., Atmospheric Environment: X, 13, 2590-1621, 100153, https://doi.org/10.1016/j.aeaoa.2022.100153, 2022.

Fiehn, A., Kostinek, J., Eckl, M., Klausner, T., Gałkowski, M., Chen, J., Gerbig, C., Röckmann, T., Maazallahi, H., Schmidt, M., Korbeń, P., Nęcki, J., Jagoda, P., Wildmann, N., Mallaun, C., Bun, R., Nickl, A.-L., Jöckel, P., Fix, A., and Roiger, A.: Estimating CH_4, CO_2 and CO emissions from coal mining and industrial activities in the Upper Silesian Coal Basin using an aircraft-based mass balance approach, Atmos. Chem. Phys., 20, 12675–12695, https://doi.org/10.5194/acp-20-12675-2020, 2020.

Fischer, M. L.; Chan, W. R.; Delp, W.; Jeong, S.; Rapp, V.; Zhu, Z. An Estimate of Natural Gas Methane Emissions from California Homes. Environ. Sci. Technol. 52, 10205– 10213, https://doi.org/10.1021/acs.est.8b03217, 2018.

Fisher, R. E., Sriskantharajah, S., Lowry, D., Lanoisellé, M., Fowler, C. M. R., James, R. H., Hermansen, O., Lund Myhre, C., Stohl, A., Greinert, J., Nisbet-Jones, P. B. R., Mienert, J. and Nisbet, E. G.: Arctic methane sources: Isotopic evidence for atmospheric inputs, Geophys. Res. Lett., 38(21), n/a-n/a, https://doi.org/10.1029/2011GL049319, 2011.

Fisher, R., Lowry, D., Wilkin, O., Sriskantharajah, S. and Nisbet, E. G.: High-precision, automated stable isotope analysis of atmospheric methane and carbon dioxide using continuous-flow isotope-ratio mass spectrometry, Rapid Commun. Mass Spectrom., 20(2), 200–208, https://doi.org/10.1002/rcm.2300, 2006.

Formolo, M.: The Microbial Production of Methane and Other Volatile Hydrocarbons, in Handbook of Hydrocarbon and Lipid Microbiology, pp. 113–126, Springer Berlin Heidelberg., 2010.

Forster, P., V. Ramaswamy, P. Artaxo, T. Berntsen, R. Betts, D.W. Fahey, J. Haywood, J. Lean, D.C. Lowe, G. Myhre, J. Nganga, R. Prinn, G. Raga, M. Schulz and R. Van Dorland, 2007: Changes in Atmospheric Constituents and in Radiative Forcing. In: Climate Change 2007: The Physical Science Basis. Contribution of Working Group I to the Fourth Assessment Report of the Intergovernmental Panel on Climate Change [Solomon, S., D. Qin, M. Manning, Z. Chen, M. Marquis, K.B. Averyt, M.Tignor and H.L. Miller (eds.)]. Cambridge University Press,

Cambridge, United Kingdom and New York, NY, USA. [online]. Available from: https://www.ipcc.ch/site/assets/uploads/2018/02/ar4-wg1-chapter2-1.pdf

France, J. L., Cain, M., Fisher, R. E., Lowry, D., Allen, G., O'Shea, S. J., Illingworth, S., Pyle, J., Warwick, N., Jones, B. T., Gallagher, M. W., Bower, K., Le Breton, M., Percival, C., Muller, J., Welpott, A., Bauguitte, S., George, C., Hayman, G. D., Manning, A. J., Myhre, C. L., Lanoisellé, M. and Nisbet, E. G.: Measurements of $\delta^{13}C$ in CH 4 and using particle dispersion modeling to characterize sources of Arctic methane within an air mass, J. Geophys. Res. Atmos., 121(23), 14,257-14,270, https://doi.org/10.1002/2016JD026006, 2016.

Fredenslund, A. M., Rees-White, T. C., Beaven, R. P., Delre, A., Finlayson, A., Helmore, J., Allen, G., Scheutz, C.: Validation and error assessment of the mobile tracer gas dispersion method for measurement of fugitive emissions from area sources, Waste Management, 83, 68-78, https://doi.org/10.1016/j.wasman.2018.10.036, 2019.

Fredenslund, A.M., Scheutz, C., Kjeldsen, P.:. Tracer method to measure landfill gas emissions from leachate collection systems, Waste Management, 30, 2146-2152, https://doi.org/10.1016/j.wasman.2010.03.013, 2010

Fries, A. E., Schifman, L. A., Shuster, W. D. and Townsend-Small, A.: Street-level emissions of methane and nitrous oxide from the wastewater collection system in Cincinnati, Ohio, Environ. Pollut., 236, 247–256, https://doi.org/10.1016/j.envpol.2018.01.076, 2018.

Fukuda, H., Fujii, T. and Ogawa, T.: Microbial Production of C 2 -Hydrocarbons, Ethane, Ethylene and Acetylene, Agric. Biol. Chem., 48(5), 1363–1365, https://doi.org/10.1080/00021369.1984.10866323, 1984.

Gallagher, M. E., Down, A., Ackley, R. C., Zhao, K., Phillips, N. and Jackson, R. B.: Natural Gas Pipeline Replacement Programs Reduce Methane Leaks and Improve Consumer Safety, Environ. Sci. Technol. Lett., 2(10), 286–291, https://doi.org/10.1021/acs.estlett.5b00213, 2015.

GERG, Methane emission estimation method for the gas distribution grid (2018). [online] Available from: https://www.gerg.eu/wp-content/uploads/2020/04/MEEM_Final_report.pdf. (Last Accessed: 25 January 2022)

GERG, Methane Emission Estimation Method for the Gas Distribution Grid (MEEM) (2020). [online], Available from: https://www.gerg.eu/wp-content/uploads/2020/04/MEEM_Final_report.pdf. (Last Accessed: 09 February 2022)

Ghadaksaz, H., Saboohi, H.: Energy supply transformation pathways in Iran to reduce GHG emissions in line with the Paris Agreement, Energy Strategy Reviews, 32, https://doi.org/10.1016/j.esr.2020.100541, 2020.

Gioli, B., Toscano, P., Lugato, E., Matese, A., Miglietta, F., Zaldei, A., and Vaccari, F. P.: Methane and carbon dioxide fluxes and source partitioning in urban areas: The case study of Florence, Italy, Environ. Pollut., 164, 125–131, https://doi.org/10.1016/j.envpol.2012.01.019, 2012.

Gogu, C.R., Gaitanaru, D., Boukhemacha, M.A., Serpescu, I., Litescu, L., Zaharia, V., Moldovan, A., Mihailovici, M.J., 2017. Urban hydrogeology studies in Bucharest City, Romania. Procedia Eng. 209, 135–142. https://doi.org/10.1016/j.proeng.2017.11.139.

Gollakota, K. G. and Jayalakshmi, B.: Biogas (natural gas?) production by anaerobic digestion of oil cake by a mixed culture isolated from cow dung, Biochem. Biophys. Res. Commun., 110(1), 32–35, https://doi.org/10.1016/0006-291X(83)91255-X, 1983.

Guisasola, A., de Haas, D., Keller, J. and Yuan, Z.: Methane formation in sewer systems, Water Res., 42(6–7), 1421–1430, https://doi.org/10.1016/j.watres.2007.10.014, 2008.

Han, Z.Y., Weng, W.G., 2010. An integrated quantitative risk analysis method for natural gas pipeline network. J. Loss Prev. Process Ind. 23, 428–436. https://doi.org/10.1016/j.jlp.2010.02.003.

Harrison, M.R., Shires, T.M., Wessels, J.K., Cowgill, R.M., 1996. Methane Emissions from the Natural Gas Industry. Gas Research Institute/Environmental Protection Agency Chicago.

Heilig, G. K.: The greenhouse gas methane (CH4): Sources and sinks, the impact of population growth, possible interventions, Popul. Environ., 16(2), 109–137, https://doi.org/10.1007/BF02208779, 1994.

Helfter, C., Tremper, A. H., Halios, C. H., Kotthaus, S., Bjorkegren, A., Sue, C., Grimmond, B., Barlow, J. F., and Nemitz, E.: Spatial and temporal variability of urban fluxes of methane, carbon monoxide and carbon dioxide above London, UK, Atmos. Chem. Phys., 16, 10543–10557, https://doi.org/10.5194/acp-16-10543-2016, 2016.

Helmig, D., Rossabi, S., Hueber, J., Tans, P., Montzka, S. A., Masarie, K., Thoning, K., Plass-Duelmer, C., Claude, A., Carpenter, L. J., Lewis, A. C., Punjabi, S., Reimann, S., Vollmer, M. K., Steinbrecher, R., Hannigan, J. W., Emmons, L. K., Mahieu, E., Franco, B., Smale, D. and Pozzer, A.: Reversal of global atmospheric ethane and propane trends largely due to US oil and natural gas production, Nat. Geosci., 9(7), 490–495, https://doi.org/10.1038/ngeo2721, 2016.

Hendrick, M. F., Ackle, R., Sanaie-Movahed, B., Tang, X., Phillips, N. G., Fugitive methane emissions from leak-prone natural gas distribution infrastructure in urban environments, Environmental Pollution, https://doi.org/10.1016/j.envpol.2016.01.094, 2016.

Hmiel, B., Petrenko, V. V, Dyonisius, M. N., Buizert, C., Smith, A. M., Place, P. F., Harth, C., Beaudette, R., Hua, Q., Yang, B., Vimont, I., Michel, S. E., Severinghaus, J. P., Etheridge, D., Bromley, T., Schmitt, J., Faïn, X., Weiss, R. F. and Dlugokencky, E.: Preindustrial 14 CH 4 indicates greater anthropogenic fossil CH 4 emissions, Nature, 578, https://doi.org/10.1038/s41586-020-1991-8, 2020.

Hoesly, R. M., Smith, S. J., Feng, L., Klimont, Z., Janssens-Maenhout, G., Pitkanen, T., Seibert, J. J., Vu, L., Andres, R. J., Bolt, R. M., Bond, T. C., Dawidowski, L., Kholod, N., Kurokawa, J.-I., Li, M., Liu, L., Lu, Z., Moura, M. C. P., O'Rourke, P. R., and Zhang, Q.: Historical (1750–2014) anthropogenic emissions of reactive gases and aerosols from the Community Emissions Data System (CEDS), Geosci. Model Dev., 11, 369–408, https://doi.org/10.5194/gmd-11-369-2018, 2018.

Hoheisel, A., Yeman, C., Dinger, F., Eckhardt, H. and Schmidt, M.: An improved method for mobile characterisation of δ 13 CH 4 source signatures and its application in Germany, Atmos. Meas. Tech., 12(2), 1123–1139, https://doi.org/10.5194/amt-12-1123-2019, 2019.

Hopkins, F.M., Ehleringer, J.R., Bush, S.E., Duren, R.M., Miller, C.E., Lai, C.-T., Hsu, Y.-K., Carranza, V. and Randerson, J.T., Mitigation of methane emissions in cities: How new measurements and partnerships can contribute to emissions reduction strategies. Earth's Future, 4: 408-425. https://doi.org/10.1002/2016EF000381, 2016a.

Hopkins, F. M., Kort, E. A., Bush, S. E., Ehleringer, J. R., Lai, C.-T., Blake, D. R. and Randerson, J. T.: Spatial patterns and source attribution of urban methane in the Los Angeles Basin, J. Geophys. Res. Atmos., 121(5), 2490–2507, https://doi.org/10.1002/2015JD024429, 2016b.

Hou, Q., Yang, D., Li, X., Xiao, G. and Ho, S. C. M., Modified Leakage Rate Calculation Models of NaturalGas Pipelines, Mathematical Problems in Engineering, https://doi.org/10.1155/2020/6673107, 2020.

Howarth, R.W., Santoro, R. & Ingraffea, A. Methane and the greenhouse-gas footprint of natural gas from shale formations. Climatic Change 106, 679. https://doi.org/10.1007/s10584-011-0061-5, 2011.

Howarth, R. W.: A bridge to nowhere: methane emissions and the greenhouse gas footprint of natural gas, *Energy Science and Engineering* 2014; 2 (2): 47–60, https://doi.org/10.1002/ese3.35, 2014.

Howarth, R. W.: Ideas and perspectives: is shale gas a major driver of recent increase in global atmospheric methane?, Biogeosciences, 16, 3033–3046, https://doi.org/10.5194/bg-16-3033-2019, 2019.

Hu, N., Liu, S., Gao, Y., Xu, J., Zhang, X., Zhang, Z. and Lee, X.: Large methane emissions from natural gas vehicles in Chinese cities, Atmos. Environ., 187, 374–380, https://doi.org/10.1016/j.atmosenv.2018.06.007, 2018.

Iacoboaea, C., Petrescu, F. Landfill monitoring using remote sensing: A case study of Glina, Romania. Waste Manag. Res. 31, 1075–1080. https://doi.org/10.1177/0734242X13487585, 2013.

Ianoş, I., Sorensen, A., Merciu, C. Incoherence of urban planning policy in Bucharest: Its potential for land use conflict. Land use policy 60, 101–112. https://doi.org/10.1016/j.landusepol.2016.10.030, 2016.

Ianoş, I., Zamfir, D., Stoica, V., Cercleux, L., Schvab, A., Pascariu, G. Municipal solid waste management for sustainable development of Bucharest metropolitan area. Environ. Eng. Manag. J. 11, 359–369. https://doi.org/10.30638/eemj.2012.045, 2012.

IPCC: Guidelines for national greenhouse inventories. [online] Available from: https://www.ipcc-nggip.iges.or.jp/public/gl/guidelin/ch1ref8.pdf, 1996.

IPCC: Climate Change 2014: Mitigation of Climate Change. Contribution of Working Group III to the Fifth Assessment Report of the Intergovernmental Panel on Climate Change. Edenhofer, O., R. Pichs- Madruga, Y. Sokona, E. Farahani, S. Kadner, K. Seyboth, A. Adler, I. Baum, S. Brunner, P. Eickemeier, B. Kriemann, J. Savolainen, S. Schlömer, C. von Stechow, T. Zwickel and J.C. Minx (eds.). Cambridge University Press, 2014.

IPCC: Refinement to the 2006 IPCC Guidelines for National Greenhouse Gas Inventories, Available from: https://www.ipcc.ch/report/2019-refinement-to-the-2006-ipcc-guidelines-for-national-greenhouse-gas-inventories/, last access: 07 April 2022, 2019.

Jackson, S.M., Morgan, G.H., Morse, A.D., Butterworth, A.L., Pillinger, C.T. The use of static mass spectrometry to determine the combined stable isotopic composition of small samples of atmospheric methane. Rapid Commun. Mass Spectrom. 13, 1329–1333. https://doi.org/10.1002/(SICI)1097-0231(19990715)13:13<1329::AID-RCM648>3.0.CO;2-P, 1999.

Jackson, R. B., Down, A., Phillips, N. G., Ackley, R. C., Cook, C. W., Plata, D. L. and Zhao, K.: Natural gas pipeline leaks across Washington, DC, Environ. Sci. Technol., 48(3), 2051–2058, https://doi.org/10.1021/es404474x, 2014.

Jackson, R. B., Saunois, M., Bousquet, P., Canadell, J. C., Poulter, B., Stavert, A. R., Bergamaschi, P., Niwa, Y., Segers, A., and Tsuruta, A.: Increasing anthropogenic methane emissions arise equally from agricultural and fossil fuel sources, 15, 071002, https://10.1088/1748-9326/ab9ed2, 2020

James, A.T., 1983. Correlation of Natural Gas By Use of Carbon Isotopic Distribution Between Hydrocarbon Components. Am. Assoc. Pet. Geol. Bull. 67, 1176–1191. https://doi.org/10.1306/03B5B722-16D1-11D7-8645000102C1865D.

Janssens-Maenhout, G., Crippa, M., Guizzardi, D., Muntean, M., Schaaf, E., Dentener, F., Bergamaschi, P., Pagliari, V., Olivier, J. G. J., Peters, J. A. H. W., van Aardenne, J. A., Monni, S., Doering, U., Petrescu, A. M. R., Solazzo, E., and Oreggioni, G. D.: EDGAR v4.3.2 Global Atlas of the three major greenhouse gas emissions for the period 1970–2012, Earth Syst. Sci. Data, 11, 959–1002, https://doi.org/10.5194/essd-11-959-2019, 2019.

Josep G. Canadell, J. G., P. M. S. Monteiro, M. H. Costa, L. Cotrim da Cunha, P. M. Cox, A. V. Eliseev, S. Henson, M. Ishii, S. Jaccard, C. Koven, A. Lohila, P. K. Patra, S. Piao, J. Rogelj, S. Syampungani, S. Zaehle, K. Zickfeld, 2021, Global Carbon and other Biogeochemical Cycles and Feedbacks. In: Climate Change 2021: The Physical Science Basis. Contribution of Working Group I to the Sixth Assessment Report of the Intergovernmental Panel on Climate Change [Masson-Delmotte, V., P. Zhai, A. Pirani, S. L. Connors, C. Péan, S. Berger, N. Caud, Y. Chen, L. Goldfarb, M. I. Gomis, M. Huang, K. Leitzell, E. Lonnoy, J.B.R. Matthews, T. K. Maycock, T. Waterfield, O. Yelekçi, R. Yu and B. Zhou (eds.)]. Cambridge University Press. In Press.

Karion, A., Sweeney, C., Pétron, G., Frost, G., Michael Hardesty, R., Kofler, J., Miller, B. R., Newberger, T., Wolter, S., Banta, R., Brewer, A., Dlugokencky, E., Lang, P., Montzka, S. A., Schnell, R., Tans, P., Trainer, M., Zamora, R. and Conley, S.: Methane emissions estimate from

airborne measurements over a western United States natural gas field, Geophys. Res. Lett., 40(16), 4393–4397, https://doi.org/10.1002/grl.50811, 2013.

Keeling, C. D.: The concentration and isotopic abundances of atmospheric carbon dioxide in rural areas, Geochim. Cosmochim. Acta, 13(4), 322–334, https://doi.org/10.1016/0016-7037(58)90033-4, 1958.

Keeling, C. D.: The concentration and isotopic abundances of carbon dioxide in rural and marine air, Geochim. Cosmochim. Acta, 24(3–4), 277–298, https://doi.org/10.1016/0016-7037(61)90023-0, 1961.

Keyes, T., Ridge G., Klein, M., Phillips, N., Ackley, R., Yang Y., An enhanced procedure for urban mobile methane leak detection. Heliyon. 9; 6 (10):e04876. https://doi.org/10.1016/j.heliyon.2020.e04876, 2020.

Kilkiş, Ş., 2016. Sustainable development of energy, water and environment systems index for Southeast European cities. J. Clean. Prod. 130, 222–234. https://doi.org/10.1016/j.jclepro.2015.07.121.

Kirchgessner, D. A., Lott R. A., Cowgill, R.M., Harrison, M. R., Shires, T. M., Estimate of methane emissions from the U.S. natural gas industry, Chemosphere, https://doi.org/10.1016/S0045-6535(97)00236-1, 1997.

Kirschke, S., Bousquet, P., Ciais, P., Saunois, M., Canadell, J. G., Dlugokencky, E. J., Bergamaschi, P., Bergmann, D., Blake, D. R., Bruhwiler, L., Cameron-Smith, P., Castaldi, S., Chevallier, F., Feng, L., Fraser, A., Heimann, M., Hodson, E. L., Houweling, S., Josse, B., Fraser, P. J., Krummel, P. B., Lamarque, J-F., Langenfelds, R. L., Quéré, C. L., Naik, V., O'Doherty, S., Palmer, P. I., Pison, I., Plummer, D., Poulter, B., Prinn, R. G., Rigby, M., Ringeval, B., Santini, M., Schmidt, M., Shindell, D. T., Simmpson, I. J., Spahni, R., Steele, L. P., Strode, S. A., Sudo, K., Szopa, S., Van der Werf, G. R., Voulgarakis, A., Van Weele, M., Weiss, R. F., Williamns, J. E., Zeng, G.: Three decades of global methane sources and sinks. Nature Geosci 6, 813–82. https://doi.org/10.1038/ngeo1955, 2013.

Kuc, T., Rozanski, K., Zimnoch, M., Necki, J.., Korus, A. Anthropogenic emissions of CO2 and CH4 in an urban environment. Appl. Energy 75, 193–203. https://doi.org/10.1016/S0306-2619(03)00032-1, 2003.

Kuenen, J. J. P., Visschedijk, A. J. H., Jozwicka, M., and Denier van der Gon, H. A. C.: TNO-MACC_II emission inventory; a multi-year (2003–2009) consistent high-resolution European emission inventory for air quality modelling, Atmos. Chem. Phys., 14, 10963–10976, https://doi.org/10.5194/acp-14-10963-2014, 2014.

Kuenen, J., Dellaert, S., Visschedijk, A., Jalkanen, J.-P., Super, I., and Denier van der Gon, H.: CAMS-REG-v4: a state-of-the-art high-resolution European emission inventory for air quality modelling, Earth Syst. Sci. Data, 14, 491–515, https://doi.org/10.5194/essd-14-491-2022, 2022.

Lamb, B. K., McManus, J. B., Shorter, J. H., Kolb, C. E., Mosher, B., Harriss, R. C., Allwine, E., Blaha, D., Howard, T., Guenther, A., Lott, R. A., Siverson, R., Westburg, H., and Zimmerman, P., Development of atmospheric tracer methods to measure methane emissions from natural gas facilities and urban areas, Environmental Science & Technology 29 (6), 1468-1479 https://doi.org/10.1021/es00006a007, 1995.

Lamb, B. K., Edburg, S. L., Ferrara, T. W., Howard, T., Harrison, M. R., Kolb, C. E., Townsend-Small, A., Dyck, W., Possolo, A., and Whetstone, J. R., Environmental Science & Technology 49 (8), 5161-5169 https://doi.org/10.1021/es505116p, 2015.

Lamb, B. K., Cambaliza, M. O. L., Davis, K. J., Edburg, S. L., Ferrara, T. W., Floerchinger, C., Heimburger, A. M. F., Herndon, S., Lauvaux, T., Lavoie, T., Lyon, D. R., Miles, N., Prasad, K. R., Richardson, S., Roscioli, J. R., Salmon, O. E., Shepson, P. B., Stirm, B. H. and Whetstone, J.: Direct and Indirect Measurements and Modeling of Methane Emissions in Indianapolis, Indiana, Environ. Sci. Technol., 50(16), 8910–8917, https://doi.org/10.1021/acs.est.6b01198, 2016.

LBEG: Geoinformation of Lower Saxony and Schleswig-Holstein, [online] Available from: https://nibis.lbeg.de/cardomap3/, 2018.

Lebel, E. D., Lu, H. S., Speizer, S. A., Finnegan, C. J. and Jackson, R. B.: Quantifying Methane Emissions from Natural Gas Water Heaters, Environ. Sci. Technol., 54(9), 5737–5745, https://doi.org/10.1021/acs.est.9b07189, 2020.

Lebel, E. D., Finnegan, C. J., Ouyang, Z., Jackson, R. B.: Methane and NO_x Emissions from Natural Gas Stoves, Cooktops, and Ovens in Residential Homes, *Environ. Sci. Technol.* 2022, 56, 4, 2529–2539, https://doi.org/10.1021/acs.est.1c04707, 2022.

Lin, Q. Vrieze, J.D., He, G., Li, X., Li, J., 2016. Temperature regulates methane production through the function centralization of microbial community in anerobic digestion. Bioresorce Tech. 216, 150-158. https://doi.org/10.1016/j.biortech.2016.05.046.

Liu, C., Liao, Y., Liang, J., Cui, Z., Li, Y., Quantifying methane release and dispersion estimations for buried natural gas pipeline leakages, Process Safety and Environmental Protection, https://doi.org/10.1016/j.psep.2020.11.031, 2021.

Liu, Y., Ni, B.J., Sharma, K.R., Yuan, Z., 2015. Methane emission from sewers. Sci. Total Environ. 524, 40-51. https://doi.org/10.1016/j.scitotenv.2015.04.029.

Lowry, D., Holmes, C. W., Rata, N. D., O'Brien, P., Nisbet, E. G. London methane emissions: Use of diurnal changes in concentration and δ 13 C to identify urban sources and verify inventories. J. Geophys. Res. Atmos. 106, 7427–7448. https://doi.org/10.1029/2000JD900601, 2001.

Lowry, D., Fisher, R. E., France, J. L., Coleman, M., Lanoisellé, M., Zazzeri, G., Nisbet, E. G., Shaw, J. T., Allen, G., Pitt, J. and Ward, R. S.: Environmental baseline monitoring for shale gas development in the UK: Identification and geochemical characterisation of local source emissions of methane to atmosphere, Sci. Total Environ., 708, 134600, https://doi.org/10.1016/j.scitotenv.2019.134600, 2020.

Luetschwager, E., von Fischer, J. C., Weller, Z. D., Characterizing detection probabilities of advanced mobile leak surveys: Implications for sampling effort and leak size estimation in natural gas distribution systems. Elementa: Science of the Anthropocene; 9 (1): 00143.https://doi.org/10.1525/elementa.2020.00143, 2021.

Luther, A., Kleinschek, R., Scheidweiler, L., Defratyka, S., Stanisavljevic, M., Forstmaier, A., Dandocsi, A., Wolff, S., Dubravica, D., Wildmann, N., Kostinek, J., Jöckel, P., Nickl, A.-L., Klausner, T., Hase, F., Frey, M., Chen, J., Dietrich, F., Nęcki, J., Swolkień, J., Fix, A., Roiger, A., and Butz, A.: Quantifying CH_4 emissions from hard coal mines using mobile sun-viewing Fourier transform spectrometry, Atmos. Meas. Tech., 12, 5217–5230, https://doi.org/10.5194/amt-12-5217-2019, 2019.

Luther, A., Kostinek, J., Kleinschek, R., Defratyka, S., Stanisavljevic, M., Forstmaier, A., Dandocsi, A., Scheidweiler, L., Dubravica, D., Wildmann, N., Hase, F., Frey, M. M., Chen, J., Dietrich, F., Necki, J., Swolkien, J., Knote, C., Vardag, S. N., Roiger, A., and Butz, A.: Observational constraints on methane emissions from Polish coal mines using a ground-based remote sensing network, Atmos. Chem. Phys. Discuss. [preprint], https://doi.org/10.5194/acp-2021-978, in review, 2021.

Lyon, D. R., Zavala-Araiza, D., Alvarez, R. A., Harriss, R., Palacios, V., Lan, X., Talbot, R., Lavoie, T., Shepson, P., Yacovitch, T. I., Herndon, S. C., Marchese, A. J., Zimmerle, D., Robinson, A. L. and Hamburg, S. P.: Constructing a Spatially Resolved Methane Emission Inventory for the Barnett Shale Region, Environ. Sci. Technol., 49(13), 8147–8157, https://doi.org/10.1021/es506359c, 2015.

Lyon, D. R., Alvarez, R. A., Zavala-Araiza, D., Brandt, A. R., Jackson, R. B. and Hamburg, S. P.: Aerial Surveys of Elevated Hydrocarbon Emissions from Oil and Gas Production Sites, Environ. Sci. Technol., 50(9), 4877–4886, https://doi.org/10.1021/acs.est.6b00705, 2016.

Ma, L., Cheng, L., Li, M., 2013. Quantitative risk analysis of urban natural gas pipeline networks using geographical information systems. J. Loss Prev. Process Ind. 26, 1183–1192. https://doi.org/10.1016/j.jlp.2013.05.001.

Maasakkers, J.D., Jacob, D.J., Sulprizio, M.P., Turner, A.J., Weitz, M., Wirth, T., Hight, C., DeFigueiredo, M., Desai, M., Schmeltz, R., Hockstad, L., Bloom, A.A., Bowman, K.W., Jeong, S., Fischer, M.L.: Gridded National Inventory of U.S. Methane Emissions, Environmental Science and Technology, 50 (23), pp. 13123-13133, https://doi.org/10.1021/acs.est.6b02878, 2016.

Maasakkers, J. D., Jacob, D. J., Sulprizio, M. P., Scarpelli, T. R., Nesser, H., Sheng, J., Zhang, Y., Lu, X., Bloom, A. A., Bowman, K. W., Worden, J. R., and Parker, R. J.: 2010–2015 North American methane emissions, sectoral contributions, and trends: a high-resolution inversion of GOSAT observations of atmospheric methane, Atmos. Chem. Phys., 21, 4339–4356, https://doi.org/10.5194/acp-21-4339-2021, 2021.

Maazallahi, H., Miandehy, M., Pakseresht, S.: Detecting methane emission using remote sensing imagery, Research and Technology Department of National Iranian Gas Company, 2017.

Maazallahi, H., Switching to the "Golden Age of Natural Gas" with a Focus on Shale Gas Exploitation: A Possible Bridge to Mitigate Climate Change?, Master degree thesis, 30 credits in Geo-Information and Earth Observation for Environmental Modelling and Management (GEM), Department of Physical Geography and Ecosystems Sciences, Lund University, 2015.

Maazallahi, H., Fernandez, J. M., Menoud, M., Zavala-Araiza, D., Weller, Z. D., Schwietzke, S., von Fischer, J. C., Denier van der Gon, H., and Röckmann, T.: MATLAB® code for evaluation of Urban Surveys, Zenodo, https://doi.org/10.5281/zenodo.3928972, 2020a.

Maazallahi, H., Fernandez, J. M., Menoud, M., Zavala-Araiza, D., Weller, Z. D., Schwietzke, S., von Fischer, J. C., Denier van der Gon, H., and Röckmann, T.: Utrecht and Hamburg city measurements data, ICOS, https://doi.org/10.18160/RAJS-KZZQ, 2020b.

Maazallahi, H., Fernandez, J. M., Menoud, M., Zavala-Araiza, D., Weller, Z. D., Schwietzke, S., von Fischer, J. C., Denier van der Gon, H. and Röckmann, T.: Virtual Tour of Urban Surveys in Utrecht, NL, and Hamburg, DE, TIB AV-Portal, https://doi.org/10.5446/49902, 2020c.

Maazallahi, H., Fernandez, J. M., Menoud, M., Zavala-Araiza, D., Weller, Z. D., Schwietzke, S., von Fischer, J. C., Denier van der Gon, H., and Röckmann, T.: Methane mapping, emission quantification, and attribution in two European cities: Utrecht (NL) and Hamburg (DE), Atmos. Chem. Phys., 20, 14717–14740, https://doi.org/10.5194/acp-20-14717-2020, 2020d.

MacFarling Meure, C., Etheridge, D., Trudinger, C., Steele, P., Langenfelds, R., van Ommen, T., Smith, A. and Elkins, J.: Law Dome CO_2 , CH_4 and N_2O ice core records extended to 2000 years BP, Geophys. Res. Lett., 33(14), L14810, https://doi.org/10.1029/2006GL026152, 2006.

Mahgerefteh, H., Oke, A., Atti, O., Modelling outflow following rupture in pipeline networks, Chemical Engineering Science, https://doi.org/10.1016/j.ces.2005.10.013, 2006.

Mays, K.L., Shepson, P.B., Stirm, B.H., Karion, A., Sweeney, C., Gurney, K.R., 2009. Aircraft-based measurements of the carbon footprint of Indianapolis. Environ. Sci. Technol. 43, 7816–7823. https://doi.org/10.1021/es901326b.

McDuffie, E. E., Smith, S. J., O'Rourke, P., Tibrewal, K., Venkataraman, C., Marais, E. A., Zheng, B., Crippa, M., Brauer, M., and Martin, R. V.: A global anthropogenic emission inventory of atmospheric pollutants from sector- and fuel-specific sources (1970–2017): an application of the Community Emissions Data System (CEDS), Earth Syst. Sci. Data, 12, 3413–3442, https://doi.org/10.5194/essd-12-3413-2020, 2020.

McKain, K., Down, A., Raciti, S. M., Budney, J., Hutyra, L. R., Floerchinger, C., Herndon, S. C., Nehrkorn, T., Zahniser, M. S., Jackson, R. B., Phillips, N. and Wofsy, S. C.: Methane emissions

from natural gas infrastructure and use in the urban region of Boston, Massachusetts, Proc. Natl. Acad. Sci., 112(7), 1941–1946, https://doi.org/10.1073/PNAS.1416261112, 2015.

MEEM, Analysing the Methods for Determination of Methane Emissions of the Gas Distribution Grid (2022). [online] Available from https://www.dbi-gut.de/emissions.html. (Last Accessed: 25 January 2022).

Menoud, M., van der Veen, C., Scheeren, B., Chen, H., Szénási, B., Morales, R.P., Pison,I., Bousquet, P., Brunner, D., and Röckmann, T. Characterisation of methane sources in Lutjewad, the Netherlands, using quasi-continuous isotopic composition measurements. Tellus B: Chemical and Physical Meteorology, https://doi.org/10.1080/16000889.2020.1823733, 2020.

Menoud, M., van der Veen, C., Necki, J., Bartyzel, J., Szénási, B., Stanisavljević, M., Pison, I., Bousquet, P., and Röckmann, T.: Methane (CH4) sources in Krakow, Poland: insights from isotope analysis, Atmos. Chem. Phys., 21, 13167–13185, https://doi.org/10.5194/acp-21-13167-2021, 2021.

Merrin, Z.; Francisco, P. W. Unburned Methane Emissions from Residential Natural Gas Appliances. Environ. Sci. Technol. 53, 5473– 5482, https://doi.org/10.1021/acs.est.8b05323, 2019.

Milkov, A.V., Schwietzke, S., Allen, G. *et al.* Using global isotopic data to constrain the role of shale gas production in recent increases in atmospheric methane. *Sci Rep* **10,** 4199 (2020). https://doi.org/10.1038/s41598-020-61035-w

Miller, S.M., Wofsy, S.C., Michalak, A.M., Kort, E.A., Andrews, A.E., Biraud, S.C., Dlugokencky, E.J., Eluszkiewicz, J., Fischer, M.L., Janssens-Maenhout, G., Miller, B.R., Miller, J.B., Montzka, S.A., Nehrkorn, T., Sweeney, C., 2013. Anthropogenic emissions of methane in the United States. Proc. Natl. Acad. Sci. U. S. A. 110, 20018–20022. https://doi.org/10.1073/pnas.1314392110.

Mischler, J.A., Sowers, T.A., Alley, R.B., Battle, M., McConnell, J.R., Mitchell, L., Popp, T., Sofen, E., Spencer, M.K., 2009. Carbon and hydrogen isotopic composition of methane over the last 1000 years. Global Biogeochem. Cycles 23, n/a-n/a. https://doi.org/10.1029/2009GB003460.

Mitchell, A. L., Tkacik, D. S., Roscioli, J. R., Herndon, S. C., Yacovitch, T. I., Martinez, D. M., Vaughn, T. L., Williams, L. L., Sullivan, M. R., Floerchinger, C., Omara, M., Subramanian, R., Zimmerle, D., Marchese, A. J. and Robinson, A. L.: Measurements of Methane Emissions from Natural Gas Gathering Facilities and Processing Plants: Measurement Results, Environ. Sci. Technol., 49(5), 3219–3227, doi:10.1021/es5052809, 2015.

Moloudi, R., Abolfazli Esfahani, J., Modeling of gas release following pipeline rupture: Proposing non-dimensional correlation, Journal of Loss Prevention in the Process Industries, https://doi.org/10.1016/j.jlp.2014.09.003, 2014.

Mønster, J. G., Samuelsson, J., Kjeldsen, P., Rella, C. W., Scheutz, C., Quantifying methane emission from fugitive sources by combining tracer release and downwind measurements – A sensitivity analysis based on multiple field surveys, Waste Management,34, 1416-1428, https://doi.org/10.1016/j.wasman.2014.03.025, 2014.

Myhre, G., Shindell, D., Bréon, F. M., Collins, W., Fuglestvedt, J., Huang, J., Koch, D., Lamarque, J. F., Lee, D., Mendoza, B., Nakajima, T., Robock, A., Stephens, G., Takemura, T., and Zhan, H.: Anthropogenic and Natural Radiative Forc-ing, in: Climate Change 2013: The Physical Science Basis, Contribution of Working Group I to the Fifth Assessment Report of the Intergovernmental Panel on Climate Change, Cambridge, UK and New York, NY, USA, available at: https://www.ipcc.ch/site/assets/uploads/2018/02/WG1AR5_Chapter08_FINAL.pdf, 2013.

Nae, M., Turnock, D. The new Bucharest: Two decades of restructuring. Cities 28, 206–219. https://doi.org/10.1016/j.cities.2010.04.004, 2011.

Naik, V., Szopa, S., Adhikary, B., Artaxo, P., Berntsen, T., Collins, W. D., Fuzzi, S., Gallardo, L., Kiendler Scharr, A., Klimont, A., Liao, H., Unger, N., Zanis, P., 2021, Short-Lived Climate Forcers. In: Climate Change 2021: The Physical Science Basis. Contribution of Working Group

I to the Sixth Assessment Report of the Intergovernmental Panel on Climate Change [Masson-Delmotte, V., Zhai, P., Pirani, A., Connors, S. L., Péan, C., Berger, S., Caud, N., Chen, Y., Goldfarb, L., Gomis, M. I., Huang, M., Leitzell, K., Lonnoy, E., Matthews, J. B. R., Maycock, T. K., Waterfield, T., Yelekçi, O., Yu, R., and Zhou, B. (eds.)]. Cambridge University, Press. 2022.

Naik, V., Voulgarakis, A., Fiore, A. M., Horowitz, L. W., Lamarque, J.-F., Lin, M., Prather, M. J., Young, P. J., Bergmann, D., Cameron-Smith, P. J., Cionni, I., Collins, W. J., Dalsøren, S. B., Doherty, R., Eyring, V., Faluvegi, G., Folberth, G. A., Josse, B., Lee, Y. H., MacKenzie, I. A., Nagashima, T., van Noije, T. P. C., Plummer, D. A., Righi, M., Rumbold, S. T., Skeie, R., Shindell, D. T., Stevenson, D. S., Strode, S., Sudo, K., Szopa, S., and Zeng, G.: Preindustrial to present-day changes in tropospheric hydroxyl radical and methane lifetime from the Atmospheric Chemistry and Climate Model Intercomparison Project (ACCMIP), Atmos. Chem. Phys., 13, 5277–5298, https://doi.org/10.5194/acp-13-5277-2013, 2013. Nam, E. K., Jensen, T. E., and Wallington, T. J.: Methane Emissions from Vehicles, Environ. Sci. Technol., https://doi.org/10.1021/ES034837G, 2004.

National Institute for Statistics (NIS) Romania, 2020. TEMPO-Online. ©The National Institute of Statistics ROMANIA 1998 – 2018. Contains public information based on Open Government License v1.0. http://statistici.insse.ro:8077/tempoonline/#/pages/ tables/insse-table.

Naus, S., Röckmann, T. and Popa, M. E.: The isotopic composition of CO in vehicle exhaust, Atmos. Environ., 177, 132–142, https://doi.org/10.1016/J.ATMOSENV.2018.01.015, 2018.

Neumann, G. and Halbritter, G.: Sensitivity analysis of the Gaussian plume model, in Studies in Environmental Science, vol. 8, pp. 57–62, Elsevier., 1980.

Nisbet, E. G., Manning, M. R., Dlugokencky, E. J., Fisher, R. E., Lowry, D., Michel, S. E., Myhre, C. L., Platt, S. M., Allen, G., Bousquet, P., Brownlow, R., Cain, M., France, J. L., Hermansen, O., Hossaini, R., Jones, A. E., Levin, I., Manning, A. C., Myhre, G., Pyle, J. A., Vaughn, B. H., Warwick, N. J., White, J. W. C., Very strong atmospheric methane growth in the 4 Years 2014–2017: implications for the Paris agreement, Global Biogeochemical Cycles, 33, 318 – 342, https://doi.org/10.1029/2018GB006009, 2019.

Nisbet, E.G., Fisher, R.E., Lowry, D., France, J.L., Allen, G., Bakkaloglu, S., Broderick, T.J., Cain, M., Coleman, M., Fernandez, J., Forster, G., Griffiths, P.T., Iverach, C.P., Kelly, B.F.J., Manning, M.R., Nisbet-Jones, P.B.R., Pyle, J.A., Townsend-Small, A., Al-Shalaan, A., Warwick, N., Zazzeri, G. Methane Mitigation: Methods to Reduce Emissions, on the Path to the Paris Agreement. Rev. Geophys. 58, 1–51. https://doi.org/10.1029/2019RG000675, 2020.

Nita, R., 2018. World's first oil refinery: the city of Ploiești. World Recor Acad. LLC 1–7.

NOAA: Trends in Atmospheric Methane, Available from: https://gml.noaa.gov/ccgg/trends_ch4/, last access: 05 April 2022, 2022.

Noorollahi, Y., Lund, H., Nielsen, S., Zinck Thellufsen, J.: Energy transition in petroleum rich nations: Case study of Iran, 3, 100026, https://doi.org/10.1016/j.segy.2021.100026, 2021.

Noël, S., Weigel, K., Bramstedt, K., Rozanov, A., Weber, M., Bovensmann, H. and Burrows, J. P.: Water vapour and methane coupling in the stratosphere observed using SCIAMACHY solar occultation measurements, Atmos. Chem. Phys., 18(7), 4463–4476, doi:10.5194/acp-18-4463-2018, 2018.

O'Shea, S. J., Allen, G., Fleming, Z. L., Bauguitte, S. J.-B., Percival, C. J., Gallagher, M. W., Lee, J., Helfter, C., and Nemitz, E.: Area fluxes of carbon dioxide, methane, and carbon monoxide derived from airborne measurements around Greater London: A case study during summer 2012, J. Geophys. Res.-Atmos., 119, 4940–4952, https://doi.org/10.1002/2013JD021269, 2014.

Okamoto, H., Gomi, Y., Empirical research on diffusion behavior of leaked gas in the ground, Journal of Loss Prevention in the Process Industries, https://doi.org/10.1016/j.jlp.2011.01.007, 2011.

Omara, M., Sullivan, M. R., Li, X., Subramanian, R., Robinson, A. L. and Presto, A. A.: Methane Emissions from Conventional and Unconventional Natural Gas Production Sites in the

Marcellus Shale Basin, Environ. Sci. Technol., 50(4), 2099–2107, doi:10.1021/acs.est.5b05503, 2016.

Paredes, M. G., Güereca, L. P., Molina, L. T. and Noyola, A.: Methane emissions from anaerobic sludge digesters in Mexico: On-site determination vs. IPCC Tier 1 method, Sci. Total Environ., 656, 468–474, doi:10.1016/j.scitotenv.2018.11.373, 2019.

Pataki, D.E., 2003. Seasonal cycle of carbon dioxide and its isotopic composition in an urban atmosphere: Anthropogenic and biogenic effects. J. Geophys. Res. 108, 4735. https://doi.org/10.1029/2003JD003865.

Peek, C.J., Montfoort, J.A., Dröge, R., Guis, B., Baas, K., van Huet, B., van Hunnik, O.R., van den Berghe, A.C.W.M. Methodology report on the calculation of emissions to air from the sectors Energy, Industry and Waste. RIVM Rep. 2019-0018 129–130. https://doi.org/10.21945/RIVM-2019-0018, 2019.

Peischl, J., Ryerson, T.B., Brioude, J., Aikin, K.C., Andrews, A.E., Atlas, E., Blake, D., Daube, B.C., De Gouw, J.A., Dlugokencky, E., Frost, G.J., Gentner, D.R., Gilman, J.B., Goldstein, A.H., Harley, R.A., Holloway, J.S., Kofler, J., Kuster, W.C., Lang, P.M., Novelli, P.C., Santoni, G.W., Trainer, M., Wofsy, S.C., Parrish, D.D. Quantifying sources of methane using light alkanes in the Los Angeles basin, California. J. Geophys. Res. Atmos. 118, 4974–4990. https://doi.org/10.1002/jgrd.50413, 2013.

Peptenatu, D., Pintilii, R.D., Draghici, C., Merciu, C., Mateescu, R.D., 2012. Management of environment risk within emergency territorial systems. case study the influence area of the bucharest city. J. Environ. Prot. Ecol. 13, 2360–2370.

Petrescu, A. M. R., Peters, G. P., Janssens-Maenhout, G., Ciais, P., Tubiello, F. N., Grassi, G., Nabuurs, G.-J., Leip, A., Carmona-Garcia, G., Winiwarter, W., Höglund-Isaksson, L., Günther, D., Solazzo, E., Kiesow, A., Bastos, A., Pongratz, J., Nabel, J. E. M. S., Conchedda, G., Pilli, R., Andrew, R. M., Schelhaas, M.-J., and Dolman, A. J.: European anthropogenic AFOLU greenhouse gas emissions: a review and benchmark data, Earth Syst. Sci. Data, 12, 961–1001, https://doi.org/10.5194/essd-12-961-2020, 2020.

Petrescu, A. M. R., Qiu, C., Ciais, P., Thompson, R. L., Peylin, P., McGrath, M. J., Solazzo, E., Janssens-Maenhout, G., Tubiello, F. N., Bergamaschi, P., Brunner, D., Peters, G. P., Höglund-Isaksson, L., Regnier, P., Lauerwald, R., Bastviken, D., Tsuruta, A., Winiwarter, W., Patra, P. K., Kuhnert, M., Oreggioni, G. D., Crippa, M., Saunois, M., Perugini, L., Markkanen, T., Aalto, T., Groot Zwaaftink, C. D., Tian, H., Yao, Y., Wilson, C., Conchedda, G., Günther, D., Leip, A., Smith, P., Haussaire, J.-M., Leppänen, A., Manning, A. J., McNorton, J., Brockmann, P., and Dolman, A. J.: The consolidated European synthesis of CH_4 and N_2O emissions for the European Union and United Kingdom: 1990–2017, Earth Syst. Sci. Data, 13, 2307–2362, https://doi.org/10.5194/essd-13-2307-2021, 2021.

Phillips, N. G., Ackley, R., Crosson, E. R., Down, A., Hutyra, L. R., Brondfield, M., Karr, J. D., Zhao, K., Jackson, R. B.: Mapping urban pipeline leaks: Methane leaks across Boston, 173, 1-4, https://doi.org/10.1016/j.envpol.2012.11.003, 2013

Picarro, G2401 Analyzer Datasheet. V1.0, 1–2. Santa Clara, CA, 2017a.

Picarro, GasScouter™ G4302 Analyzer Datasheet. V1.0,1–2. Santa Clara, CA, 2017b.

Picarro, G2301 Analyzer Datasheet. V1.1, 1–2. Santa Clara, CA, 2019.

Popa, M. E., Vollmer, M. K., Jordan, A., Brand, W. A., Pathirana, S. L., Rothe, M. and Röckmann, T.: Vehicle emissions of greenhouse gases and related tracers from a tunnel study: CO : CO2 , N2O : CO2 , CH4 : CO2 , O2 : CO2 ratios, and the stable isotopes 13C and 18O in CO2 and CO, Atmos. Chem. Phys., 14(4), 2105–2123, doi:10.5194/acp-14-2105-2014, 2014.

Prather, M. J. et al.,: Atmospheric Chemistry and Greenhouse Gases. In: Climate Change 2001: The Physical Science Basis. Contribution of Working Group I to the Third Assessment Report of the Intergovernmental13 Panel on Climate Change [Y. Ding, D.J. Griggs, M. Noguer, P.J. van

der Linden, X. Dai, K. Maskell, andC.A. Johnson (eds.)]. Cambridge University Press, Cambridge, United Kingdom and New York, NY, USA, pp.15 239–287, 2001.

Prather, M. J.: Lifetimes and time scales in atmospheric chemistry, Phil. Trans. R. Soc. A.3651705–1726http://doi.org/10.1098/rsta.2007.2040, 2007.

Prather, M.J., Holmes, C.D., Hsu, J. Reactive greenhouse gas scenarios : Systematic exploration of uncertainties and the role of atmospheric chemistry. Geophys. Res. Lett. 39, 6–10. https://doi.org/10.1029/2012GL051440, 2012.

Quay, P., Stutsman, J., Wilbur, D., Snover, A., Dlugokencky, E., and Brown, T.: The isotopic composition of atmospheric methane, *Global Biogeochem. Cycles*, 13(2), 445– 461, doi:10.1029/1998GB900006, 1999.

Rasmussen, R. A., and Khalil, M. A. K., Atmospheric methane (CH_4): Trends and seasonal cycles, J. Geophys. Res., 86(C10), 9826– 9832, https://doi.org/10.1029/JC086iC10p09826, 1981.

Rijksoverheid: Emissieregstratie. [online] Available from: http://www.emissieregistratie.nl/erpubliek/erpub/facility.aspx (Accessed 9 December 2019), 2019.

Röckmann, T. and the The ROMEO team: ROMEO - ROmanian Methane Emissions from Oil and Gas , EGU General Assembly 2020, Online, 4–8 May 2020, EGU2020-18801, https://doi.org/10.5194/egusphere-egu2020-18801, 2020.

Röckmann, T., Eyer, S., van der Veen, C., Popa, M. E., Tuzson, B., Monteil, G., Houweling, S., Harris, E., Brunner, D., Fischer, H., Zazzeri, G., Lowry, D., Nisbet, E. G., Brand, W. A., Necki, J. M., Emmenegger, L. and Mohn, J.: In situ observations of the isotopic composition of methane at the Cabauw tall tower site, Atmos. Chem. Phys., 16(16), 10469–10487, https://doi.org/10.5194/acp-16-10469-2016, 2016.

Rogelj, J., D. Shindell, K. Jiang, S. Fifita, P. Forster, V. Ginzburg, C. Handa, H. Kheshgi, S. Kobayashi, E. Kriegler, L. Mundaca, R. Séférian, and M.V. Vilariño, 2018: Mitigation Pathways Compatible with 1.5°C in the Context of Sustainable Development. In: Global Warming of 1.5°C. An IPCC Special Report on the impacts of global warming of 1.5°C above pre-industrial levels and related global greenhouse gas emission pathways, in the context of strengthening the global response to the threat of climate change, sustainable development, and efforts to eradicate poverty [Masson-Delmotte, V., P. Zhai, H.-O. Pörtner, D. Roberts, J. Skea, P.R. Shukla, A. Pirani, W. Moufouma-Okia, C. Péan, R. Pidcock, S. Connors, J.B.R. Matthews, Y. Chen, X. Zhou, M.I. Gomis, E. Lonnoy, T. Maycock, M. Tignor, and T. Waterfield (eds.)]. In Press. Available online; https://www.ipcc.ch/site/assets/uploads/sites/2/2019/02/SR15_Chapter2_Low_Res.pdf, last access: 23 April 2022, 2019.

Sandulescu, E. The contribution of waste management to the reduction of greenhouse gas emissions with applications in the city of Bucharest. Waste Manag. Res. 22, 413–426. https://doi.org/10.1177/0734242X04048519, 2004.

Sapart, C., Monteil, G., Prokopiou, M. *et al.* Natural and anthropogenic variations in methane sources during the past two millennia. *Nature* **490,** 85–88. https://doi.org/10.1038/nature11461, 2012.

Sargent, M. R., Floerchinger, C., McKain, K., Budney, J., Gottlieb, E. W., Hutyra, L. R., Rudek, J., Wofsy, S. C.: Majority of US urban natural gas emissions unaccounted for in inventories, Proceedings of the National Academy of Sciences Nov 2021, 118 (44) e2105804118; https://doi.org/10.1073/pnas.2105804118, 2021.

Saunois, M., Bousquet, P., Poulter, B., Peregon, A., Ciais, P., Canadell, J. G., Dlugokencky, E. J., Etiope, G., Bastviken, D., Houweling, S., Janssens-Maenhout, G., Tubiello, F. N., Castaldi, S., Jackson, R. B., Alexe, M., Arora, V. K., Beerling, D. J., Berga-maschi, P., Blake, D. R., Brailsford, G., Brovkin, V., Bruhwiler, L., Crevoisier, C., Crill, P., Covey, K., Curry, C., Frankenberg, C., Gedney, N., Höglund-Isaksson, L., Ishizawa, M., Ito, A., Joos, F., Kim, H.-S., Kleinen, T., Krummel, P., Lamarque, J.-F., Langen-felds, R., Locatelli, R., Machida, T.,

Maksyutov, S., McDonald, K. C., Marshall, J., Melton, J. R., Morino, I., Naik, V., O'Doherty, S., Parmentier, F.-J. W., Patra, P. K., Peng, C., Peng, S., Peters, G. P., Pison, I., Prigent, C., Prinn, R., Ramonet, M., Riley, W. J., Saito, M., Santini, M., Schroeder, R., Simpson, I. J., Spahni, R., Steele, P., Takizawa, A., Thornton, B. F., Tian, H., Tohjima, Y., Viovy, N., Voulgarakis, A., van Weele, M., van der Werf, G. R., Weiss, R., Wiedinmyer, C., Wilton, D. J., Wiltshire, A., Worthy, D., Wunch, D., Xu, X., Yoshida, Y., Zhang, B., Zhang, Z., and Zhu, Q.: The global methane budget 2000–2012, Earth Syst. Sci. Data, 8, 697–751, https://doi.org/10.5194/essd-8-697-2016, 2016.

Saunois, M., Bousquet, P., Poulter, B., Peregon, A., Ciais, P., Canadell, J. G., Dlugokencky, E. J., Etiope, G., Bastviken, D., Houweling, S., Janssens-Maenhout, G., Tubiello, F. N., Castaldi, S., Jackson, R. B., Alexe, M., Arora, V. K., Beerling, D. J., Bergamaschi, P., Blake, D. R., Brailsford, G., Bruhwiler, L., Crevoisier, C., Crill, P., Covey, K., Frankenberg, C., Gedney, N., Höglund-Isaksson, L., Ishizawa, M., Ito, A., Joos, F., Kim, H.-S., Kleinen, T., Krummel, P., Lamarque, J.-F., Langenfelds, R., Locatelli, R., Machida, T., Maksyutov, S., Melton, J. R., Morino, I., Naik, V., O'Doherty, S., Parmentier, F.-J. W., Patra, P. K., Peng, C., Peng, S., Peters, G. P., Pison, I., Prinn, R., Ramonet, M., Riley, W. J., Saito, M., Santini, M., Schroeder, R., Simpson, I. J., Spahni, R., Takizawa, A., Thornton, B. F., Tian, H., Tohjima, Y., Viovy, N., Voulgarakis, A., Weiss, R., Wilton, D. J., Wiltshire, A., Worthy, D., Wunch, D., Xu, X., Yoshida, Y., Zhang, B., Zhang, Z., and Zhu, Q.: Variability and quasi-decadal changes in the methane budget over the period 2000–2012, Atmos. Chem. Phys., 17, 11135–11161, https://doi.org/10.5194/acp-17-11135-2017, 2017.

Saunois, M. and Stavert, A. R. and Poulter, B. and Bousquet, P. and Canadell, J. G. and Jackson, R. B. and Raymond, P. A. and Dlugokencky, E. J. and Houweling, S. and Patra, P. K. and Ciais, P. and Arora, V. K. and Bastviken, D. and Bergamaschi, P. and Blake, D. R. and Brailsford, G. and Bruhwiler, L. and Carlson, K. M. and Carrol, M. and Castaldi, S. and Chandra, N. and Crevoisier, C. and Crill, P. M. and Covey, K. and Curry, C. L. and Etiope, G. and Frankenberg, C. and Gedney, N. and Hegglin, M. I. and Höglund-Isaksson, L. and Hugelius, G. and Ishizawa, M. and Ito, A. and Janssens-Maenhout, G. and Jensen, K. M. and Joos, F. and Kleinen, T. and Krummel, P. B. and Langenfelds, R. L. and Laruelle, G. G. and Liu, L. and Machida, T. and Maksyutov, S. and McDonald, K. C. and McNorton, J. and Miller, P. A. and Melton, J. R. and Morino, I. and Müller, J. and Murguia-Flores, F. and Naik, V. and Niwa, Y. and Noce, S. and O'Doherty, S. and Parker, R. J. and Peng, C. and Peng, S. and Peters, G. P. and Prigent, C. and Prinn, R. and Ramonet, M. and Regnier, P. and Riley, W. J. and Rosentreter, J. A. and Segers, A. and Simpson, I. J. and Shi, H. and Smith, S. J. and Steele, L. P. and Thornton, B. F. and Tian, H. and Tohjima, Y. and Tubiello, F. N. and Tsuruta, A. and Viovy, N. and Voulgarakis, A. and Weber, T. S. and van Weele, M. and van der Werf, G. R. and Weiss, R. F. and Worthy, D. and Wunch, D. and Yin, Y. and Yoshida, Y. and Zhang, W. and Zhang, Z. and Zhao, Y. and Zheng, B. and Zhu, Q. and Zhu, Q. and Zhuang, Q.: The Global Methane Budget 2000–2017, 12, 1561-1623, http://dx.doi.org/10.5194/essd-12-1561-2020, 2020.

Scarpelli, T. R., Jacob, D. J., Maasakkers, J. D., Sulprizio, M. P., Sheng, J.-X., Rose, K., Romeo, L., Worden, J. R., and Janssens-Maenhout, G.: A global gridded (0.1° × 0.1°) inventory of methane emissions from oil, gas, and coal exploitation based on national reports to the United Nations Framework Convention on Climate Change, Earth Syst. Sci. Data, 12, 563–575, https://doi.org/10.5194/essd-12-563-2020, 2020.

Schaefer H., Mikaloff Fletcher S. E., Veidt C., Lassey K. R., Brailsford G. W., Bromley T. M., Dlugokencky E. J., Michel S. E., Miller J. B., Levin I., Lowe D. C., Martin R. J., Vaughn B. H., White J. W.: A 21st-century shift from fossil-fuel to biogenic methane emissions indicated by $^{13}CH_4$. Science. 2016 Apr 1;352(6281):80-4. doi: https://doi.org/10.1126/science.aad2705.

Schaum, C., Lensch, D., Bolle, P. Y. and Cornel, P.: Sewage sludge treatment: Evaluation of the energy potential and methane emissions with cod balancing, J. Water Reuse Desalin., 5(4), 437–445,

doi:10.2166/wrd.2015.129, 2015.
Scheutz, C., Samuelsson, J., Fredenslund, A. M., Kjeldsen, P., Quantification of multiple methane emission sources at landfills using a double tracer technique, Waste Management, 31, 1009-1017, https://doi.org/10.1016/j.wasman.2011.01.015, 2011.
Schmidt, G. A. and Shindell, D. T.: Atmospheric composition, radiative forcing, and climate change as a consequence of a massive methane release from gas hydrates, Paleoceanography, 18(1), n/a-n/a, doi:10.1029/2002PA000757, 2003.
Schoell, M. Recent advances in petroleum isotope geochemistry. Org. Geochem. 6, 645–663. https://doi.org/10.1016/0146-6380(84)90086-X, 1984.
Schoell, M. Multiple origins of methane in the Earth. Chem. Geol. 71, 1–10. https://doi.org/10.1016/0009-2541(88)90101-5, 1988.
Schollaert, C., Ackley, R. C., DeSantis, A., Polka, E., & Scammell, M. K., Natural gas leaks and tree death: A first-look case-control study of urban trees in Chelsea, MA USA. Environmental Pollution, 263. https://doi.org/10.1016/j.envpol.2020.114464, 2020.
Schwietzke, S., Sherwood, O., Bruhwiler, L. *et al.* Upward revision of global fossil fuel methane emissions based on isotope database. *Nature* **538,** 88–91. https://doi.org/10.1038/nature19797, 2016.
Sclater, J., Royden, L., Horath, F., Burchfield, B., Semken, S., Stegena, L. The formation of the intra-carpathian basins as determined from subsidence data. Earth Planet. Sci. Lett. 51, 139–162. https://doi.org/10.1016/0012-821X(80)90262-9, 1980.
Sheng J-X., Jacob, D. J., Maasakkers, J. D., Sulprizio, M. P., Zavala-Araiza, D., Hamburg, S. P.: A high-resolution (0.1° × 0.1°) inventory of methane emissions from Canadian and Mexican oil and gas systems, 158, 211-215, https://doi.org/10.1016/j.atmosenv.2017.02.036, 2017
Sherwood, O. A., Schwietzke, S., Arling, V. A., and Etiope, G.: Global Inventory of Gas Geochemistry Data from Fossil Fuel, Microbial and Burning Sources, Version 2017, Earth System Science Data, 9, 639–656, https://doi.org/10.5194/essd-9-639-2017, 2017.
Shindell, D., Kuylenstierna, J. C. I., Vignati, E., Van Dingenen, R., Amann, M., Klimont, Z., Anenberg, S. C., Muller, N., Janssens-Maenhout, G., Raes, F., Schwartz, J., Faluvegi, G., Pozzoli, L., Kupiainen, K., Höglund-Isaksson, L., Emberson, L., Streets, D., Ramanathan, V., Hicks, K., Oanh, N. T. K., Milly, G., Williams, M., Demkine, V., Fowler, D.: Simultaneously Mitigating Near-Term Climate Change and Improving Human Health and Food Security, Science (80-.)., vol. 335, no. 6065, pp. 183–189, doi: 10.1126/science.1210026., 2012.
Simpson, I. J., Chen, T.-Y., Blake, D. R., Rowland, F. S., Implications of the recent fluctuations in the growth rate of tropospheric methane, *Geophys. Res. Lett.*, 29(10), doi:10.1029/2001GL014521, 2002.
Simpson, I. J., Rowland, F. S., Meinardi, S., and Blake, D. R., Influence of biomass burning during recent fluctuations in the slow growth of global tropospheric methane, *Geophys. Res. Lett.*, 33, L22808, doi:10.1029/2006GL027330, 2006.
Sowers, T., 2010. Atmospheric methane isotope records covering the Holocene period. Quat. Sci. Rev. 29, 213–221. https://doi.org/10.1016/j.quascirev.2009.05.023Townsend-Small, A., Tyler, S.C., Pataki, D.E., Xu, X., Christensen, L.E., 2012. Isotopic measurements of atmospheric methane in Los Angeles, California, USA: Influence of “fugitive” fossil fuel emissions. J. Geophys. Res. Atmos. 117, 1–11. https://doi.org/10.1029/2011JD016826.
Spahni, R., Chappellaz, J., Stocker, T. F., Loulergue, L., Hausammann, G., Kawamura, K., Flückiger, J., Schwander, J., Raynaud, D., Masson-Delmotteand , V., Jouzel, J.: Atmospheric Methane and Nitrous Oxide of the Late Pleistocene from Antarctic Ice Cores, 310, 1317-1321, https://doi.org/10.1126/science.1120132, 2005
Sperlich, P., Uitslag, N.A.M., Richter, J.M., Rothe, M., Geilmann, H., Veen, C. Van Der, Röckmann, T., Blunier, T., Brand, W.A. Development and evaluation of a suite of isotope reference gases

for methane in air. Atmos. Meas. Tech. 9, 3717–3737. https://doi.org/10.5194/amt-9-3717-2016, 2016.

Stephenson, M. and Stickland, L. H.: Hydrogenase: The bacterial formation of methane by the reduction of one-carbon compounds by molecular hydrogen, Biochem. J., 27(5), 1517–1527, doi:10.1042/bj0271517, 1933.

Stern, D. I., Kaufmann, R. K.: Estimates of global anthropogenic methane emissions 1860–1993, Chemosphere, 33, 159-176, https://doi.org/10.1016/0045-6535(96)00157-9, 1996

Subak, S.:Methane from the House of Tudor and the Ming Dynasty: Anthropogenic emissions in the sixteenth century, Chemosphere, 29, 843-854, https://doi.org/10.1016/0045-6535(94)90157-0, 1994

Thauer, R. K.: Biochemistry of methanogenesis: a tribute to Marjory Stephenson:1998 Marjory Stephenson Prize Lecture, Microbiology, 144(9), 2377–2406, doi:10.1099/00221287-144-9-2377, 1998.

Thorpe, A. K., Frankenberg, C., and Roberts, D. A.: Retrieval techniques for airborne imaging of methane concentrations using high spatial and moderate spectral resolution: application to AVIRIS, Atmos. Meas. Tech., 7, 491–506, https://doi.org/10.5194/amt-7-491-2014, 2014.

Tong, L. I., Chang, C. W., Jin, S. E. and Saminathan, R.: Quantifying uncertainty of emission estimates in National Greenhouse Gas Inventories using bootstrap confidence intervals, Atmos. Environ., 56, 80–87, https://doi.org/10.1016/j.atmosenv.2012.03.063, 2012.

Townsend-Small, A., Tyler, S. C., Pataki, D. E., Xu, X., and Christensen, L. E., Isotopic measurements of atmospheric methane in Los Angeles, California, USA: Influence of "fugitive" fossil fuel emissions, *J. Geophys. Res.*, 117, D07308, https://doi.org/10.1029/2011JD016826, 2012.

Townsend-Small, A., Marrero, J.E., Lyon, D.R., Simpson, I.J., Meinardi, S., Blake, D.R. Integrating Source Apportionment Tracers into a Bottom-up Inventory of Methane Emissions in the Barnett Shale Hydraulic Fracturing Region. Environ. Sci. Technol. 49, 8175–8182. https://doi.org/10.1021/acs.est.5b00057, 2015.

Townsend-Small, A., Disbennett, D., Fernandez, J. M., Ransohoff, R. W., Mackay, R. and Bourbonniere, R. A.: Quantifying emissions of methane derived from anaerobic organic matter respiration and natural gas extraction in Lake Erie, Limnol. Oceanogr., 61(S1), S356–S366, https://doi.org/10.1002/lno.10273, 2016a.

Townsend-Small, A., Botner, E.C., Jimenez, K.L., Schroeder, J.R., Blake, N.J., Meinardi, S., Blake, D.R., Sive, B.C., Bon, D., Crawford, J.H., Pfister, G., Flocke, F.M. Using stable isotopes of hydrogen to quantify biogenic and thermogenic atmospheric methane sources: A case study from the Colorado Front Range. Geophys. Res. Lett. 43, 11,462-11,471. https://doi.org/10.1002/2016GL071438, 2016b.

Tu, Q., Schneider, M., Hase, F., Khosrawi, F., Ertl, B., Necki, J., Dubravica, D., Diekmann, C. J., Blumenstock, T., and Fang, D.: Quantifying hard coal mines CH_4 emissions from TROPOMI and IASI observations using high-resolution CAMS forecast data and the wind-assigned anomaly method, Atmos. Chem. Phys. Discuss. [preprint], https://doi.org/10.5194/acp-2022-41, in review, 2022.

Turner, A. J., D. J. Jacob, J. Benmergui,S. C. Wofsy, J. D. Maasakkers, A. Butz,O. Hasekamp, and S. C. Biraud,A large increase in U.S. methane emissions over the past decade inferred from satellite data and surface observations,Geophys. Res. Lett.,43, 2218–2224, https://doi.org/10.1002/2016GL067987, 2016.

Turner, A. J., Frankenberg, C. and Kort, E. A.: Interpreting contemporary trends in atmospheric methane, Proc. Natl. Acad. Sci., 116(8), 2805–2813, https://doi.org/10.1073/PNAS.1814297116, 2019.

Turner, D. B.: Workbook of Atmospheric Dispersion Estimates, U.S. Environmental Protection Agency. [online] Available from: https://nepis.epa.gov/Exe/ZyPDF.cgi/9101GKEZ.PDF?Dockey=9101GKEZ.PDF, 1969.

U.S. EIA: Natural gas consumptions in the United States, [online] Available from: https://www.eia.gov/energyexplained/natural-gas/use-of-natural-gas.php (Accessed 16 June 2020), 2019.

U.S. EPA, 2020. Greenhouse Gas Equivalencies Calculator. https://www.epa.gov/energy/greenhouse-gas-equivalencies-calculator. (Accessed 05 February 2021).

Ulrich, B. A., Mitton, M., Lachenmeyer, E., Hecobian, A., Zimmerle, D., and Smits,K. M., Natural Gas Emissions from Underground Pipelines and Implications for Leak Detection, Environmental Science & Technology Letters, 6 (7), 401-406, https://doi.org/10.1021/acs.estlett.9b00291, 2019.

Umezawa, T., Brenninkmeijer, C. A. M., Röckmann, T., van der Veen, C., Tyler, S. C., Fujita, R., Morimoto, S., Aoki, S., Sowers, T., Schmitt, J., Bock, M., Beck, J., Fischer, H., Michel, S. E., Vaughn, B. H., Miller, J. B., White, J. W. C., Brailsford, G., Schaefer, H., Sperlich, P., Brand, W. A., Rothe, M., Blunier, T., Lowry, D., Fisher, R. E., Nisbet, E. G., Rice, A. L., Bergamaschi, P., Veidt, C. and Levin, I.: Interlaboratory comparison of $\delta^{13}C$ and δD-CH_4 measurements of atmospheric CH4 for combined use of data sets from different laboratories, Atmos. Meas. Tech., 11(2), 1207–1231, https://doi.org/10.5194/amt-11-1207-2018, 2018.

Umweltbundesamt, Berichterstattung unter der Klimarahmenkonvention der Vereinten Nationen und dem Kyoto-Protokoll 2021, [Online], Available from: https://www.umweltbundesamt.de/sites/default/files/medien/5750/publikationen/2021-05-19_cc_43-2021_nir_2021_1.pdf, (Last Accessed: 08 February 2022).

UNEP and CCAC: United Nations Environment Programme and Climate and Clean Air Coalition. Global Methane Assessment: Benefits and Costs of Mitigating Methane Emissions. Nairobi: United Nations Environment Programme. Available at: https://www.ccacoalition.org/en/file/7941/download?token=q_bCnfYV. last access: 06 April 2022, 2021, 2021.

UNFCCC: United Nations Framework Convention on Climate Change: Paris Agreement, Available from: https://unfccc.int/process-and-meetings/the-paris-agreement/the-paris-agreement, last access: 08 April 2022, 2015.

UNFCCC: Third National Communication to United Nations Framework Convention on Climate Change, Available from: https://unfccc.int/sites/default/files/resource/Third%20National%20communication%20IRAN.pdf, last access: 11 April 2022, 2017.

UNFCCC: Annual European Union greenhouse gas inventory 1990–2017 and inventory report 2019, https://unfccc.int/documents/65886, last access: 28 April 2022, 2018.

UNFCCC: Romania's Fourth Biennial Report under the UNFCCC, Available from: https://unfccc.int/sites/default/files/resource/BR4-Romania.pdf, last access: 11 April 2022, 2019.

UNI MISKOLC and ETE: A register of all gas regulations and norms concerning the necessary gas quality for allowing the transport in the natural gas grid. [online] Available from: https://ec.europa.eu/energy/intelligent/projects/sites/iee-projects/files/projects/documents/redubar_a_register_of_all_gas_regulations.pdf, 2008.

US Census Bureau: U.S. and World Population Clock, [online] Available from: https://www.census.gov/popclock/ (Accessed 20 June 2020), 2020.

Van Ulden, A. P. and Wieringa, J.: Atmospheric boundary layer research at Cabauw, Boundary-Layer Meteorol., 78(1–2), 39–69, doi:10.1007/BF00122486, 1996.

Veolia, K., 2013. Glina Wastewater Treatment Plant , Romania Bioflex – increased biological capacity | Case Study.

Von Fischer, J. C., Cooley, D., Chamberlain, S., Gaylord, A., Griebenow, C. J., Hamburg, S. P., Salo, J., Schumacher, R., Theobald, D., and Ham, J.: Rapid, Vehicle-Based Identification of Location

and Magnitude of Urban Natural Gas Pipeline Leaks, Environ. Sci. Technol., 51, 4091–4099, https://doi.org/10.1021/acs.est.6b06095, 2017.

Vogel, F., Ars, S., Wunch, D., Lavoie, J., Maazallahi, H., Röckmann, T., Necki, J., Bartyzel, J., Jagoda, P., Lowry, D., France, J., Fernandez, J., Bakkaloglu, S., Fisher, R., Lanoiselle, M., Chen, H., Oudshoorn, M., Yver-Kwok, C., Defratyka, S., Morgui, J. A., Estruch, C., Curcoll, R., Grossi, C., Chen, J., Dietrich, F., Forstmaier, A., Denier van der Gon, H., Dellaert, S. N. C., Salo, J., Corbu, M., Iancu, S. S., Tudor, A. S., Scarlat, A. I., Calcan, A.: Ground-based mobile measurements to track urban methane emissions from natural gas in twelve cities across eight countries, in press.

Weller, Z. D., Roscioli, J. R., Daube, W. C., Lamb, B. K., Ferrara, T. W., Brewer, P. E., and von Fischer, J. C.: Vehicle-Based Methane Surveys for Finding Natural Gas Leaks and Estimating Their Size: Validation and Uncertainty, Environ. Sci. Technol., 52, 11922–11930, https://doi.org/10.1021/acs.est.8b03135, 2018.

Weller, Z. D., Yang, D. K., and von Fischer, J. C.: An open source algorithm to detect natural gas leaks from mobile methane survey data, edited by: Mauder, M., PLoS One, 14, e0212287, https://doi.org/10.1371/journal.pone.0212287, 2019.

Weller, Z. D., Hamburg, S. P., and von Fischer, J. C., A National Estimate of Methane Leakage from Pipeline Mains in Natural Gas Local Distribution Systems, Environmental Science & Technology, 54 (14), 8958-8967, https://doi.org/10.1021/acs.est.0c00437, 2020.

Wennberg, P.O., Mui, W., Wunch, D., Kort, E.A., Blake, D.R., Atlas, E.L., Santoni, G.W., Wofsy, S.C., Diskin, G.S., Jeong, S., Fischer, M.L. On the sources of methane to the Los Angeles atmosphere. Environ. Sci. Technol. 46, 9282–9289. https://doi.org/10.1021/es301138y, 2012.

West, J. J., Fiore, A. M., Horowitz, L. W. and Mauzerall, D. L.: Global health benefits of mitigating ozone pollution with methane emission controls., Proc. Natl. Acad. Sci. U. S. A., 103(11), 3988–93, https://doi.org/10.1073/pnas.0600201103, 2006.

Whiticar, M.J., 1990. A geochemial perspective of natural gas and atmospheric methane. Org. Geochem. 16, 531–547. https://doi.org/10.1016/0146-6380(90)90068-B.

Wiesner, S., Gröngröft, A., Ament, F. et al. Spatial and temporal variability of urban soil water dynamics observed by a soil monitoring network. J Soils Sediments 16, 2523–2537. https://doi.org/10.1007/s11368-016-1385-6, 2016

WMO, 2020. The State of Greenhouse Gases in the Atmosphere Based on Global Observations through 2019. WMO Greenh. Gas Bull. 16, 1-9. https://gaw.kishou.go.jp/static/publications/bulletin/Bulletin2019/ghg-bulletin-16.pdf

Worden, J. R., Anthony Bloom, A., Pandey, S., Jiang, Z., Worden, H. M., Walker, T. W., Houweling, S., Röckmann, T., , Reduced biomass burning emissions reconcile conflicting estimates of the post-2006 atmospheric methane budget, Nature Communications 8, 2227 https://doi.org/10.1038/s41467-017-02246-0, 2017

Wunch, D., Toon, G.C., Hedelius, J.K., Vizenor, N., Roehl, C.M., Saad, K.M., Blavier, J.-F.L., Blake, D.R., Wennberg, P.O., 2016. Quantifying the loss of processed natural gas within California's South Coast Air Basin using long-term measurements of ethane and methane. Atmos. Chem. Phys. 16, 14091–14105. https://doi.org/10.5194/acp-16-14091-2016.

Xu, L. and Jiang, C.: Initial desorption characterization of methane and carbon dioxide in coal and its influence on coal and gas outburst risk, Fuel, 203, 700–706, doi:10.1016/J.FUEL.2017.05.001, 2017.

Xueref-Remy, I., Zazzeri, G., Bréon, F.M., Vogel, F., Ciais, P., Lowry, D., Nisbet, E.G. Anthropogenic methane plume detection from point sources in the Paris megacity area and characterization of their $\delta^{13}C$ signature. Atmos. Environ. 222. https://doi.org/10.1016/j.atmosenv.2019.117055, 2020.

Yacovitch, T. I., Herndon, S. C., Roscioli, J. R., Floerchinger, C., McGovern, R. M., Agnese, M., Pétron, G., Kofler, J., Sweeney, C., Karion, A., Conley, S. A., Kort, E. A., Nähle, L., Fischer,

M., Hildebrandt, L., Koeth, J., McManus, J. B., Nelson, D. D., Zahniser, M. S. and Kolb, C. E.: Demonstration of an Ethane Spectrometer for Methane Source Identification, Environ. Sci. Technol., 48(14), 8028–8034, https://doi.org/10.1021/es501475q, 2014.

Yacovitch, T. I., Herndon, S. C., Pétron, G. P., Kofler, J., Lyon, D., Zahniser, M. S. and Kolb, C. E.: Mobile Laboratory Observations of Methane Emissions in the Barnett Shale Region, , https://doi.org/10.1021/es506352j, 2015.

Yacovitch, T. I., Neininger, B., Herndon, S. C., Van der Gon, H. D., Jonkers, S., Hulskotte, J., Roscioli, J. R. and Zavala-Araiza, D.: Methane emissions in the Netherlands: The Groningen field, Elem Sci Anth, 6(1), 57, https://doi.org/10.1525/elementa.308, 2018.

Yan, Y., Dong, X., Li, J., Experimental study of methane diffusion in soil for an underground gas pipe leak, Journal of Natural Gas Science and Engineering, https://doi.org/10.1016/j.jngse.2015.08.039, 2015.

Yarnes, C., 2013. $\delta^{13}C$ and $\delta^{2}H$ measurement of methane from ecological and geological sources by gas chromatography/combustion/pyrolysis isotope-ratio mass spectrometry. Rapid Commun. Mass Spectrom. 27, 1036–1044. https://doi.org/10.1002/rcm.6549, 2013.

Yuhua, D., Huilin, G., Jing'en, Z., Yaorong, F., Evaluation of gas release rate through holes in pipelines, Journal of Loss Prevention in the Process Industries, https://doi.org/10.1016/S0950-4230(02)00041-4, 2002.

Zavala-Araiza, D., Lyon, D. R., Alvarez, R. A., Davis, K. J., Harriss, R., Herndon, S. C., Karion, A., Kort, E. A., Lamb, B. K., Lan, X., Marchese, A. J., Pacala, S. W., Robinson, A. L., Shepson, P. B., Sweeney, C., Talbot, R., Townsend-Small, A., Yacovitch, T. I., Zimmerle, D. J., and Hamburg, S. P.: Reconciling divergent estimates of oil and gas methane emissions, P. Natl. Acad. Sci. USA, 112, 15597–15602, https://doi.org/10.1073/pnas.1522126112, 2015.

Zazzeri, G., Lowry, D., Fisher, R. E., France, J. L., Lanoisellé, M. and Nisbet, E. G.: Plume mapping and isotopic characterisation of anthropogenic methane sources, Atmos. Environ., 110, 151–162, https://doi.org/10.1016/j.atmosenv.2015.03.029, 2015.

Zazzeri, G., Lowry, D., Fisher, R.E., France, J.L., Lanoisellé, M., Kelly, B.F.J., Necki, J.M., Iverach, C.P., Ginty, E., Zimnoch, M., Jasek, A., Nisbet, E.G. Carbon isotopic signature of coal-derived methane emissions to the atmosphere: from coalification to alteration. Atmos. Chem. Phys. 16, 13669–13680. https://doi.org/10.5194/acp-16-13669-2016, 2016.

Zazzeri, G., Lowry, D., Fisher, R.E., France, J.L., Lanoisellé, M., Grimmond, C.S.B., Nisbet, E.G. Evaluating methane inventories by isotopic analysis in the London region. Sci. Rep. 7, 4854. https://doi.org/10.1038/s41598-017-04802-6, 2017.

Zhao, W., Zhang, T., Wang, Y., Qiao, J. and Wang, Z.: Corrosion Failure Mechanism of Associated Gas Transmission Pipeline., Mater. (Basel, Switzerland), 11(10), https://doi.org/10.3390/ma11101935, 2018.

Zimmerle, D. J., Williams, L. L., Vaughn, T. L., Quinn, C., Subramanian, R., Duggan, G. P., Willson, B., Opsomer, J. D., Marchese, A. J., Martinez, D. M. and Robinson, A. L.: Methane Emissions from the Natural Gas Transmission and Storage System in the United States, Environ. Sci. Technol., 49(15), 9374–9383, https://doi.org/10.1021/acs.est.5b01669, 2015.

Zimnoch, M., Godlowska, J., Necki, J.M., Rozanski, K. Assessing surface fluxes of CO_2 and CH^4 in urban environment: a reconnaissance study in Krakow, Southern Poland. Tellus B Chem. Phys. Meteorol. 62, 573–580. https://doi.org/10.1111/j.1600-0889.2010.00489, 2010.

Zimnoch, M., Necki, J., Chmura, L., Jasek, A., Jelen, D., Galkowski, M., Kuc, T., Gorczyca, Z., Bartyzel, J. and Rozanski, K.: Quantification of carbon dioxide and methane emissions in urban areas: source apportionment based on atmospheric observations, Mitig. Adapt. Strateg. Glob. Chang., 24(6), 1051–1071, https://doi.org/10.1007/s11027-018-9821-0, 2019.

Zolin, M.B. The extended metropolitan area in a new EU member state: Implications for a rural development approach. Transit. Stud. Rev. 14, 565–573. https://doi.org/10.1007/s11300-007-0154-z, 2007.

Scientific articles

Maazallahi, H., Fernandez, J. M., Menoud, M., Zavala-Araiza, D., Weller, Z. D., Schwietzke, S., von Fischer, J. C., Denier van der Gon, H., and Röckmann, T.: Methane mapping, emission quantification, and attribution in two European cities: Utrecht (NL) and Hamburg (DE), Atmos. Chem. Phys., 20, 14717–14740, https://doi.org/10.5194/acp-20-14717-2020, 2020.

Maazallahi, H., Delre, A., Scheutz, C., Fredenslund, A. M., Schwietzke, S., Denier van der Gon, H., and Röckmann, T.: Intercomparison of detection and quantification methods for methane emissions from the natural gas distribution network in Hamburg, Germany, Atmos. Meas. Tech. Discuss. [preprint], https://doi.org/10.5194/amt-2022-134, in review, 2022.

Fiehn, A., Kostinek, J., Eckl, M., Klausner, T., Gałkowski, M., Chen, J., Gerbig, C., Röckmann, T., Maazallahi, H., Schmidt, M., Korbeń, P., Nęcki, J., Jagoda, P., Wildmann, N., Mallaun, C., Bun, R., Nickl, A.-L., Jöckel, P., Fix, A., and Roiger, A.: Estimating CH_4, CO_2 and CO emissions from coal mining and industrial activities in the Upper Silesian Coal Basin using an aircraft-based mass balance approach, Atmos. Chem. Phys., 20, 12675–12695, https://doi.org/10.5194/acp-20-12675-2020, 2020.

Chen, J., Dietrich, F., Maazallahi, H., Forstmaier, A., Winkler, D., Hofmann, M. E. G., Denier van der Gon, H., and Röckmann, T.: Methane emissions from the Munich Oktoberfest, Atmos. Chem. Phys., 20, 3683–3696, https://doi.org/10.5194/acp-20-3683-2020, 2020.

Menoud, M., van der Veen, C., Lowry, D., Fernandez, J. M., Bakkaloglu, S., France, J. L., Fisher, R. E., Maazallahi, H., Stanisavljević, M., Nęcki, J., Vinkovic, K., Łakomiec, P., Rinne, J., Korbeń, P., Schmidt, M., Defratyka, S., Yver-Kwok, C., Andersen, T., Chen, H., and Röckmann, T.: Global inventory of the stable isotopic composition of methane surface emissions, augmented by new measurements in Europe, Earth Syst. Sci. Data Discuss. [preprint], https://doi.org/10.5194/essd-2022-30, in review, 2022.

Fernandez, J.M., Maazallahi, H., France, J.L., Menoud, M., Corbu, M., Ardelean, M., Calcan, A., Townsend-Small, A., van der Veen, C., Fisher, R.E., Lowry, D., Nisbet, E.G., Röckmann, T., Street-level methane emissions of Bucharest, Romania and the dominance of urban wastewater., Atmospheric Environment: X (2022), doi: https://doi.org/10.1016/j.aeaoa.2022.100153.

Menoud, M., van der Veen, C., Lowry, D., Fernandez, J. M., Bakkaloglu, S., France, J. L., Fisher, R. E., Maazallahi, H., Stanisavljević, M., Nęcki, J., Vinkovic, K., Łakomiec, P., Rinne, J., Korbeń, P., Schmidt, M., Defratyka, S., Yver-Kwok, C., Andersen, T., Chen, H., and Röckmann, T.: Global inventory of the stable isotopic composition of methane surface emissions, augmented by new measurements in Europe, Earth Syst. Sci. Data Discuss. [preprint], https://doi.org/10.5194/essd-2022-30, in review, 2022.

Korbeń, P., Jagoda, P., Maazallahi, H., Kammerer, J., Nęcki, J. M., Wietzel, J., Bartyzel, J., Radovici, A., Zavala-Araiza, D., Röckmann, T., Schmidt, M., Quantification of methane emission rate from oil and gas wells in Romania using ground-based measurement techniques, [under preparation]

Vogel, F., Ars, S., Wunch, D., Maazallahi, H., Röckmann, T., Necki, J., Bartyzel, J., Jagoda, P., Lowry, D., France, J., Fernandez, J., Bakkaloglu, S., Fisher, R., Lanoiselle, M., Chen, H., Oudshoorn, M., Yver-Kwok, C., Defratyka, S., Morgui, J. A., Dietrich, F., Zhao, X., Chen, J., Denier van der Gon, H., Dellaert, S. N. C., Salo, J.: Ground-based mobile measurements to track urban methane emissions from natural gas in twelve cities across eight countries, [under preparation].

Fiehn, A., Eckl, M., Kostinek, J., Galkowski, M., Gerbig, C., Röckmann, T., Menoud, M., Maazallahi, H., Schmidt, M., Korben, P., Necki, J., Stanisavljevic, M., Swolkien, J., Fix, A., Roiger, A.: Isotopic characterization of methane emissions from the Upper Silesian Coal Basin, Poland, [under preparation].

de Groot, T. R., Menoud, M., van Bleijswijk, J., Hernando-Morales, V., Czerski, H., Maazallahi, H., Walter, S., Meijninger, B. M. L., Rush, D., Röckmann, T., Niemann, H.: Tidal and seasonal control on the efficiency of water column methanotrophy at shallow water cold seeps, [under preparation].

Public outreach
Articles

Scientists discover more methane leakages in Utrecht's gas distribution network, Utrecht University, 7 December 2020, Online, Available from: https://www.uu.nl/en/publication/scientists-discover-more-methane-leakages-in-utrechts-gas-distribution-network, last access: 12 August 2022.

Mobile measurements help quantify and attribute methane emission sources in urban areas, Atmospheric Chemistry and Physics, 7 December 2020, Online, Available from: https://www.atmospheric-chemistry-and-physics.net/about/news_and_press/2020-12-07_mobile-measurements-help-quantify-and-attribute-methane-emission-sources-in-urban-areas.html, last access: 12 August 2022.

Scientists Discover 50 Methane Leaks in City of Hamburg's Gas Utility Network, Environmental Defense Fund, 7 December 2020, Online, Available from: https://www.edf.org/media/scientists-discover-50-methane-leaks-city-hamburgs-gas-utility-network, last access: 12 August 2022.

Universiteit ontdekt tientallen lekken in Utrechts aardgasnetwerk, NU, 7 December 2020, Online, Available from: https://www.nu.nl/utrecht/6095050/universiteit-ontdekt-tientallen-lekken-in-utrechts-aardgasnetwerk.html, last access: 12 August 2022.

Tientallen lekken ontdekt in het Utrechts aardgasnetwerk, DUIC, 7 December 2020, Online, Available from: https://www.duic.nl/algemeen/tientallen-lekken-ontdekt-in-het-utrechts-aardgasnetwerk/, last access: 12 August 2022.

Nieuwe meetmethode ontdekt tientallen lekken in Utrechts gasnetwerk, Gelderlander, December 2020, Online, Available from: https://www.gelderlander.nl/utrecht/nieuwe-meetmethode-ontdekt-tientallen-lekken-in-utrechts-gasnetwerk~ae49446f/, last access: 12 August 2022.

Onderzoekers ontdekken methaanlekken in Utrechts aardgasnetwerk, Utrecht Nieuws, 7 December 2020, Online, Available from: https://utrecht.nieuws.nl/onderwijswetenschap/76915/onderzoekers-ontdekken-methaanlekken-in-utrechts-aardgasnetwerk/, last access: 12 August 2022.

Decaying Urban Gas Lines Are Fueling Global Warming, Bloomberg, 28 January 2021, Online, Available from: https://www.bloomberg.com/news/articles/2021-01-28/decaying-urban-gas-lines-leaking-methane-fuel-global-warming?srnd=author, last access: 12 August 2022.

Study shows urban gas leaks are a climate problem in Europe. But there is a clear technology solution, Climate and Clean Air Coalition, 13 January 2021, Online, Available from: https://www.ccacoalition.org/en/news/study-shows-urban-gas-leaks-are-climate-problem-europe-there-clear-technology-solution, last access: 12 August 2022.

Video interviews

Scientists sniff for hidden methane leaks to combat global warming, 13 September 2021, Online, Available from: https://www.euronews.com/green/2021/09/13/scientists-in-utrecht-sniff-out-methane-to-help-protect-the-environment, last access: 12 August 2022.

Methan: Die Jagd nach dem unbemerkten Klimaschädling, 13 September 2021, Online, Available from: https://de.euronews.com/green/2021/09/13/methan-die-jagd-nach-dem-unbemerkten-klimaschadling, last access: 12 August 2022.

Científicos cazan fugas "invisibles" de metano por Europa para luchar contra el cambio climático, 13 September 2021, Online, Available from: https://es.euronews.com/green/2021/09/13/cientificos-cazan-fugas-invisibles-de-metano-por-europa-para-luchar-contra-el-cambio-clima, last access: 12 August 2022.

Réchauffement climatique : sur la piste des fuites de methane, Online, Available from: https://fr.euronews.com/green/2021/09/13/rechauffement-climatique-sur-la-piste-des-fuites-de-methane, last access: 12 August 2022.

Scovare il metano per ridurre il riscaldamento climatico, 13 September 2021, Online, Available from: https://it.euronews.com/green/2021/09/13/scovare-il-metano-per-ridurre-il-riscaldamento-climatico, last access: 12 August 2022.

A caça ao metano escondido para travar aquecimento global, 13 September 2021, Online, Available from: https://pt.euronews.com/green/2021/09/13/a-caca-ao-metano-escondido-para-travar-aquecimento-global, last access: 12 August 2022.

В поисках утечек метана, 13 September 2021, Online, Available from: https://ru.euronews.com/green/2021/09/13/cl-09-methane, last access: 12 August 2022.

تتبع أثر تسرب الميثان المسبب للاحتباس الحراري، ۰۶ صفر ۱۴۴۳، عبر الانترنت، متاح من: https://arabic.euronews.com/green/2021/09/13/tracking-the-impact-of-global-warming-methane-leaks, آخر ولوج: ۱۴ محرم ۱۴۴۳.

Kutatás a rejtett metán után, 13 September 2021, Online, Available from: https://hu.euronews.com/green/2021/09/13/kutatas-a-rejtett-metan-utan, last access: 12 August 2022.

Bilim insanları, küresel ısınmayla mücadele için metan sızıntısı avında, 13 September 2021, Online, Available from: https://tr.euronews.com/green/2021/09/13/bilim-insanlar-kuresel-s-nmayla-mucadele-icin-metan-s-z-nt-s-av-nda, last access: 12 August 2022.

Η ανάγκη μείωσης των εκπομπών μεθανίου - Ο καιρός τον Αύγουστο, 13 September 2021, Online, Available from: https://gr.euronews.com/green/2021/09/13/i-anagki-meiosis-ton-ekpobon-methaniou-o-kairos-ton-avgousto, last access: 12 August 2022.

تغییرات آب‌وهوایی؛ شکار ذرات متان برای شناخت منشئهای پنهان نشت این گاز، ۱۳ سپتامبر ۲۰۲۱، برخط، قابل دسترس از: https://per.euronews.com/green/2021/09/13/chasing-methane-particles-to-find-leak-sources-in-cities، آخرین دسترسی: ۲۱ مرداد ۱۴۰۱.

Gefährliches Gas - auf der Jagd nach den Methanlecks, 01 September 2022, Online, Available from: https://www.3sat.de/wissen/wissenschaftsdoku/220901-sendung-wido-104.html, last access: 01 September 2022.

Acknowledgement

Now, it comes to the point when I must write the acknowledgement which is unavoidable. I noticed to start writing this important part of the thesis and find a structure to it, I must travel through space and time. The best day I could imagine of was the first day of September 2022, exactly five years after I started my PhD journey. But I still have to find a place to write down the memories and nowhere is better than sitting on a grey wooden bench in the botanical garden under shadow of an Oak tree after walking from Olympos, the sport centrum, along the canal and a row of nineteen walnut trees. After entering the garden through the rotating door and climbing the mountains, walking around the lake, greenhouses, and through the arch toward the east side of the garden I was approaching the bench I wanted to write these lines. On the way to the bench in the botanical garden, I passed a triceraptops close to a narrow bush-walled pathway. But before starting my walk from the Olympos, I had to picture the flashbacks in more details, so I started walking toward the science park on the same pathways like the first time and walked toward the university.

It was Friday and after dropping my luggage in my studio in the University College Utrecht in 2017, I walked toward de Uithof. I passed a welcoming sign from the university on my way to meet my supervisor, Prof. Thomas Röckmann. Gradually, while walking under a bridge toward the science park a building was showing up from behind a row of trees with a written Utrecht University (UU) on top, and once the name was fully readable, there was a sunrise. This was the building I was supposed to start the research. I was a bit earlier than our first scheduled meeting with Prof. Röckmann, I knocked at his door, entrance permission was granted, and I opened the door. The first seconds went in silence because Thomas and Elena were in a meeting, and I guess the conversation they were having was deep. After some moments, Thomas recognized me and ask the question for the confirmation. We had a conversation about my trip and accommodation, and we went toward the lab. In the corridor we met Carina and had a bit of chat, then he showed me the instrument I have been using for the last five years. Afterwards, we went to my first office which we shared first with Iris and Marco and later with Sophie and Malika. At this point it was the lunch time, we gathered in front of the elevator to have the lunch together when I met Sylvia. We went to the educatorium sitting next to a large window to get some warmness from the sun. Today, before walking to this bench, I passed next to the educatorium and then went through a green tunnel close to the garden toward Olympos, it was a nice flashback. The next week after my arrival, I got to know my second supervisor, Dr. Hugo Denier van der Gon, who came to IMAU (Institute for Marine and Atmospheric research Utrecht) and we had a meeting with him in Thomas's office. It was a pleasant chat talking about past but mainly future. Hugo invited me to meet colleagues and atmosphere of TNO (Netherlands Organisation for Applied Scientific Research) in the coming days, where my longest secondment was assigned within the MEMO^2 (MEthane goes MObile, MEasurements and MOdelling) project. The PhD journey started when I was in Tehran for the first interview after applying for the ESR10 (Early-Stage Researcher) position of the MEMO^2 project, while Thomas was in Utrecht and Hugo was in Chile.

Thomas, in the last years we have been to so many campaigns in different European countries. When I look back into the last years, I notice our understanding about methane emissions from different sources are on a positive trend, still a lot more to learn but this is the nature of science. I thank you for all the coordination mainly in the MEMO^2 project, the ROMEO (ROmanian Methane Emissions from Oil & gas) campaign and the city campaigns. I appreciate the opportunities I received to participate in research activities. There have been many rocks on the roads but those didn't stop us to reach the goals, these have been learning school for me through out these years. I thank you for all the meetings we had to discuss about the measurements and evaluations and writings which was very useful and made me think more and more. Thank you for all the comments I received on the manuscripts and thesis, those improved the manuscripts to be remained for future studies under open science frameworks. It was also indeed joyful to have group events at your house and your invitation for watching the UEFA (Union of

European Football Associations) champions league final in your house with your family and neighbors right after I came back from the Hamburg measurement campaign in 2020.

Hugo, together with Thomas I learned a lot from your supervisions. I understood that how useful it can be to learn from experienced supervisors who can provide feedbacks from different perspectives. I learned from you how to simplify messages and being to the point. The possibility I received from TNO to use the methane:ethane instrument together with the use of carbon dioxide instrument from UU brought us a whole new chapter of understanding in the methane emission studies. Borrowing the binoculus to watch the NEOWISE comet was a good idea, because the next time it will be in couple of thousands of years. The comments you provided on the manuscripts and thesis and guidance of yours as an inventory expert were very useful in my learning process. I appreciate all the time we spent walking in nature and city and chatting about different topics within or out of scope of work. And of course, the tea/coffee breaks at your house. The invitation to watch the football match between Utrecht FC and AFC Ajax in the Utrecht stadium was a very good idea.

The MEMO^2 project was full of activities and memories over dimension of time and space. We had several meetings, campaigns, conferences etc. in different countries. I thank all the work groups of the project whose contribution made this happen in the right way. I am pleased for having the chance of getting to know so many nice people with different expertise. The diversity was the key. Sylvia, I thank you for your project management skills, and it was indeed great to spend some time with you in a measurement cruise to the North Sea. Tim and Helge thank you for providing the chance to be part of the cruise. I extend my regards to all the ESRs, Juli, it was great to perform the measurement together with you in Bucharest and thank you for the discussions we had in the following months which ended in chapter 3 in this book, thank you for all your ideas, sampling advice and motivations you provided, Piotr, it was great measuring with you in Poland and thank you for your host in the workshop we had in Heidelberg, Malika it was nice measuring together and filling the sample bags and seeing your enthusiasm, thank you for all the invites and your warm visit with a delicious baking, Anja it was nice to see your simulations and talk about how plumes move around, Barbara thank you for the chats we had every now and then, Mila thank you for your host in the COMET (Carbon Dioxide and Methane mission) campaign and showing Krakow, Katarina, thank you for your host in Groningen and it was nice to see how to make smoothie with bicycle, Jonas and Randulph, thank you for providing the EMPA (Swiss Federal Laboratories for Materials Science and Technology) flag to find wind direction, Patryk, thank you for the meeting we had in Lund, a very nice city to study, Sara thank you for the host at LSCE (Climate and Environment Sciences Laboratory), Semra, it was nice talking to you as a person from a neighbor country.

The MEMO^2 project had other dimensions which was created by contributions of partners. Martina, thank you for the chats we had about measurements and instruments, your host and showing us the botanical garden at Heidelberg university, Jarek, it was always interesting to talk to you about the numbers from statistical point of view. I thank you Ilona, Pim and Arjan for the school you organized in Petten and the cruise measurements we had in the North Sea, it was gezellig, Bill, it was nice hearing your advices, Magdalena it was great to be in contact with a person from Picarro to talk about the instruments I used, Phillippe, thank you for the school we had at LSCE, Dominik and Lukas, thank you for your host at EMPA for the annual meeting and the arrangement of enjoying cheese fundoe on top of a hill in a cottage and the trip to the Jungfraujoch station, Dorien, thank you for the measurements we had in the beginning of my PhD, Euan, thank you for sharing the experiences you gained through time in different places and conditions, it was always interesting to hear your stories. I appreciate all the supervisors, technicians and staff members who were moving the project forward. I thank the administration of Lund university who informed alumni of the university through an email about ESR openings of MEMO^2 project, and thanks to Maria who had informed me about this newsletter.

The ROMEO and COMET campaigns were the true examples of applying wide range of measurement techniques in action from different platforms from ground all the way up to the sky. Many thanks to all the coordinators, researchers, assistance and all the people who were part of it. Anke,

Alina, Andreas, Andreas, Jarek and the teams for your coordination and arrangements in the COMET project and later discussions we had over the datasets. My visit to the DLR (German Aerospace Center) was absolutely unforgettable where I had a very nice parking spot. Andreas, it was indeed nice to talk to you about your total column measurement technique and the drive we had together in upper Silesia, and of course your help in the translation of the summary. Participating in the ROMEO campaign with more than 70 people from several countries was absolutely a learning opportunity, Thomas, thank you for the coordination, Andrea, Magdalena, Marius, Sebastian and all the other member of INCAS (National Institute for Aerospace Research "Elie Carafoli") who helped us during the ROMEO campaign and Bucharest city measurements. A good host is a crucial part of a measurement campaign, and you did it so well. Mackenzie it was great talking about your flight measurement and later communications talking about the dataset to find new insights of methane emissions from large area and compare it to the models. Michael, Mariano, Patrick, Samuel and James, thank you for the model outputs, evaluations and discussion we had in the last years, it is very useful to compare results of the simulations and measurements.

Hamburg, a beautiful city where I drove thousands of kilometers and had the chance to see all corners of this city. It was always nice to come back to this city and review the memories in different neighborhoods. A very warm appreciation to all people who contributed to the measurements we had in Hamburg where I learned a lot on streets. It stated in 2018, when we had great hosts from Geomatikum of Hamburg university and Max Planck institute and started the communications with Gasnetz Hamburg, the results of this campaign are provided in chapter 2. This campaign was the start of further measurement campaigns in Hamburg in 2020 and 2021. I extend my warm appreciations to all colleagues who helped enthusiastically to move our understandings forward. In 2020, we started another measurement campaign in Hamburg to find out the differences between different quantification techniques, the results are provided in chapter 4. I thank the suction team for applying their method on the gas leak locations and providing their results with further discussion before and after the campaign. I thank colleagues from DBI who have been actively contributing in the discussion meetings we had over the findings of the 2018 and 2020 campaigns. I thank Charlotte, Antonio, Vincent and Anders from Technical University of Denmark for applying the tracer method and providing the results and dataset. The results of this campaign are provided in chapter 4. I thank colleagues from DVGW (German association for gas and water) for the discussion we had about the results and their hosts during the EGATECH (European Gas Technology Conference) conference in Hamburg. In 2021, we had another campaign in Hamburg to combine the mobile method with total column measurements. I thank Jia, Andreas, Florian, Dominik and Juan for not only the measurements we had in Hamburg, but also the Oktoberfest campaign in Munich, 2018. During the Hamburg campaign we had a good synergy, and I am looking forward to reading the publication. I thank Daniel and Stefan from Environmental Defence Fund (EDF) with whom we performed several methane measurement campaigns, it was very useful to learn from your past experiences and discuss the results of our measurements.

Vienna, a nice city where one of the main conferences in our field happens, EGU (European Geoscience Union) general assembly, where it is quite often to meet colleagues and friend from the past or learn about the ongoing research world-wide. It has been always nice to travel to this city for a reason or another. Sigi, one of the most beautiful moments I had in my memory in the last years happened in the arrangements you provided for Gerhard. He was a true friend with great mentorship skills who was very helpful throughout my research life and his advice remain on my mind for taking decision in future, thank you so much for all the moments you created.

Utrecht, a pleasant city where during my PhD I was based at IMAU and member of the APCG (Atmopsheric Physics and Chemistry Group) where I had chance to work, enjoy and grow. It was always nice to have the weekly group meetings we had, thank you Elena for arranging the meetings and all the other times we spent chatting in the breaks, and thank you for showing us Bucharest during the ROMEO campaign. Thank you, Iris, for your invite to your house, Marco for the conversations we had about your models, wish you both well with your families. Maarten, it was always nice to talk about

riddles and come up with new ideas and thank you for the dinner we had at your place, it was delightful. I thank Rupert and Dušan for the Climate Change in Context course where I had a chance to act as teaching assistant together with Sophie and Malika, Guus, thank you for the student projects we had together and the datasets you provided, Sophie, it was always nice to hear about your nice sport activities, including climbing, cycling, climbing, running and climbing, and thank you for the summary translation and all the chats we had about this and that topic, Robbert, I think we need to find a way how to compete in a sport and accept the results. Malavika, thank you for the invite to your house with nice atmosphere. Getachew, thank you for the laughers you brought to the group, Juhi, there is no problem at all and thank you for the invites to your house, it is always nice to have a good neighbor. Lila, it was really nice to play basketball with you, I absolutely enjoyed it, although maybe it was better trying something different. Carina, Marcel, Henk, Giorgio, Roy and David thank you for your supports in during all the measurement campaigns we had in the last years in different places and providing the ideas how to solve technical issues. Sudhanshu, thank you for the understanding of methane emission you provided from space, Sander, thank you for the coordination of the RITA (Ruisdael land-atmosphere Interactions Intensive Trace gas and Aerosol) campaign in Rotterdam. Thank you, Julie, for your great help and coordination in the mobile measurements of the RITA campaign. Thank you, Bernadette, for showing Vienna in a trip I had there and hearing about your research. Jin, it was interesting to see your model results and chat every now and then. Hanne, it was very nice to meet a person from the north, heldigvis, a very good reminder for me about the vibes I had some years ago, if I may say. Thank you for all your supports which saved me significant amount of time in the extremely critical period, thank you for your time commenting on the introduction and translating the summary, you are right, having a tablet holder is always good idea in an outreach.

It is extremely important to bridge science to the public in a proper way, which require expertise and detailed attentions. I appreciate the journalist we were interviewed by, Jeremy, Daniel, Paul, Aschwin, Jarno and all your crew members who transferred the scientific messages to the eyes and ears of public. It was very nice to hold conversation with you about your experiences filming science in all the other fields of science in different part of the world in the fields or labs.

Working with students at IMAU was extremely pleasant. I had the opportunity to be in contact with students who were either attending courses in which I was supposed to contribute to the education as teaching assistance or performing course projects for which we had field works together, or those who performed their theses at IMAU. It was also useful for me when I was receiving questions or ideas from the student who were viewing topics of discussions from another perspective, and it was also nice seeing them answering questions. Carsten, it was great seeing your motivation and efforts in the Hamburg campaign in 2021 and later detailed evaluations you performed, Paula, thank you for the measurements you did in Amsterdam and your contribution to the reduction of methane emissions from gas leaks, Daan, thank you for the quantifications you performed from the Amsterdam port and finding another scientific way once a required dataset was not available. Ina and Lena, thank you for your work in the MAIO course project, Jasper, Marc, Roel, Feliks, Yujie, Socorro, Foteini, Laura, Reinaart, Bente, Marius, Elian, your enthusiasm, teamwork and evaluations in the ACCP projects were impressive.

At IMAU there are/were so many other faces with whom the institute has been running on the right direction. Floor and Clara, it was nice having you at the institute which brough happiness even sometimes with a sweet package in our mailboxes. Sandra, thank you for giving some tips in the first days of my arrival. Mariken, Judith, it is great to see you onboard the IMAU, and thank you for your welcoming attitude and helps you provided in the process of arrangements for my defence session. Claudia, it is always important to measure temperature, that's why we research to address global warming. Erik, thank you for the meetings we had to talk about the progress of research and great to see your achievements, it was nice having quick morning chats. Isolde, your suggestion of attending the kickbag class was life changing, I really appreciate it, and I thank Jojanneke and Denise whose training skills are incredibly powerful, and Rens for the nice spinning classes, Arianna, thank you for being so friendly, Aarnout, thank you for the opportunity of giving a presentation in the lunch talk,

Peter, it was interesting to randomly seeing you cycling somewhere. Paul, thank you for the support around the wind measurements and nice to hear about your campaigns, Maurice, it is interesting to hear about your field experiences in Greenland, Christian, thank you for the chats we had about different topics around the world complications, Abdel, thank you for the tea times, Stefanie, thank you for the explanation around how particles move in a medium. Janneke, thank you for the chats we had every now and then, Daniel, thank you for the conversations about the lama teapot, Meike, it was nice seeing you play video games, Arthur thank you for bringing initiatives to the community and the conversations we had at your place about physics and chemistry. Darshika, thank you for the chats in tea times, Daan, thank you for the conversation we had about the social media. André, Daniele and Martina, thank you for all the invites and your lovely host, Ann-Sofie, I still think some words should be pronounced differently, it was nice to see your attempts in the water-bottle challenge. Julia, it has been always nice hearing your enthusiasm about field works. Sacha, I think we need to play chess more, Sanne, thank you for the chats we had about this joyful game, we still need to play it. Jinyang, thank you for the comments on the introduction, Tim, your comments were also useful and thank you and, Laurence, for the help in the Utrecht measurement campaign. Simon, thank you for the chats we had about the vocabularies, Valérian, it was interesting to see your creativity about how to use glasses in different occasions, Max, thank you for the explanations about Dutch culture. Bas, thank you for the invite to have hotpot at your place and it was great following your efforts in your startup at Utrecht Inc.

It was great meeting Stefan, Robin, Cerina and Lina, Paul and Jorg at Utrecht Inc. I thank you so much for the efforts preparing the validation programs, meetings, workshops and events for those who seek the entrepreneurship. I thank all the mentors, experts who provided advice and hints on how to move forward in raising a startup. I thank Ana and Nienke from Impact office of UU with whom we had very informative meetings. I would also like to thank Hamid for the great designs of the startup's logo and the thesis cover. Maaz Maps kindly thank you all warmly.

It was a great experience participating in the GERG (European Gas Research Group) project in Zelzate, Belgium. I thank colleagues from Fluxys for the host, Jonathan from Bureau Veritas for the coordination, Tania, Violeta from Enagás for the managements before, during and after the campaign. I thank colleagues from the GERG who provided this opportunity for the Maaz Maps to be involved in such a large-scale project with several measurement technologies aiming to reconcile the methane emission techniques. I thank all the colleague involved in the project for their times, explaining their techniques onsite, in the meetings and providing their results and reports.

I thank Michiel and the IMAU board for supporting our futsal team, Ijsbeercelona. Ijsbeercelona, a futsal team of passionate players with incredible motivations with brilliant fan team; these are the two wings which let the polar bears fly. I enjoyed every single moment of being in this team and watching your contributions to reach the team goals was extremely indescribable. It was great to see the pressure you were putting in all the spots of the field. Bas, jimmy and Erwin thank you for keeping the goal safe, Bouke, thank you for your return to your team, Léo thank you for all the runs you had, Matías, thank you for your energy and determination, Arthur, your skill improvements was exponential, thank you for all the efforts, Claudio, thank you for your enthusiasm in the field, Joey, nice defending technique, John, great moves and skills, Maurice, great to have you as captain, Tim, it was incredible to see you everywhere in the field, Stan, a player with footbally structured mindset, great to hear your thoughts, Manuel, thank you for keeping the mid-field in right order, Kaylee, thank you for making sub decisions easy, Simon, impressive four minutes, well done, Kilian, we need to play one more game at least, Mees, Mart, Thomas and Chiel for the supports when needed. It was just with the brilliant and lovely fan club that the atmosphere in the games enhanced by a factor of nine at least, endless thanks go to Sacha, Simon, Julia, great mascot, Hanne, Juhi, Getachew, Valérian, Malika, Elena, Sanne, Esther, Ann-Sofie, Meike, Bernadette, Miriam, Dani, Sanne, Max, Isabel, Jippe, Vittoria, Darshika, Christian, Brice, Zhongyang, Laura, Malavika, Jorjo, René and Petra.

It was extremely fortunate that I could find the Annatommie Medical Centre in Utrecht where I was treated with expertise in a very professional, nice and friendly environment. First of all, I appreciate

Caroline for recommending the Annatommie MC. This brilliant suggestion was in the middle of my search for a medical centre, I will not forget it. This is a true example of talking about right place at the right time. The Annatommie MC specialists, staffs and physiotherapists were those whom I have been looking for to get reliable treatment with clear medical procedure in the last year of my PhD right before the thesis submission. I would like to thank Rosa Bas who prepared me with the exercises for the operation and for the continuation of the exercises in the recovery phase. The energy, motivation and exercises I receive in the sessions have been extremely useful. I extend my appreciations to Dr. Marwan Shadid for the clear explanations in the appointments and reconstruction of the ligament. So far, although it has just been few months after the operation, I have been seeing the improvements slowly but continuously and I can see many moves back. I thank the anesthesia team who were extremely friendly before the operation, for the instruction before the anesthesia and also waking me up afterwards for giving me the ice cream. I thank, all the staff and operation room technicians who brought me a good memory from that day. I thank the receptionists who have always welcomed me to the centre and answered my enquiries adequately. I am very happy that I trusted your expertise.

I started living at the UCU when I moved to Utrecht in 2017, and a year later I found a lovely house with international and Dutch students. Very good memories of living with them, probably it will take some time to go through all the events, but I would like to thank them all with whom we became a dynamic and diverse family. It was brilliant to see how our family were supporting each other in the moments of need. Bastiaan, Stan, and Manuel, living with you was a big mistake, but we need to go to restaurants more often or play pool, if not, carting should be a good reason to show the virtually practiced skills. Amanda, it has been great knowing you and spending time with you and thank you for the summary translation, Ilse, thank you for the smartiz, it was a great idea, and nice to see your painting skills, Isabel, thank you for being so happy and energetic with great singing skills, Jippe, thank you for the time you spent to keep me mobile, Aura, thank you for all the games you played and motivations, Thorsten, thank you for the language lessons and help, Mees, thank you for the amazing and informative flyers and accessories, Ada, it was great seeing your sketches and interesting conversations we had about cultural similarities, Vittoria, thank you for the happiness you brought, Fenny, it was great seeing your passion about horses and conversation we had about how to deal with them, Levi, thank you for the poster and bringing nice atmosphere with your drawings, they looks great, Melissa, thank you for the game we played and the summary translation.

It is not possible to finish the acknowledgment without writing some lines about family. My mother, Zahra, my appreciation ability is limited but I thank you for your dedications, supports to the family, the joy you brought to us throughout years, I thank you for all the moments you created, the lessons you taught us, memories remain forever, My stepmother, Mehri, I thank you for all the happy moments you brought to our family, I thank you for your presence, my father, Majid, thank you for all days and nights you spent to keep eye on us and all the advice you gradually taught us. I thank all my siblings, nieces, and nephews whose continuous encouragements have been only raised over time. I thank my family for providing an atmosphere which enabled me to grow and learn life lessons and for all the supports while going through all the up and downs.

Now, it is time to pack and leave the grey bench, exit the garden, pass next to the walnut trees toward the sport centre. Once reaching the tennis courts, the Olympos should be to the left and a pathway on the right side which will lead to the spot for taking the September photo at the running track between the football fields, but this time close to the finish line.

Curriculum Vitae

Hossein started his methane studies from his bachelor's degree, petroleum engineering, when he was investigating kinetics and thermodynamics of gas hydrate formations and extractions in a teamwork. In his bachelor, he worked as student assistance to some bachelor's and master's lab measurement projects at the Biochemical and Bio-Environment Research Center and Institute for Biotechnology and Environment at Sharif University of Technology in Tehran, Iran. After his bachelor's studies, he attended a joint master's program, Geo Information and Earth Observation for Environmental Modelling and Management (GEM), between ITC/University of Twente, Netherlands, and Lund University, Sweden, when he used remote sensing and geo-information science to learn how to address environmental issues. In his master's thesis, he used Airborne Visible/Infrared Imaging Spectrometer (AVIRIS) to detect and quantify methane emissions from shale gas activities in Marcellus shale basin, Pennsylvania, USA. After his master's study, he returned to Iran and worked as a researcher to detect and quantify methane emissions from Iran's gas activities at National Iranian Gas Company (NIGC) using satellite imageries. This project was a joint project between NIGC and Iran's National Elites Foundation to fulfill his service. After this project, he started his PhD in the MEMO^2 (MEthane goes Mobile, MEasurements and MOdelling) project at Utrecht University (UU), Utrecht, Netherlands. In his PhD studies, he participated in several mobile methane measurement campaigns in European countries and learned from international collaborations. He is currently post-doc researcher at UU aiming to perform urban methane emission measurements in Seoul, South Korea. During his PhD, he noticed that to speed-up the efforts aiming to reduce methane emissions, a startup would be very useful, hence he founded Maaz Maps B.V. (www.maazmaps.com) in the Netherlands. He currently aims to expand the company with talented experts to be part of the global efforts in the framework of methane emission reduction pledge.

He enjoys sport activities a lot, and practicing several different sports is part of his lifestyle including football, futsal, chess, martial arts and some others. He has a good memory of participating in futsal leagues during his bachelor's, master's and PhD studies. In the latest league, he very much enjoyed being part of the Ijsbeercelona, the futsal team of IMAU (Institute for Marine and Atmospheric research Utrecht). He likes travelling and astrophysics could be another choice for his studies.

He has been living as an international student in the last years. He has been enjoying learning and experiencing different cultures and views of different people about same topics. He thinks that without constructive international collaborations, it is extremely difficult, if not impossible, to address global environmental issues.